Use of transaminases for the biosynthesis of enantiopure building blocks of two essential medicines: Ethambutol and Dolutegravir

2023

Josephine Tshegofatso Maboya

Supervisors: Prof Dean Brady & Dr Daniel Pienaar

A DISSERTATION SUBMITTED TO THE FACULTY OF SCIENCE, UNIVERSITY OF THE WITWATERSRAND, IN FULFILMENT OF THE REQUIREMENTS FOR THE DEGREE OF MASTER OF SCIENCE

Declaration

I declare that the work presented in this dissertation is my own work and has not been submitted before for any degree or qualification in this or any other university. A dissertation submitted to the Faculty of Sciences at the University of the Witwatersrand, Johannesburg, for the Degree of Master of Sciences.

Josephine Tshegofatso Maboya
Date : 25-03-2024

Abstract

(S)-2-Amino butan-1-ol and (*R*)-3–amino butan-1-ol play an important role as intermediates in the synthesis of the anti-tuberculosis drug ethambutol and HIV integrase inhibitor drug dolutegravir respectively. The current industrial preparation of these enantioenriched amino alcohols is quite a challenging process; it typically involves the use of harsh chemicals, results in low yields, and generates hazardous waste materials. Consequently, these methods tend to be expensive, and it has been demonstrated that the cost of these intermediates has a significant impact on the overall costs of the synthesis of the entire drug. Therefore, it is not surprising that the convenient, cost–effective, and environmentally benign production of these optically pure amino alcohols is still the subject of ongoing investigations. The chemo-enzymatic approach holds great potential to replace the conventional routes for the synthesis of enantiopure amines. Transaminase enzymes (ATAs), in particular, have gained much attention over time due to their remarkable capability to transform inexpensive ketone starting materials into valuable enantiopure amino alcohols.

Through the utilization of the isopropyl amine donor system, pro-chiral ketone starting materials were effectively transformed into the desired (*S*)-isopropyl 2-aminobutanoate and (*R*)-isopropyl 3-aminobutanoate using transaminase biocatalysis. These reactions proceeded well under milder conditions such as ambient temperature and pressure conditions, and impressively under an aqueous environment. Three (*S*)-enantiomer selective “hit “enzymes were discovered (ATA-189, ATA-194, and ATA-254) for the biotransformation of alpha-keto ester substrate into an enantio-enriched amino ester product, with enantiomeric excess ranging between 95-99% and the yield was 15-73% depending on the enzyme and reaction conditions. However, when it came to dolutegravir intermediate, a different scenario unfolded. In this case, the majority of the ATA enzymes in our enzyme library fortuitously exhibited selectivity for the (*R*)-enantiomer. In particular, four highly enantioselective enzymes (ATA-254, ATA-261, ATA-262, and ATA-234) were discovered, demonstrating % e.e ranging from 93% to 99.99%, with corresponding yields from 38% to 45%. The successful biotransformation of an inexpensive pro-chiral starting material into highly valuable enantioenriched amino ester intermediates represents a significant achievement. Coupled with an effective reduction method to convert these intermediates into the corresponding amino alcohols, this biotransformation process holds immense potential for enabling the sustainable and cost-effective production of both of the valuable ethambutol and dolutegravir amine intermediates.

Acknowledgments

I extend my sincere gratitude to Prof. Dean and Dr Danie for their unwavering support and exceptional mentorship. Their guidance and wealth of knowledge have been pivotal in shaping my journey, and I am immensely thankful for the opportunities to learn and grow under their tutelage.

I want to express my profound gratitude to Thapelo, Refilwe, and Dr. Eric for their invaluable support in utilizing GCMS and HPLC-MS techniques. Furthermore, I extend my deepest thanks to Professor Fernandes for conducting the single-crystal analysis and to Dr. Sam Gittings from Prozomix for generously providing us with enzyme samples. Your expertise and collaborative efforts have significantly elevated the quality of my research, far beyond what I could have accomplished on my own

I extend my warmest thanks to Dr. Maphupha, Dr Thabo, and Dr. Charles for their significant contributions and guidance throughout this journey. Your insights have been invaluable in shaping the trajectory of my work. To my wonderful lab mates – Kabelo, Lebo, Khanya, Chris, Nduduzo, Mpumi, Cecilia and Bongi – your camaraderie and support have turned the laboratory into a place of both productivity and enjoyment. I am truly thankful for the shared experiences that made this journey memorable.

To my beloved siblings, whose belief in me has been a constant source of inspiration, and to my mom, whose prayers and emotional support have been my pillars of strength – your unwavering faith has been instrumental in my success, and for that, I am truly grateful.

I would also like to express my gratitude to my best friend, Dinah. The late nights we spent together in the laboratory, pushing through challenges, were made enjoyable by your presence. Your unwavering companionship has been a constant source of motivation. Lastly, I want to thank Shibo, Tshego, Mkhulule, Bongi and Saki for their unwavering emotional support. Your encouragement and understanding have been a guiding light, helping me navigate both the highs and lows of this journey.

To everyone mentioned above including the whole of organic group, your support has been invaluable, and I am deeply thankful for your roles in my academic and personal growth.

With heartfelt appreciation,

Table of Contents

List of Figures

List of Schemes

List of abbreviations

AIDS	Acquired Immune Deficiency Syndrome
API	Active pharmaceutical ingredients
α-TAms	Alpha transaminases
ART	Antiretroviral therapy
ATAs	Amino transaminases
$BF_3.(OEt)_2$	Boron trifluoride diethyletherate
DCC	N, N'-Dicyclohexylcarbodiimide
DCM	Dichloromethane
DKR	Dynamic kinetic resolution
DMAP	4-dimethylamino pyridine
DNA	Deoxyribonucleic acid
DIPEA	N, N-Diisopropylethylamine
e.e	Enantiomeric excess
FDA	Food and Drug Administration
HILIC	Hydrophilic interaction chromatography
HIV	Human immunodeficiency virus
InSTI	Integrase strand transfer inhibitor
IREDs	Imine Reductases
IPA	Isopropyl amine
KR	Kinetic resolution
K^+P_i	Potassium monophosphate buffer
LCMS	liquid chromatograph mass spectrometer
MAO	Monoamine oxidases
NADP	Nicotinamide adenine dinucleotide phosphate (NADP)
NRTIs	Nucleoside reverse transcriptase inhibitors
PLP	Pyridoxal-5-phosphate
PMP	Pyridoxamine-5-phosphate
PPM	Part per million
THF	Tetrahydrofuran
ω-TAms	Omega transaminases
WHO	World Health Organization

CHAPTER 1:

1. INTRODUCTION

Aminotransferases (ATAs), also known as transaminases (EC 2.6.1.-), are groups of enzymes that catalyse the interconversion of amine and keto groups in the presence of pyridoxal-5-phosphate (PLP) enzyme co-factor. These enzymes play a major role in central metabolism in both animals and plants.[1] ATAs are commonly found in all parts of the plants, and they are responsible for the catalysis of the reversible transaminase between glutamate and pyruvate into oxoglutarate and alanine, which plays a major role in the protein synthesis.[1–3]

ATAs have a tissue-specific distribution in humans, some are found in the kidneys, cardiac and skeletal muscle but the major distribution is found in the liver.[2,3] The importance of transaminase in glucose formation is illustrated in *Fig.1*. In the muscle cell, pyruvate and glutamate are converted to alanine and α-ketoglutarate. The alanine product then enters the blood circulation and is taken up by the liver where alanine transaminase hepatocytes convert it back to pyruvate, which plays a major role in glucose synthesis (*Fig. 1*). This function is essential for glucose regulation, particularly during stressful conditions like vigorous exercise and food deprivation.[1,2,4] Generally, ATAs play a crucial role in cell viability, metabolism, and excretion of toxic substances in the body.

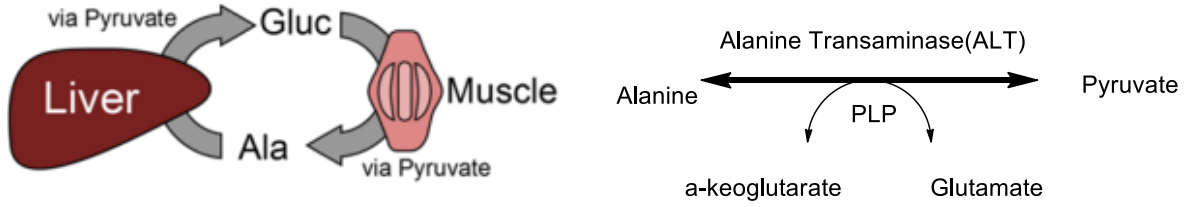

Figure 1: The collective alanine transaminase function in the human liver and skeletal muscle cells.[3]

In bacterial cells (e.g. *E. coli*), there are several overlapping ATAs enzyme activities that collectively participate in the biosynthesis of alanine, which is a major building block of the bacterial cell wall, while they also catalyse alanine degradation depending on the metabolic and environmental conditions.

The enzymatic function of ATAs and their biological significance was discovered and recognized by Braunstein and his colleagues in the late 1930s.[5] Their discoveries resolved several biochemical puzzles despite working with limited resources and this team continued

over decades advancing the study of ATAs and other PLP-dependant enzymes. Cooper and Meister published a historical review paper in 1988 as a tribute to Braunstein; the paper gave a detailed explanation of the events and pioneers involved in the discovery of ATAs, as well as enzyme characteristics.[5] Their findings involve:

- The mechanism of action of aspartate transaminase enzymes.
- Biological significance of ATAs, wherein they observed the conversion of glutamate and aspartate to succinate when using muscle tissue extracts and concluded that a mammalian cell should at least contain two different ATAs, a glutamate-pyruvate ATAs and aspartate-pyruvate ATAs.
- The importance of PLP as an enzyme co-factor was also highlighted.
- The stereospecificity of the ATAs reaction was observed as they found only one enantiomeric configuration between the reversible interconversion of alanine and glutamate.

Since the first ATA demonstration by Braunstein in the 1930s, various ATAs were subsequently discovered. ATAs are now classified into two different groups, the α-transaminases (α-TAms) or ω-transaminases (ω-TAms) depending on their substrate specificity. [6]In the case of α-TAms, the presence of a carboxylic group in the α-position to the carbonyl functionality is exclusively required, hence α-TAms only allow for the formation of α-amino acids and the corresponding α- keto acids. [7,8] *ω*-TAms are technically more useful than α-TAms as they allow amination of non-alpha positioned substrates thus having a wide range of substrates including ketones, aldehydes, and keto acids.

ω-TAms exhibit enantio-preferences, being either *R* or *S*–selective. Over decades the majority of ω-TAms discovered in nature have been (*S*)-selective; it is only recently that (*R*)-selective ω-TAms have been identified or engineered. [9]ω-TAms biocatalysis is currently applied in pharmaceuticals, chemical and agricultural industries for the interconversion of pro-chiral ketones into high-value enantiopure intermediates.

Mechanism of action of ATAs

1.1.1 **The role of PLP-cofactor**

Pyridoxal-5-phosphate (PLP), also known as an active form of vitamin B6, represents the most versatile organic co-factor utilized in biochemistry. PLP-dependent enzymes are involved in the catalysis of numerous chemical reactions, including those catalysed by transaminases, racemases, aldolases, decarboxylases, lyases and others.[10] Besides this broad functional diversity, all PLP-dependent enzymes are structurally grouped into seven-fold types based on different evolutionary lineages. Of all 7-fold types, fold type 1 is the most populated and is more structurally and functionally diverse compared to the others.[11] The family of aminotransferases are a part of this widely diverse fold-type I PLP–dependent enzymes. Fold type I enzymes share certain mechanistic characteristics with other fold types such as a covalent binding of PLP with lysine residue to form a Schiff base *(Fig. 2*).[10]

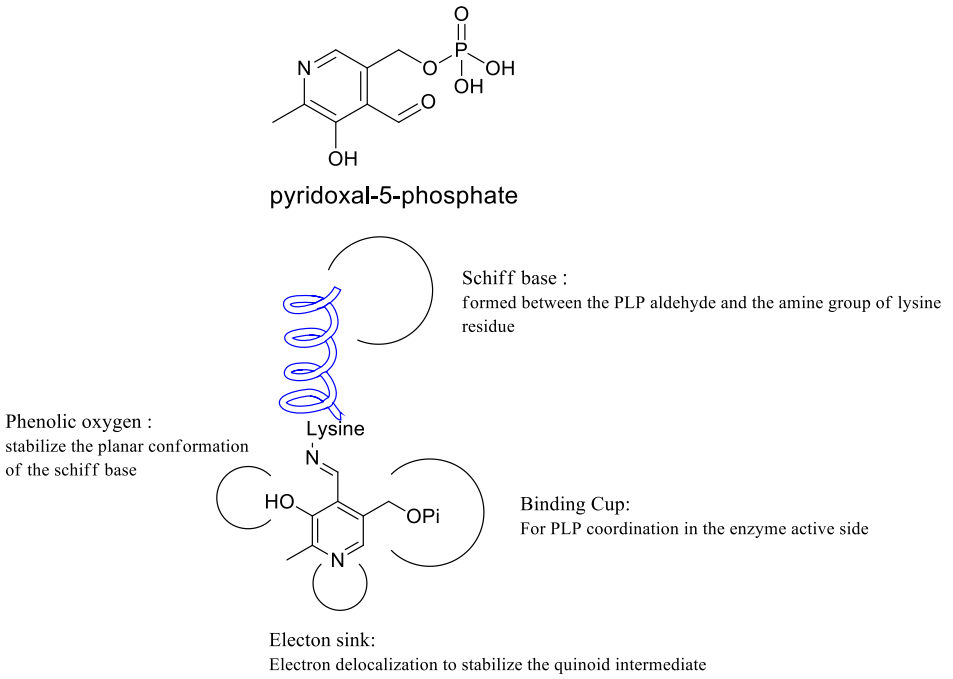

Figure2: The significance of PLP functional groups on its overall function, redrawn from reference.[12]

PLP acts as a co-factor because of its specific structural properties. The structure of PLP contains a phosphate group and a hetero aromatic pyridine ring bearing a hydroxyl and an aldehyde group (*Fig. 2*). All functional groups in PLP are vital in the mode of action and binding interaction of PLP–dependent enzymatic reactions. The aldehyde group is responsible for imine formation (Schiff base) with the free unprotected amine, i.e. the internal aldimine is formed with the lysine residue of the enzyme, and the external aldimine formed with the amine of the amino donor or a substrate (*Fig. 2)*.[10] The interconversion between internal and external

aldimine is a reversible process due to its thermodynamic properties, which makes it possible for the binding of the substrate, product release, and the regeneration of the co-factor (PLP).[10] The phenolic oxygen of the PLP is responsible for maintaining the planar conformation of the Schiff base, which is essential for electron delocalization. The oxygen also interacts with the imine nitrogen through keto-enol tautomerization which favours the keto-enamine tautomer and the planer conformation of imine and the pyridine ring (*Fig. 2*). The pyridine ring is important for the stabilization of the carbaionic intermediate that is formed in the reaction, this is done through resonance stabilization and delocalization of electrons by the electron-sink character of PLP (further discussed below). The PLP binds in the active site through the phosphate group, however, exceptions are observed in some fold types. The phosphate group was also proposed to function as an acid-base catalyst, which promotes proton transfer during external aldimine formation.[10]

1.1.2 **Transaminase reaction mechanism**

The reaction mechanism of transaminases was extensively studied by crystallographic investigation of enzyme and substrate complexes. Although there are different sub-classes of transaminases (2.6.1.1-2.6.1.6), they all follow the same mechanism but differ significantly in substrate specificity. ATAs catalyse the oxidative deamination of amine donor and reductive amination of amine acceptor, thus the whole mechanism is divided into two distinct half-reactions (*Scheme 1).*[7,13,14] The first half-reaction involves the conversion of the amine donor to its corresponding ketone, while the PLP cofactor is interconverted into its amine version, pyridoxamine-5-phosphate (PMP).[14] In the second half-reaction, the amine acceptor (ketone) is converted into a final amine product and PLP is regenerated.[14]

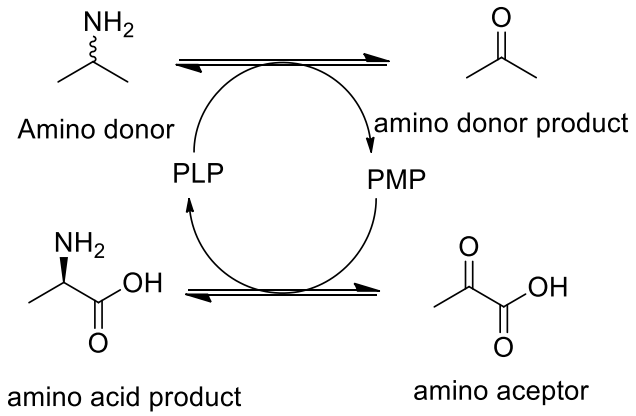

Scheme 1: The summary of the overall ATAs reaction mechanism.

The first step in transamination involves the formation of the internal aldimine (Schiff base).[10,14] This is followed by a nucleophilic attack of the amino donor at the iminium carbon of PLP thus undergoing transaldimination transformation to form external aldimine.[7,14] The proton on Cα is abstracted by the lysine residue resulting in a planar quinoid intermediate, which is followed by the carbanion resonance stabilization over the entire compound (electron sink effect) resulting in new bond formation.[7,14,15] Catalytic lysine then donates a proton at C4 resulting in a ketimine intermediate. Finally, ketimine is hydrolyzed to a keto acid and PMP, thus one-half reaction is complete followed by a second half which constitutes the same intermediates but in the reversed order resulting in a corresponding new amine product as well as PLP regeneration.[14]

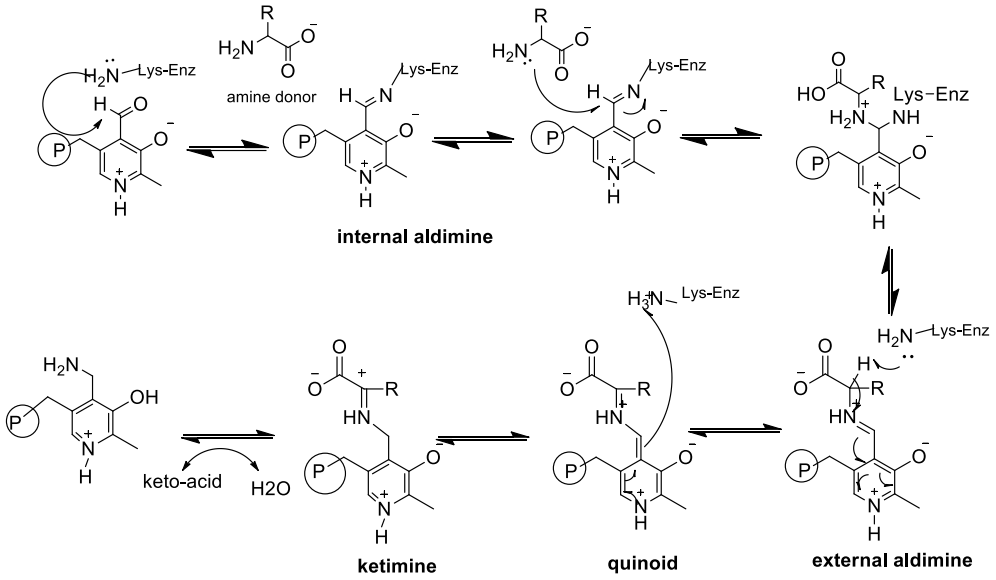

Scheme 2: The transamination reaction mechanism.[14]

Chiral amines

Chiral amines play an increasingly important role as building blocks in the pharmaceutical and agrochemical industries.[16] In the case of a racemic compound, both *R* and *S* enantiomers may have the same structural and physical characteristics, however, they often have different biological responses. The most famous example of the importance of chirality is thalidomide, which is the drug that was used in the early 1960s for the treatment of nausea and alleviation of morning sickness in pregnant women.[17] The use of racemic thalidomide resulted in a lot of infants being born with deformities of limbs and only half of these children survived. This effect was due to the biological response from one of the enantiomers, the *R* enantiomer was a potent drug with multiple therapeutic applications, while the *S* enantiomer had severe

teratogenic side effects.[17] The US Food and Drug Administration (FDA) and the European Committee for Proprietary Medicinal Products introduced strict regulation requiring the synthesis of single stereoisomer drugs, and this came into effect in 1992.[18.]

More than 90% of Top selling drugs originate from enantiopure chiral amines, *Fig.3* shows examples of drugs containing a single amine enantiomer.[18]

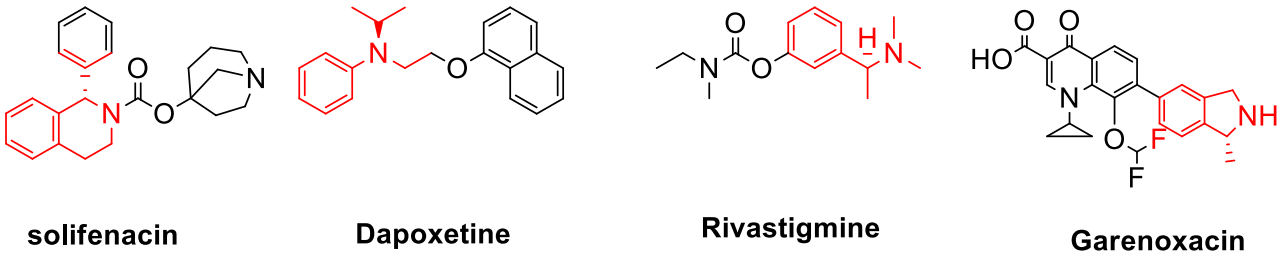

Figure 3 :The examples of chiral amine-containing pharmaceutical drugs.[18]

1.1.3 **Chemical synthesis of amines**

The are numerous chemical reaction techniques that can be used to synthesize amines. The most facile route includes the direct substitution of an alkyl halide in a simple SN2 reaction (*Scheme 3).* The problem with the substitution reaction is the requirement of an excessive amount of ammonia in order to drive the reaction to a desired product. The primary amine product is also reactive towards the alkyl halide; therefore this results in an unfavourable over-alkylation if minimum amount of ammonia is used. Alternative synthesis of amines includes the reductive amination reaction, which is the most commonly used and versatile way of forming C-N bonds (*Scheme 3).* The are two steps involved in this reaction, this includes the imine / the enamine formation from the corresponding ketone or aldehyde followed by the reduction reaction. The most common reducing reagent for this purpose is sodium triacetoxyborohydride ($NaBH(OAc)_3$) which can selectively reduce imines in the presence of aldehydes into amines. Other reducing agents such as sodium borohydride ($NaBH_4$) and sodium cyanoborohydride ($NaBH_4CN$) can also be used. Amines can also be formed from the reduction of other nitrogen-containing functional groups, amides, nitriles, and azides *(Scheme 3).*

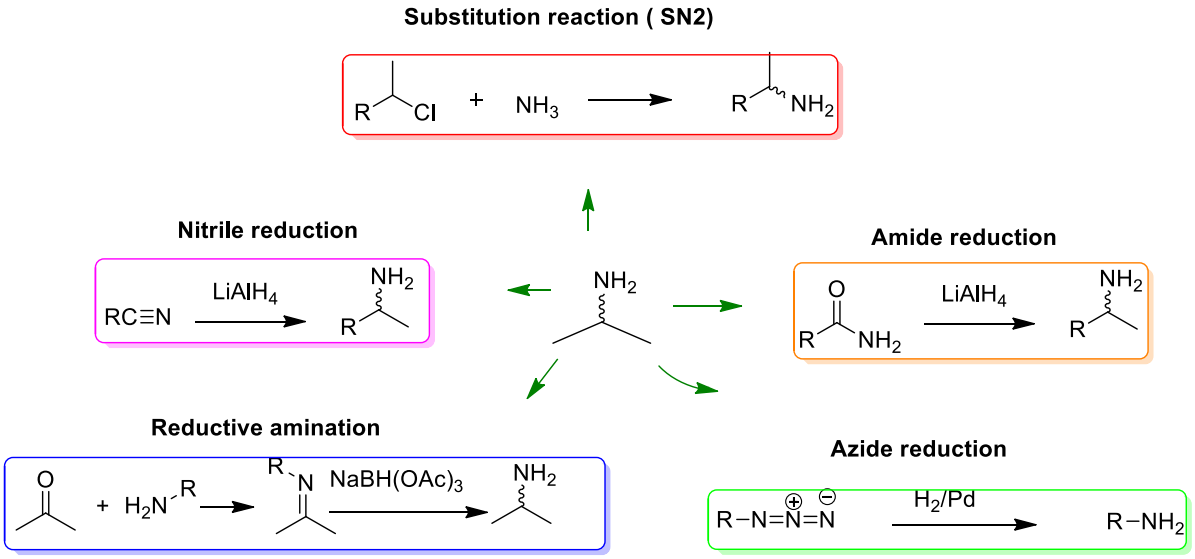

Scheme 3: Different schematic routes for the synthesis of primary racemic amines.

All the reactions mentioned above result in the racemic mixtures of amine products. To achieve a single enantiomer, a chiral resolution step needs to be applied. The most commonly used resolution step for large-scale production includes recrystallization of the desired enantiomer by forming a diastereoisomeric salt.[19] Formation of diastereoisomers from different resolution agents (mostly carboxylic chiral agents) results in two compounds with different physical properties, thus making them easy to be separated via distillation, crystallization, etc.[19] During chiral resolution steps, only 50% of the initial quantity of the reactants can be converted to the desired product whilst the other 50% can be recovered as an unwanted precusor.[20] However, if the undesired enantiomer can be racemized, it is possible to undergo the whole optical resolution repeatedly until all the products are in a single enantiomer form (*Fig. 4).*

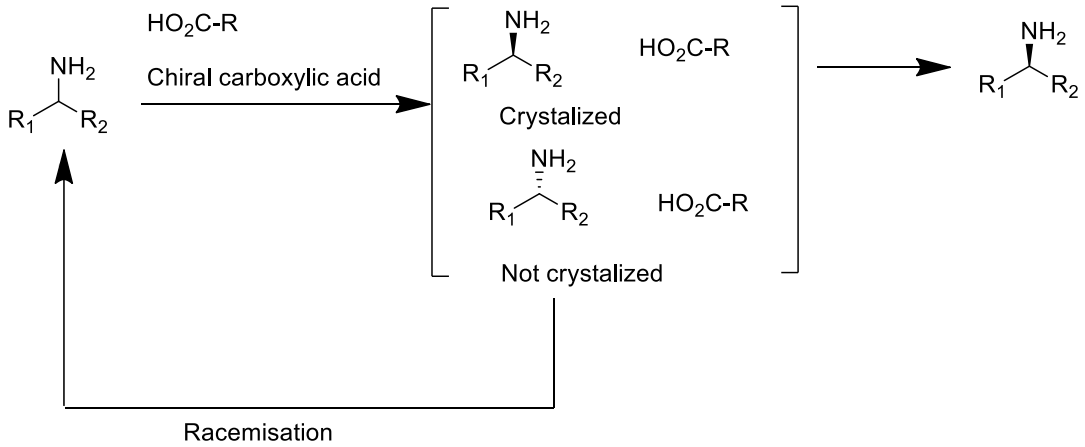

Figure 4: An example of chiral resolution using the crystallization method.

Chemical synthesis strategies for stereospecific synthesis of chiral amines is still a challenging process, it requires time-consuming resolution steps, uses harsh chemicals, results in low

product yield, and generates toxic waste material.[21,22] Even the recent synthesis approaches, which involve high temperature and pressure conditions, harsh chiral auxiliaries, and transition metals (like expensive ruthenium catalyst, which are non-reusable), are far from perfect. A more convenient and greener route for the production of optically pure amines is needed and is still an ongoing investigation. Biocatalysis, which is the use of biological substances to catalyse a chemical reaction, bears great potential for the synthesis of optically pure amines and thus has gained much attention in the past years.[20]

1.1.4 **Biocatalytic Synthesis of chiral amines**

An efficient and sustainable synthesis of enantiopure amines is of great importance in the pharmaceutical industries and now there is a shift to the application of biocatalysis in the production of enantiopure amine-containing drugs. Biocatalytic synthesis of chiral amines has emerged as a green alternative route to chemical synthesis, they often work under milder conditions, operate in aqueous media and they are insensitive.[23] The most appealing aspect of biocatalysis is that many enzymes are extremely stereoselective, often leading to enantioenriched amine compounds (sometimes achieving 99.9% e.e).[20] In theory, various enzymatic pathways can be used to synthesize optically active amines, originating from different enzyme classes including transferases, hydrolases, and oxidoreductases (*Scheme 4).* Some enzymes, such as amine oxidases, transaminases, lipases, and other hydrolases, can distinguish between enantiomers of racemic substrates and thus can be used for a chiral resolution step. Others are capable of the more atom economical enantiospecific synthesis (imine reductases, amine dehydrogenases and again transaminases).

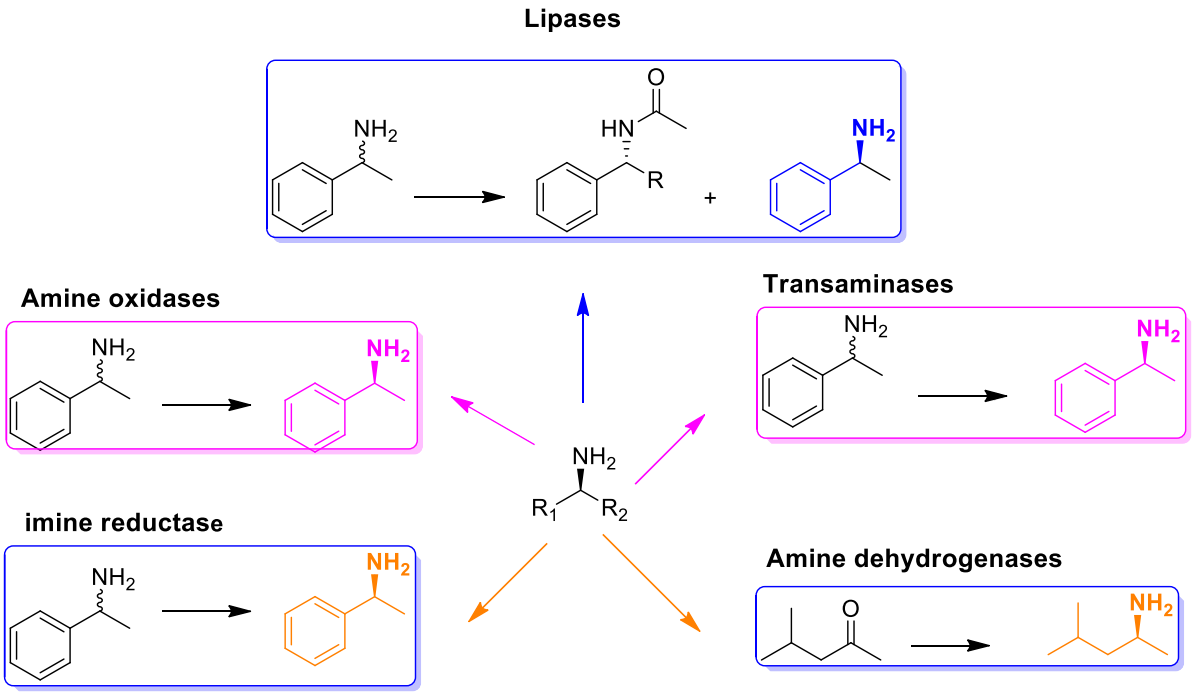

Scheme 4: Different schematic routes for the synthesis of optically pure amine.[20]

1.1.4.1 The use of hydrolases for resolution of racemic amines.

Hydrolase enzymes can be used for the kinetic resolution of racemic amines to obtain optically pure compounds. The protease family of hydrolases, including penG acylase, lipases, and amidases, inherently catalyses the stereoselective hydrolysis of amides.[20] These enzymes work by preferentially attacking one enantiomer, and the final product contains a mixture of a single amine enantiomer and the amide form of the other enantiomer. BASF agricultural solution industry in Germany uses *Burkholderia plantarii* lipase at a large-scale for the production of optically pure aliphatic amines and amino alcohols.[20] Although the method has been highly optimized to be performed on a large scale for the resolution of a wide variety of amines, kinetic resolution yields are still limited to less than 50% unless racemization is performed to facilitate the dynamic kinetic resolution (DKR) step.

The kinetic dynamic resolution was applied to the synthesis of the anti-depressant pharmaceutical norsetraline (1*R*, 4*S*) by Bäckvall's group.[24] Initially, the racemic 1-aminotetralin underwent the dynamic resolution step using *Candida antarctica* lipase B (CALB) followed by the racemization using Ru-Shvo catalyst and this resulted in a 70% yield of the intermediate (*Scheme 5*). Five more steps were followed to afford 28% norsertraline.[24]

This example highlights how the lipase kinetic resolution step can be improved by incorporating racemization to facilitate dynamic kinetic resolution. The drawback is that most of the racemization catalysts are transition metal catalysts, so they are expensive and some produce toxic waste. To solve this problem, enzymes that are able to promote racemization must be incorporated.

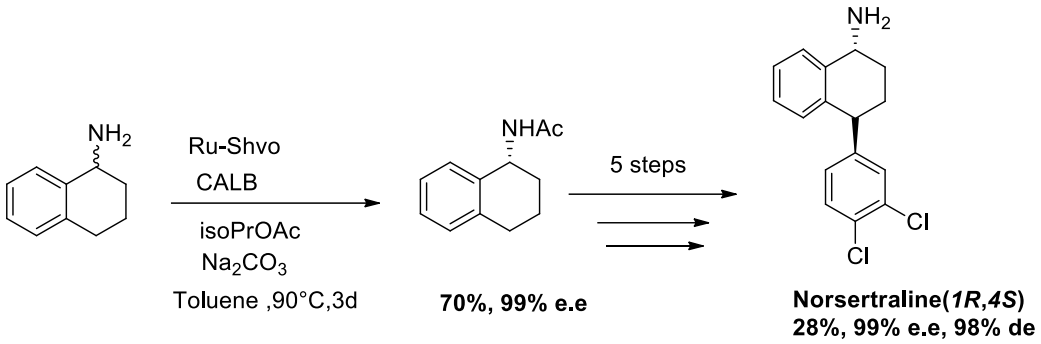

Scheme 5: An example of the application of dynamic kinetic resolution in improved hydrolases resolution % yield of the enantiopure products.

1.1.4.2 The use of monoamine oxidases (MAO) for the synthesis of enantiopure amines

Monoamine oxidases (MAO) are members of the oxidoreductase class of enzymes and they play a major role in the catalysis of redox reactions, particularly oxidation.[16,18] MAO catalyses the enantioselective oxidation of a racemic amine to form an imine and a single enantiomer (*Scheme 6*). The most efficient approach that harnesses the catalytic power of MAO is deracemization, in which the enantioselective oxidation is coupled with the concurrent non-selective chemical reduction. The process can occur recursively until a 100% yield of the single enantiomer is reached. This resolution step is more advantageous compared to lipase DKR because no additional organometallic catalyst is required for the deracemization step.

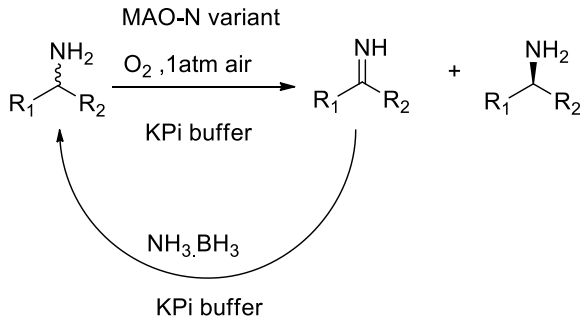

Scheme 6: Kinetic resolution of racemic amine using MAO followed by deracemization.

The chiral resolution of MAO reveals a rather impressive technique to synthesize a single enantiomer in 100% yield. A disadvantage of this reaction is that it requires a non-selective chemical reducing agent to facilitate the deracemization step, and ammonium borane ($NH_3.BH_3$) is most commonly used for this purpose. Boron-containing reducing agents are inconvenient to use because they often lead to undesirable boron-amine complex formation. An alternative non-boron containing reducing agent such as lithium aluminium hydride must be employed for the reduction of imines.

1.1.4.3 **The use of imine reductase (IREDs) for the synthesis of enantiopure amines.**

Imine reductases are NADPH–dependent enzymes that are able to catalyse the stereoselective reduction of imine to their corresponding amines.[25] The most interesting part of the IRED resolution step is that it allows for the asymmetric synthesis of optically pure amines, both reductive amination reactions and imine reductions are possible (*Scheme 7*). Due to the unfavourable equilibrium of imine formation in aqueous media, IRED reactions have received little attention in the past few years. For this reaction to be successful, the enzyme must be chemo selective enough to avoid reduction of the carbonyl to the corresponding alcohol.

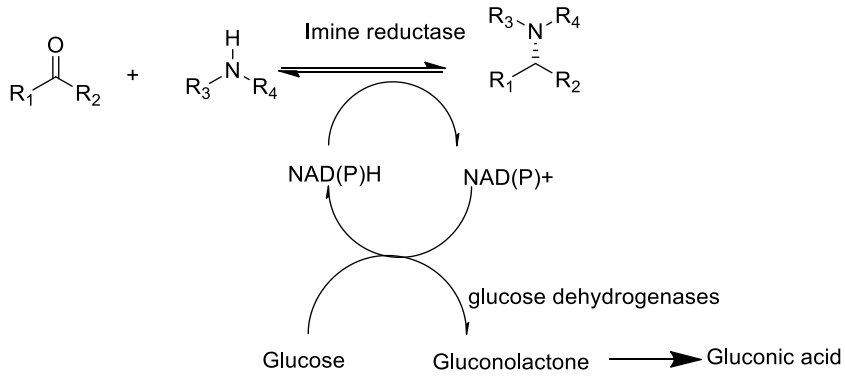

Scheme 7: Asymmetric synthesis of optically pure amines using imine reductases.

In 2010, Mitsukura's group discovered two different stereoselective IREDs in filamentous bacteria. *Streptomyces* species GF3587 and 3546 exhibited a highly enantioselective reduction of 2-methyl-1-pyrroline to 2-methyl-1-pyrrolidine, yielding ~99.2% e.e (*R*) and 99.3% e.e (*S*) enantiomers with excellent conversion .[25] Since then IREDs have become highly recognised and now it is used in the industrial synthesis of suvorexant (a drug used for the treatment of insomnia).[26] Although this reaction has excellent stereoselectivity, it also has limited substrate specificity as the reductive amination of aldehydes with amines has proven difficult. It is clear that enzymatic reduction occurs when prochiral imines are formed, however, there has been

little evidence for the role of enzymes in imine formation. Understanding the substrate specificity of IRED requires further understanding of the overall mechanistic reaction.

1.1.4.4 **The use of amine dehydrogenase (AmDHs) for the synthesis of enantiopure amines.**

Amine dehydrogenases catalyse the stereoselective reductive amination of ketones and aldehydes to enantiopure chiral amines. AmDHs allow the asymmetric synthesis of chiral amines, initializing from a prochiral substrate (*Scheme 8*). This reaction is different from other NADPH- dependent enzymes (such as IRED) in the sense that it accepts ammonia as an amino donor, however, other primary amine donors such as methylamine, ethylamine, and cyclopropyl amines and have been reported when operating under high concentrations.[27] Mayol's group successfully catalysed the stereoselective synthesis of (*S*)-4-aminopentanoic acid from the corresponding ketone substrate using the AmDHs enzyme derived from the *Clostridium sticklandii* strain (*Scheme 8*).[28] Only a single enantiomer was obtained (99.5% e.e) with an excellent 90% conversion. AmDHs are extremely enantioselective thus there are no additional racemization or DKR step required. The problem with this reaction is that AmDHs have a limited substrate scope and are only often involved in the formation of primary amines. More amino donors need to be discovered for the expansion of the substrate range in order to allow the synthesis of secondary and tertiary amines, and further engineering still needs to be investigated to improve the substrate specificity of the enzyme.

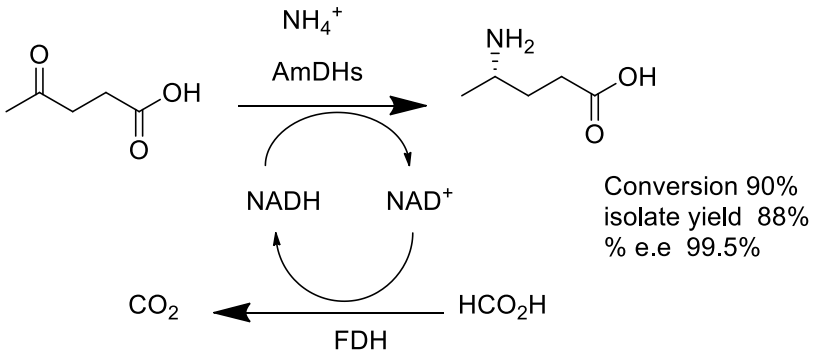

Scheme 8: Example of AmDHs enzyme catalysed reaction.[27]

Types of transaminases reaction

1.1.5 **Kinetic resolution transaminase reaction**

KR transaminase reactions involve the resolution of a racemic mixture of amines to generate one enantiomer. In this case, a single enantiomer of a racemic mixture donates its amino group to form a corresponding ketone and the other enantiomer is then isolated from the reaction mixture (Scheme 9). Pyruvate is the most commonly used amino acceptor for this reaction, and only a half equivalence is required for the resolution of a single enantiomer, this behaviour favours the forward reaction thus making the KR reaction more thermodynamically favourable compared to the asymmetric synthesis. As in any other KR step, the maximum yield that can be obtained is 50%. To overcome this limitation, ATAs are typically coupled to oxidizing enzymes such as amine oxidases to facilitate DKR or the alanine by-product is deracemized in a single pot reaction. Rozzell and Turner's groups demonstrated an efficient chiral resolution method utilizing ATAs in tandem with amino acid oxidases, and a product in 99.99% e.e with a substrate conversion of 99% was obtained.[32]

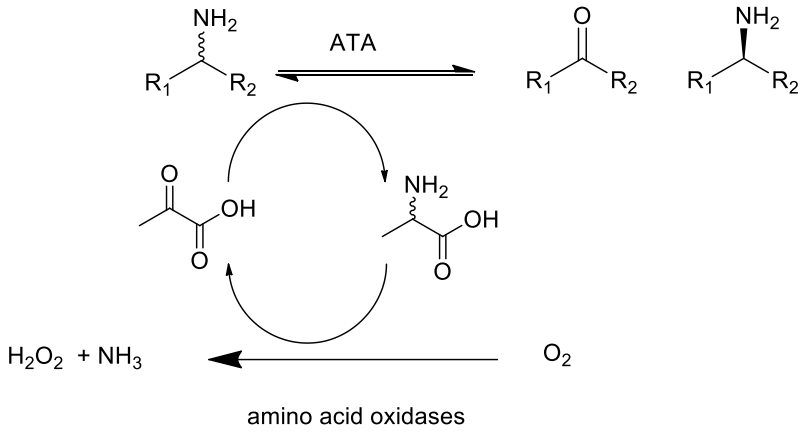

Scheme 9: ATA kinetic resolution coupled with amine oxidases.[32]

Kroutil's group also applied ATAs to kinetic resolution in the synthesis of mexiletine, a drug used for the treatment of cardiac diseases and muscle stiffness.[33] They successfully isolated 99% yield of a single enantiomer using a single pot reaction which consists of two different transaminase reactions (*Scheme 10*). The first step involves the deamination of a single enantiomer (*R*–enantiomer in *Scheme 10*) to a ketone intermediate, this was followed by the recycling of pyruvate by amino acid oxidases which convert alanine back to pyruvate in the presence of oxygen. *R*-ATAs are then deactivated by heat followed by the addition of a second stereoselective ATAs to afford the conversion of the ketone intermediate to the amine, so using this step both R and S enantiomers can be isolated in a good yield. KR using ATA is only

efficient if the racemic starting material is inexpensive, when dealing with an expensive racemic compound asymmetric synthesis of amines using ATAs can be employed.

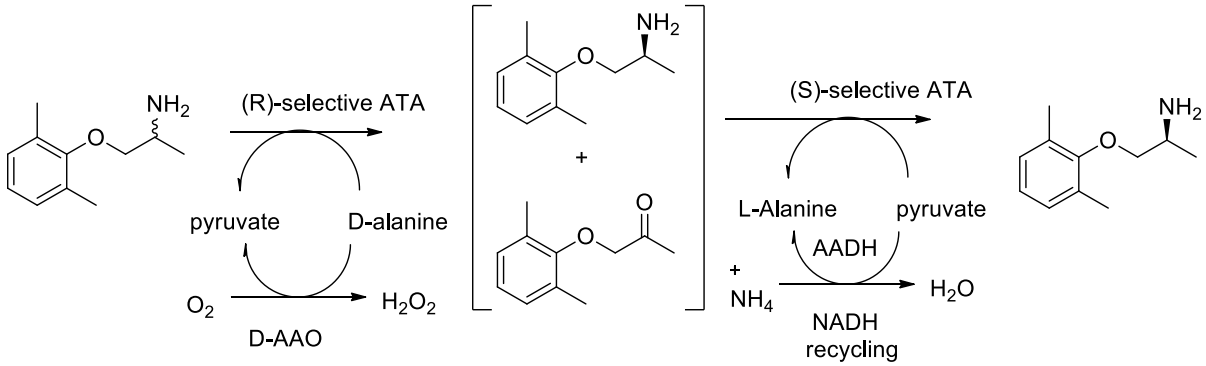

Scheme 10: The application of sequential stereoselective ATA catalysed reactions to synthesise mexiletine.[33]

1.3.2 Asymmetric synthesis of chiral amines using ATAs.

ATAs together with AmDHs have emerged as important tools in biocatalysis because they are both capable of catalyzing direct conversion of a prochiral carbonyl group into an optically pure amine.[18] These two enzymatic routes have several advantages compared to other routes (routes that include KR and DKR steps), the most obvious advantage of this route is initializing the reaction with the cost-effective starting material (prochiral ketone) which is capable of reducing the overall cost of the entire synthetic route. Asymmetric synthesis often results in a 100% theoretical yield and also has less waste generation, these properties are highly desired in both pharmaceutical and agrochemical manufacturing companies.[8]

AmDHs rely on nicotinamide cofactors ($NAD(P)^+$ /NAD(P)H) for the reaction to take place, however, these cofactors are expensive to use *in vitro*. To solve this problem whole cells can be used to eliminate the need to supply the expensive co-factor. Although these enzymes are extremely stereoselective, their application is not necessarily economically attractive because it involves high process costs. ATAs on the contrary do not belong to the family of nicotinamide–dependent enzymes, they use PLP co-factors that regenerate themselves during the synthetic reaction.

The application of asymmetric transaminase reaction has only gained much attention after 20 centuries their discovery, primarily due to constraints such as unfavourable equilibrium, enzyme instability, and limited substrate specificity profile.[34] The first asymmetric synthesis of amines was demonstrated by Shim and Kim, they used ATAs originating from *Vibrio fluvialis* to convert acetophenone to (*S*)-α-methyl benzylamine using L-alanine amino donor

(*Scheme 11*).[35] To overcome the thermodynamic bias towards the starting material they used an excessive amount of amino donors and removed the pyruvate co-product by converting it to lactate to afford 90% yield of the product with 99 % e.e (*Scheme 11*).[35]

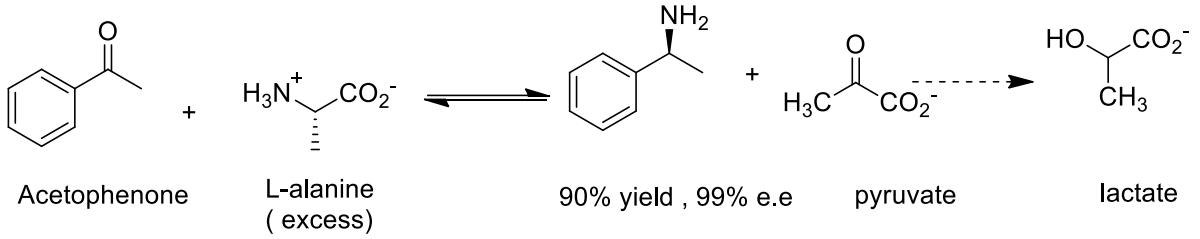

Scheme 11: The conversion of acetophenone to (*S*)-α-methyl benzylamine reaction performed by Shin and Kim.[30]

In recent years, asymmetric synthesis of achiral amines is widely used in both academia and industries to synthesize a different range of pharmaceutically active compounds or intermediates. Researchers from Merck and Codexis did several rounds of directed evolution and structurally guided protein engineering to form an *R*-selective ωTAms variant derived from *Arthrobacter* sp, this was applied for the asymmetric synthesis of sitagliptin (an anti-diabetic drug) from prositagliptin.[7,29] Most notably, the use of ATAs to biosynthesize the blockbuster sitagliptin was shown to be more economically competitive than using a traditional chemical method, i.e. a chiral ruthenium-based catalyst to reductively aminate the ketone intermediate. The same mutant Arthmut11-ATA which allows bulky substrates was later applied for the asymmetric synthesis of the intermediate of ramastroban, which is a thromboxane receptor antagonist currently used for the treatment of asthma and coronary disease.[36]

Rivastigmine (*Fig. 5*), the most potent drug used in the treatment of early stages of Alzheimer's disease as well as Parkinson's disease was synthesized using ATA (Vfl-ATA) to form enantiopure chiral amine in 71% yield and 99% e.e.[37] Mutti and colleagues also published a paper using different enzyme mutants to form amine products, a few of these products formed shows potential in API precursor production.[37] This includes the production of Dilevalol (a hypertension drug) and formoterol (β-2 agonist). All of the examples mentioned above emphasize the value of biocatalysis and how pharmaceuticals are continuously moving toward a greener and a sustainable approach to the synthesis of APIs.

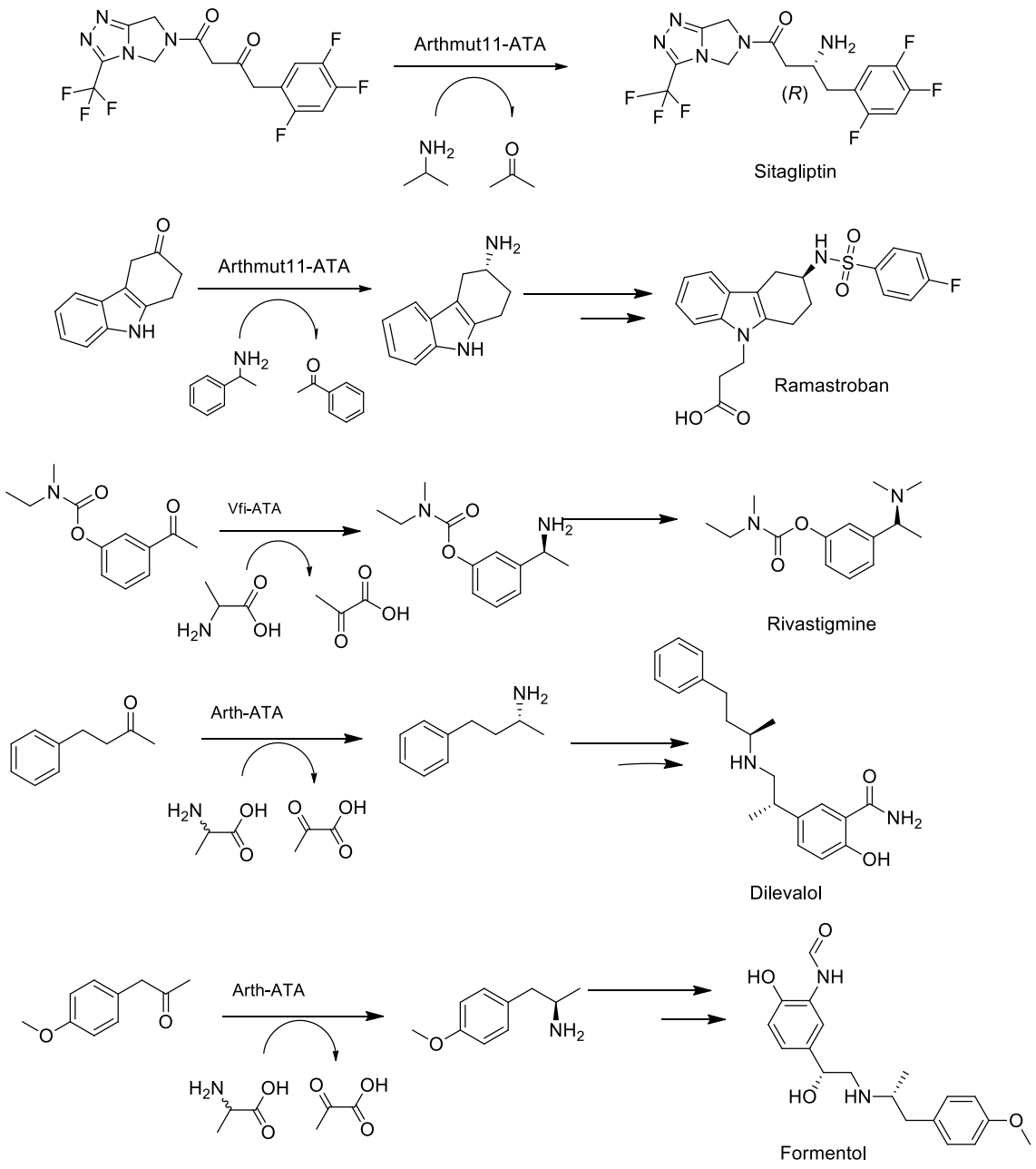

Figure 5: Biocatalytic application of ATAs for the synthesis of pharmaceutically active compounds.

General developments and challenges of asymmetric ATAs reaction

1.1.6 **Expansion of substrate scope and a choice of amino donor**

Over the years, significant improvements have been made to overcome the previously mentioned limitations (section 1.3.2) of ATAs in asymmetric synthesis. Through different enzyme engineering and evolution techniques, the enzyme variants that allow bulky substrates have been identified (i.e. *Arthrobacter sp* for the synthesis of Sitagliptin), which resulted in the

expansion of the substrate scope. Transamination can now be carried out in a wide range of substrates varying in size and constituents.

Another major constraint was the unfavourable equilibrium due to the reversible nature of the reaction. To achieve a good conversion, the carbonyl co-product should be removed to prevent the reverse reaction. Shin and Kim investigated the transamination reaction and indicated that the choice of the amine donor and amine acceptor together with the possible product and coproduct is crucial in an ATA-catalysed reaction.[35] In most circumstances, the equilibrium was far on the reactant side therefore there was a major need for equilibrium displacement.[14] A natural amino acid, alanine has proven to be the most commonly used amine donor in ATA-catalysed reactions, however using it results in an unfavourable equilibrium (only a small amount of the desired amine products is formed, often less than 5%).[14] Increasing the quantity of the alanine amine donor also did not lead to any improvement in the yield for most substrates; however, the was an exception when aminating the 4-methoxyphenyl acetone into a desired amine, 94% conversion was isolated with 16–fold alanine amino donor.[11] The equilibrium can be displaced when using alanine by removing the pyruvate co-product. Lactate dehydrogenase is usually coupled in the reaction in order to convert the pyruvate by-product into lactic acid in the presence of NADH (nicotinamide adenine dinucleotide).[11] This reaction requires an additional regeneration enzyme to recycle NADH and in most cases, glucose dehydrogenase and glucose are usually used.[6]

The are many other reactions that can be performed in tandem with the ATAs reaction to remove the pyruvate, however, it is clear that they are many biological compounds associated with this reaction thus using alanine as an amino donor in the ATAs reaction presents a relatively expensive synthetic route. This has driven a search for other suitable amino donors. Isopropyl amine (IPA) is the most convenient and promising amino donor, it is readily obtainable and cost-effective and the co-product acetone can be easily removed to shift the equilibrium.[30,38] From an economic point of view, IPA is the most preferred amino donor in industries for ATA-mediated reactions (i.e. biosynthesis of sitagliptin).[7,29] Although IPA performs better than alanine, an excessive amount is still required to drive the forward reaction to completion.

1.4.2 Continuous flow biotransformation

Substrate insolubility and enzyme instability are one of the challenges that were causing a major restriction on the application of ATAs in asymmetric reductive amination reactions. This problem can be improved by incorporating ATAs catalysed reactions into optimized flow

chemistry.[39,40] The application of this technique is not a recent development; however, only limited examples regarding its applications on ATAs have been published. Flow chemistry is rapidly developing in both industry and academia and it was proposed that this technique has the ability to improve half of biocatalytic processes.[39,40] Continuous flow chemistry is mostly used in large-scale production, the system can be run for longer periods to increase productivity.[44] Another advantage of continuous flow biotransformation is that it allows for substrates with low solubility and it is typically more reproducible and economically attractive compared to the comparable batch processes.[39,41]

Enzyme immobilization is often a vital component for successful flow chemistry, although enzymes can be used on their own, attachment of a cell to a protein structure is always advantageous. Furthermore, some enzymes exist in small quantities, and attachment of the enzyme to a reactor reduces the quantities required for processing.[40] Enzyme immobilization has been shown to improve the selectivity, stability of the enzymes and reaction rates. During the process, the enzyme is retained and this behaviour results in the simplification of the purification process.[39] Many different immobilization techniques have been applied to the ATAs flow chemistry reactions. Kroutil et al. applied continuous flow chemistry by first immobilizing an enzyme using methacrylate polymeric resin (*Fig. 6*).[40] The immobilized enzyme was then loaded into a packed bed –reactor and the necessary reactant (transferred through syringes) were passed through the reactor to allow continuous flow asymmetric amination of ketone substrate, this resulted in an excellent conversion (70-94%) and greater than 99% e.e .[40]

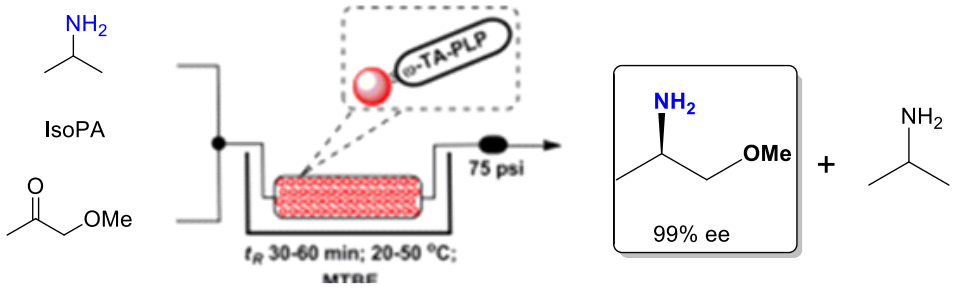

Figure 6: Immobilization of *E. coli* cells and PLP in methacrylate polymeric resin followed by flow chemistry transformation[40]

Major improvements have been made in transaminase biocatalysis, and now the use of enzymes in pharmaceutical industries is expanding. Enzymes are easily accessible, and they are produced from inexpensive renewable resources. The application of biocatalysis in industries

does not only reduce the cost of production but also shifts the synthesis into a greener approach and sustainable industrial processes.

Chiral amino alcohols

Chiral amino alcohols are alcohol and amine–containing class of compounds with diverse applications, abundantly featured in many natural products, pharmaceuticals, and other bioactive molecules. These compounds can be derived from natural molecules, particularly amino acids, and they are widely involved in the synthesis of several bioactive compounds. Chiral amino alcohols also serve as a cost–effective precursors for the synthesis of organic and inorganic chiral ligands and chiral auxiliaries.[41]1,2-Amino alcohol and 1,3-amino alcohol motifs, which are the primary focus of this project, are present in pharmaceutical active compounds.[42] The are several amino-alcohol-containing drugs on the market, this includes ethambutol, raltegravir, embamide, tembamide, dolutegravir, arbutamine, and antibiotics such as lincomycin and levomycetin[37] (*Fig. 7*).

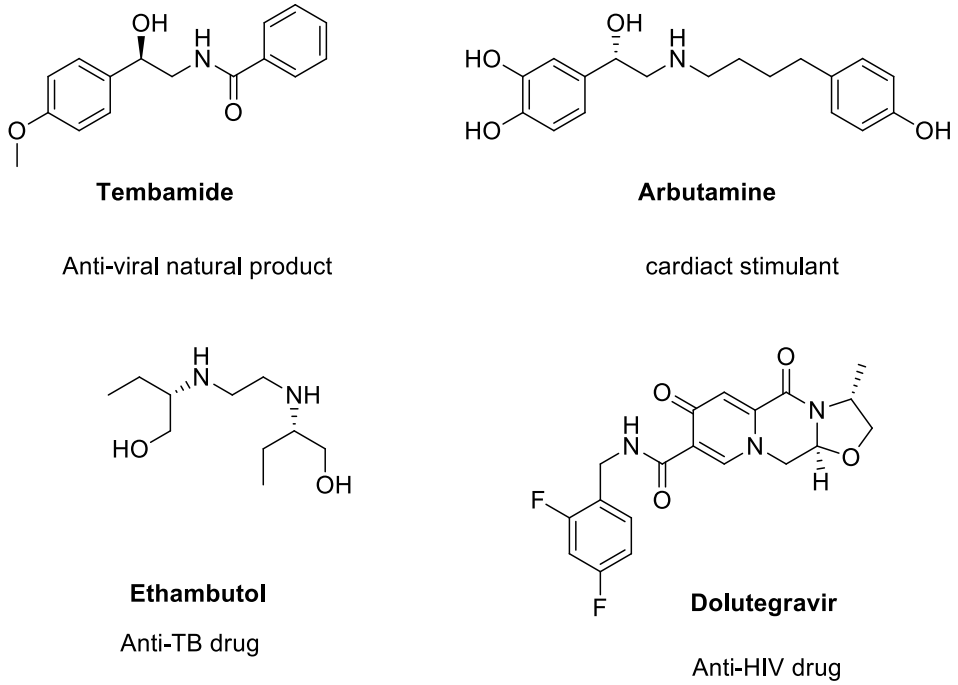

Figure 7: Amino alcohol-containing drugs.

In this study, we focus on two of these active pharmaceutical ingredients (APIs), ethambutol and dolutegravir. The reason why both APIs are included here is that we plan to use one key enabling chemistry that will be applicable to both APIs. The key step in the preparation of both enantiopure amino-alcohols (2-(*S*)-aminobutan-1-ol for ethambutol and 3-(*R*)-aminobutan-1-

ol for dolutegravir) is the conversion of cheap achiral starting material into enantiopure amino-alcohols using transaminase enzymes.

1.1.7 **Ethambutol**

Ethambutol is listed as an essential World Health Organization (WHO) drug for use in combination drug therapy against tuberculosis (TB), which is considered the most infectious disease worldwide, resulting in the most human fatalities annually.[43] Although ethambutol was discovered more than 50 years ago[44], many decades of synthesizing and screening libraries of similar compounds have not led to the discovery of new compounds with improved potency and pharmacokinetic properties.[45] Therefore, ethambutol remains a mainstay of TB treatment to this day and is on South Africa's essential medicines list. Ethambutol plays a crucial role in lowering the incidence of the development of mycobacterial resistance against the other treatments (isoniazid, rifampin and pyrazinamide) which are used in combination with ethambutol in standard TB treatment.[46]

(*S*)-2-Amino butanoic acid **3** is the most important chiral building block for the chemical synthesis of ethambutol **1**. According to Wilkinson and his colleagues, the (*S*, *S*)-configured diastereomer of ethambutol is the most effective agent against almost all the strains of mycobacterium.[46–48] It has the highest biological activity compared to other derivatives and it is approximately 500 times more potent than the (*R*, *R*)-diastereomer.[47,48]

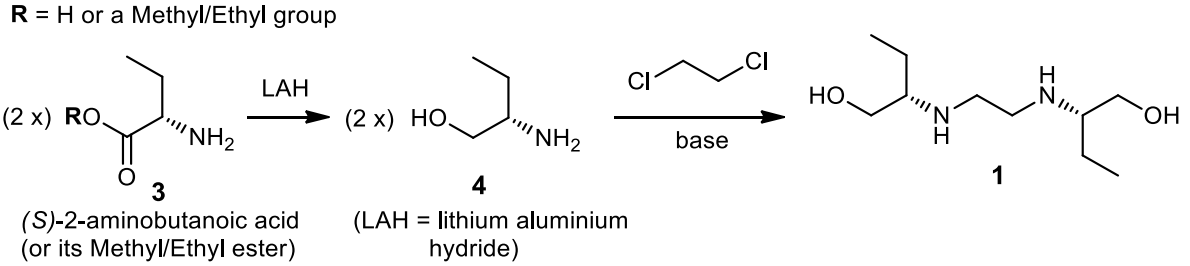

Scheme 12: Facile synthesis of Ethambutol from unnatural amino acid **3**

Since the discovery of ethambutol in the 1960s, (*S*)-2-amino-1-butanol **4** has been used as a main precursor for its industrial-scale production.[29] This amino alcohol can be prepared from amino butanoic acid or its ester **3**. (*S*)-2-Amino butanoic acid can be easily reduced into amino-alcohol **4**, followed by a reaction with 1,2-dichloroethane resulting in desired enantiomer of ethambutol **1** (*Scheme 12*). Since the synthesis initializes with an unnatural amino acid **3,** this represents a relatively expensive starting material. Our aim is to reduce the cost of the starting material by using transaminase biocatalysis for its preparation, thus making the route more economically attractive.

1.1.7.1 How will it improve the manufacturing process?

This asymmetric synthetic route would have several advantages over the existing industrial synthesis of ethambutol. A well-known, industrial synthesis of ethambutol contains a critical chiral resolution step of amino alcohol **4**, by first converting the intermediate racemic (50/50 *R* and *S*) mixture of **4** into the corresponding (+)-tartrate salts. The required 2-(*S*) salt of **4** is selectively precipitated and only this component can be used subsequently. This creates waste, as more than 50% of the racemic compound **4** (the *R* component) is effectively discarded. It also results in a low yield, as only a maximum yield of 50% of the desired (*S*)-**4** can be obtained in this way.

1.1.7.2 Tuberculosis disease and its prevalence.

Tuberculosis (TB) is an infectious disease caused by a bacterium known as *Mycobacterium* tuberculosis.[49] TB primarily targets the respiratory system; however, it can also spread to other parts of the body, including muscles and bones.[50] The disease is transmitted when an infected individual expels the bacteria into the air through actions like sneezing or coughing, and another person inhales these airborne particles. Although this bacterium was discovered more than a century ago, it still remains the major cause of morbidity and mortality worldwide.[51] According to the World Health Organization (WHO), TB claimed the lives of 1.6 million people in 2021, ranking it as the 13th leading cause of death and the second most prevalent infectious disease after COVID-19.[52] South Africa continues to be the epicentre of the TB epidemic (172,200 TB cases were reported in 2021) and this nation still faces challenges in managing the treatment process.[53]

These challenges are exacerbated by human resource shortages and the disruptions from the impact of the COVID-19 pandemic.[53] TB is curable and preventable. The current treatment regimen involves using first-line anti-TB drugs for new TB cases, and second-line anti-TB drugs are employed for cases of multi-drug resistance. Ethambutol, pyrazinamide, isoniazid, and rifampin are combination drug regimens that are used to treat TB bacterial infection in the initial intensive phase of therapy (*Fig.8*).

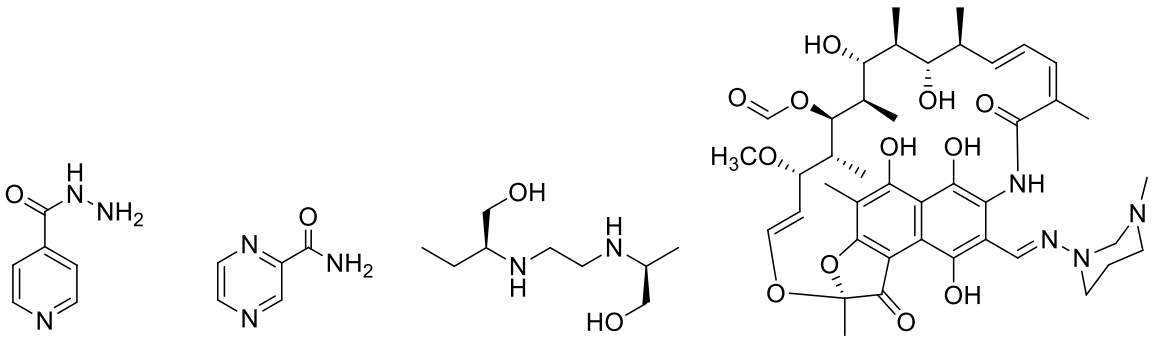

Figure 8: First-line Anti-TB drug combination.

1.5.2 Dolutegravir

Dolutegravir is a potent, new-generation integrase strand transfer inhibitor drug against HIV that was fast-tracked for approval by the FDA in 2013.[54] In June 2020, it was approved for the treatment of children born with HIV, from as young as 4 weeks old.[45] As of the end of 2019, dolutegravir is one of the drugs recommended for first-line antiretroviral treatment (ART) for treatment-naïve individuals in South Africa.[54] It is also recommended that people experiencing side effects with other treatment regimens switch to the new regimen of dolutegravir, tenofovir disoproxil fumarate and lamivudine, known as TLD. This is a fixed-dose combination including one integrase inhibitor (dolutegravir) and two NRTIs. With about 4.8 million people currently on antiretroviral treatment in South Africa,[54] local demand for antiretroviral drugs such as dolutegravir is high, and dolutegravir is considered an essential medicine in South Africa. The new regimen that includes dolutegravir has a number of advantages, including the fact that it has fewer interactions with other medicines, such as those used to treat tuberculosis, which is a common co-morbidity in South Africa.[43]

The most efficient industrial synthesis of dolutegravir is dependent on the economic access to chiral amine building block (*R*)-3-amino-1-butanol (**5**) (see step 8 in red, *Scheme 13)*. This is quite an expensive building block because it cannot be prepared from naturally occurring amino acids. Our aim is to develop an improved and convenient selective route for the synthesis of 3-aminobutanol using economical, cheap, and easily available starting materials.

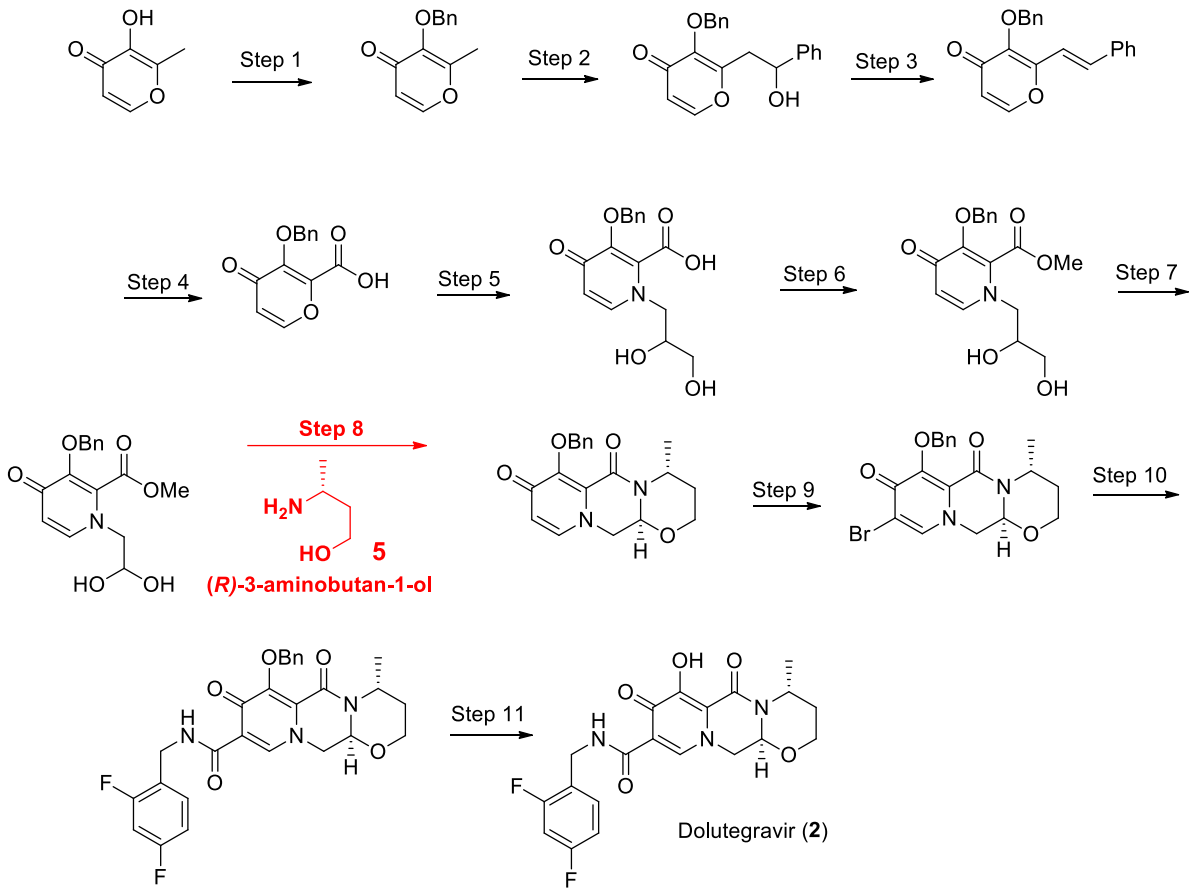

Scheme 13: The most economical industrial synthesis of dolutegravir developed to date.[55]

Based on a materials requirement calculation for the route shown in *Scheme 13*, for every kilogram of dolutegravir produced, 463 g of (*R*)-3-aminobutan-1-ol (**5**) are required.[55]Thus, a cost reduction in this key building block will lead to a cost reduction in the reported synthesis. We plan to demonstrate the cost-effective preparation of **5** from an achiral ketone using transaminase.

1.1.7.3 **1.5.2.1 Human Immunodeficiency Virus and its prevalence.**

Human Immunodeficiency Virus (HIV) is a pathogen that specifically targets and affects the individual's CD4 T lymphocytes, resulting in a compromised immune system. This weakened immune system makes the body susceptible to other infectious diseases, including tuberculosis (TB). If left untreated, HIV infection can progress to an extremely serious condition known as Acquired Immune Deficiency Syndrome (AIDS). HIV has evolved into one of the most critical global public health challenges since it was initially reported in 1981.[56] Since the beginning of this epidemic, over 40.4 million lives were tragically lost.[57] Currently, there are approximately 39 million individuals living with HIV and a significant majority of them, roughly two-thirds

(25.6 million) reside in African countries.[56] Over the past two decades, significant global efforts have been made to combat the HIV epidemic, and this resulted in a substantial progress on the number of infected individuals. For instance, in South Africa, there has been a notable decline in the number of new infections. In 2010, there were 401,608 new infections, whereas in 2021, that number decreased to 198,311, marking a 51% reduction (*Fig.*9).[53]

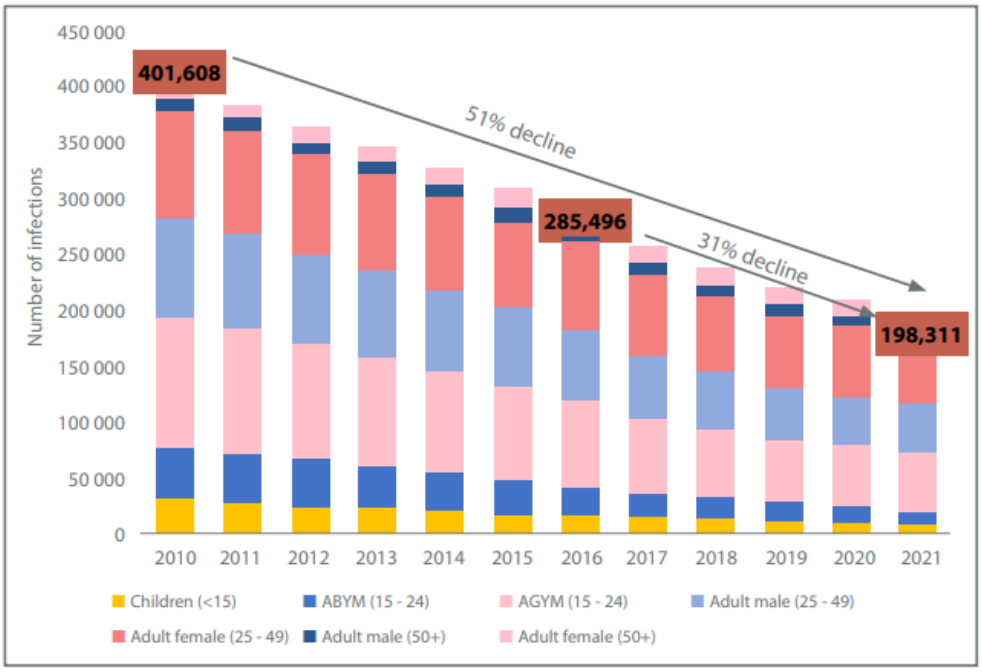

Figure 9:The population of new HIV infections in South Africa categorized by sex and gender from 2010 to 2021.[53.]

The decline in HIV cases can primarily be attributed to improved HIV awareness and prevention efforts, as well as enhanced HIV treatment programs. Since the development of antiretroviral therapy, there has been a notable decline in the mortality rates among HIV-infected patients. Antiretroviral therapy is categorized into six distinct classes based on the drug's molecular mechanism and resistance profiles.[57] The recommended optimal initial regimens for most patients typically include a combination of two nucleoside reverse transcriptase inhibitors (NRTIs) along with an integrase strand transfer inhibitor (InSTIs).[58] InSTIs represent the newest class of antiretroviral drugs and they function by blocking the viral intergrase enzymes which play a major role in the insertion of viral's DNA into DNA of a host's T-lymphocytes.[59] There are currently four FDA-approved InSTI drugs, these include the first-generation raltegravir and elvitegravir, as well as the second-generation dolutegravir and

bictegravir drugs.[60] Dolutegravir is mostly preferred in first-line HIV therapy, and it is used in combination with either abacavir-lamivudine or tenofovir-emtricitabine NRTIs.[60]

Aims and Objectives

1.6.1 Aims

The aim of this project is to use transaminase enzymes to convert cheap achiral ketone starting materials into high value enantiopure amino alcohols required as key building blocks in the synthesis of dolutegravir and ethambutol.

1.6.2 Objectives

- Introduction of new keto ester enzyme substrates with improved enzyme-substrate binding properties to improve enzyme efficiency.
- The screening of the substrates with different ω-Transaminases to discover new active enzymes with greater activity and stereoselectivity.
- Identification of stereoselective enzymes from a given library of enzymes.
- Biocatalytic synthesis of chiral amino alcohols for the industrial synthesis of ethambutol and dolutegravir.

Chapter 2:

2. Synthesis of an Ethambutol intermediate

Ethambutol **1** is manufactured on an industrial scale through the process outlined in Scheme 14.[61,62] During the process, nitropropane undergoes oxymethylation with formaldehyde resulting in 2-nitrobutanol which is subsequently reduced to form racemic amino butanol (*Scheme14).*[61] The desired (*S*)-amino butanol is resolved using tartaric acid followed by the reaction with 1,2-dichloroethane to form (*S,S*)ethambutol **1.** When assessing the overall expenses of the entire reaction scheme, it is evident that steps 1 and 2 account for approximately 75% of the total reaction costs (*Table 8*). Furthermore, only 50% of the desired enantiomer can be theoretically obtained, so this scheme is expensive and generates a substantial amount of waste. Due to unattractive environmental and economic consequences associated with a significant amount of side products in an industrial process, it is evident that there is a pressing need for the development of new efficient and sustainable synthetic routes to (*S*)-2-amino alcohol intermediate.

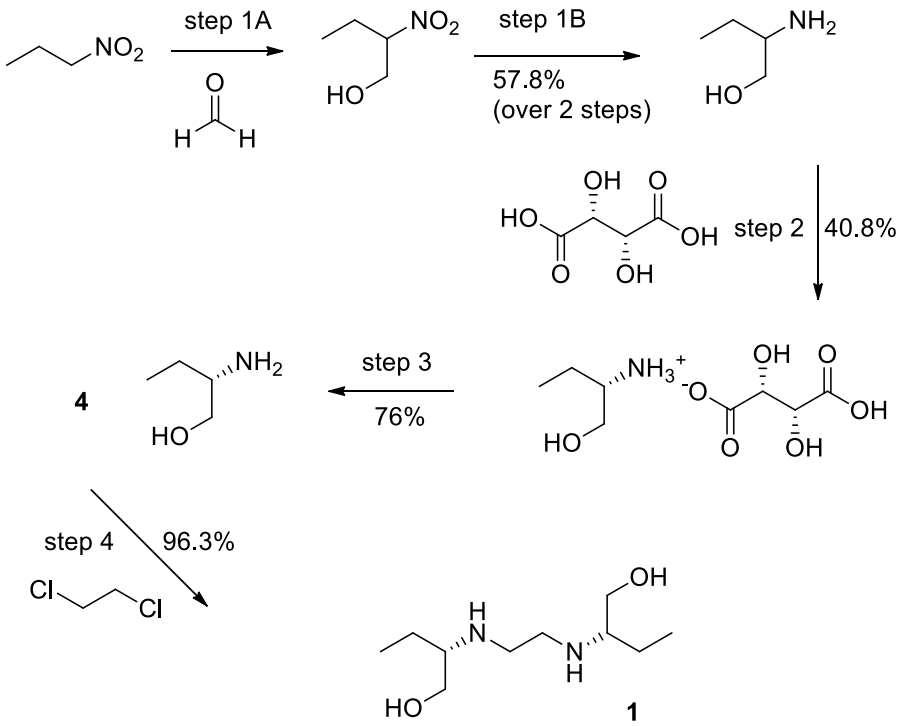

Scheme 14: Industrial synthesis of Ethambutol **1** .[61,62]

In this chapter, we are exploring an alternative greener and enzymatic approach to the synthesis of (*S*)-2-amino butanol **4** intermediate. In this case, we entail to use transaminase enzymes to directly convert an affordable prochiral ketone **7** into (*S*)-amino ester **8**, which can be subsequently reduced to the desired (*S*)-2-amino butanol **4**(*Scheme 15*). This schematic route has the potential of decreasing the costs of synthesis of the intermediate which can decrease the overall cost of the production of the drug. As mentioned previously, South Africa still experience challenges with the TB-treatment, with one of the prominent obstacles being the high cost of medications. Reducing the cost of this drug could enhance affordability and potentially stimulate price-based competition within the local pharmaceutical industries.

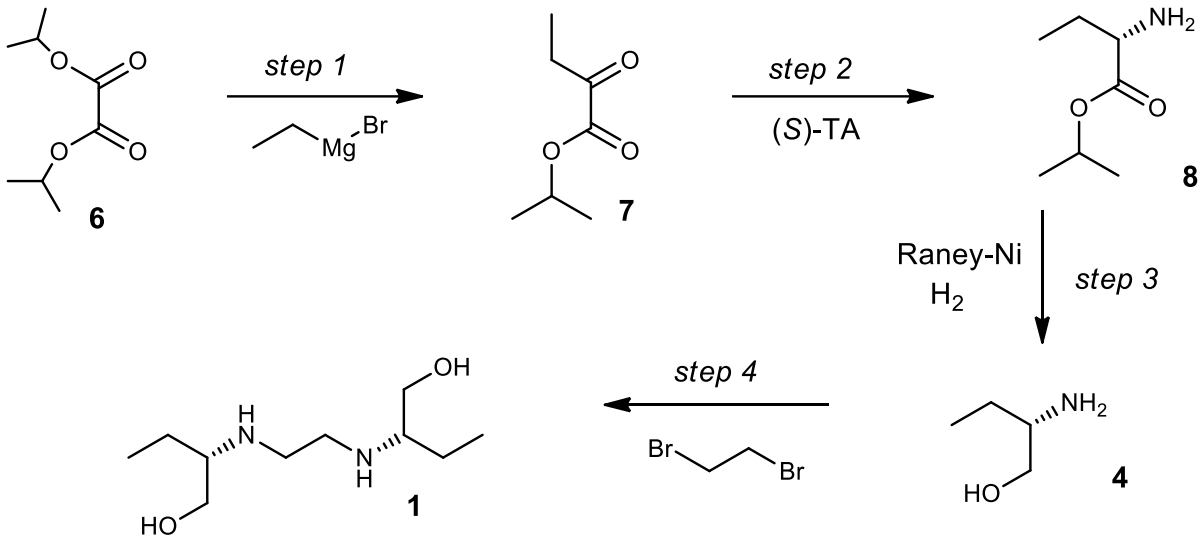

Scheme 15: Our proposed synthesis route to produce Ethambutol **1**

Substrate selection

Transaminases allow the biotransformation of carbonyl groups (ketones, aldehydes, and keto acids) into the corresponding amine. There are various aspects that have to be taken into consideration before choosing an ATAs substrate. This includes the solubility of reactants in water, the extraction of the amine product from the aqueous media and the binding interaction between the enzyme and the substrate.

ATAs catalysis often requires organic co-solvents to enhance the solubility of reactants in aqueous media; however, the utilization of high concentrations of water-miscible organic solvents decreases the stability of ATAs enzymes. To prevent this the substrate should be soluble enough in an aqueous solvent in order to allow catalysis to take place.

Extraction of organic compounds is usually achieved by using the liquid-liquid extraction method, which is the distribution of the product between the aqueous and organic layers. In this case, the extraction efficiency is strongly dependent on the chemical structure and dissociation state of the amine or amino alcohol. Distribution of amines in an organic layer can only be achieved by changing the dissociation state of the amine through the adjustment of the pH using a specific base. Amino-alcohol has two polar groups, the amino group, and the alcohol group, that can undergo hydrogen bonding with the water molecule thus forming strong hydrogen bond interactions. The H-bonding properties of these types of compounds make the extraction difficult; this becomes a problem because it can result in a dramatic loss of product through poor recovery. To combat this issue, the substrate should be less polar enough in order to achieve a less polar product that can be easily extractable compared to amino alcohol.

Previous structural studies have revealed that there are two pockets (P and O) in the active side of the ω-TAms (*Fig.10)*. The P-pocket is located near the phosphate group of PLP, whereas the O-pocket is positioned in the proximity of the O3′ atom on PLP.[63] The two pockets differ from each other in size, depending on the class of ω-TAms. The docking study that was done by Zhang and his colleagues on keto butyric acid indicates that the small pocket displays steric constraints, prohibiting the substituent with a larger group from binding while the larger pocket can accommodate the bulkier substituents (*Fig. 10*).[64] The choice of the ATAs substrate is highly dependent on the enzyme's active site, the substrate should have small constituents (ethyl and methyl groups are recommended) on one end to fit in the small pocket of the active site, and it should also have a larger constituent at the other end to fit in the larger pocket of the active side.

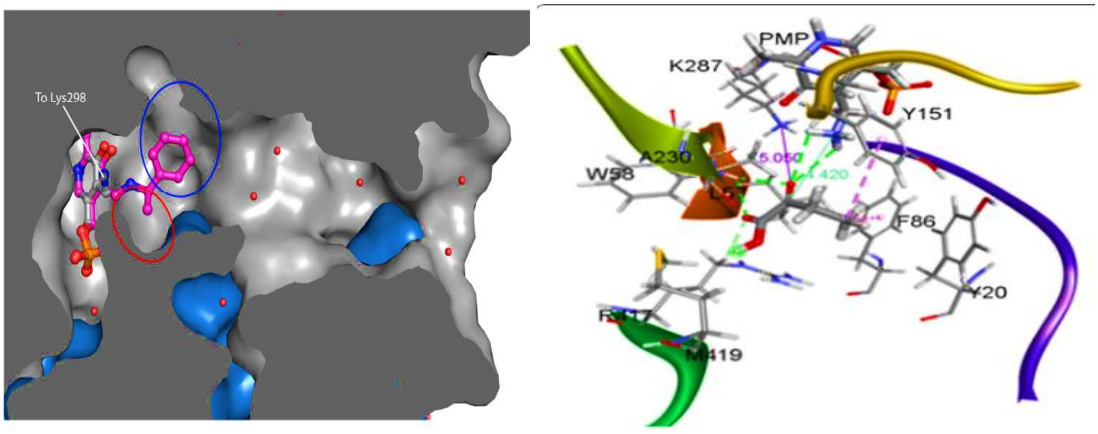

Figure 10: Docking of keto butyric acid in the ATA active site.[64]

In this study, the desired (*S*)-amino butanol **4** can be accessed by the transaminase biotransformation on pro-chiral hydroxyl ketone **9** or alpha-ketoseter (*Scheme 16*)**.** The hydroxyl ketone (**9**) is a commercially available compound that provides the most facile single-step route for the synthesis of enantiopure amino alcohol **4**. Hydroxyl ketones are quite soluble in water; therefore, no additional solvents like DMSO are required. Although this substrate allows a direct conversion into the desired product, amino alcohols are often difficult to extract from the aqueous layer. Furthermore, hydroxyl ketone **9** is relatively expensive (a gram of it costs R2472 from Sigma Aldrich), therefore using it is inconvenient in this project as the main objective is to decrease the cost of the production of ethambutol **1**. The starting material, alpha keto esters are often cheap renewable compounds that can undergo biotransformation into amino esters **3** which are easily extractable in the aqueous media (*Scheme 16*). In this study, we introduce a cheap novel ATAs substrates (ethyl keto ester and isopropyl ketoesters) with the aim of decreasing the costs of synthesis of the high-valued (*S*)-amino alcohol **4** intermediate.

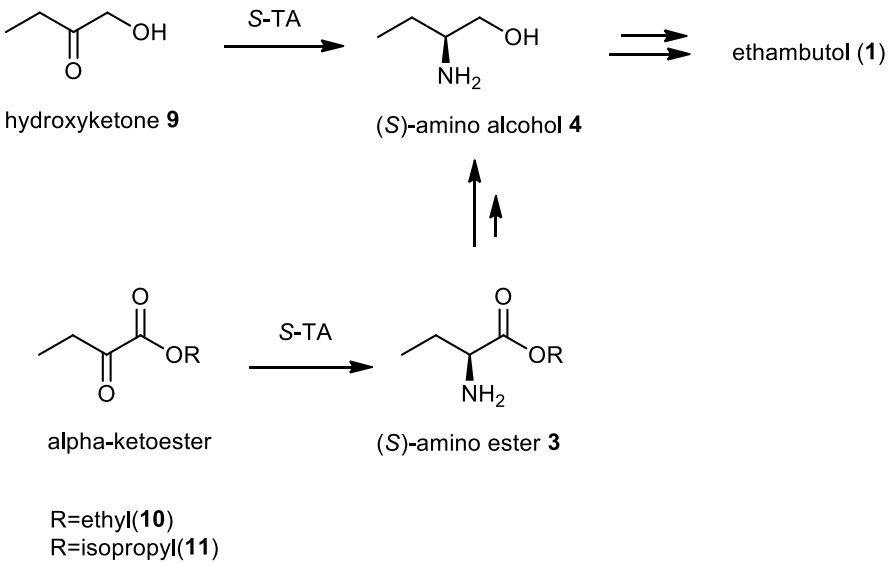

Scheme 16: Different routes for biotransformation of pro-chiral ketones into amines using ATAs.

Substrate synthesis

Initially, there were two different substrates of interest in this part of the project, ethyl keto ester **10** and isopropyl keto ester **11 (***Scheme 16***)**. Our substrates were not commercially available; hence they were chemically synthesized in the lab. The Grignard reaction, which is

most commonly used in pharmaceuticals for the introduction of new-carbon-carbon bonding, was utilized. The starting material for ethyl keto ester substrate **10**, diethyl oxalate, is a cheap, and commercially available compound. The diethyl oxalate was reacted with the Grignard reagent that was successfully synthesized using magnesium turnings and bromoethane (*Scheme 17*). The reaction was controlled at a low temperature (0°C) under nitrogen gas for 2 hours (*Scheme 17*). No over-substitution of an ester (to form 3, 4-hexadione) was observed, and only residual starting material (which can be recycled) and the desired product were isolated. The purification was achieved using silica-column chromatography and by using ethyl acetate-hexane mobile phase, only 15 % of the product was isolated. Substrate **10** is very volatile, so most of the product was lost during the solvent removal step. To avoid this issue, purification by distillation was attempted, however, it was unsuccessful as the product carried over together with the starting material. The purification solvent was then changed to 1% ether – hexane and only slight changes were observed as the yield increased from 15 to 25%. The product was characterised using a proton and a carbon NMR .^{1}H NMR spectrum shows a peak integrating 2H at chemical shift of 2.80 ppm indicating a newly formed ethyl group adjacent to the carbonyl group whilst the deshielded ester CH_2 group was observed at 4.22 ppm. The ^{13}C NMR spectrum confirmed that the is no longer a symmetry in the compound as 6 carbon peaks were observed.

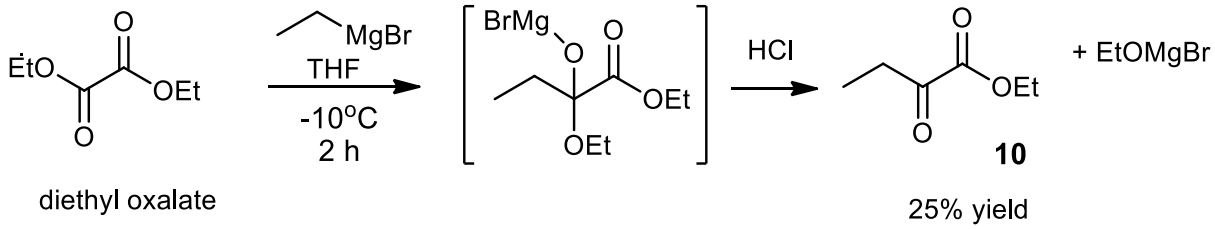

Scheme17: Grignard reaction to prepare ATA substrate **10**.

In contrast to the synthesis of substrate **10**, diisopropyl oxalate **12**, is not commercially available. However, it can be readily prepared by performing a simple nucleophilic substitution reaction between oxalyl chloride and isopropanol in the presence of a base (*Scheme 18*). This method resulted in 67% yield of product **12**, a ^{1}H NMR spectrum shows a doublet peak at 1.37 ppm integrating for 12 protons (all the methyl groups are in the same chemical environment), and a heptet peak at 5.16 ppm with a coupling constant of 6.5 Hz for protons adjacent to methyl groups. Although the reaction was successful, most of the product was lost during the solvent

and pyridine removal. To solve this problem, Pyridine was replaced with DIPEA, and a more volatile solvent was used (DCM). With the new conditions, the reaction time was reduced to 5 hours and the yield was improved to 80%.

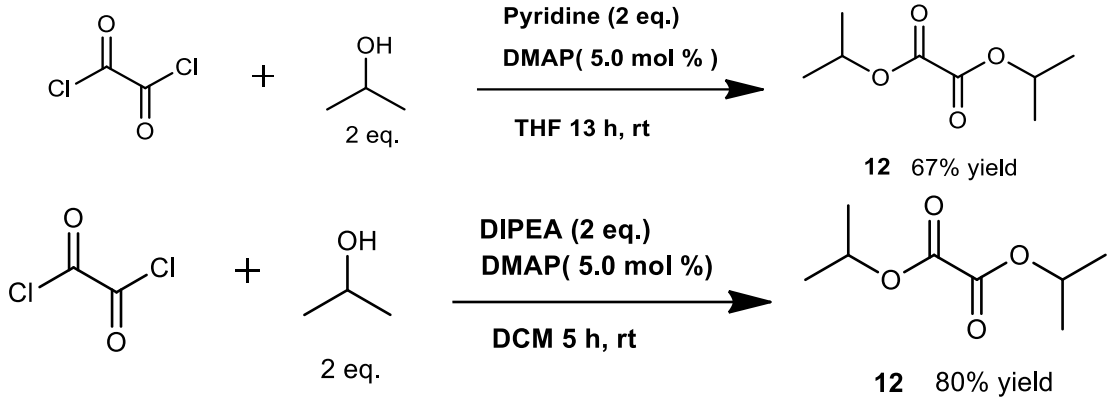

Scheme 18: The synthesis of diisopropyl oxalate **12**

Diisopropyl oxalate **12** undergone a Grignard reaction following the same procedure as in substrate **10** (*Scheme 19*). The same extraction procedure was used and the purification was modified by adding 1 % of toluene in the mobile phase (1-3% ether hexane). The product was isolated in the yield of 50% yield. The ^{1}H NMR spectrum shows a quartet peak at 2.8 ppm with the coupling constant of 7.2 Hz representing the newly formed CH_2 adjacent to the methyl and the carbonyl group. The ^{13}C NMR spectrum also confirmed that the is no longer a symmetry in the compound as 6 carbon peaks were observed.

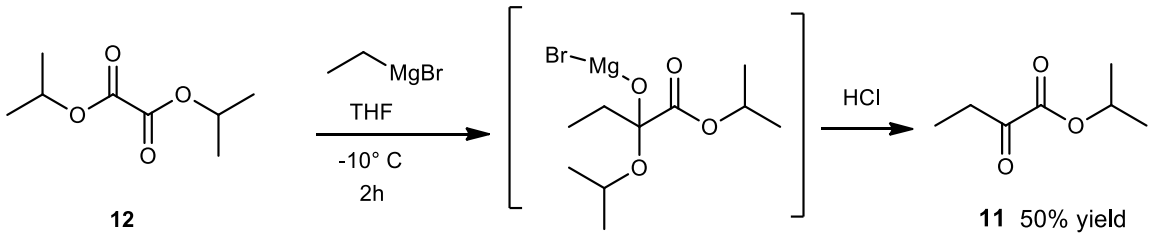

Scheme 19: Grignard reaction to prepare ATA substrate **11.**

Grignard reaction resulted in an incomplete conversion of the starting material to the product and there were various challenges encountered during the purification procedure, this led to the exploration of different techniques to synthesis the substrates. The simple Fischer esterification reaction was investigated using a keto butyric acid starting material, this starting material is commercially available and in the presence of an alcohol and acid catalyst, it results in the formation of an ester (*Scheme 20).* In this reaction, no purification procedure was required, and the yield of the ethyl substrate **10** ranged from 79-82% whilst the isopropyl substrate **11** ranged from 80-95%.

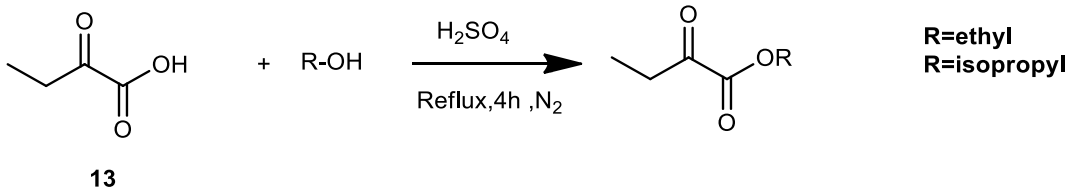

Scheme 20: Fisher esterification for the synthesis of ATA substrates.

Enzyme screening

2.1.1 **Enzyme Screening Method Development**

In 2014, the Turner group at the Manchester Institute of Biotechnology published a very useful ATA screening method that can be applied to test for ATA enzyme activity on a specific ketone substrate, within any library of given ATA enzyme variants.[65] The method entails using a smart donor amine that, upon substrate conversion to the desired amine product, will result in an easily detectable colour change, from colourless/yellowish to dark purple-black. Our group at Wits has acquired an extensive library of more than 30 ATA enzymes from UK enzyme producers Prozomix in Northumberland. Previous research in our lab applied the Turner method to screen for ATA enzyme activity on substrate **10**, and it was found that almost all of the enzymes in our library were active in producing the desired amine product to varying degrees. The presence of the product was also confirmed by semi-quantitative HPLC-high-resolution mass spectrometry. These results motivated us to investigate this reaction further using the same substrate **10** and an additional substrate **11**, which is a novel ATA substrate. Although the use of smart donors has proved to displace challenging reaction equilibria, applying this procedure in large-scale reactions can be a problem as it may lead to the introduction of many side reactions (diamine smart donors often result in amine side product, and amines are very reactive thus susceptible to side reactions).[65] In this project, the isopropyl amino donor was utilized because it has proven to be convenient in large-scale transamination (isopropylamine is used as an amine donor in the production of sitagliptin).[7,29]

Enzyme activity is broadly dependent on the defined conditions such as temperature, pH and the nature and strength of the ions, therefore the enzyme activity can only be accurately compared if such conditions are standardised. For our screening method development, we began by using pH 7.5 and a temperature of 30°C, these are typical optimal conditions that are used for enzymatic reactions. Monophosphate buffer (100 mM) was used to stabilize the pH; the more concentrated a buffer is, the higher the capacity to stabilize the pH. However, ATAs accept moderate ionic strength between 0.005 M to 0.1 M (only halophilic and thermophilic

enzymes prefer high concentrations). In this method, there is no observable colour change expected as in when using a diamine donor in the Turner method and the desired amine products are also UV inactive, so monitoring the reaction as time progresses is quite challenging.[65] In our initial screening procedure, the reactions were left stirring (250 rpm) for a maximum of 24 hours to ensure completion, this is the duration that is normally used in the literature. Scheme 21 shows the route and the initial conditions that were used for our screening process.

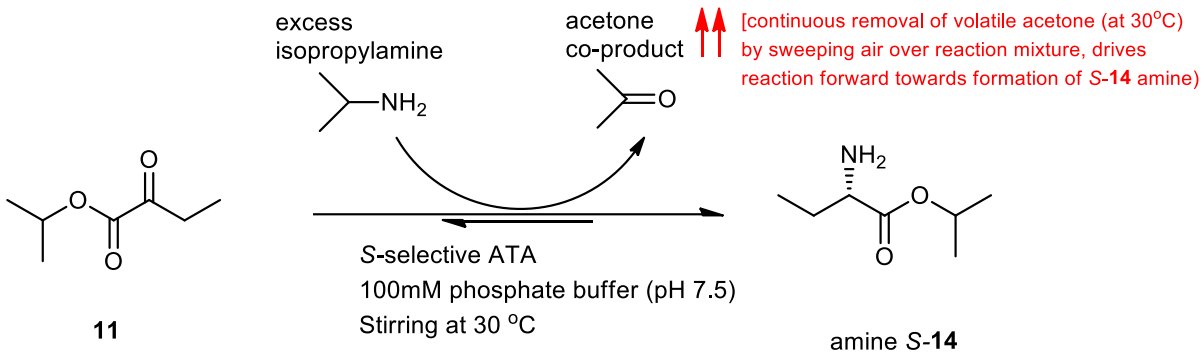

Scheme 21: Proposed ATA biotransformation towards the synthesis of (*S*)-amino butanol

2.1.2 **Method development for product isolation and quantification**

Developing a method for quantitative and qualitative analysis of the enzyme amine products requires standard compounds, However, both, ethyl 2-aminobutanoate and isopropyl 2-aminobutanoate (whether enantio-enriched or racemates) are not commercially available. These standards were therefore prepared using a non-biocatalytic synthetic approach. Scheme 22 shows all attempted reductive amination reactions for the synthesis of *rac-**14**,* unfortunately all the reactions didn't work and only traces of the product *rac-**14*** was observed in proton NMR and mass spectrum.

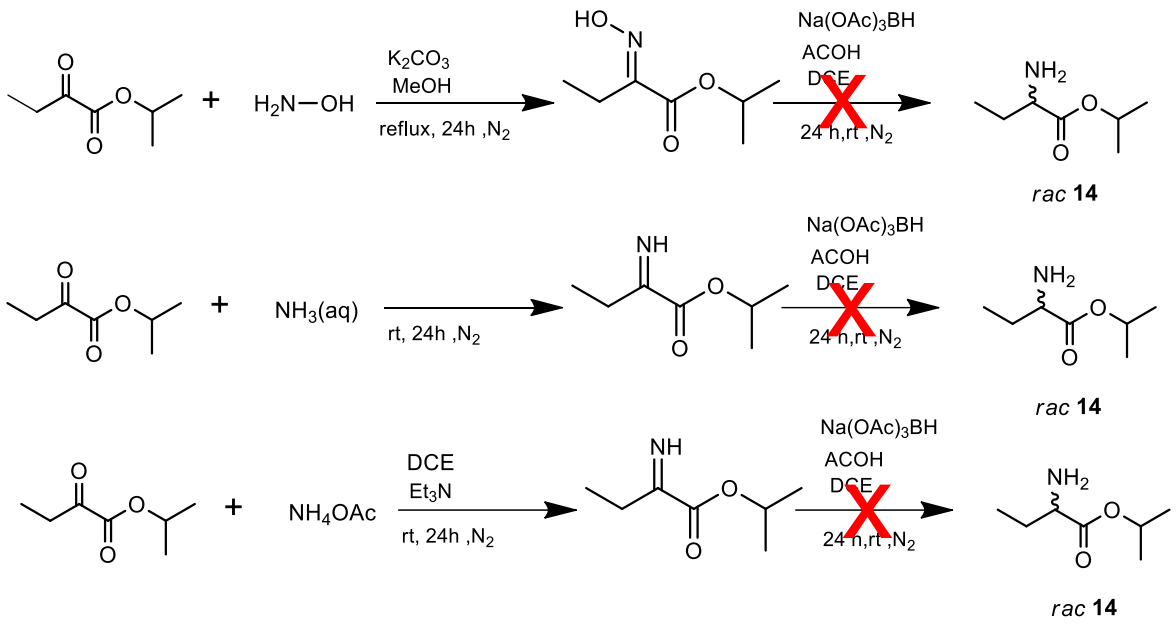

Scheme 22: Reductive amination reaction to synthesis the racemic amino ester **14** standard

These unsuccessful reactions emphasise how difficult the reductive amination is and how the emergence of the ATA biocatalysis reaction can overcome this. This synthesis was only essential for method development and validation, therefore we compromised and decided to use some expensive commercially available (*S*) and (*rac*)-aminobutyric acid **15** to synthesis our standards. Simple acyl halide reaction was carried out in the presence of isopropanol to afford yellow oil product with an excellent yield of 78-86% for *rac-**14*** and *(S)-**14** (Scheme23).* The products were characterised using ^{1}H and ^{13}C NMR. As expected, the same NMR pattern was observed in both racemate and (*S*)-enantiomer .^{1}H NMR spectrum shows a newly formed doublet of doublet peak with a coupling constant of 6.1 and 3.4 Hz integrating for six protons, these indicate the presence of two methyl groups that are in the same chemical environment. The proton adjacent to the methyl group was also observed as a multiplet at 5.11-5.00 ppm. These results indicate that the reaction was a success, and it was further confirmed by the presence of an additional methyl carbon at 20.9 ppm in ^{13}C NMR spectrum.

The ethyl 2-aminobutanoate rac-***16*** and *(S)-**16*** standard were also successfully synthesised to afford a yellow oil product with the yield of 68-85 % and the product was also characterised using ^{1}H and ^{13}C NMR (*Scheme 23*). The ^{1}H NMR spectrum shows a new quartet peak (J=6.5Hz) at 4.18 ppm indicating the presence of CH_2 adjacent to the methyl group, the newly formed methyl group was also observed as a triplet (J=7.5 Hz) at 1.28 ppm. This serves as a confirmation of successful esterification formation.

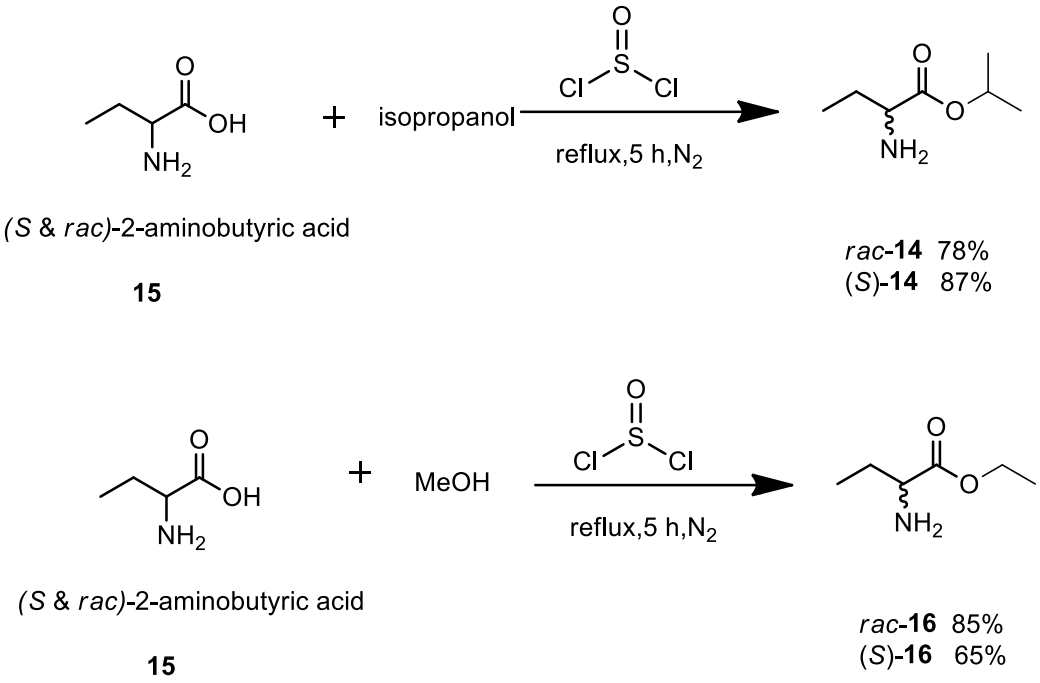

Scheme 23: The synthesis of amino-ester standards using nucleophilic reaction.

Our desired amine products are very small compounds and not UV active, the most convenient characterization technique that can be utilized in this project is gas chromatography-mass spectrometry (GC-MS) and liquid chromatography-mass spectrometry (LC-MS). Using the standard amine **14**, we were able to develop a LC-MS reverse phase gradient method (5-95% H_2O /ACN), retention time: 15 minutes, flow rate: 0.300 ml/min). The standard curve (*Fig.11)* was then developed using different concentrations of the standard amine (S)-**14**. Additionally, the excellent R^2 value indicates that there is a perfect correlation between the variables thus the concentration of the enzyme product can be quantified accurately.

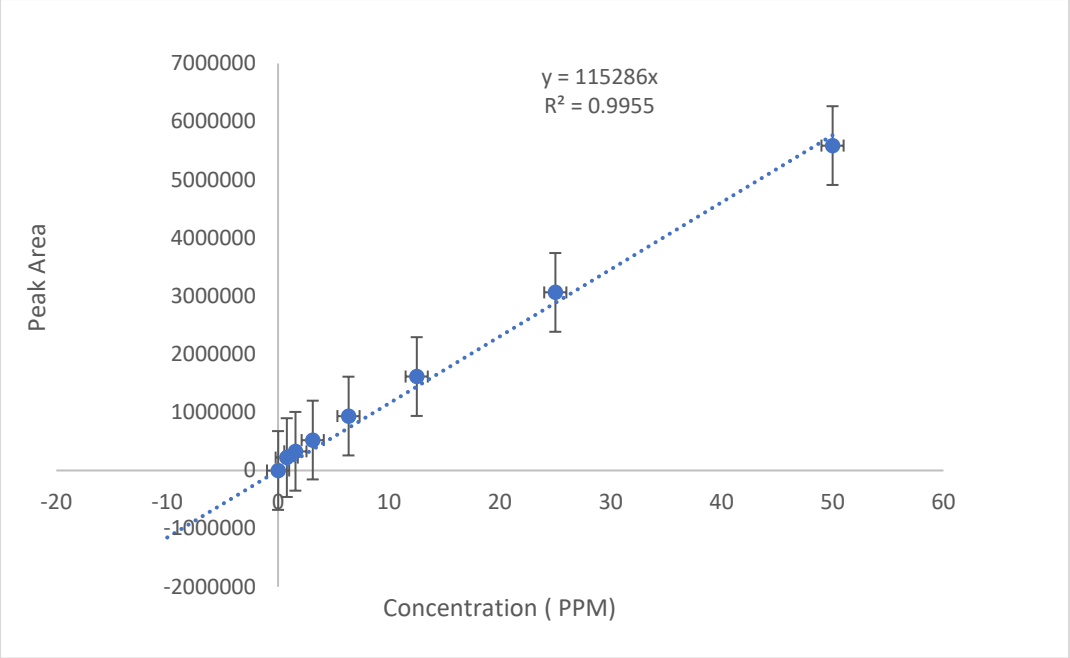

Figure 11: The standard curve of concentration of amino ester **versus** peak area by LCMS (number of variables, (n)= 8).

2.1.3 **Enzyme screening results**

The ATA enzymes were screened using assays in order to discover their substrate specificity profile and their ability to form interesting stereo-selective amines. Qualitative and quantitative analysis of enzyme amine products are often difficult to achieve when working in a small scale. As a result, most ATA reactions are monitored via the detection of the ketone starting material. However, in this study, our keto substrates are quite unstable during analysis by LCMS, thus making them difficult to monitor, therefore the enzyme reaction progress was monitored using the amine products.

Initially, 28 enzymes were selectively screened against substrate **10** and substrate **11** using the conditions illustrated in Scheme 21. The products were processed and extracted with HPLC-grade acetonitrile and directly injected into the LCMS vials for characterization. *Fig. 12* shows a comparison between the amino-ester standard **14** and the enzyme product **14** LCMS results. Two peaks eluting at a retention time of 3.5 min ($[M+H]^+$ =146.1164 and $[M+H]^+$ =104.0708) and 8.9 min($[M+H]^+$ =146.1164 and $[M+H]^+$ =104.0708),slightly shifted in the standard compound were observed .The product existing in two different forms, the ionic and the neutral form, thus separating when using the HILIC column. Fragment $[M+H]^+$=146.1164 represent the full mass of our desired product and $[M+H]^+$=104.0708 corresponds to our product without the isopropyl ester group. From these results, we can

deduce that ATA-230 successfully catalysed the synthesis of amino ester **14** from a pro-chiral ketone **11**.

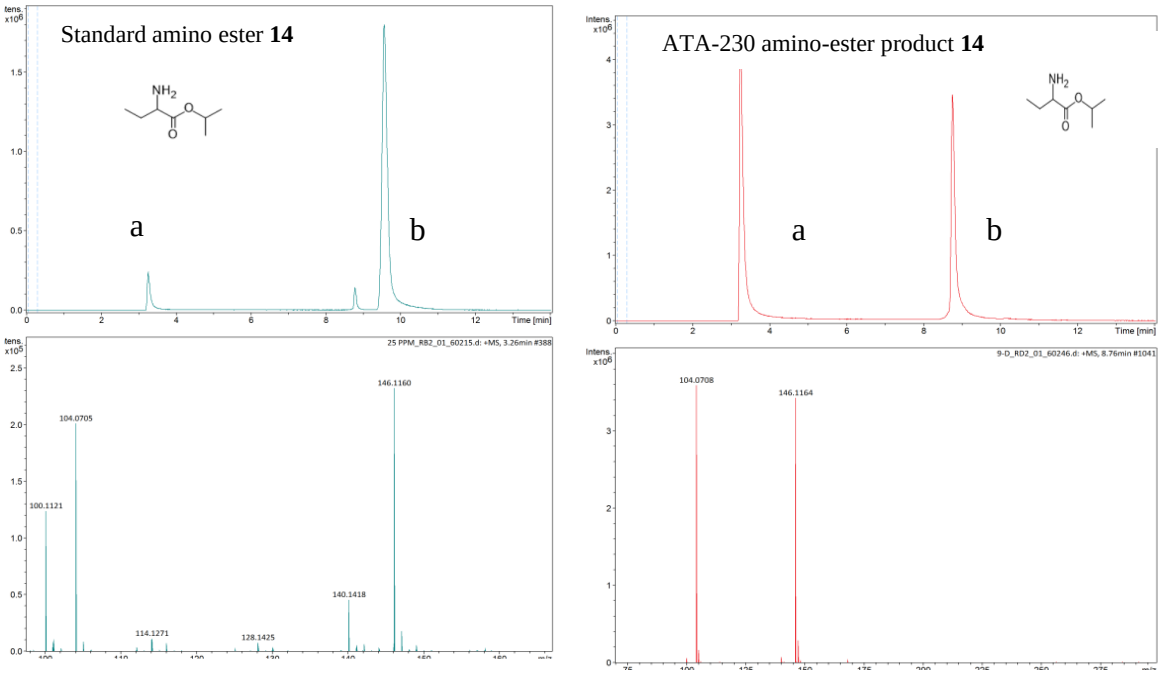

Figure 12: Comparison between LCMS results of ATA-230 and the standard amino ester products.

From the LCMS data obtained, the peak of the neutral amine product **11** (8.9 min) was selected, it was then integrated, and the peak area of each enzyme product was compared. The graph in Figure 13 illustrates the comparison of the peak area of the amine product catalysed by different enzymes on substrate **10.** Sixteen enzymes were active against our substrate and ATA-231, ATA-250 and ATA-247 showed the greatest activity while the activity of others, for example ATA-241 and ATA-239, were insignificant.

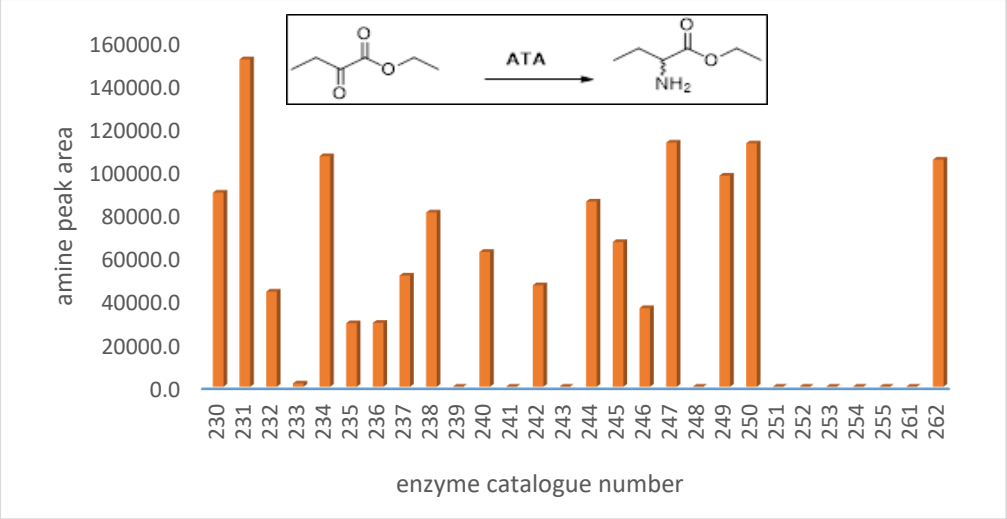

Figure 13: A graph illustrating the comparison between the activities of the enzymes on substrate **10**.

Moving to substrate **11**, only few enzymes from the selected assay were active in comparison to substrate **10**, however, the activity was more than 100-fold greater than substrate **10** (*Fig. 14*). An in-depth investigation of the comparison of these two substrates is beyond the scope of this project; however, from the results presented in the graphs, it is clear that substrate **11** gives better activity than substrate **10**. Due to this reason, we decided to eliminate substrate **10** and further investigate substrate **11**.

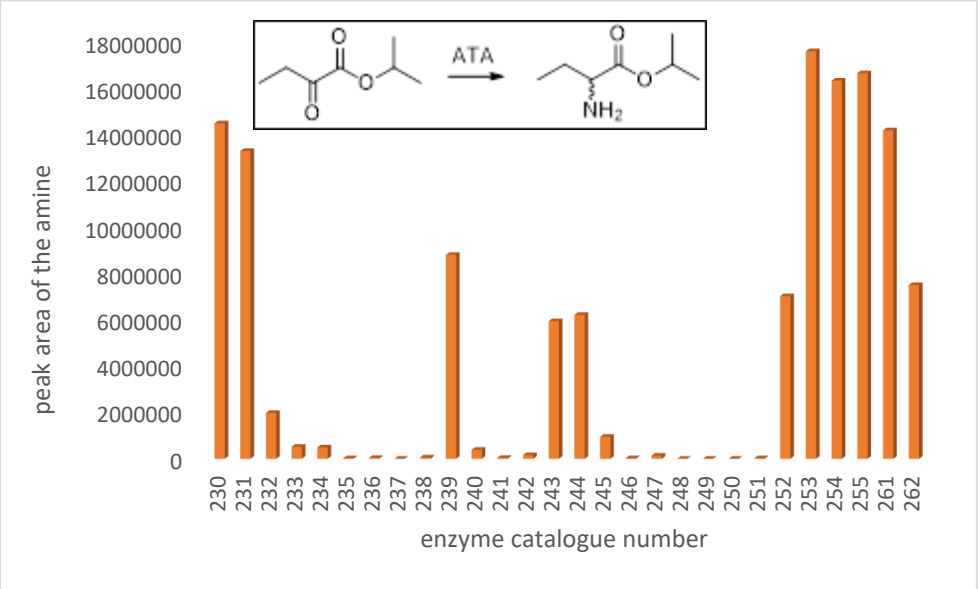

Figure 14: A graph illustrating the comparison between the activities of the enzymes on substrate **11.**

2.1.4 **Development of HPLC method for separation of *R* and *S* enantiomers.**

Determination of the presence of chiral compounds using chiral HPLC is becoming an essential tool in organic chemistry. This analytical technique makes it possible to efficiently obtain target enantiomers in high enantiomeric purities. Therefore, many of the detection methods have already been coupled to chiral HPLC to determine the enantiomeric excess of different enantiomers. In this project, direct chiral resolution of the racemic amino ester **14** was difficult to perform. Only a single peak eluted and the use of different solvents (methanol, water and acetonitrile) and solvent constituents (gradient and isocratic) proved to be unsuccessful. There are many techniques that can be used to improve the separation of the enantiomeric compounds, such as the increase in the number of theoretical plates or increasing the length of the column. In this case, two different columns that vary in column length and particle size were investigated; however, neither of them resulted in better separation.

Derivatization is the most commonly used technique to improve the separation of enantiomers; this method works efficiently especially when using small analytes such as our isopropyl amino ester**.** The derivatization of amino ester was subsequently performed order to establish a method for the chiral HPLC detection of the derivative amide (*Scheme 24)*. Primary amines are strong bases and in the presence of carboxylic acids they undergo a fast acid-base reaction to form a salt. In this case the amidation reaction is favoured if high-temperature conditions (< 100°C) are employed; however, this is inconvenient because our isopropyl amino ester (**14**) will not survive those conditions. To favour the amidation route, coupling reagents are normally used. Our first attempt involved the use of CDI (carbonyl imidazole) coupling reagent, unfortunately the reaction didn't work, only traces of the product was observed (*Scheme 24*). Various solvents and temperatures were investigated, however, none of those optimizations resulted in an improved yield. CDI was then replaced with a more flexible and less expensive coupling reagent, dicyclohexylcarbodimine (DCC). DCC is one of the most widely used coupling reagents and it has been utilized since 1955 for peptide synthesis, it is also widely used along with DMAP in esterification reactions. The use of DCC reagent resulted in a good outcome compared to the CDI, the maximum yield of amide obtained was 60%, and the only problem encountered was the purification procedure as there were a lot of by-products and starting material spots on the TLC plate. The purification procedure was achieved using silica column and 10-25% ethyl acetate-hexane to afford a light-yellow powder product **17**. The product was characterised using NMR and mass spectrometer. The ^{1}H NMR spectrum shows the present of two aromatic peaks at 8.35 – 8.27 ppm and 8.03 – 7.94 ppm .The NH peak

was also observed at 6.90 ppm, this indicate that the coupling was a success and it was further confirmed by the presence of an amide carbon at 164.6 ppm in the ^{13}C NMR spectrum .The mass spectrum also shown the fragment with the mass of $[M+H]^+$= 295.1295 which correspond to the expected mass of our product **17**. Using the same reaction procedure as in Scheme 24, the (*S*)-**17** amide was synthesised from the (*S*)-**14** amine. As expected, the NMR and the mass spec data of the (*S*)-**17** corresponded to its racemate.

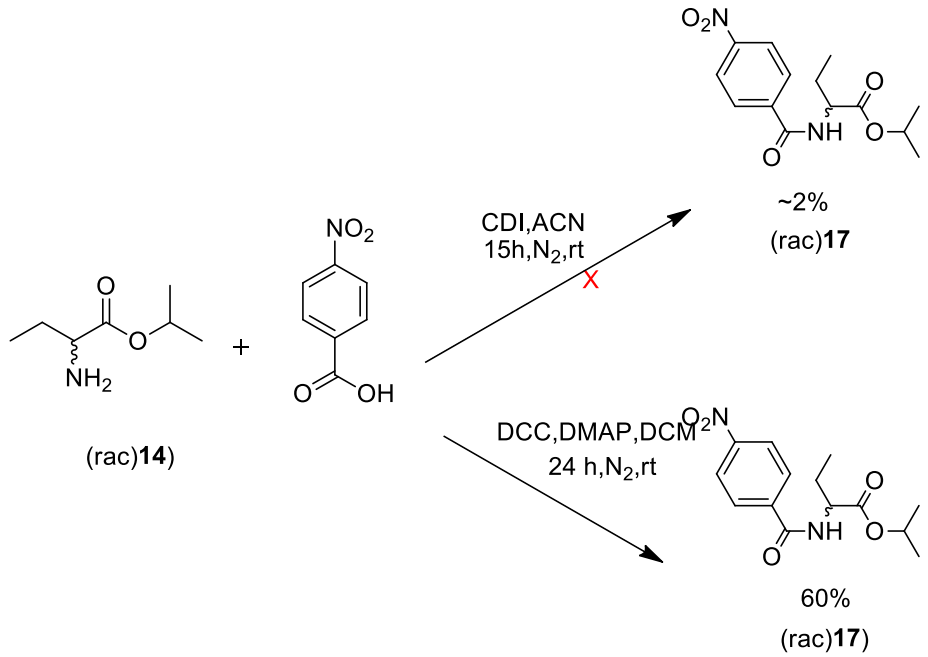

Scheme 24: The derivatization of amino ester 14 into a corresponding amide **17** to improve chiral HPLC separation.

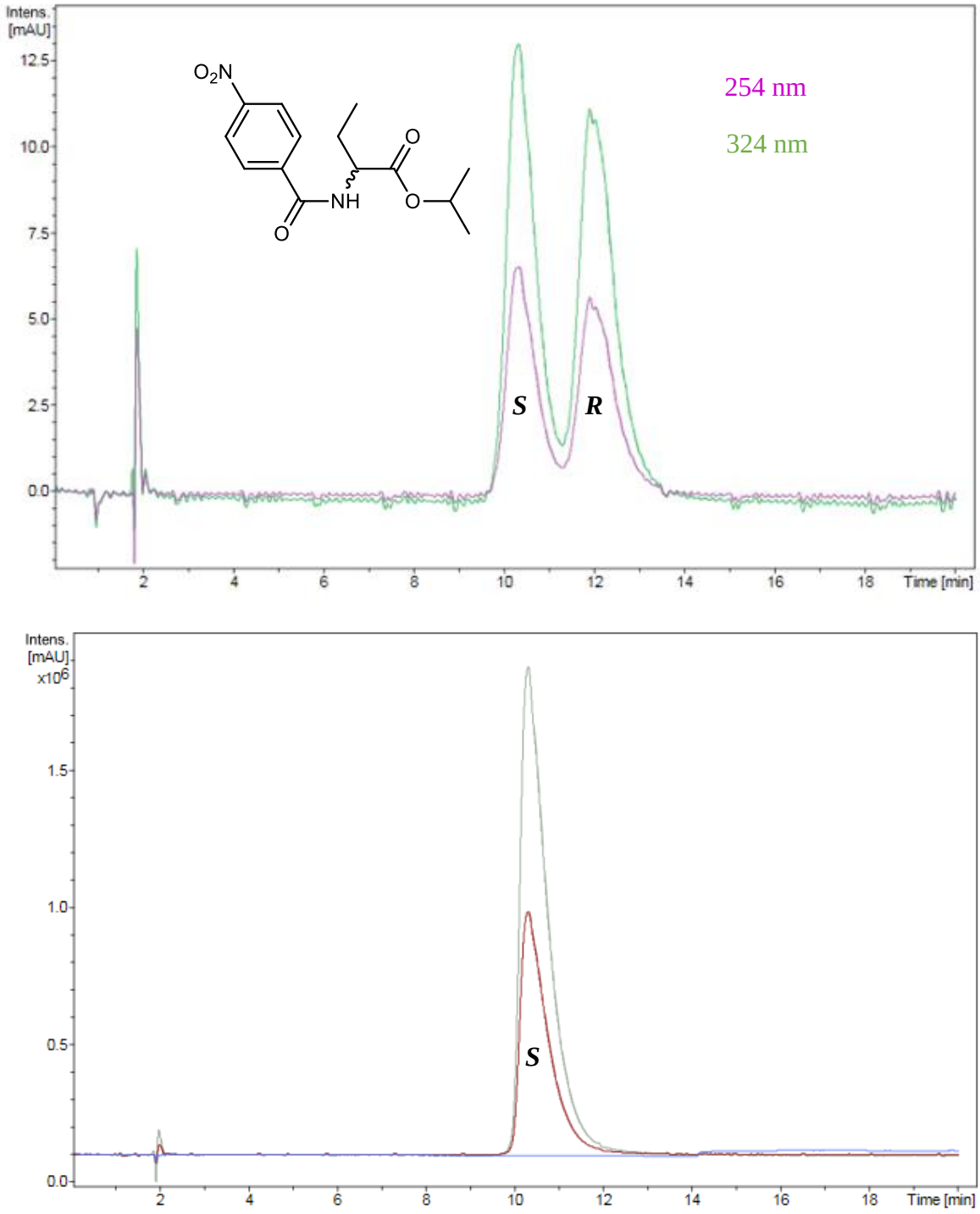

Figure 15: The LCMS chromatography peaks of the derivatized (*rac*)-**17** (above) and (*S*)-standard **17** (below).

The resolution of two enantiomers proved to be successful as a clear baseline was detected between the two enantiomers using a Chiralpak® AD column, a mobile phase of water/ acetonitrile (95:5) isocratic, UV detection at 254 and 324 nm and mass spec detection (*Fig. 16*). The *S*-derivative standard was also run on the instrument, using the same method and

conditions. It eluted at a retention time of 9.8 minutes; these results indicate that the *S*-enantiomer elutes first followed by the *R*-enantiomer. Standards were run immediately before running samples in order to achieve accurate results or elution time.

2.1.5 **Determination of stereochemistry of the enzyme products.**

Transaminase reactions were scaled up to 10 ml scale to provide a sufficient product for accurate analysis; this was followed by the derivatization to form the amide **17** (*Scheme 25)*. Table 2 shows the summarised results obtained when using different enzymes, the % e.e. was derived from the enantiomer peak areas, and the value of the yields represents the % yield of the amino ester products. The yields of the amino ester products were relatively good; this was followed by the derivatization with the yield ranging from 25-45%. The NMR and the mass spec data of the derivatized compounds correspond well with the standard data.

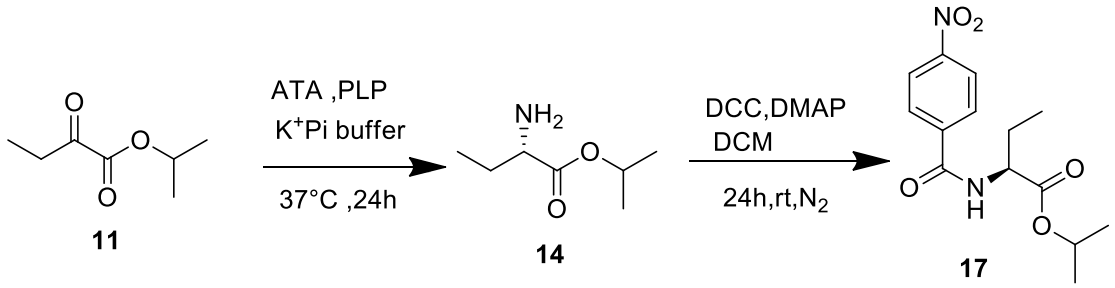

Scheme 25: The enzymatic synthesis of the amino ester **14** followed by the derivatization to form the UV active amide **17.**

ATA-230 gave an excellent conversion of starting material to the product (87% yield) with an excellent % e.e; however, the stereochemistry was undesired (96% *R*). As noted in the introductory chapter ethambutol exist as three diastereomers, the *S, S* being the therapeutically active while *R, S* is 16 times less potent and *R, R* is 500 less potent, this enzyme is not useful for our intended product, however, it can be applied in the synthesis of other products for example, (*R*)-amino alcohol can be used for chiral resolution of the optical isomers of 1,1′-binaphthalene-2,2′-diyl hydrogen phosphate which is a chiral ligand used for hydro carboxylation reactions.

ATA– 262, 239, 251 and 261 gave rise to *R*-enriched products, therefore like ATA-230 they are not applicable in the synthesis of ethambutol. In nature, (*S*)-selective transaminases are more abundant than the (*R*)-selective enzymes, and therefore more information concerning (*R*)-

selective transaminases is necessary. For a long time mainly (*S*)-selective transaminases were known and extensively investigated, and (*R*)-amines were mainly prepared by kinetic resolution of racemic amines by (*S*)-transaminases, which only gave a maximum yield of 50%. (*R*)-selective enzymes, are currently under investigation regarding their substrate scope.

A few (*S*)-enriched enzyme products were obtained, but the percentage conversion of some (ATA-252, 232 and 190) were relatively low. More impressive results were obtained from ATA-189, 194 and 254; these enzymes are very (*S*)-selective and gave rise to % e.e ranging from 95-99 %; unfortunately, the yields were relatively low for ATA-189 and 194. However, various optimizations can be made to improve the yield. ATA-254 belongs to Class III transaminases, which are (*S*)-preferential, the *S*-conformation is expected.[66]

Table 2: The % yield and % e.e of amino ester 14 product catalysed by different enzymes.

Enzyme catalogue number PRO(ATA)	**% e.e**	**% yield**
ATA-230	96% R	87%
ATA-251	54% R	26%
ATA-261	78% R	54%
ATA-262	63% R	65%
ATA-239	70% R	33%
ATA-232	46% R	45%
ATA-252	48% S	30%
ATA-253	45% S	38%
ATA-195	41% S	38%
ATA-190	53% S	48%
ATA-191	40% S	47%
ATA-253	55% S	55%
ATA-194	94% S	37%
ATA-254	97% S	73%
ATA-189	98% S	39%

The derivatised product was also analysed by crystallography to determine the stereochemistry as a confirmation of the chiral-HPLC data. The product **17** was crystalized by a slow

evaporation of ethyl acetate /hexane solution. White fibre crystals were formed and then subjected to X-ray diffraction (XRD) to determine the single crystal structure. The resultant molecular structure of compound **17** is given in *Fig. 17*, the selected bond length, torsion angle, and crystal structure refinements are included in additional information (Table 11, *Chapter 5*). This molecule contains an aromatic group, nitro group, amide, and an ester group, we can therefore conclude that our enzyme catalysis was a success, and we successfully synthesized an amide derivative. This crystal structure also confirms our stereochemistry, as the absolute configuration was determined to be that of the (*S*) enantiomer.

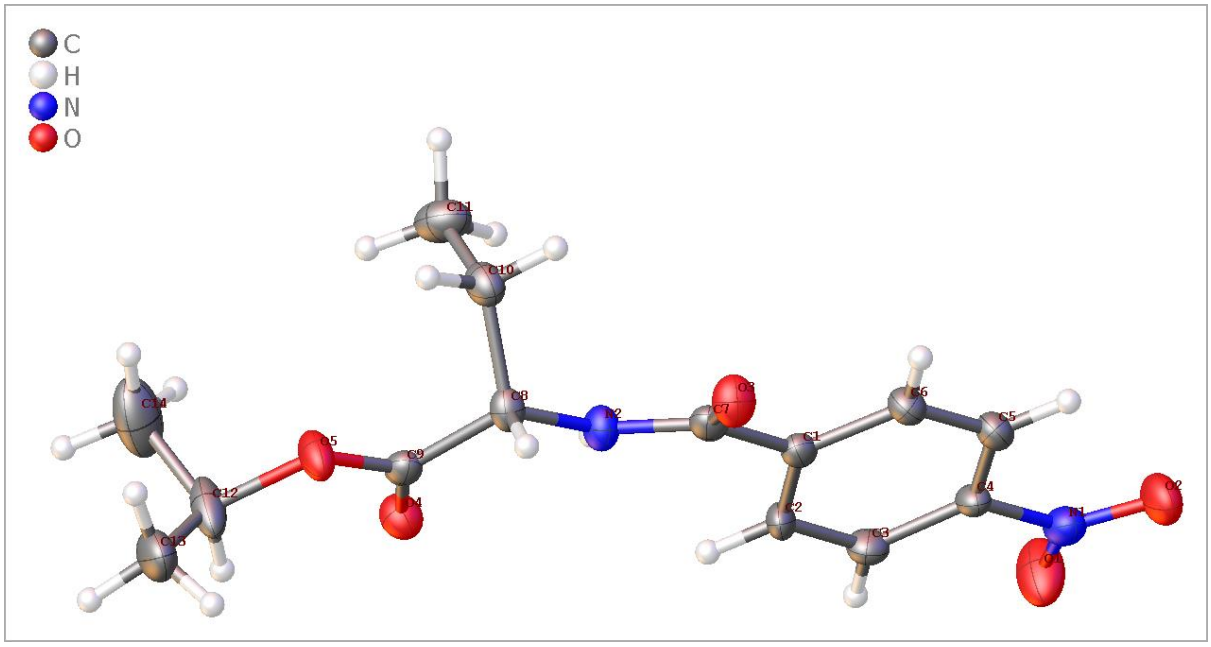

Figure 16: The crystal structure of the derivative **17** of the ATA-189 enzyme product.

2.1.1 **The quantitative analysis of the isopropyl amino ester 14**

From the previous section, it was proven that a few of the enzymes were able to catalyse the conversion of the substrates to the amine product (the LCMS of the enzyme product matches the standards). Consequently, it was now important to improve the method in order to ensure reproducibility and accuracy. All the assays of the active enzymes that were identified in *Fig.14* were repeated, together with an additional 20 new enzymes (*Fig.15*). The experimental conditions of both batches were kept the same: the reactions were run at 30°C using the same substrate and isopropyl amine stock solutions for 24 hours. However, there was a difference in the extraction procedure between the two sets of reactions.

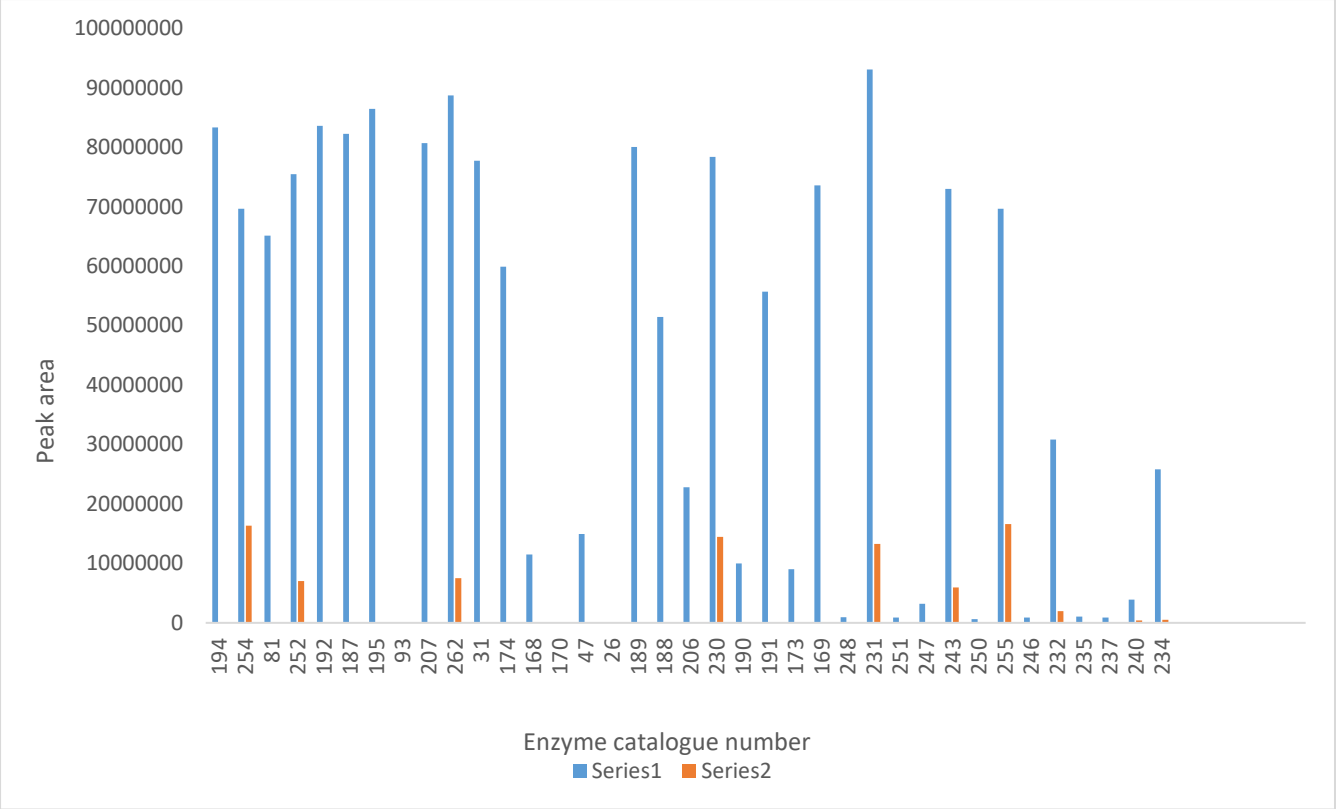

Figure 17: A graph illustrating the comparison between the activities of the enzymes, Series **1** (blue) represents the activity of the enzymes in a repeat experiment, and Series **2** (orange), represents the activity of the first screen.

To improve the accuracy of the analysis the method was modified to enhance product recovery. The volume of the sample was increased from 100 µl to 120 µl to obtain more significant and detectable results for accurate quantitative analysis. The volume of the sodium bicarbonate base was also increased, this has the potential of adjusting the pH to ensure that the amine is in neutral form. Additionally, the volume of brine was increased. This increase in brine volume was aimed to enhance the separation of the organic solvent and the aqueous phase, improving the overall efficiency of the extraction process.

The modification in the extraction procedure resulted in an increase in the peak areas as the concentration of the product that was extracted per batch was increased, these allowed us to accurately quantify our products and also allowed us to discover other active enzymes that were not observed because the products were too dilute to be detected. Looking at the peak area of ATA-254 in *Fig.15,* it is evident that the is a substantial 78% increase in peak area when comparing the second screen with the first screen (*Fig. 15).* This was observed with all repeated reactions. This finding emphasizes the significance of optimizing the extraction procedure.

To quantify the products, the standard curve in *Fig. 11* was used to estimate the concentration of the amine product at a given peak area. Multiple dilutions of the enzyme products were made in order to bring the peak area into the linear range of the standard curve (*Calculations in chapter 5*). Table 1 illustrates the % yield of the selected enzyme product, the highest yield obtained was 23%, which is relatively low.

Table 1: % yield of the amino ester from the different enzyme-catalysed reaction

Enzyme catalogue number	% yield
ATA-194	22.05
ATA-254	18.39
ATA-81	17.19
ATA-252	19.93
ATA-192	22.07
ATA-187	21.73
ATA-195	22.83
ATA-93	0.00
ATA-207	21.31
ATA-262	23.42
ATA-31	20.52
ATA-174	15.82

Although the change in extraction procedures has been shown to increase the yields, the extracting solvent used (acetonitrile) has high polarity index and it is miscible in water. Less polar organic solvents, such as ethyl acetate must be employed to ensure the complete extraction of the product. There are many ways that can also be used to optimize the yield, however since there were a lot of active enzymes, we decided to determine the stereochemistry before yield optimizations so that we can filter off enzymes with undesired stereochemistry.

2.1.2 **Enzyme kinetics**

As mentioned in Chapter 1, one of the limitations of the application of transaminases in industries is the reaction's unfavourable equilibrium, when there is a high concentration of acetone co-product the equilibrium is pushed to the left thus favouring the reverse reaction. Acetone is a volatile solvent with a boiling point of 56°C. The temperature that was used initially in the screening process (30°C) is insufficient for efficient acetone removal. Acetone can be removed in the reduced pressure system or an increased temperature; however, this is

widely dependent on two factors, the volatility of the substrate and the operational temperature of the enzyme. In 2015, Cerioli published an article focusing on the behaviour of transaminase enzymes under different temperature conditions.[67] The activity increased as temperature increased until it reached the optimum temperature of 50°C followed by the decrease in activity and denatured at 60°C.[67] With the motivation from these results, we decided to increase the temperature to 40-42°C and interesting results were obtained.

The temperature optimizations were applied in a time-based reaction in order to further investigate the behaviour of the enzymes at different time intervals. Theoretically, we expect the concentration of the product to increase with time (the steady state) until it reaches the equilibrium.

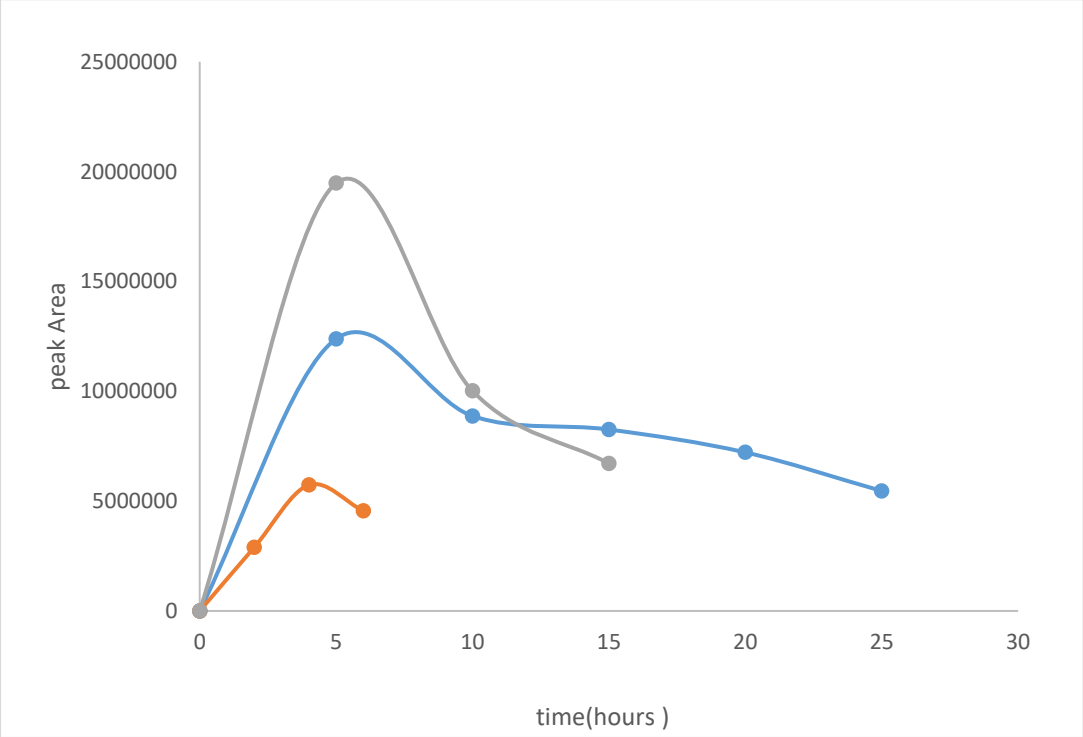

Figure 18:Peak area versus time graph of the ATA-194 (blue), ATA-254 (grey) and ATA-189 (orange) catalysed reaction at 40°C.

All the enzymes followed the same behaviour, the is a steady state until 4-5 hours, the maximum yield is obtained at 5 hours followed by a decrease in concentration (*Fig. 18*). The decrease could be due to the accumulation of acetone co-product in the reaction which results in a reverse reaction. ATA-254 gave the highest activity, followed by ATA-194 and ATA-189, from all of these results, we can conclude that the reaction goes to completion between 4-5 hours, and this is comparatively good as most reported transaminase reactions often take about 15-48 hours to run to completion.[68]

2.3.7 Scale–up of ATAs reaction for ethambutol synthesis

The enzyme reactions were scaled up to generate sufficient material to generate the amino alcohol **4**. The subsequent synthesis is required as a demonstration of the reaction and a source of material as an independent confirmation of the stereochemistry. The kinetics and the stereochemistry of the products produced in a scaled-up reactions were studied, and the following results were obtained.

Table 3: The % yield and % e.e. of amino ester product catalysed by different enzymes.

Enzyme catalogue number	Time (min)	% Yield	% e.e.
ATA -254	30	65%	99% S
	300	73 %	65% S
ATA-194	30	58%	98% S
	300	40%	96% S
ATA -189	30	48%	95% S
	300	32%	95% S

Interesting results were obtained when using ATA-254, the reaction resulted in exceptional % e.e at 40 ℃ and the yield was relatively good (65%), however, the % e.e. decreased with increased reaction time. This effect is known as the racemization effect, which can be defined as the irreversible conversion of optically active compounds into racemates. The racemization is induced by heat or a certain chemical reaction; in this case, the same conditions were used for all the enzyme reactions, however, racemization was only observed when using ATA-254. Since we are working with unpurified enzymes, side reactions could occur, so it is safe to assume that there is an undesired side enzyme reaction that is occurring which results in an undesired change in stereochemistry. ATA-254 is an interesting enzyme, and it does not only prefer (*S*)-conformation but was also found to possess some (*R*)–preference when using different substrate (Chapter 3), in-depth investigation of this of the enzyme is important and the docking study of this enzyme on both substrates might help us understand the reason for racemization.

2.3 Reduction of amino ester to the amino alcohol

The most essential step in our proposed synthesis of ethambutol is the reduction of amino ester **14** to the desired amino alcohol **4** (*Scheme 26)*. The racemic and *S*-standards were initially used

for the development of an efficient reduction method. The first attempt includes the use of lithium aluminium hydride (LAH), a very powerful non-selective hydride transfer reagent that can reduce esters directly into alcohols (*Scheme 26*). The reaction was investigated using different reaction conditions (time, co-solvent, and LAH quantity), however, none of these resulted in the formation of the desired product. Neither aldehyde intermediate nor starting material was detected, therefore, the reaction was unsuccessful. The starting material **14** consists of a very reactive amino group. To improve the LAH reaction; the amine can be protected by forming an amide **17** followed by the reduction of both amide and ester to an amino alcohol. Since the LAH reduction requires further investigation, which includes the introduction of more reaction steps, and considering the difficulties in the work-up procedure, alternative approaches were explored.

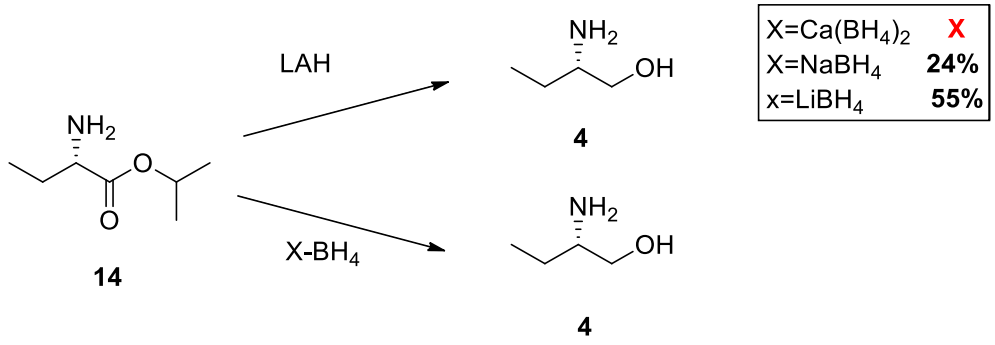

Scheme 26: Reduction of amino ester **14** into corresponding amino alcohol **4**.

Borohydride reduction is the most commonly used hydride transfer for the reduction of different functional groups.[69] Sodium borohydride is a mild reducing agent, and it can reduce carboxylic esters, however, the method is not efficient because the reaction often takes long, and it requires an excessive amount of the reagent. Replacing sodium with calcium has been proven to improve the reduction of esters into alcohols. In this case, we attempted to replace sodium with calcium using $NaBH_4$ and $CaCl_2$. This was followed by the reduction reaction; unfortunately, the reaction was unsuccessful, and we suspect that the $CaCl_2$ was not dry enough. $NaBH_4$ was then used in excess amount (5 equivalents) and quite surprisingly the reaction worked, however only 24% of the product was isolated. We then decided to investigate $LiBH_4$ and the yield was increased significantly to 55%. The NMR data corresponded to that in the literature, and therefore the reaction was successful.

The same method used for the reduction of standards was also applied on an enzyme product (*Scheme 27).* The product was isolated as a borohydride–amino alcohol complex, the mass spec data correspond to the complexation of borohydride to both amine and an alcohol group. The

peaks in the ^{1}H NMR spectrum was also slightly shifted, to free the borohydride from our alcohol, the product was heated in the presence of potassium hydroxide solution for 3 hours, however, this resulted in the decomposition of the product.

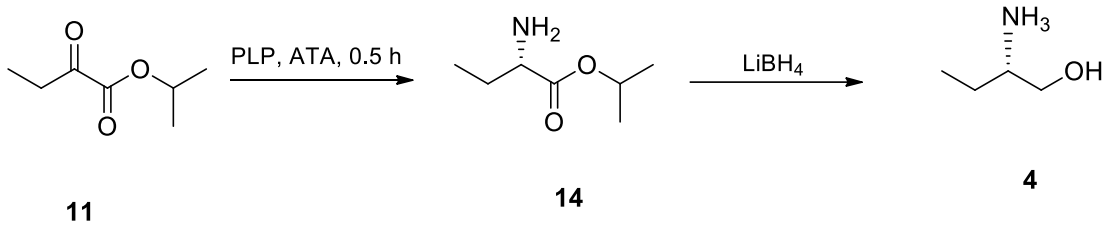

11 **14** **4**

Scheme 27: Enzyme route for the synthesis of (*S*)-amino alcohol **4**.

We repeated the reaction using the same conditions and employed concentrated (10%) HCl to cleave the boron complex, and the results obtained was quite remarkable. Notably, no mass of complexed amino alcohol molecular ion was detected, as shown in *Fig.19*. Only the starting material and the product masses were observed (*Fig.19*). Despite obtaining a low yield (7%) after purification, we managed to determine the optical rotation of our product in methanol. The specific rotation of our enzyme product **4** wa**s** determined to be $\alpha\,^{21}_{598\,nm}$ = -16.800°, while for our (S)-standard, it measured -17.1579°. When comparing this to the literature values, this allowed us to calculate the enantiomeric excess (% e.e), resulting in a value of 97.91% (*S*). This outcome serves as further confirmation that ATA-254 is indeed selective for the (S)-enantiomer.

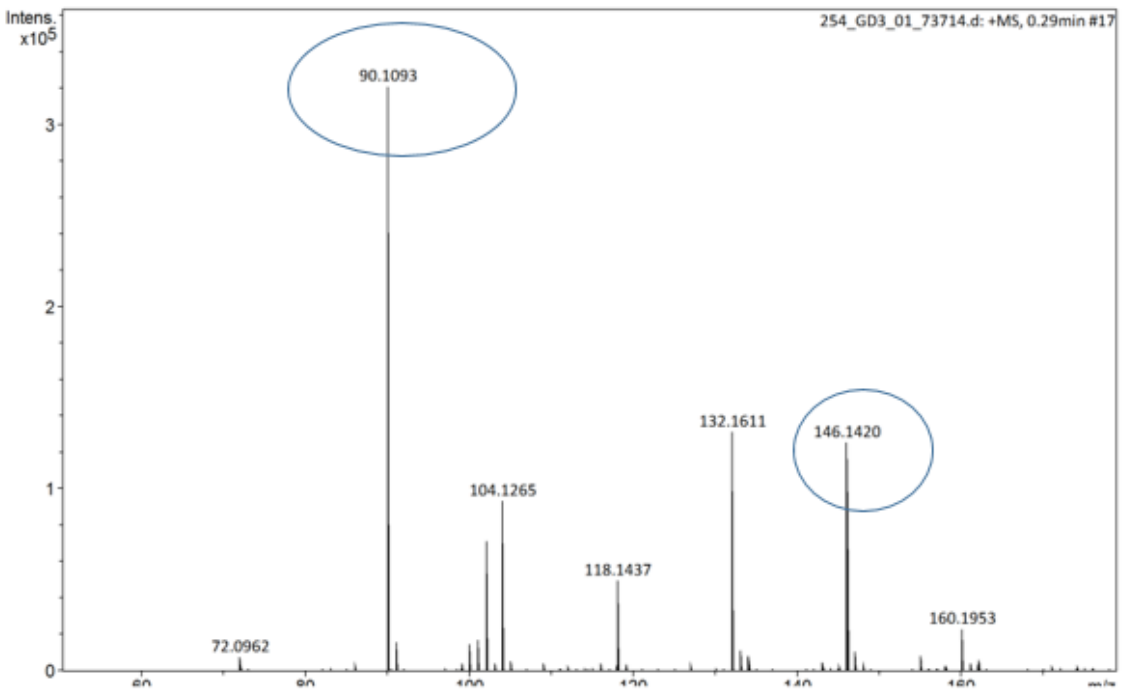

Figure 19:Mass spectrum of ATA-254 catalysed amino alcohol product.

2.4 Conclusion and Future Work

A novel isopropyl ketoester **11** substrate was introduced in this thesis, together with a substrate that had previously undergone screening in our laboratory, the ethyl keto ester substrate **10.** The only distinction between the two substrates lay in the presence of an extra methyl group in the isopropyl ketoester **11**, and it's worth noting that these ester groups are the ones that interact with the enzyme at its larger active site. As previously discussed, the enzyme's larger active site can readily accommodate substituents with bulkier groups. These two substrates exhibited distinct behavior and displayed significant differences in activity. Therefore, we can infer that the introduction of the additional methyl group in the isopropyl substrate **11** introduced a new, potentially hydrophobic binding interaction between the substrate and the enzyme, resulting in distinct behavior compared to the ethyl substrate **10**.

Additionally, the isopropyl ester 1**1** substrate exhibited significantly higher activity when compared to the ethyl ester substrate **10**. Therefore, it can be concluded that the greater the size of the substituent at the enzyme's large active site, the higher the enzyme's activity. In the future, a more comprehensive comparison between these two substrates could be conducted to gain a deeper understanding of the obtained results.

Isopropyl ketoester substrate **11** was successfully screened against ω-TAms using isopropyl donor system, giving rise to amino ester product **14**. The mass spectra and the liquid chromatograms of our enzymatically synthesized amine **14** corresponded to our standard amine **14**. The only noticeable distinction was observed in the proton NMR spectrum, where the proton at the stereogenic centre exhibited a dramatic shift in the enzyme product (Fig .*20*). The shielding was also observed in ^{13} C NMR spectrum and DEPT NMR spectrum confirmed that the peak belongs to the CH group.

Possible explanation for this phenomenon could be the formation of a salt, where a protonated amine forms a strong complex with the phosphate anion thus effecting the chemical shift of the proton adjacent to it. As demonstrated earlier, when this product is employed in subsequent reactions, such as derivatization or reduction, the resulting product corresponds to the standard. Therefore, it raises the possibility that the issue may be related to the extraction procedure. Alternatively, it might be worthwhile to explore whether the buffer system plays a role in this discrepancy by testing a different buffer system to verify its influence on the observed proton NMR shift.

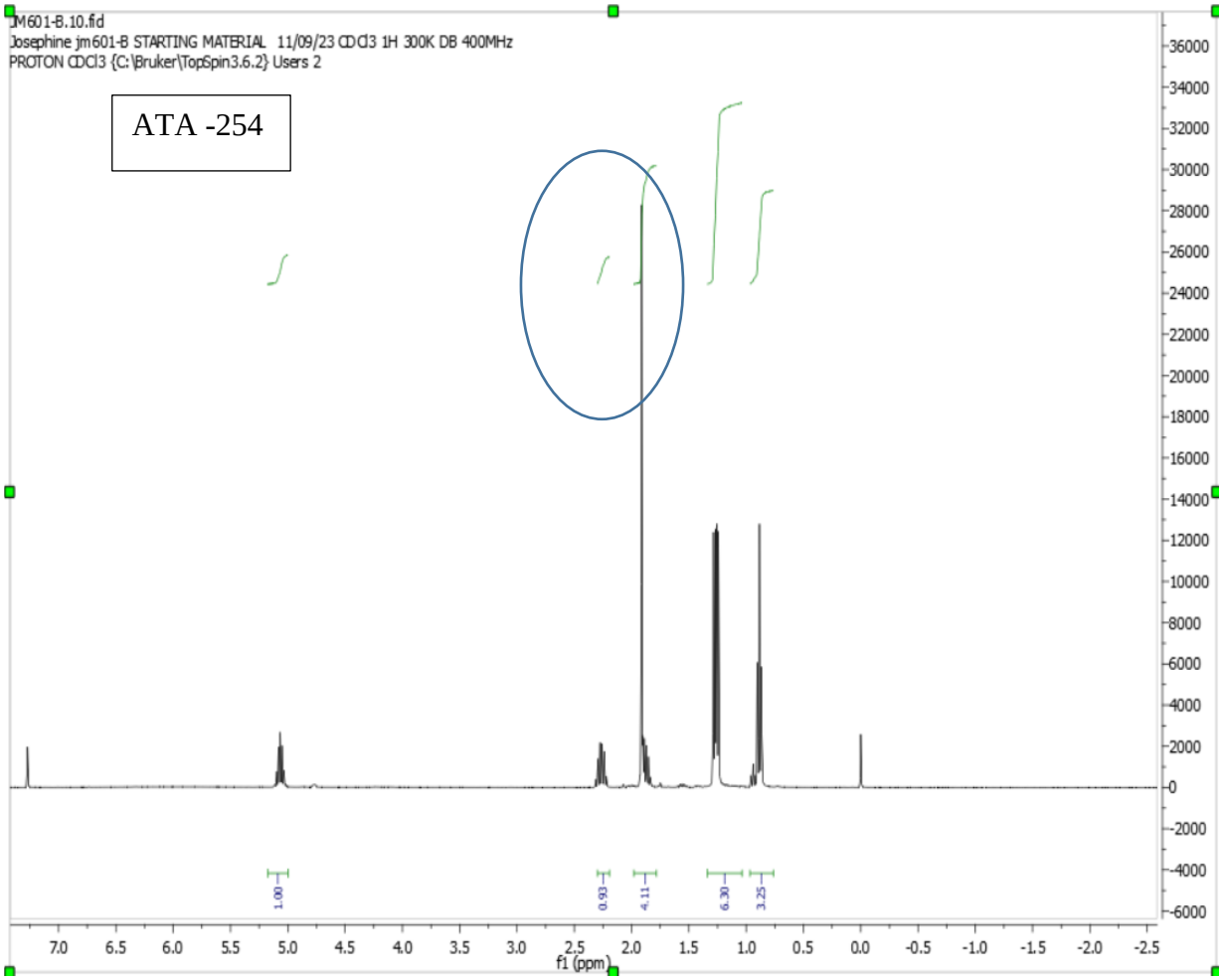

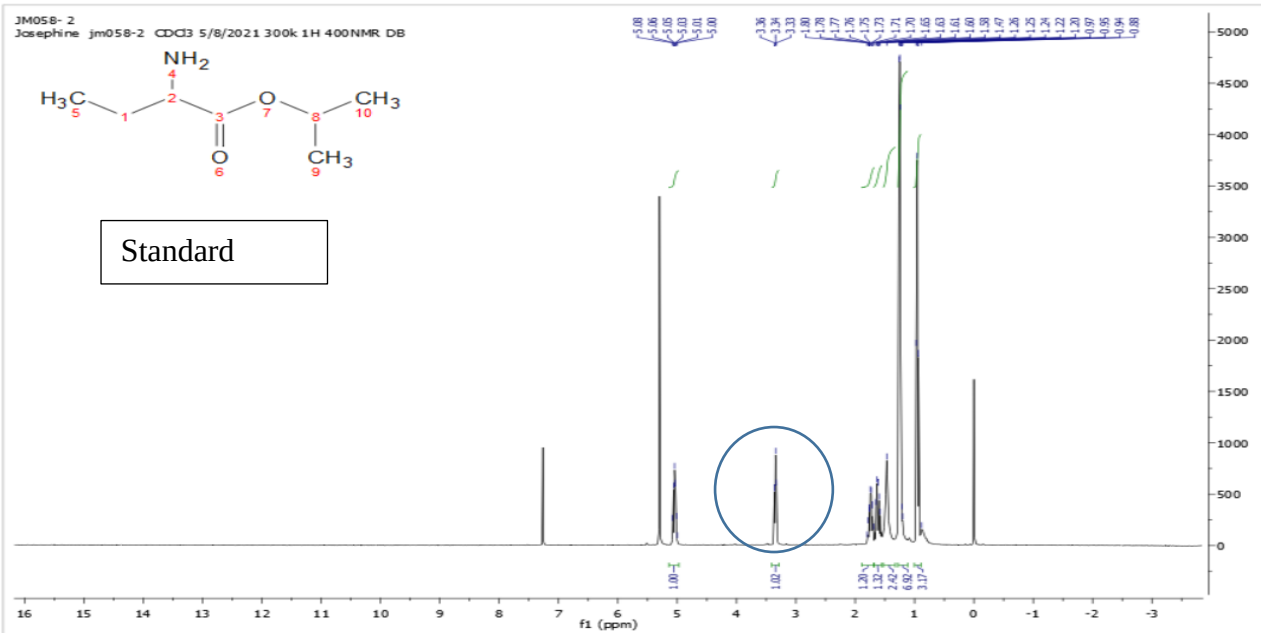

Figure 20: In the ^{1}H NMR spectrum of the enzyme product (above), the stereogenic proton has shifted from 3.5 ppm to 1.8 ppm in comparison to the standard spectrum (below).

The NMR, LCMS, and crystal structure analysis of the derivatized amine product **17** were in complete agreement with those obtained for the standard. Additionally, we successfully determined the enantiomeric excess (% e.e), revealing the presence of three highly (*S*)-stereoselective enzymes, namely ATA-189, ATA-254, and ATA-194. This stereochemistry was further confirmed by polarimetry measurements conducted on the amino alcohol **4** and the derivatized amine.

In summary, we achieved the conversion of cost-effective pro-chiral starting materials into enantioenriched amines, which were subsequently reduced to alcohols. However, we encountered significant challenges during the reduction process, particularly with the formation of boron complexes with our amino alcohol. Nonetheless, we developed a method to cleave these complex bonds; however, the yield obtained was very poor.

For future work, it is imperative to explore alternative reducing reagents to circumvent the issue of boron complexation. One promising route to investigate is hydrogenation, employing organometallic complexes like palladium complexes for the reduction of esters into alcohols. Once an efficient reduction procedure is established, (*S*)-amino butanol can then be used to complete the synthesis of ethambutol.

Chapter 3:

3.Synthesis of a chiral Dolutegravir intermediate

Substrate selection

(*R*)-3-amino-1-butanol (**5**) is a key precursor in the production of the anti-viral drug dolutegravir. As mentioned in Chapter 1, decreasing the cost of the synthesis of this intermediate has the potential of decreasing the overall production costs of the drug. There are two different asymmetric reductive amination routes reported in the literature for the synthesis of (*R*)-3-amino-1-butanol **5** (*Scheme 28*).[70,71]Method **A** involves the use of an expensive ruthenium catalyst and the reaction is usually carried out at high temperature and pressure, although this method works efficiently it is still not economically attractive (*Scheme 28*).[71] Transaminase biocatalysis emerged as a promising catalysis for the replacement of toxic and expensive metal catalysts. A wide range of (*R*)–selective ATAs have been discovered as reported in the literature and some have been shown to exhibit the highest activity towards 4-hydroxy-2-butanone **19** resulting in enantiopure (*R*)-3-amino-1-butanol (**5**).[71] Although Method **B** illustrates an excellent greener synthetic approach, it is still economically unsustainable because hydroxyl ketones are relatively expensive pro-chiral starting materials (*Scheme 28*). In this chapter, we are introducing a new inexpensive starting material in order to make method **B** economically attractive (*Scheme 29*).

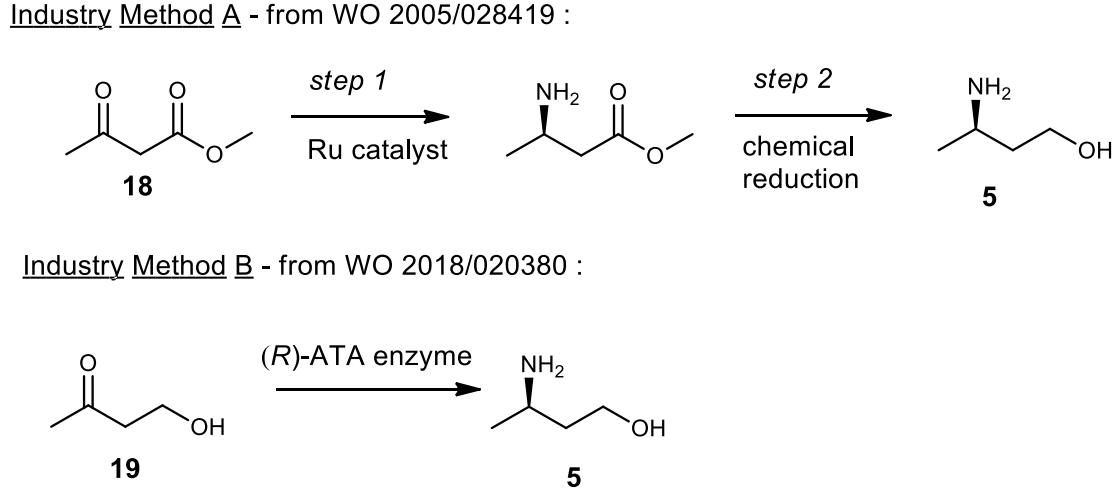

Scheme 28: The current industrial methods for the production of (*R*)-3-amino-1-butanol (**5**) intermediate.

Keto-esters such as ethyl and methyl acetoacetate have received less attention as substrates for transaminase biotransformation (*Scheme 29*). These pro-chiral ketones are readily and

inexpensively available from suppliers such as Sigma Aldrich and have the great potential of improving production costs. In Chapter 2, it was revealed that a substrate that has an isopropyl group at the larger pocket of the enzyme's active site has shown greater enzyme activity compared to the substrate with an ethyl group. These results motivated us to investigate the isopropyl acetoacetate **20** as an ATA substrate. Here we concisely focus on the biotransformation of isopropyl acetoacetate **20** into (*R*)-amino ester **21** followed by the reduction to a desired (*R*)-amino butanol **5** *(Scheme 29*).

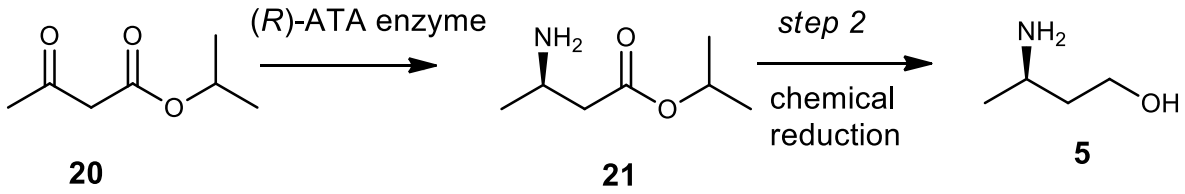

Scheme 29: Proposed ATA biotransformation for the synthesis of the dolutegravir intermediate (**5**)

3.2 Substrate synthesis

Transesterification is a process where an ester is transformed into another ester through the interchange of an alky group (*Scheme 30*). This procedure was found to be efficient for the synthesis of a wide range of beta-keto ester derivatives. The reaction is in equilibrium and can be accelerated by a Bronsted acid, Lewis acid, or a base catalyst. Yang and his colleagues investigated the behaviour of transesterification reactions using different catalysts under different conditions and the Boron trifluoride diethyl etherate (BF_3OEt) Lewis acid catalyst was found to work efficiently for β-keto esters.[72]

Our first attempt involved the transesterification of ethyl acetoacetate **22** with isopropanol to form isopropyl acetoacetate **20** using the conditions similarly reported in the literature (*Scheme 30*). The reaction was initially refluxed for 5 hours but, unfortunately, only a slight conversion of the starting material to the product was detected (< 15%). Furthermore, separation of these two compounds on TLC was also challenging as they do not differ much in polarity. To improve the conversion, the reaction time was increased to 12 hours. After several failed separation attempts, 64% of the yellow oil product was finally isolated by running a long silica chromatography column using hexane as a mobile phase. The ^{1}H NMR spectrum of the product shows a doublet peak at 1.24 ppm integrating for six protons, this indicate the presence of two methyl peak and the peak of proton adjacent to the methyl groups is also observed at 5.03 ppm

as a septet. The results were confirmed by the presence of newly formed isopropyl CH peak in ^{13}C NMR spectrum.

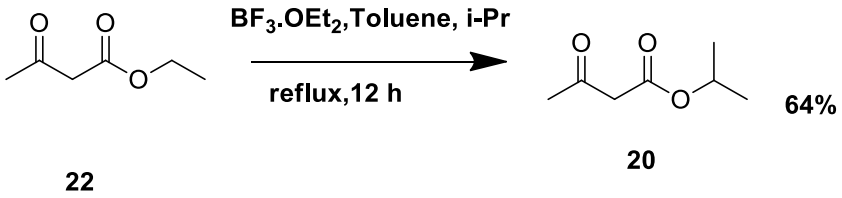

Scheme 30: Transesterification of ethyl acetoacetate **22** with isopropanol to synthesize the isopropyl acetoacetate **20.**

Due to the previous tedious purification procedure, we decided to replace ethyl acetoacetate **22** with methyl acetoacetate **20** (*Scheme 31*). The reaction proceeded better compared to the previous ethyl ester reaction in that 80% of the product was isolated after an adjustment of the purification procedure (5% ether/hexane). The polarity of methyl acetoacetate **18** and isopropyl acetoacetate **20** are significantly different and thus were easy to separate using silica column chromatography. From these results we can deduce methyl acetoacetate **18** provides a facile transesterification into isopropyl acetoacetate **20** thus it is a more convenient starting material to use.

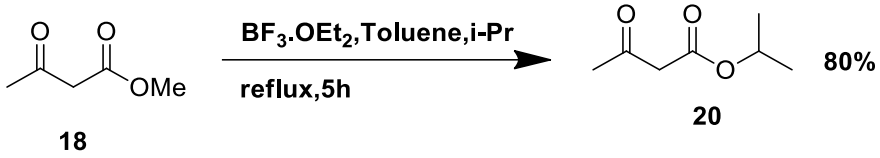

Scheme 31: Transesterification of methyl acetoacetate **18** with isopropanol to synthesize the isopropyl acetoacetate **20.**

3.3 Quantification and stereochemistry determination

As in Chapter 2, it is very important to have the reference amino ester compounds for the development of quantitative and qualitative analysis methods. Our first attempt at the synthesis of the racemic amino ester **18** involved reductive amination using aqueous ammonia as an amine source (*Scheme 32, step 1*). This reaction is often effective for the synthesis of primary amines and ammonia itself is an inexpensive commodity compound and also readily available. The reaction was performed at room temperature from 16-24 hours and the product was characterized using NMR spectroscopy.

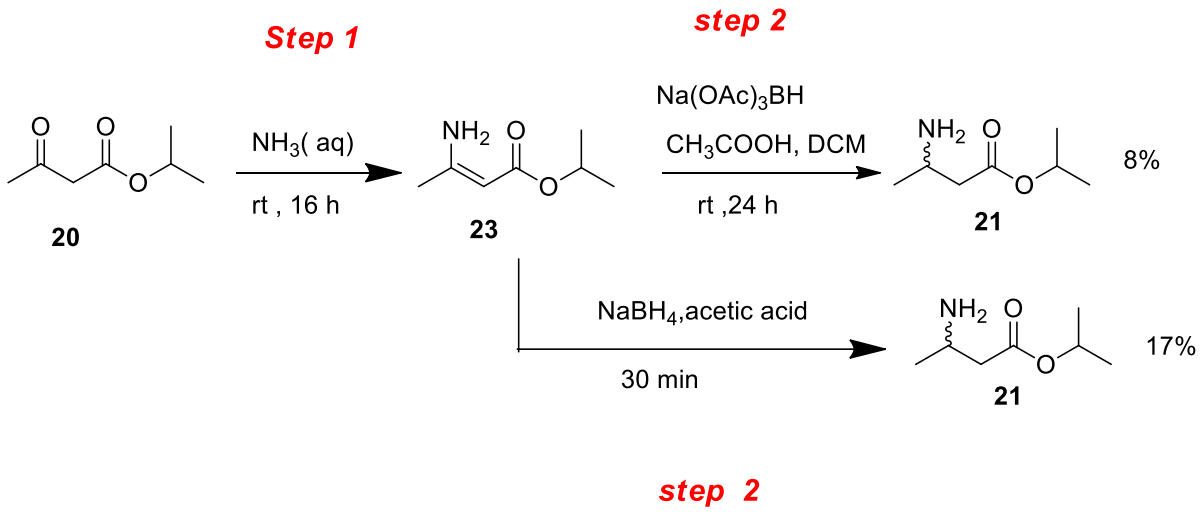

Scheme 32: Reductive amination of isopropyl acetoacetate **20** into a (*rac*) - amino ester **21.**

^{1}H NMR spectrum of enamine **23** shows a new distinct singlet peak at 4.5 ppm which integrates for a single proton, this indicates the presence of a double bond in the beta position (*Fig. 22*). The broad NH_2 singlet peak integrating 2H was also detected at 7.8 ppm (*Fig. 22*). These two distinct peaks indicate the presence of the desired product; however, there were still few small peaks of the starting material detected (peak at 3.3 ppm in *Fig. 19*). The estimated conversion obtained from the integration of the peak was found to be relatively good (70%). Without any further purification procedure, step 2 was investigated (*Scheme 32, step 2*).

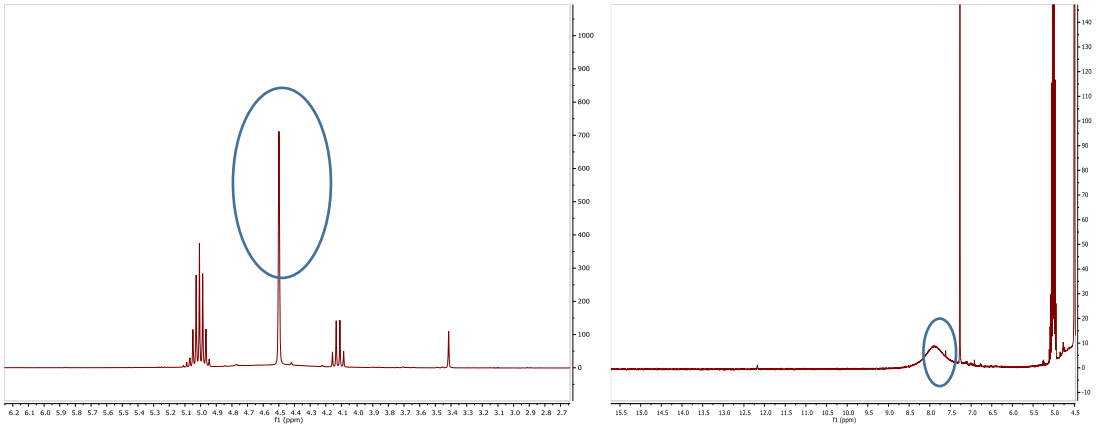

Figure 21: ^{1}H NMR data of an enamino ester **21** illustrating the two distinct peaks that distinguish a product from the starting material.

Our first attempt at the reduction of the enamine ester **23** into desired amino ester **21** involved the use of the most popular and selective sodium triacetoxyborohydride reducing agent. This reagent directly reduces imines and enamines to amines without interfering with any carbonyl groups that are present . The ^{1}H NMR of the product showed a multiplet peak at 2.5 ppm

intergrating 2H, this indicate the presence of ethyl group, hence the peak was assigned to two protons adjacent to the stereogenic centre .The intensity of the product peaks was quite low, this suggests that only a small quantity of the product is formed, and a major compound was a starting material. Different optimizations were investigated in order to improve the conversion (change in reaction time, acid, and solvent), however, none of these resulted in improved results.

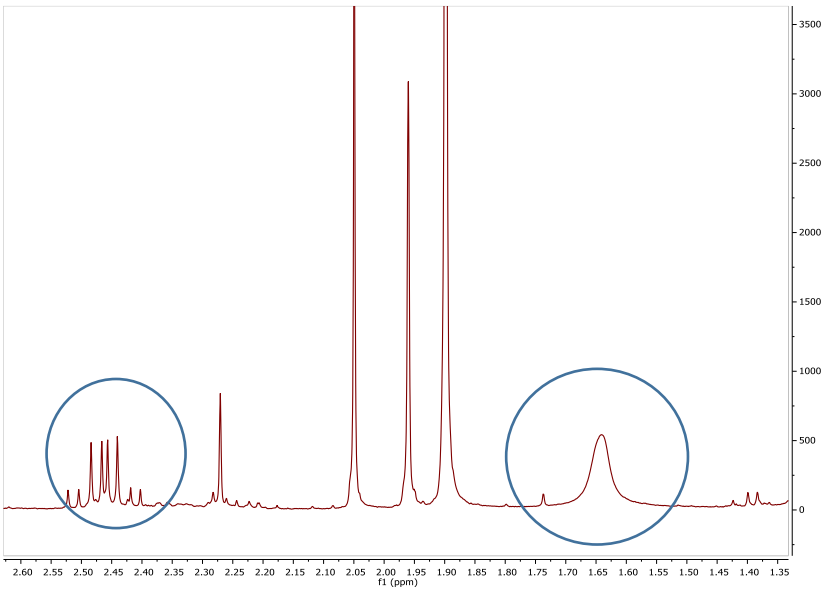

Figure 22: ^{1}H NMR showing the indication of newly formed stereogenic centre when utilizing sodium triacetoxyborohydride reagent.

Considering the unsatisfactory yields, we decided to investigate the solvent-free reduction of enamine using sodium borohydride in the presence of citric acid wherein the reagents were ground in a mortar for 30 minutes (*Scheme 32)*. Interestingly the reaction proceeded well, there was no sign of the starting material in the ^{1}H NMR but only 17% of the desired product was isolated. The decrease or an increase in the quantity of the reducing reagent did not result in yield improvement; we suspect that most product is lost due to ester hydrolysis into an acid, which could have been removed in the work-up procedure by washing with a saturated bicarbonate solution. An alternative synthesis was sought. Fortunately, racemic aminobutyric acid **24** is commercially available; this reagent was treated with thionyl chlorine and isopropanol to allow the alkyl halide substitution reaction (*Scheme 33*). The same reaction was performed using (*S*)-3-aminobutyric acid to afford the (*S*)-enantiomer of **21**. Yields ranging from 75-90% were achieved for both the single enantiomer and racemic standards.

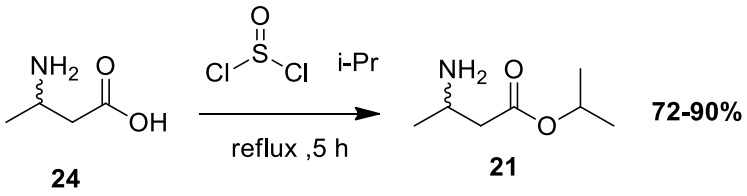

Scheme 33: An alternative synthesis of racemic and (*S*)-amino ester reference compound **21.**

An achiral HPLC method for quantitative analysis was successfully developed using a reverse phase column. Our β-amino ester **20** behaved in the same manner as the α-amino ester **14** obtained in Chapter 2, they both exist in two different forms, the ionized and the neutral form, thus separating when using the HILIC column (*Fig.24).* The product **21** peak eluting at 8.9 minutes was chosen as a quantifier ion, it was then integrated at different concentrations to develop a standard curve (*Fig. 25).* The correlation coefficient of the standard curve obtained (R^2 = 0.9878) indicates a good correlation between the variables, therefore the concentration of an unknown solution can be estimated for the quantitative analysis.

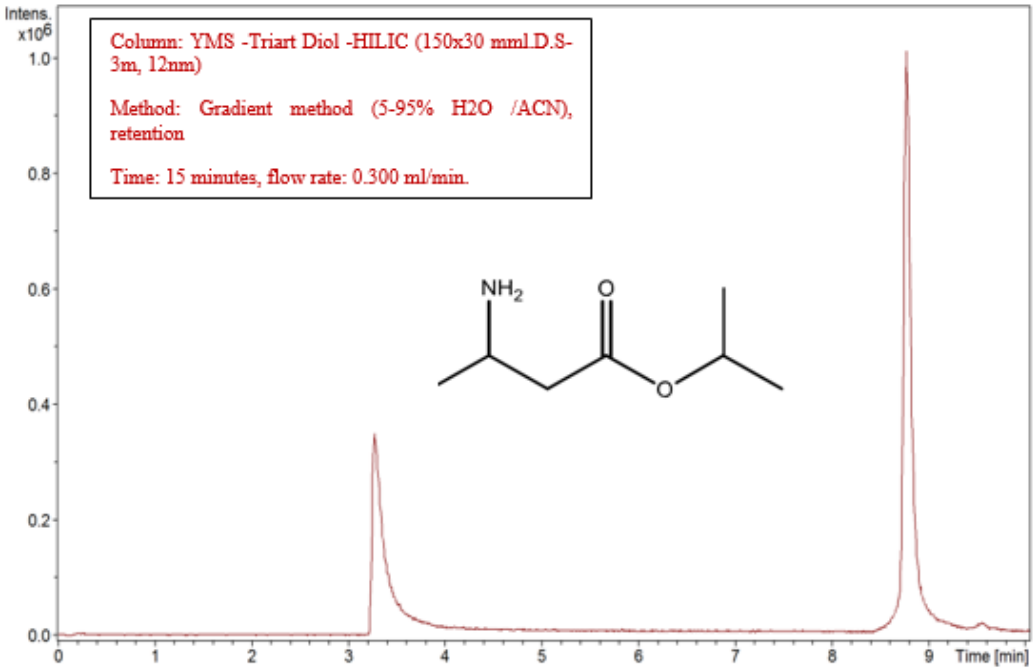

Figure 23: Liquid chromatogram of the standard amino ester **21** obtained when using an achiral reverse phase column.

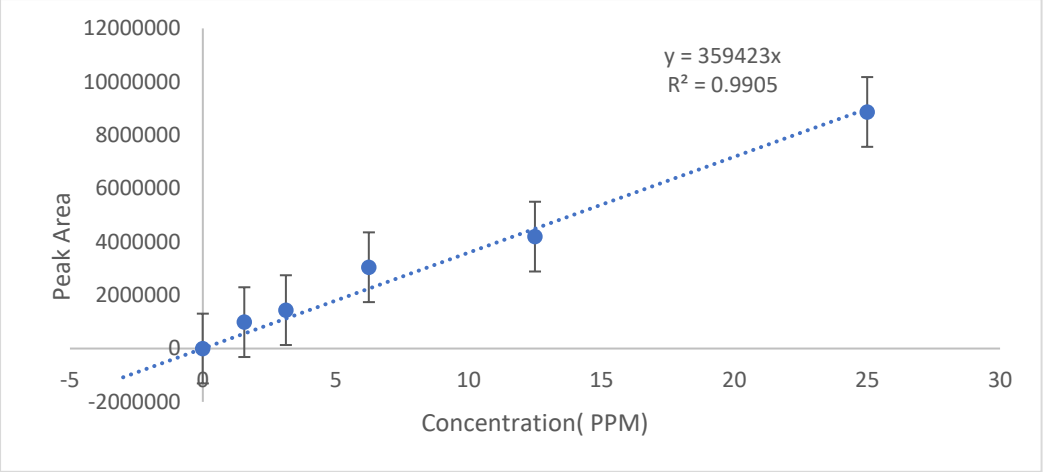

Figure 24: Standard curve of peak area of the amine reference product **21** versus the concentration (ppm) (n=6).

The next step was to develop a method for the determination of the stereochemistry; our standard amines were successfully derivatized into amides as in Chapter 2 using a similar procedure. Scheme 31 shows the reaction conditions used for the amidation reaction; *para*-nitro benzoic acid was replaced with *para*-nitro benzoyl chloride in order to avoid the tedious purification procedure that was experienced when using *para*-nitro benzoic acid as a starting material (*Scheme 34*). The reaction does not need any coupling reagents, only an excess amount of a base is required for neutralizing the acid that is released during the reaction. The reaction was performed at room temperature for 24 hours to afford a light-yellow powder **25** product with a yield of 60 %. The ^{1}H NMR spectrum of **25** shows the present of two aromatic peaks at 8.33 – 8.22 ppm and 7.99 – 7.89 ppm. The NH peak was also observed at 1.60 ppm, this indicate that the coupling was a success and it was further confirmed by the presence of an amide carbon at 164.2 ppm in the ^{13}C NMR spectrum .The mass spectrum also shown the fragment with the mass of $[M+H]^{+}$= 295.1296 which correspond to the expected mass of our product **25**. Using the same reaction procedure as in Scheme 35, the (*S*)-**25** amide was synthesised from the (*S*)-**21** amine. As expected, the NMR and the mass spec data of the (*S*)-**17** corresponded to its racemate.

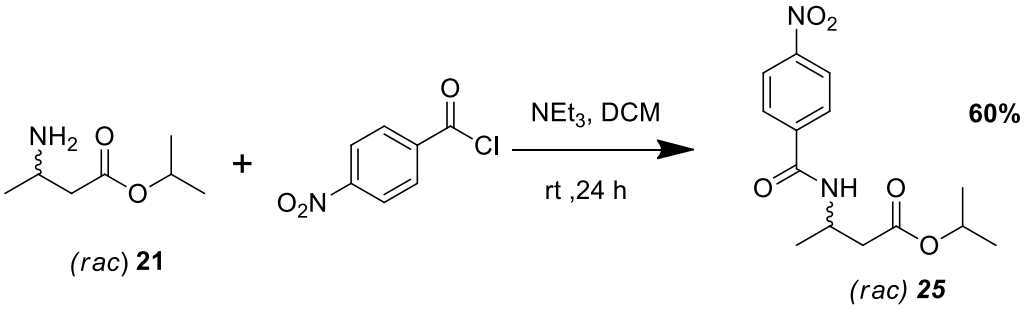

(*rac*) **21** (*rac*) ***25***

Scheme 34: Derivatization of the standard amine **21** using para- nitro benzoyl chloride to form amide **25.**

The resolution of two enantiomers proved to be successful as a clear baseline was detected between the two enantiomers using a Daicel Chiralpak AD-RH chiral column (4.6 x 150 mm, 5 µm)), an isocratic mobile phase of water/acetonitrile (50:50), UV detection at 254 and 324 nm, and mass spec detection (*Fig. 26*). The (*S*)-derivative **25** standard was also run on the instrument, using the same method and conditions. It eluted at a retention time of 4.5 minutes; these results indicate that the (*S*)-enantiomer **21** elutes first followed by the desired (*R*)-enantiomer **21.**

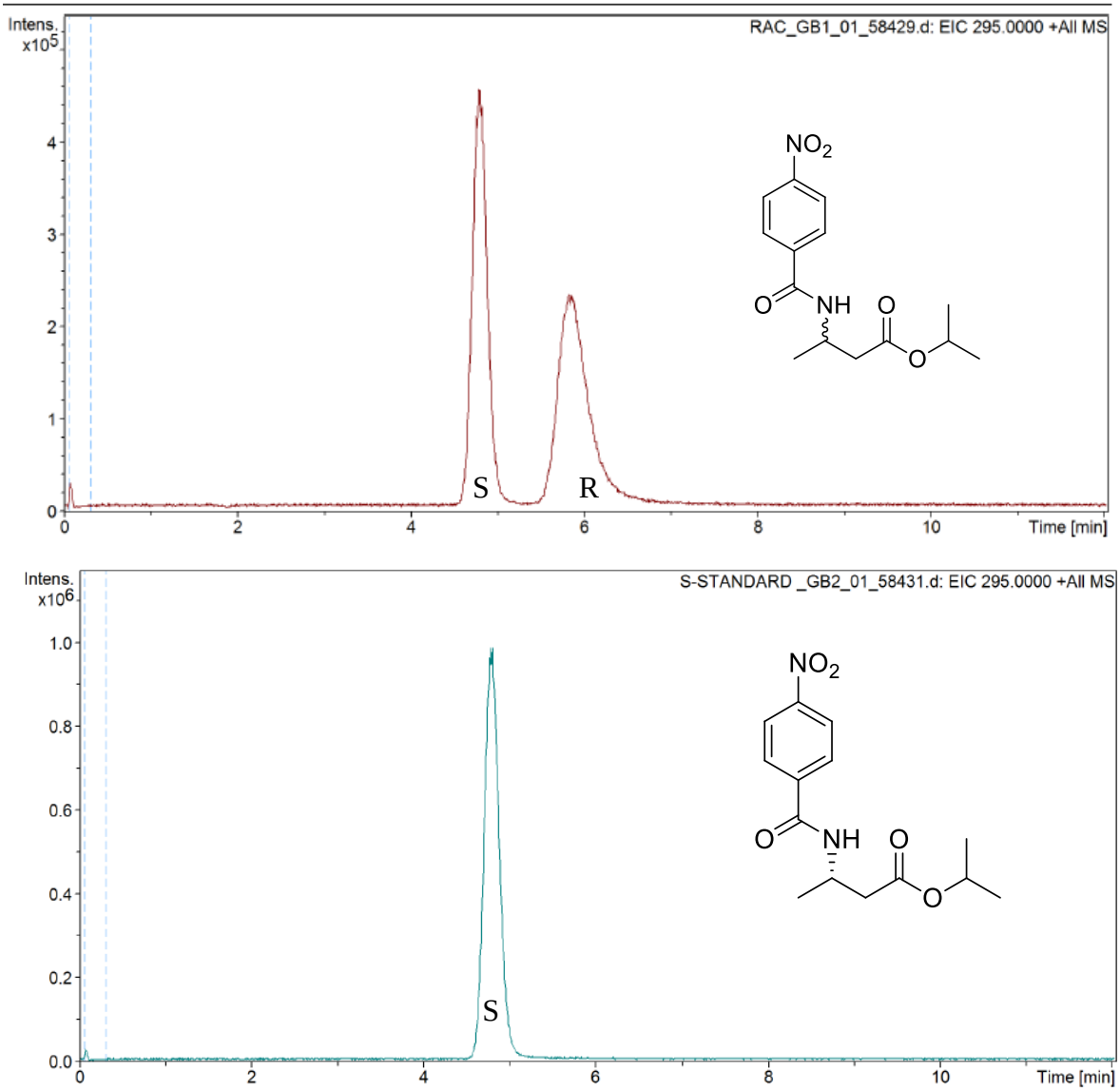

Figure 25: LCMS chromatography peaks of the derivatized r*ac*-**25** and enantiopure (S)-**25** (below).

3.4 Enzyme screening

Following the same approach as in Chapter 2, a total of 28 different ATAs were subsequently tested against substrate **20** with the aim of converting the pro-chiral ketone **20** into (*R*)-amino ester product **21** *(Scheme 35*)**.** The graph in Figure 27 illustrates the comparison between the peak areas of the enzymes active in this reaction and overall, 39% of the screened enzymes were active against the substrate **20**. ATA-261 and ATA-262 showed the greatest activity against substrate **17,** these results were impressive because both ATA-261 and ATA-262 are well known to be (*R*)-selective in literature (which is our desired enantiomer). All the results illustrated in the bar graph below (*Fig. 27*) were obtained from characterization using HR-LCMS against the reference compound data.

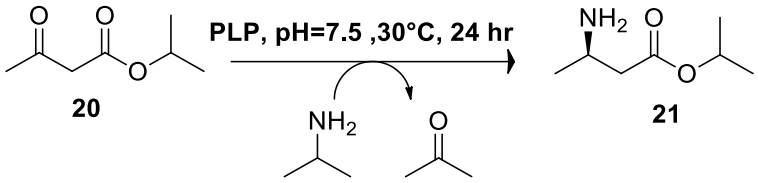

Scheme 35: Proposed biotransformation towards the synthesis of (*R*)-amino ester **21.**

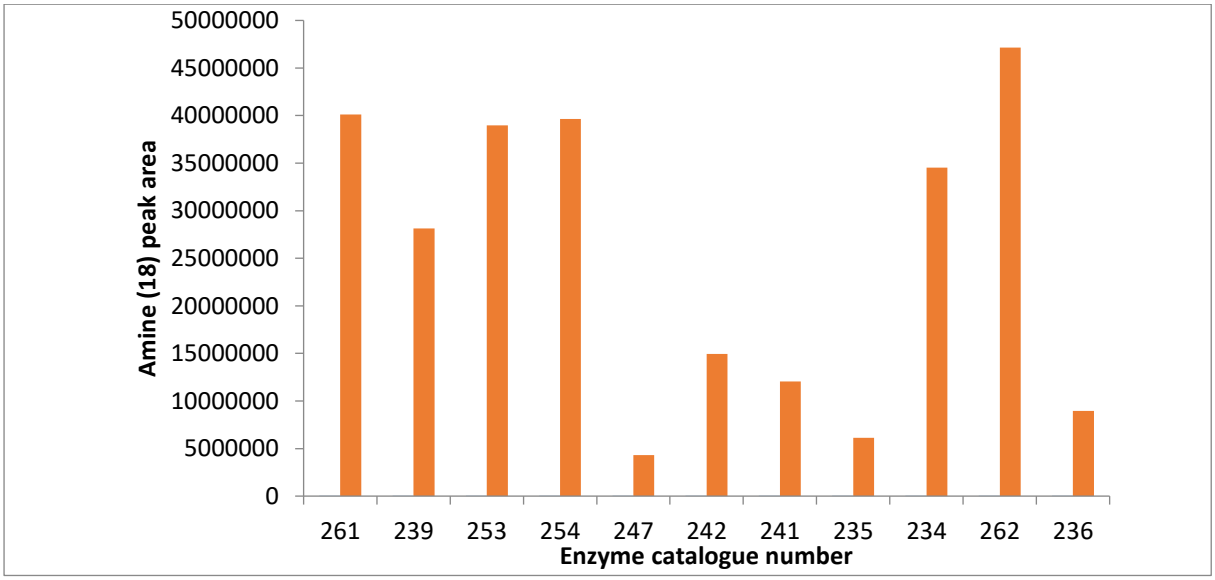

Figure 26: Comparison between the activities of active enzymes towards the biotransformation of pro-chiral **20** into the corresponding amino-ester **21.**

Quantitative analysis was usefully determined using the standard curve in Figure 25. Multiple dilutions of the enzyme products were performed for the peak area to lie within the quantification range. Table 4 illustrates the mol % yield of the selected amine enzyme products, the highest yield obtained was 45% which is acceptable, however, other enzymes such as ATA-

235 gave a very poor yield (*Table 4*). When scaling up the reaction, we frequently encountered issues with emulsion formation during the extraction process for our enzyme amine product **21**, particularly when employing ethyl acetate as the extraction solvent. Unfortunately, the addition of sodium chloride, or even sodium sulphate did not break the emulsion and only centrifugation was able to separate the two liquids. We speculate that much of our product could have been lost during this process. Other possible explanations include the unfavoured equilibrium, which has been covered extensively in Chapter 2.

Table 4:% yield of amino ester **21** obtained from different ATA enzyme-catalyzed reactions.

Enzyme catalog number	**Mol% yield**
ATA-261	41.89
ATA-262	45.13
ATA-254	43.10
ATA-234	37.93
ATA-242	1.87
ATA-241	1.48
ATA-235	0.69
ATA-236	1.07
ATA-247	0.44

The enzyme amine product **21** was derivatized into amide **25** for stereochemistry determination. Most of our active enzymes exhibited the desired (*R*)-selectivity (*Table 5*). ATA-261 and 254 gave an excellent enantiomeric excess (% e.e) with relatively good yields, these enzymes can further be utilized for the synthesis of our desired amino alcohol **5**. ATA-241 also gave an excellent % e.e; however, the yield was extremely poor. ATA-234 and 262 gave good conversions and reasonably high % e.e, but with some (*S*)-enantiomer impurities, the enantiomeric excess can then be further improved by optimizing the reaction conditions. The % e.e of ATA-236, 235 and 247 were difficult to obtain because of poor % yield. Figure 28 shows an example of the chromatograms obtained from ATA-261 which shows a single

peak eluting at the same retention time as an (*R*)-enantiomer and ATA-241 which shows the presence of both enantiomers, however, the desired (*R*)–enantiomer is in excess.

Table 5:% yield and % e.e of amino ester **21** obtained from different ATA enzyme-catalysed reactions.

Enzyme catalog number	**Mol% yield**	**% e.e**
ATA-261	41.89	99.99% R
ATA-262	45.13	85.14% R
ATA-254	43.10	95.08 % R
ATA-234	37.93	93.85 % R
ATA-242	1.87	55.93 % R
ATA-241	1.48	97.99% R

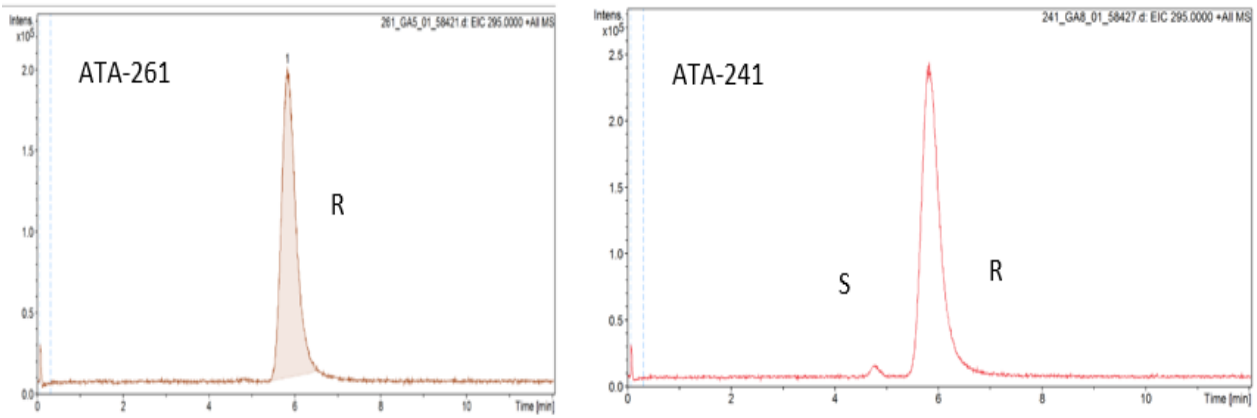

Figure 27: Chiral liquid chromatogram showing the (*R*)-selectivity of ATA-261 and ATA-241.

3.5 Reduction of amino ester **21** into amino alcohol **5**

The next objective was the reduction of the amino ester **21** into corresponding amino alcohol **5.** Lithium borohydride reduced standard α–amino ester into amino alcohol quite well in Chapter 2. We then decided to investigate this reagent on our β-amino ester **21,** unfortunately, the reaction did not proceed well. The NMR peaks were slightly shifted and the mass spectrum data indicated the presence of boron complexation with both hydroxyl and amino group forming a compound **24** (*Scheme 36*).We then attempted to cleave the complex using HCl as

previously investigated, unfortunately the boron remained attached to the compound .The boron complexed compound can still be used for confirmation of the stereochemistry in the polarimeter analysis. Additionally, we can grow a crystal and further confirm the absolute configuration using an X-ray crystal structure .

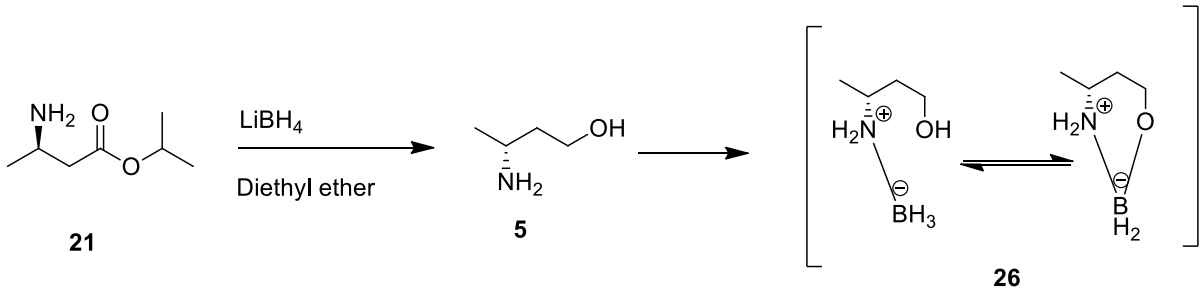

Scheme 36: Reduction of amino ester **21** into corresponding amino alcohol **5.**

The enzyme reaction was scaled up into 25-5ml (2.5 to 10 mmol)–scale (as in chapter 2) using both (*R*)-selective ATA-241 and ATA-254.Unfortunately, we were only able to isolate the starting material.

We then decided to downscale the reaction back to 5 ml scale and combined the product until we reached a total of 30 mg of the amino ester **21** starting material. Proceeding to the next reduction reaction using the same conditions as in the standard, the reaction outcome was unfortunately unsuccessful. The was no sign of the product, complexed product and even a starting material on the proton NMR analysis. It is evident that working with a beta-substrate **20** presents a significant challenge, specifically regarding the yields. To address this issue effectively, a major yield optimization strategy must be implemented in order to obtain an enough material for the reduction reaction.

3.6 Conclusion and Future work

Isopropyl β-ketoester substrate **20** was successfully screened against ω-Tams using isopropyl donor system, giving rise to amino ester product **21**. The mass spectra and the liquid chromatograms of our enzyme synthesized amine **21** corresponded to our standard amine **21**. This compound also behaved in the same manner as in chapter 2 where the proton NMR of the enzyme product differed from the standard. The proton at the stereogenic centre also exhibited a dramatic shift in the enzyme product (*Fig .29*).

When this product is employed in subsequent reactions, such as derivatization, the results of the amide **25** product obtained correspond to the standard amide **25**. From the LCMS data, we

can conclude that our reaction was a success, however further investigation has to be employed to further understand the NMR data obtained.

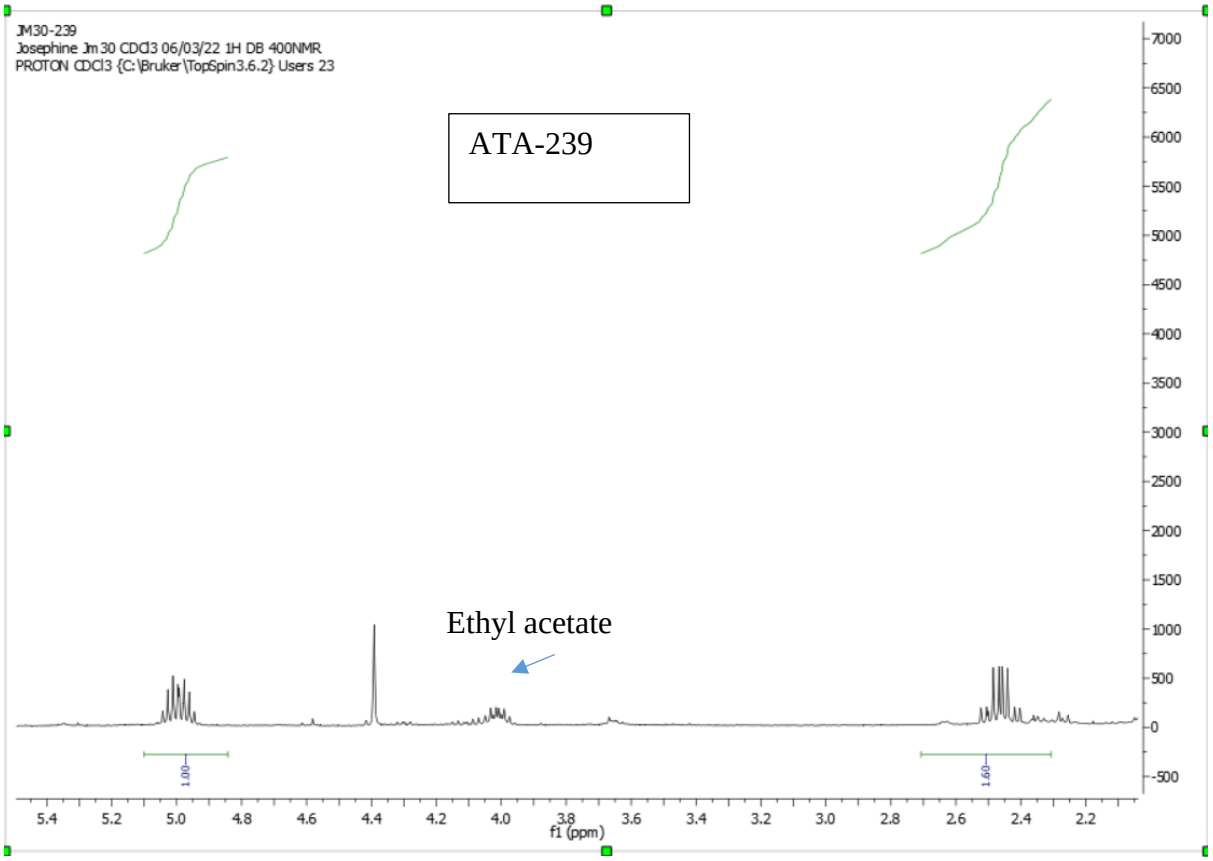

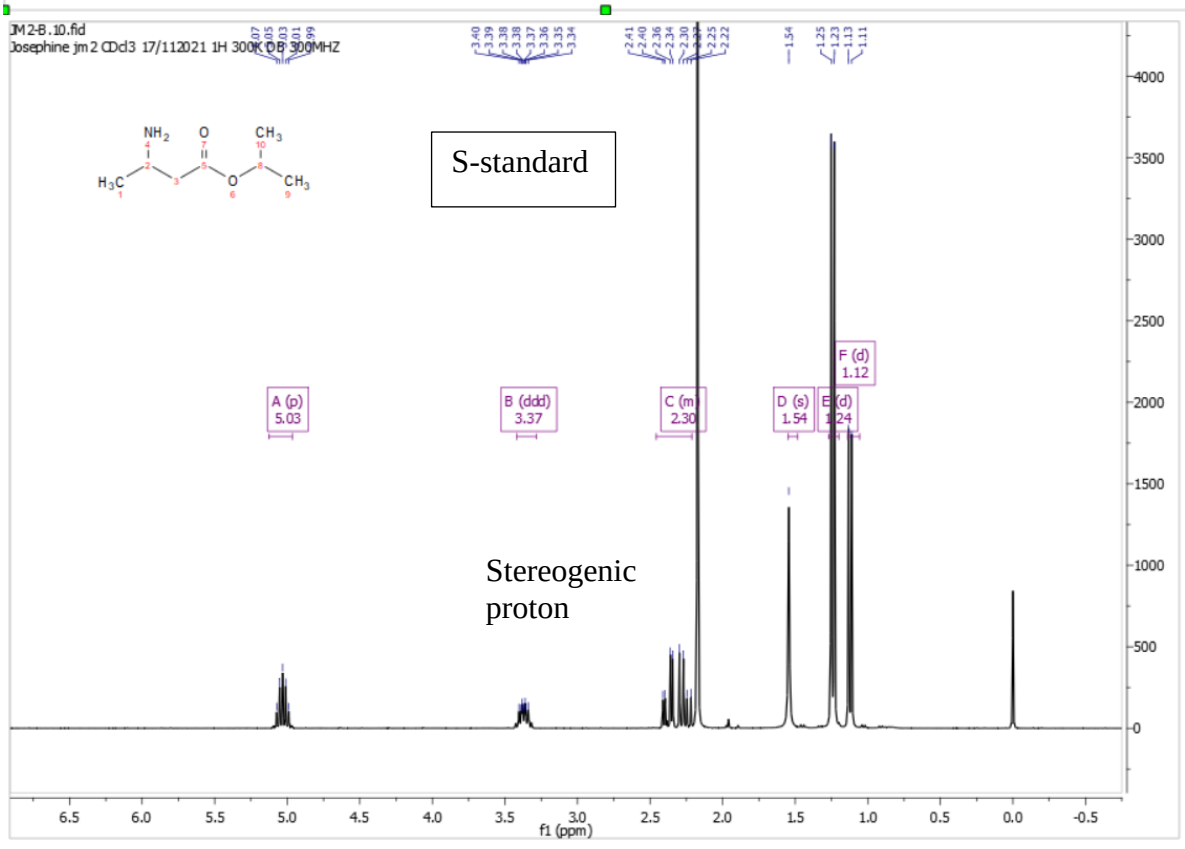

Figure 28: In the ^{1}H NMR spectrum of the enzyme product (above), the stereogenic proton has shifted from 3.5 ppm to 1.8 ppm in comparison to the standard spectrum (below).

Our derivatized amines **25** allowed us to determine the % e.e of our products. Within our library of ATA enzymes, the majority displayed (*R*)-selectivity, and we particularly identified five (*R*)-selective enzymes, ATA-254, 241, 261, 262, and 234, which exhibited % e.e values ranging from 85% to an impressive 99.99%. Additionally, their yields fell within the range of 38% to 45%. A significant challenge arose when attempting to scale up the reaction, to address this issue, we propose immobilizing our enzymes, with the goal of recycling and by incorporating it with flow chemistry, we can successfully improve our yields and facilitate large scale reactions.

In conclusion, the biotransformation of a cheap pro-chiral starting material **20** into a highly valuable enantioenriched amino ester intermediates **21** was successful. Although challenges were encountered in completing the final reduction step due to yield limitations, this approach still holds a potential to be used for the efficient and cost-effective production of the dolutegravir intermediate.

Chapter 4:

4. General conclusion and future work

In this study, we employed transaminase biocatalysis to efficiently transform inexpensive ketones into valuable amino ester products in only a single step. This method stands out significantly when compared to the conventional commercial synthesis processes, which typically involve a four-step procedure to achieve the same product. What makes our approach particularly noteworthy is that our synthesis operates under mild environmental conditions. While commercial synthesis often relies on methanol as a solvent, our method uses water, which is readily available and considerably more environmentally friendly. Furthermore, our process functions optimally at standard temperature and pressure conditions, eliminating the need for the high pressure and temperature typically required in the commercial method for the hydrogenation of nitro groups into amines in ethambutol synthesis and ruthenium catalysis in the synthesis of dolutegravir intermediate.

Developing our method revealed stereo-selective enzymes that exhibited exceptional enantiomeric excess, reaching an impressive 99.99% e.e, with unoptimized yields ranging from 40% to 75%. This is a substantial improvement over the conventional approach, where the maximum yield achievable is capped at 50% due to the chiral resolution step. Moreover, our enzymatic process stands out for its efficiency in waste reduction. Since our enzymes are stereoselective, there is no production of waste material (only acetone is released, and it can be recovered). In contrast, the commercial method generates substantial waste as approximately 50% as the undesired enantiomer is discarded. This not only underscores the sustainability of our approach but also highlights its economic and environmental advantages.

We conducted a cost estimation for our synthetic route using ethyl-2-oxobutanoate as a reference starting material, instead of isopropyl-2-oxobutanoate (*Table 9, appendix*). These two pro-chiral ketones are produced following the same basic schematic route, differing primarily in the choice of alcohol. In summary, the cost of these ketones is notably influenced by the price of the alcohol employed. The use of lithium borohydride as a reducing agent in large-scale synthesis is not cost-effective, and the associated extraction process can be hazardous, making it unsuitable for industrial applications. As previously mentioned, an alternative worth exploring is hydrogenation, a method commonly employed in the industry.

When using hydrogenation method, the total cost of the reaction comes to $54 per kilogram of ethambutol, assuming efficient recycling of tetrahydrofuran and alcohol (*Table 9, appendix*). This cost is approximately half of the cost of the existing industrial synthesis of ethambutol outlined in Table 8 in the appendix ($110.25 per kilogram). For future research, we can consider incorporating enzymes into the final reduction step to make the entire process more environmentally friendly. Furthermore, by immobilizing our enzymes and efficiently regenerating our co-factor, we can potentially achieve even further cost reductions in our synthetic route.

In the context of dolutegravir intermediate synthesis, we also conducted a cost estimation using ethyl acetoacetate instead of isopropyl acetoacetate (*Table 12, appendix*). Once again, it's essential to note that the cost of the starting material is closely linked to the price of the alcohol used. Based on our calculations, the cost comes to $126.09 per kilogram of the intermediate (*Table 12, appendix),* which is less expensive compared to the hydroxyl ketone method ($239.74 per kg, *Table 11, appendix*). The ruthenium method appears to be the most cost-effective among the asymmetric synthesis ($102.37 per kg, *Table 10, appendix*). However, as discussed previously, the ruthenium method may not align with our goal of green chemistry due to its environmental concerns. Our primary objective is to employ an environmentally friendly and cost-efficient method.

To further reduce the cost of our route, we can explore enzyme recycling and optimization of the reduction method. Additionally, we can investigate the incorporation of lipase catalysis in the transesterification process, converting the less expensive methyl acetoacetate into isopropyl acetoacetate. This approach not only lowers costs but also enhances the overall environmental sustainability of the route.

In conclusion, our method for the synthesis of (*S*)-2-aminobutanol and (*R*)-isopropyl-3-aminobutanoate holds a potential to replace existing methods, primarily due to its cost-effectiveness and environmentally friendly nature.

Chapter 5:

5. Experimental

5.1 General reagents and instrumentation

All reagents were obtained from commercial sources (Radchem and Sigma Aldrich) and they were used as received unless specified otherwise. The transaminase enzymes that were used throughout the project were purchased from Prozomix Limited (UK) and they were used without any further purification, estimated purity of the enzymes was 20 % w/w. NMR spectra were recorded at room temperature (295 K) using Avance 300 and 400 Bruker NMR spectrometers (300 and 400 MHz for ^{1}H spectra and 75 and 101 MHz for ^{13}C spectra). The samples were dissolved in deuterated solvents and the NMR data was processed and analyzed using MestreNova software. A Thermo Scientific Dionex Ultimate 3000 UHPLC instrument coupled to a Bruker Compact Q-TOF mass spectrometer was used for quantitative, qualitative, and stereoselectivity determination. Achiral HPLC analysis was performed under reverse phase conditions (5-95% acetonitrile/water) on a YMS-Triart Diol-Hydrophilic interaction chromatography column (HILIC) (150x30 mml D.S 3 µm, 12 nm). Chiral HPLC analysis was performed under the isocratic method conditions (water /acetonitrile) on an Astec Chirobiotic HPLC column (10 cm x 4.6 mm, 5 μm) and Daicel Chiralpak AD-RH chiral column (4.6 x 150 mm, 5 μm). Mass spectrometry analysis was performed using a positive mode electron ionization source (ESI).

5.2 Experimental procedures

5.2.1 Synthesis of diisopropyl oxalate 12

Method A

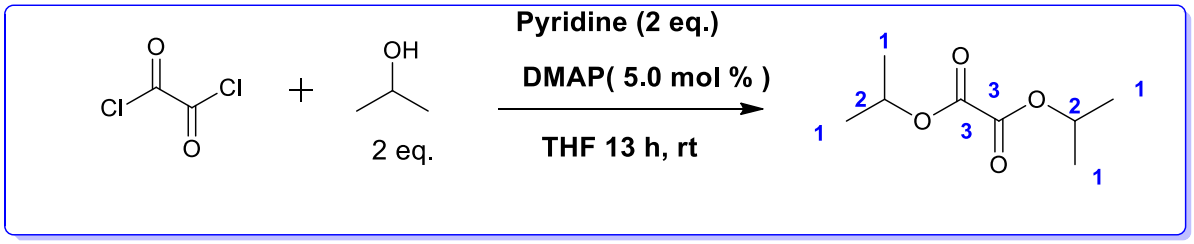

N, N'-dimethyl amino pyridine (DMAP)(722 mg, 5.91 mmol), dry pyridine (19.12 ml, 236.4 mmol), isopropanol (18.10 ml, 236.4 mmol), and THF (100 ml) were added into a dry 2-neck round bottom flask. While stirring, 10 ml oxalyl chloride was added dropwise into the reaction mixture and the reaction was left stirring for 13 hours at room temperature. The reaction mixture was diluted with saturated aq. NH_4Cl solution and extracted with diethyl ether (3x50 ml). The combined organic layers were washed with saturated aq. $NaHCO_3$ (100 ml), brine (100 ml), and dried over $MgSO_4$, then filtered and concentrated under reduced pressure. The yellow-orange oil crude product **12 (**67 %) was characterized using ^{1}H NMR and ^{13}C NMR. Diisopropyl oxalate is a known compound and the NMR data obtained correspond to those given in the literature. ^{1}H NMR (300 MHz, $CDCl_3$) δ 5.16 (hept, J = 6.3 Hz, 2H (*H2*)), 1.36 (d, J = 6.3 Hz, 12H(*H1*)). ^{13}C NMR (75 MHz, $CDCl_3$) δ = 158.2(*C3*), 71.3(*C2*), 21.7(*C1*)

Method B

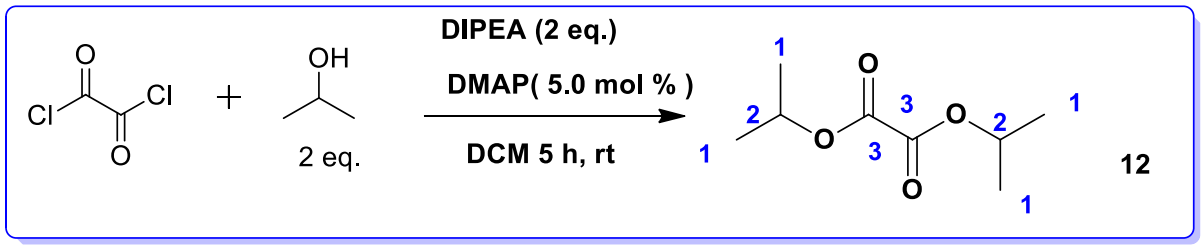

N, N'-Dimethyl amino pyridine (DMAP) (1.5 g,), diisopropylethylamine (DIPEA) (85 ml), isopropanol (40 ml), and dry DCM (150 ml) were added into a dry 2-neck round bottom flask. While stirring, 20 ml oxalyl chloride was added dropwise and the reaction was left stirring for 5 hours at room temperature. The reaction mixture was diluted with saturated aq. NH_4Cl solution and extracted with diethyl ether (3x50 ml). The combined organic layers were washed with saturated aq. $NaHCO_3$ (100 ml), brine (100 ml), and dried over $MgSO_4$, and then filtered and concentrated under reduced pressure. The orange oil crude product (80%) was characterized using ^{1}H NMR and ^{13}C NMR. ^{1}H NMR (300 MHz, $CDCl_3$) δ 5.16 (hept, J = 6.3 Hz, 2H(*H2*)), 1.36 (d, J = 6.3 Hz, 12H(*H1*)). ^{13}C NMR (75 MHz, $CDCl_3$) δ = 158.2(*C3*), 71.3(*C2*) 21.7(*C1*)

5.2.2 Grignard reaction for the synthesis of α-Keto-butyric-isopropyl ester substrate and α-Keto-butyric-ethyl ester 11

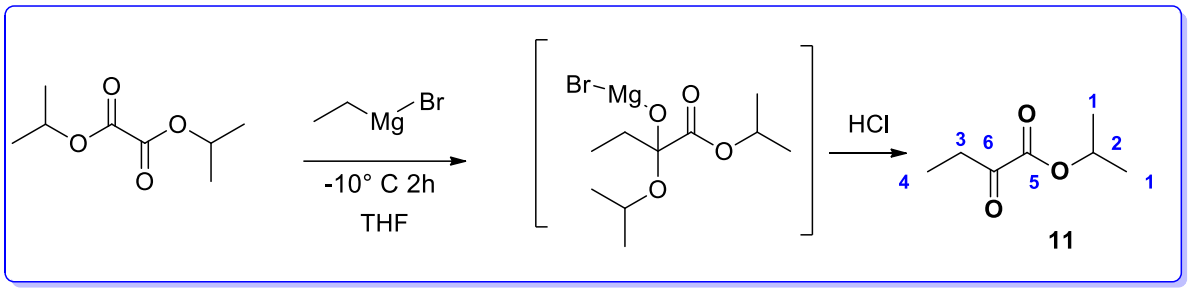

A mass of 2.53 g (23.23 mmol) of magnesium turnings and freshly distilled THF was added into an oven-dried two-neck round bottom flask. The mixture was gently stirred, and this was followed by the addition of 5% mmol of 1, 2-dibromoethane catalyst. The flask was gently heated to 60°C to expose the surface area of the magnesium turnings for the reaction to occur. Ethylene bromide (23.23 mmol) was added dropwise over a period of 15 minutes under stirring. During the addition, the mixture became turbid and warmed up to the boiling point, so that the rate of addition of ethyl bromide was controlled to maintain the mixture slightly boiling. When the addition was complete, the mixture was stirred for an hour; it was cooled and transferred into the dropping funnel. The Grignard reagent was added dropwise into the mixture of 60 ml THF and (23.23 mmol) alkyl oxalate. The reaction was stirred for 2 hours while maintaining the temperature of -10℃. The reaction was neutralized by quickly adding a solution of hydrochloric acid in water. The product was extracted with diethyl ether, washed with NH_4Cl (2×50 ml), $NaHCO_3$ (2x50 ml), and brine (2x50 ml) and dried over $MgSO_4$ then filtered and concentrated under reduced pressure. The product was purified using ether /hexane (1-3%) on a silica stationary phase to isolate 30-50 % of the product as a yellow oil. The products were characterized using ^1H and ^{13}C NMR. ^1H NMR (400 MHz, $CDCl_3$) δ 5.22 – 5.09 (m, 1H (*H2*)), 2.85 (q, *J* = 7.2 Hz, 2H(*H3*)), 1.33 (dd, *J* = 12.5, 5.3 Hz, 6H(*H1*)), 1.13 (t, *J* = 7.2 Hz, 3H (*H4*)). ^{13}C NMR (101 MHz, $CDCl_3$) δ 195.1(*C6*), 160.9(*C5*), 70.8(*C2*), 33.2 (*C3*), 21.8 (*C1*), 6.6(*C4*). **HRMS** (ESI+): calculated $C_7H_{12}O_3$ $[M+H]^+$ 145.0865, found $[M+H]^+$ 145.0866

Method B

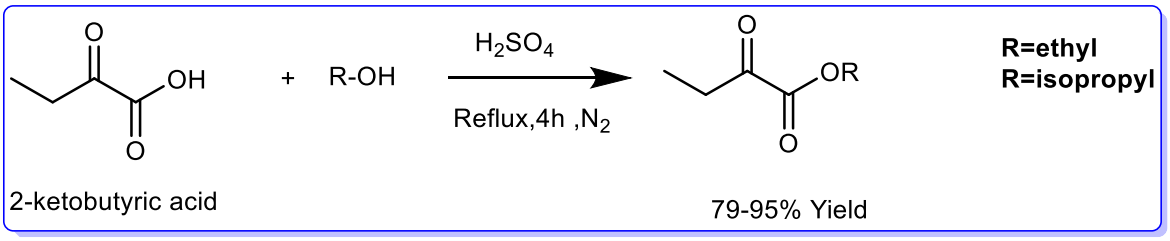

2-Oxobutanoic acid (2 g, 19.59 mmol) was dissolved in alcohol (ethanol or isopropanol), this was followed by the addition of H_2SO_4 (6.856 mmol). The mixture was refluxed for 4 hours under N_2 gas, cooled down, and dissolved in saturated $NaHCO_3$(100 ml). The product was extracted with ethyl acetate, washed (7x 40ml) with brine to ensure complete removal of the alcohol, dried over $MgSO_4$, and concentrated at reduced pressure. The product was isolated as a yellow oil with a yield ranging from 79-95 % and characterized using NMR spectroscopy; the NMR data correspond to those obtained when using the Grignard method.

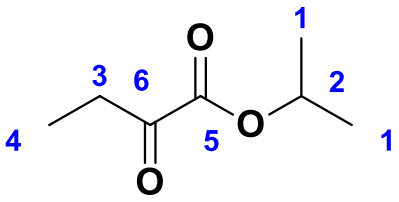

11

^{1}H NMR (400 MHz, $CDCl_3$) δ 5.22 – 5.09 (m, 1H(*H2*)), 2.85 (q, *J* = 7.2 Hz, 2H(*H3*)), 1.33 (dd, *J* = 12.5, 5.3 Hz, 6H(*H1*)), 1.13 (t, *J* = 7.2 Hz, 3H(*H4*)). ^{13}C NMR (101 MHz, $CDCl_3$) δ 195.1(*C6*), 160.9(*C5*), 70.8(*C2*) 33.2(*C3*), 21.8(*C1*), 6.6(*C4*). **HRMS** (ESI+): calculated $C_7H_{12}O_3$ $[M+H]^+$ 145.0865, found $[M+H]^+$ 145.0866

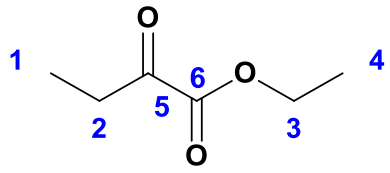

10

^{1}H NMR (400 MHz, $CDCl_3$) δ= 4.22 ppm (q, J = 7.2 Hz, 2H (*H3*), 2.80 ppm (q, *J* = 7.2, 2H(*H2*)), 1.30 ppm (t, *J* = 7.2 Hz, 3H(*H4*)), 1.06 ppm (t, J = 7.2 Hz, 1H(*H1*))]. ^{13}C NMR (101 MHz, $CDCl_3$) δ = 194.1 (*C5*), 159.9(*C6*), 61.4(*C3*), 31.6(*C2*), 12.9(*C4*) 5.6(*C1*)]. **HRMS** (ESI+): calculated $C_6H_{10}O_3$ $[M+1]^+$ 131.0708, found $[M+H]^+$ 131.0695.

5.2.3 Transesterification reaction for the synthesis of isopropyl acetoacetate 20.

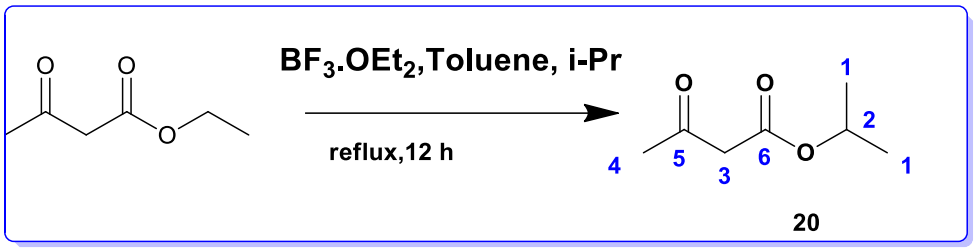

Ethyl acetoacetate (93 mmol, 10 ml) and isopropanol (139 mmol) were dissolved in dry toluene. While stirring, 15 mol% of BF3.OEt2 (13.9 mmol, 1.50 ml)was added dropwise to the mixture, and the resulting reaction mixture was refluxed for 12 hours under N_2 gas. The reaction mixture was cooled, and the catalyst was quenched with water and left to stir for 10 minutes. The product was extracted with DCM (2x 70 ml), washed with brine(2x 50ml) dried with anhydrous $MgSO_4$ and concentrated at reduced pressure. The product was purified using hexane on a silica stationary phase to isolate 8.575 g (64 %) of the product as orange oil. The product was characterized using ^{1}H and ^{13} C NMR. ^{1}H NMR (300 MHz, CDCl3) δ 5.07 (m, 1H(*H2*)), 3.42 (s, 2H(*H3*), 2.27 (s, 3H(*H4*)), 1.27 (d, J = 6.3 Hz, 6H(*H1*)). ^{13}C NMR (101 MHz, CDCl3) δ = 200.7(*C5*), 166.7(*C6*), 69.1(*C2*), 50.5(*C3*), 30.1(*C4*), 21.7(*C1*). **HRMS** (ESI+): calculated $C_7H_{12}O_3$ $[M+H]^+$ 145.0865, found $[M+H]^+$ 145.0864.

Method B

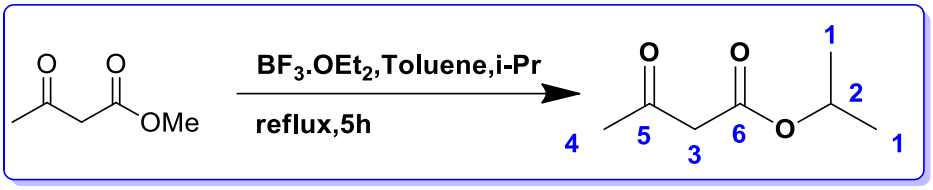

Methyl acetoacetate (95 mmol, 10 ml) and isopropanol (139 mmol) were dissolved in dry toluene. While stirring, 15 mol% of BF3.OEt2 (14.4 mmol, 2.02 ml) was added dropwise to the mixture, and the resulting reaction mixture was refluxed for 5 hours under N_2 gas. The reaction mixture was cooled, and the catalyst was quenched with water, and left to stir for 10 minutes.The product was extracted with DCM (2x 70 ml), washed with brine (2x 50 ml), dried with anhydrous $MgSO_4$ and concentrated at reduced pressure. The product was purified using ether/hexane on a silica stationary phase to isolate 10.830 g (80 %) of the orange oil product. The product was characterized using ^{1}H and ^{13} C NMR. ^{1}H NMR (300 MHz, CDCl3) δ 5.07 (m, 1H(*H2*)), 3.42 (s, 2H(*H3*), 2.27 (s, 3H(*H4*)), 1.27 (d, J = 6.3 Hz, 6H(*H1*)). ^{13}C NMR (101 MHz, CDCl3) δ = 200.7(*C5*), 166.7(*C6*), 69.1(*C2*), 50.5(*C3*), 30.1(*C4*), 21.7(*C1*). **HRMS** (ESI+): calculated $C_7H_{12}O_3$ $[M+H]^+$ 145.0865, found $[M+H]^+$ 145.0864.

5.2.4 Synthesis of reference *rac a*nd *(S)* -2-aminobutyric –isopropyl ester and reference *rac* & *(S)* -2-aminobutyric –ethyl ester.

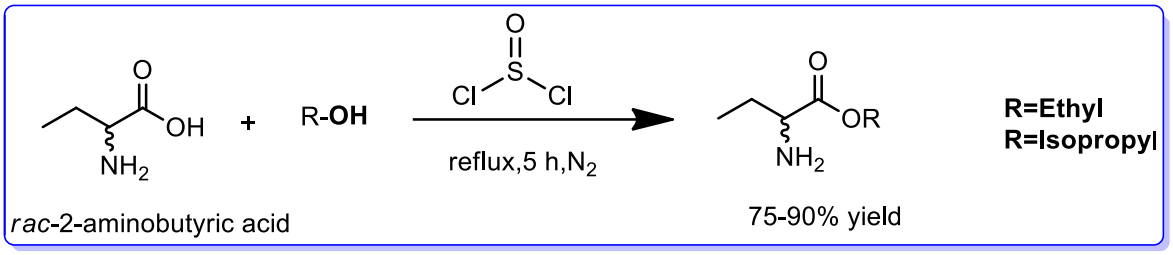

A mass 100 mg (0.97 mmol) of *rac*-2-aminobutyric acid was dissolved in 5 ml of alcohol (ethanol or isopropanol) in a dry 2-neck round bottom flask. while stirring, 85 µl of thionyl chloride (1.16 mmol) was added dropwise in room temperature. The reaction was then refluxed under nitrogen for 5 hours. The reaction mixture was cooled down and the pH was adjusted to 9.0 using NaOH. The product was extracted using ethyl acetate, washed with brine (2x5 ml), dried over $MgSO_4$, then filtered and concentrated under reduced pressure. The products were isolated as yellow oil with yields ranging from 75-95% and characterized using ^{1}H and ^{13}C NMR.

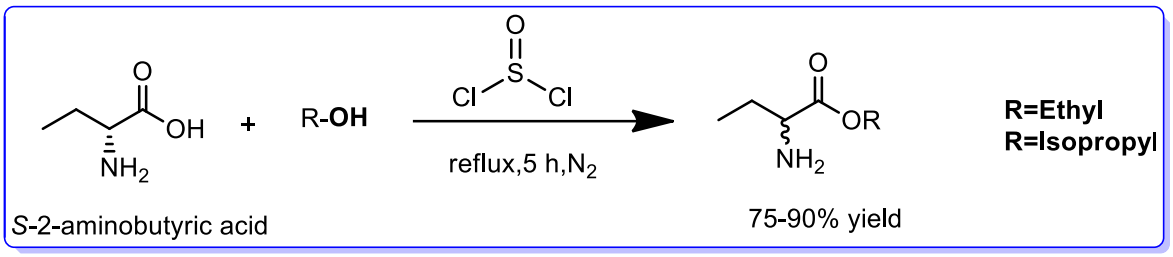

A mass 100 mg (0.97 mmol) of *S*-2-aminobutyric acid was dissolved in 5 ml of alcohol (ethanol or isopropanol) in a dry 2-neck round bottom flask .while stirring, 85 µl of thionyl chloride (1.16 mmol) was added dropwise in room temperature. The reaction was then refluxed under nitrogen for 5 hours. The reaction mixture was cooled down and the pH was adjusted to 9.0 using NaOH. The product was extracted using ethyl acetate, washed with brine (2x5 ml), dried over $MgSO_4$, then filtered and concentrated under reduced pressure. The products were isolated as yellow oil with yields ranging from 75-95% and characterized using ^{1}H and ^{13}C NMR.

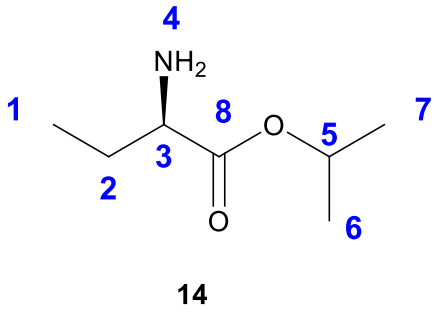

14

1H NMR (400 MHz, CDCl3) δ 5.11 – 5.00 (m, 1H(*H5*)), 3.34 (t, J = 6.2 Hz,1H(*H3*), 1.81 – 1.70 (m, 1H(*H2*)), 1.66 – 1.61 (m, 1H(*H2*), 1.47 (s, 2H(NH_2)), 1.25 (dd, J = 6.1, 3.4 Hz, 6H (*H7&H8*)), 0.95 (t, J = 7.5 Hz, 3H(*H1*) .^{13}C NMR (101 MHz, $CDCl_3$) δ 168.2 (*C8*), 70.8(*C5*), 54.2 (*C3*), 23.5(*C2*), 20.9(*C7&C8*), 9.2(*C1*). **HRMS** (ESI+): calculated $C_7H_{15}NO_2$ $[M+H]^+$ 146.1181, found $[M+H]^+$ 146.1160

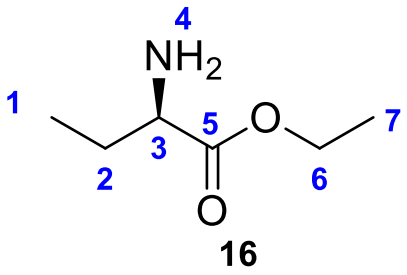

16

^{1}H NMR (400 MHz, $CDCl_3$) δ= 4.18 (q, *J*= 6.5 Hz, 2H (*H6*)), 3.38 (t, *J* = 6.3 Hz, 1H (*H3*)), 1.84 – 1.70 (m, 1H(*H2*)), 1.69 – 1.57 (m, 1H(*H2*)), 1.48 (s, 2H(NH_2)), 1.28 (t, *J* = 7.1 Hz, 3H(*H7*)), 0.96 (t, *J* = 7.5 Hz, 3H(*H1*)).

5.2.5 Synthesis of reference *rac a*nd *(S)* -3-aminobutyric–isopropyl ester 21.

2.1.2.1 **5.2.5.1 Reductive amination using ammonia.**

Step 1

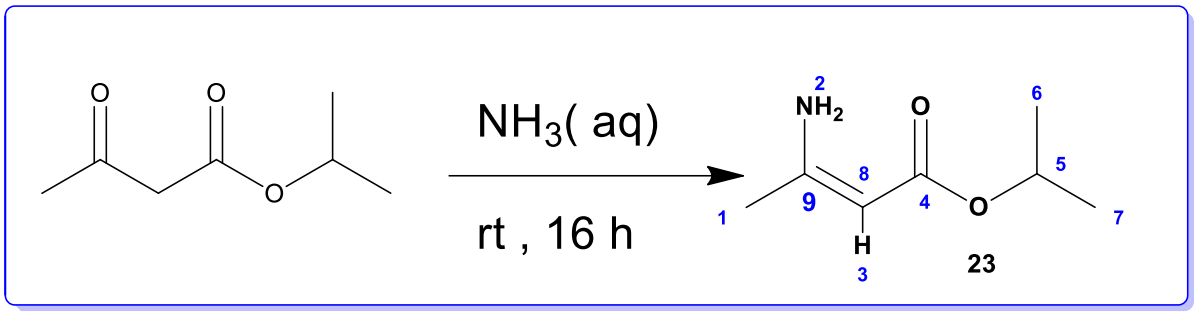

23

A mixture of isopropyl acetoacetate (3.85 mmol, 0.5 ml) and 25% aqueous ammonia (25.83mmol, 0.5 ml) was stirred at room temperature for 30 minutes, additional 0.5 ml of ammonia was added into the reaction and the mixture was left stirring for 16 hours in atmospheric temperature. The resulting mixture was dissolved in 0.3 ml $NaHCO_3$ and extracted with 0.5 ml ethyl acetate (3x). The organic layer was dried over $MgSO_4$ and concentrated under reduced pressure. The crude product was characterized using ^{1}H NMR. ^{1}H NMR (300 MHz,

$CDCl_3$) δ 7.92 (s, 2H(NH2))5.07 – 4.94 (m, 1H(*H5*)), 4.50 (s, 1H (*H3*)), 1.90 (s, 3H(*H1*)), 1.27 – 1.20 (m, 6H(*H6&H7*)).

Step 2: Method A

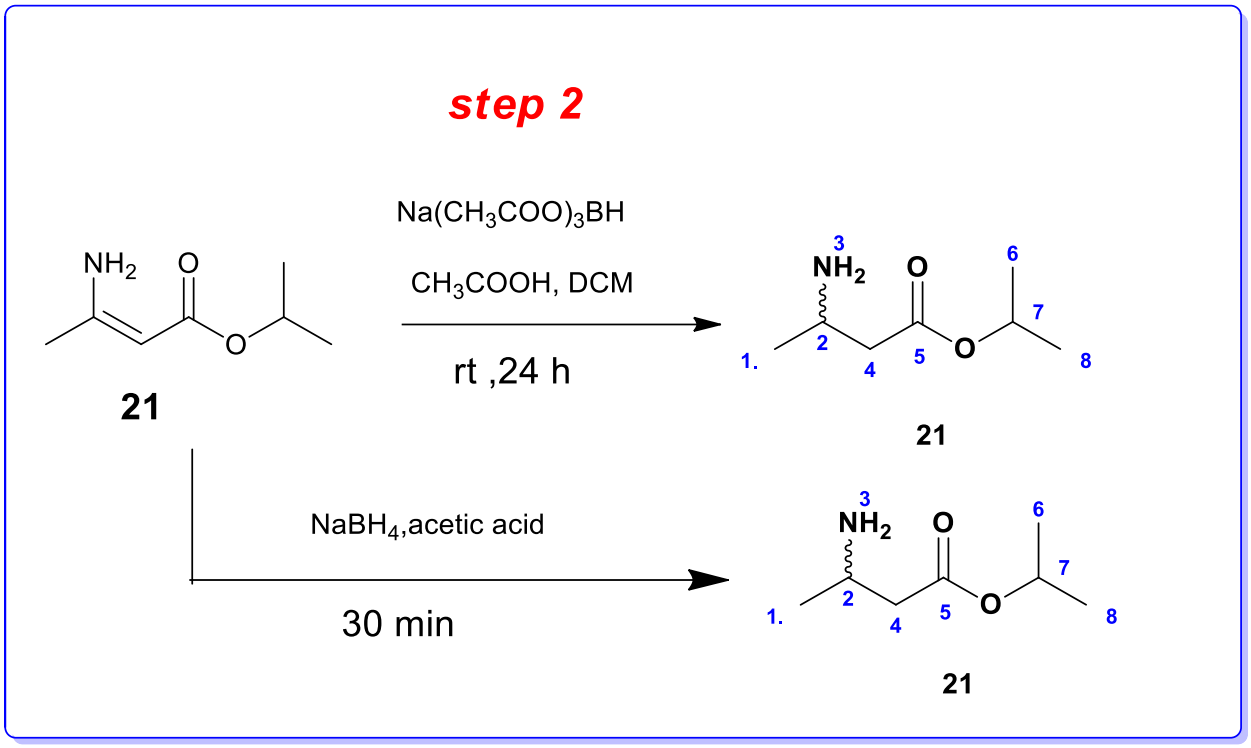

Enamine ester (50.00 mg,0.3492 mmol) and acetic acid (0.5238 mmol, 29.95 μL) was dissolved in 10 ml DCM. This was followed by addition of Na $(CH_3COO)_3BH$, and the mixture was stirred overnight under N_2 at room temperature. The mixture was dissolved in DCM, washed with $NaHCO_3$(2x 10ml) and brine (2x 10ml) then dried over anhydrous $MgSO_4$ and concentrated under reduced pressure. The product was characterized using ^1H and ^{13} C NMR. ^1H NMR (300 MHz, $CDCl_3$) δ= 5.03 (h, *J* = 6.3 Hz, 1H(*H7*)), 3.40 – 3.34 (m, 1H(*H2*)), 2.46 – 2.21 (m, 2H(*H4*)), 1.54 (s, 2H(NH_2)), 1.24 (d, *J* = 6.3 Hz, 6H(*H6&H8*)), 1.12 (d, *J* = 6.4 Hz, 3H(*H1*)).^{13}C NMR (75 MHz, $CDCl_3$) δ 171.9(*C5*), 67.6(*C7*), 44.7(*C9*), 44.1(*C4*), 23.5(*C6&C8*), 21.9(*C1*). **HRMS** (ESI+): calculated $C_7H_{15}NO_2$ $[M+H]^+$ 146.1164, found $[M+H]^+$ 146.1177.

Step 2: Method B- solvent free method

Enamino ester (500mg, 3.492 mmol) was accurately weighed and transferred into a mortar, a mole equivalent quantity of citric acid was added, and the mixture was ground with a pestle for a minute. $NaBH_4$ was added and the resulting mixture was further grounded for 30 minutes. The borohydride was quenched with water and the product was extracted with ethyl acetate. The organic layer was dried over anhydrous $MgSO_4$ and concentrated under reduced pressure to afford a yellow oil product (17%). The product was characterized using ^{1}H and ^{13} C NMR. ^{1}H NMR (300 MHz, $CDCl_3$) δ= 5.03 (h, *J* = 6.3 Hz, 1H (*H7*)), 3.40 – 3.34 (m, 1H(*H2*)), 2.46 – 2.21 (m, 2H (*H4*)), 1.54 (s, 2H(NH_2)), 1.24 (d, *J* = 6.3 Hz, 6H(*H6&H8*)), 1.12 (d, *J* = 6.4 Hz, 3H(*H1*)).^{13}C NMR (75 MHz, $CDCl_3$) δ 171.9(*C5*), 67.6(C7), 44.7(*C9*), 44.1(*C4*), 23.5(*C6&C8*), 21.9(*C1*). **HRMS** (ESI+): calculated $C_7H_{15}NO_2$ $[M+H]^+$ 146.1164, found $[M+H]^+$ 146.1165.

5.2.5.2 Alternative approach for the synthesis of rac and (S)-3-aminobutyric–isopropyl ester 21.

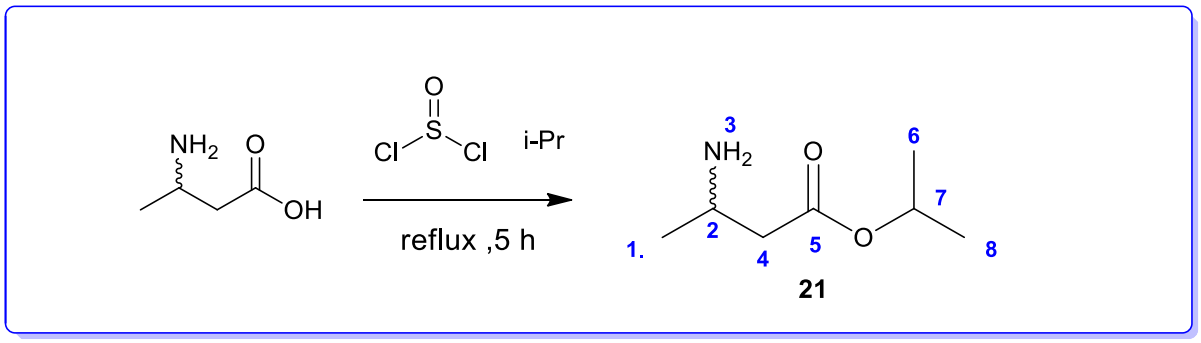

A mass 100 mg (0.97 mmol) of (*S*)-3-aminobutyric acid was dissolved in isopropanol in a dry 2-neck round bottom flask while stirring, 85 µl of thionyl chloride (1.16 mmol) was added dropwise in room temperature. The reaction was then refluxed under nitrogen for 5 hours. The reaction mixture was cooled down and the pH was adjusted to 9 using 2M NaOH. The product was extracted using ethyl acetate, washed with brine (2x5 ml), dried over $MgSO_4$, then filtered and concentrated under reduced pressure. The products were isolated as yellow oil with the yield of 90% and characterized using ^{1}H and ^{13} C NMR. ^{1}H NMR (300 MHz, $CDCl_3$) δ= 5.03 (h, *J* = 6.3 Hz, 1H(*H7*)), 3.40 – 3.34 (m, 1H(*H2*)), 2.46 – 2.21 (m, 2H (*H4*)), 1.54 (s, 2H(NH_2)), 1.24 (d, *J* = 6.3 Hz, 6H(*H6&H8*)), 1.12 (d, *J* = 6.4 Hz, 3H(*H1*)).^{13}C NMR (75 MHz, $CDCl_3$) δ 171.9(*C5*), 67.6(*C7*), 44.7(*C9*), 44.1(*C4*), 23.5(*C6&C8*), 21.9(*C1*). **HRMS** (ESI+): calculated $C_7H_{15}NO_2$ $[M+H]^+$ 146.1164, found $[M+H]^+$ 146.1170.

5.2.**6 Derivatization of 2-aminobutyric–isopropyl ester into para-nitro benzoic-isopropyl ester 17 for HPLC method development**.

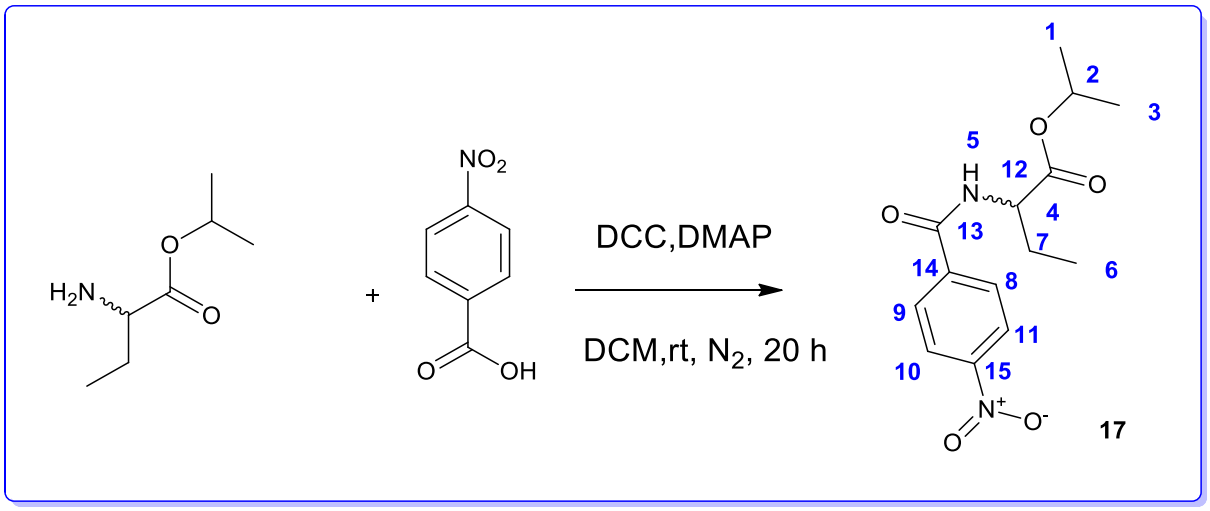

Para–nitro benzoic acid (103.65 mg, 0.6202 mmol), DCC (153.56 mg, 0.7442 mmol) coupling reagent and DMAP (15.15 mg, 0.1240 mmol) catalytic base were dissolved in 15 ml DCM. The reaction mixture was stirred at room temperature, under N_2 gas for 24 hours. The product was extracted with DCM (2x 50ml), washed with $NaHCO_3$ (2x 20ml), brine (2x 20ml), dried over $MgSO_4$ then filtered and concentrated under reduced pressure. The product was purified using 10-25% ethyl acetate-hexane to afford a light-yellow powder (109.52 mg, 60% yield). ^{1}H NMR (300 MHz, $CDCl_3$) δ 8.35 – 8.27 (m, 2H(*H10&H11*)), 8.03 – 7.94 (m, 2H (*H9&H8*)), 6.90 (d, *J* = 7.2 Hz, 1H(*H5*)), 5.12 (hept, *J* = 6.3 Hz, 1H(*H2*)), 4.77 – 4.66 (m, 1H *H4*)), 2.12 – 1.97 (m, 1H (*H7*)), 1.93 – 1.81 (m, 1H(*H7*)), 1.30 (dt, *J* = 11.7, 5.9 Hz, 6H(*H1&H3*)), 0.98 (t, *J* = 7.5 Hz, 3H(*H6*)). ^{13}C NMR (101 MHz, $CDCl_3$) δ = 171.8(*C12*), 164.6(*C13*), 150.1(*C15*), 139.2(*C14*), 128.3(*C9&C8*), 124.0(*C11&C10*), 69.1(*C2*), 53.3(C4), 26(*C7*), 21.4(*C1&C3*), 8.8(*C6*). **HRMS** (ESI+): calculated $C_{14}H_{18}N_2O_5$ $[M+H]^+$ 295.1294, found $[M+H]^+$ 295.1295 .

5.2.7 Derivatization of 3-aminobutyric–isopropyl ester into para-nitro benzoic-isopropyl ester for HPLC method development.

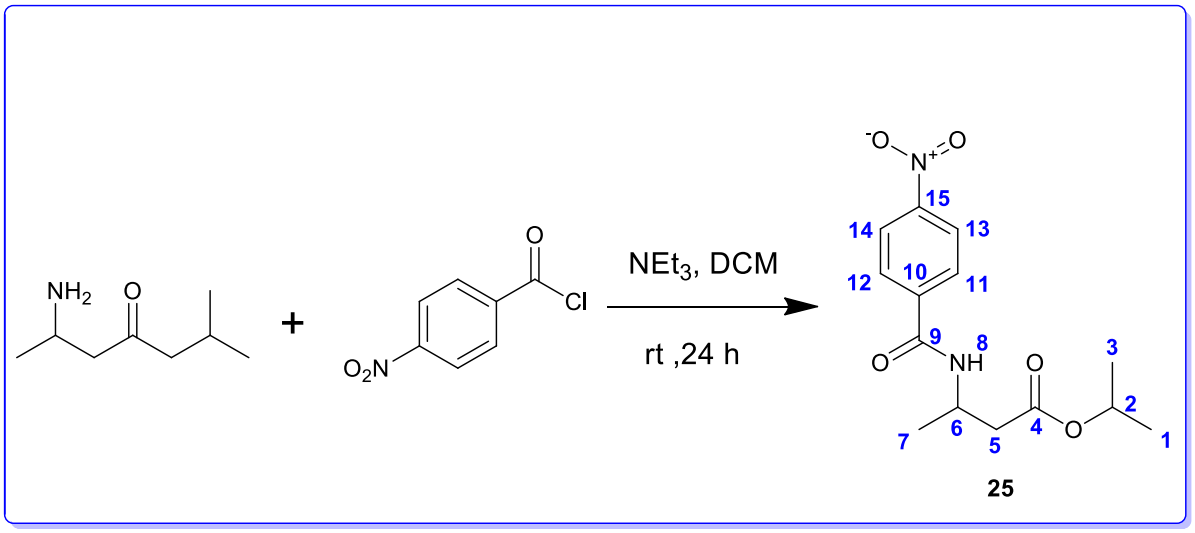

Para-nitrobenzyl chloride (57 mg, 0.3411 mmol), was dissolved in 5 ml of dry DCM. This solution was added dropwise to a mixture of amino ester (50 mg, 411 mmol), triethyl amine (29.!) and 7 ml DCM. The reaction was left stirring at room temperature, under N_2 gas for 24 hours. The product was extracted with DCM (2x 30ml) and washed with $NaHCO_3$ (2x 20 ml) and brine (2x 20 ml), dried over $MgSO_4$ then filtered and concentrated under reduced pressure. The product was purified using 10-25% ethyl acetate-hexane to afford 60.24 mg of a light-yellow powder. ^{1}H NMR (400 MHz, $CDCl_3$) δ 8.33 – 8.22 (m, 2H(*H14&H13*)), 7.99 – 7.89 (m, 2H(*H11&H12*)), 5.12 – 5.01 (m, 1H(*H2*)), 4.68 – 4.47 (m, 1H(*H6*)), 2.74 – 2.46 (m, 2H(*H5*)), 1.60 (s, 1H(*H8*), 1.35 (d, *J* = 6.8 Hz, 6H(*H1&H3*)), 1.30 – 1.25 (m, 3H(*H7*)).^{13}C NMR (101 MHz, $CDCl_3$)δ=171.8(*C4*), 164.2(*C9*), 139.8(*C15*), 128.3(*C10*), 123.9 (*C11&C12*), 69.0(*C2*), 43.1(*C6*), 39.7(*C5*), 21.9 (*C1&C3*), 19.6(*C7*).

5.2.8 Reduction of 2-aminobutyric–isopropyl ester into 2-aminobutanol 4

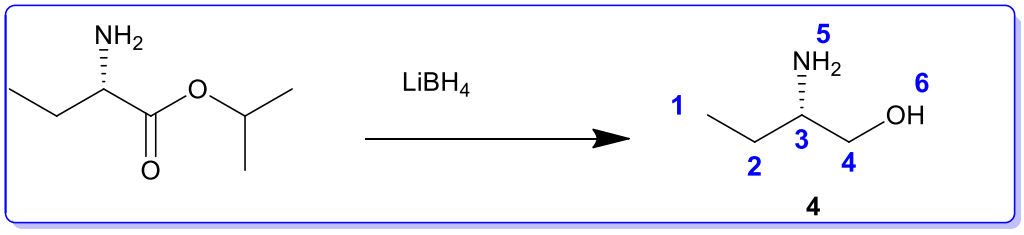

2-Aminobutyric–isopropyl ester (100 mg, 0.688mmol) was dissolved with 20 ml dry diethyl ether, while stirring, 2.5 equivalence of lithium borohydride (37.6 mg, 1.72mmol) was added into the mixture. The reaction mixture was stirred in room temperature for 30 minutes, followed by refluxing at 40°C for 6- 24 hours. The mixture was cooled down and the lithium borohydride was quenched with 1 ml of water, pH was then adjusted to 11 using 20 mM of NaOH. The product was extracted with ethyl acetate (2x 40ml), washed with brine (2x 30ml), dried over $MgSO_4$ then filtered and concentrated under reduced pressure. The yellow oil was isolated with 50% yield (30.66 mg) and characterized using NMR spectroscopy. ^{1}H NMR (300 MHz, $CDCl_3$) δ= 4.37 (d, *J* = 12.1 Hz, 1H(*H6*)), 3.92 (dt, *J* = 10.5, 5.2 Hz, 1H(*H4*)), 3.60 (d, *J* = 6.4 Hz, 1H(*H4*)), 3.2 (s, 2H(*H5*)), 2.76 (dtd, *J* = 9.0, 5.8, 3.1 Hz, 1H(*H3*), 1.80– 1.75(m, 1H(*H2*)), 1.60 – 1.38 ppm (m, 1H(*H2*)), 1.08 – 0.89 ppm (m, 3H(*H1*)) .^{13}C NMR (75 MHz, $CDCl_3$) δ = 60.8(*C4*), 59.6(*C3*), 22.3(*C2*), 9.4(*C1*). **HRMS** (ESI+): calculated $C_4H_{11}NO$ $[M+H]^+$ =90.0919, found $[M+H]^+$ = 90.0925.

5.2.9 Reduction of 3-aminobutyric–isopropyl ester into 3-aminobutanol 5

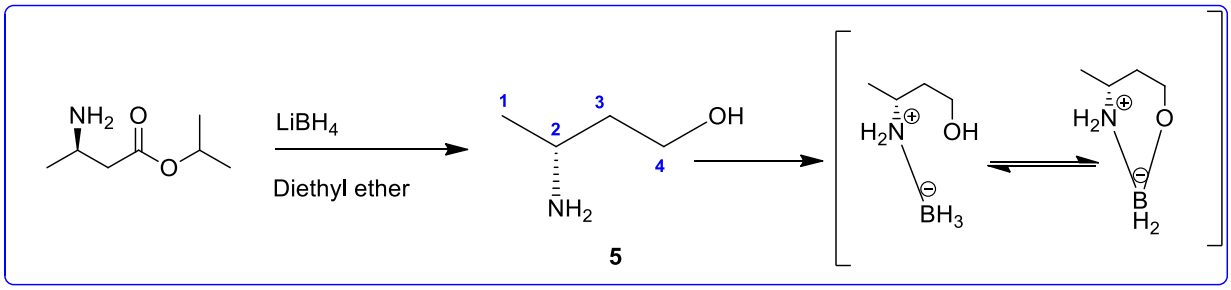

3-Aminobutyric –isopropyl ester (100 mg, 0.688 mmol) was dissolved with 20 ml dry diethyl ether while stirring, 2.5 equivalence of lithium borohydride (37.6 mg, 1.72 mmol) was added into the mixture. The reaction mixture was stirred in room temperature for 30 minutes, followed by refluxing at 40°C for 24 hours. The mixture was cooled, and the lithium borohydride was quenched with 1 ml of water, pH was then adjusted to 11 using 20 mM of NaOH. The product was extracted with ethyl acetate (2x 40ml), washed with brine (2x 30ml), dried over $MgSO_4$ then filtered and concentrated under reduced pressure. The yellow oil was isolated with 42% yield (25.76 mg) and characterized using NMR spectroscopy. ^{1}H NMR (400 MHz, $CDCl_3$) δ 4.89 (s, 1H), 3.96 – 3.71 (m, 2H), 3.35 (s, 1H), 3.03 (d, *J* = 3.0 Hz, 1H), 1.80 – 1.65 (m, 3H), 1.25 (d, *J* = 6.6 Hz, 3H). ^{13}C NMR (101 MHz, $CDCl_3$) δ = 59.9(*C4*), 53.1(*C3*), 34.8(*C2*), 18.3 (*C1*). **HRMS** (ESI+): calculated $C_4H_{13}NO$ $[M+H]^+$ =102.1012 found $[M+H]^+$ =102.1047.

5.3 Enzyme reaction

5.3.1 General enzyme screening procedure

Transamination of ketoesters substrates were run at 1 ml scale using an isopropyl amine donor system under the following conditions: 100 mM potassium phosphate buffer, 5 mg/l pyridoxal-5-phosphate, 1 M isopropyl amine, 20 mM ketoesters substrate and 5 mg transaminase (ATA). Reactions were run at 30℃, pH 7.5 in an incubator shaker (250 rpm) for 24 hours. 28 Prozomix enzymes were screened using the same conditions. The products were extracted by dissolving 120 µl of the crude product into 500 μL of HPLC acetonitrile, 100 µl of brine, and $NaHCO_3$. The organic layer was separated by centrifugation (5 minutes, 13000 rpm). The top clear layer was extracted and directly injected into high-resolution LCMS for qualitative analyses.

Preparation of stock solution

Pyridoxal-5-phosphate (5 mg/l) was added into potassium phosphate buffer solution (pH 7.5). The 40 Mm keto-ester substrate and 2M isopropyl amine stock solutions were then prepared using PLP-containing phosphate buffer solution.

Scaled -up reaction procedure.

ATA-enzyme (250 mg) was weighed into 100 ml Erlenmeyer flask followed by addition of 25ml of 40 mM of substrate stock solution and 25 ml of 2M isopropyl amine stock solution. The reaction was conducted at 40℃ in an incubator shaker (250 rpm) for 5 hours. The pH of the reaction mixture was adjusted to 9 using $NaHCO_3$(aq) and 0.5 g of NaCl was added. The product was extracted (3x) using 50 ml ethyl acetate. The organic layers were combined, dried over $MgSO_4$ then filtered and concentrated under reduced pressure. The resulting yellow oil was isolated and characterized using NMR and LCMS

Enzyme product NMR data

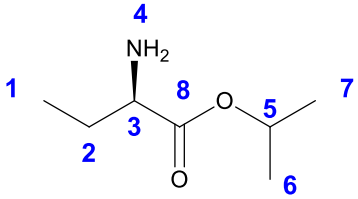

1H NMR (400 MHz, CDCl3) δ 5.11 – 5.00 (m, 1H(*H5*)), 1.63 – 1.61 (m,1H(*H3*), 1.81 – 1.70 (m, 1H(*H2*)), 1.66 – 1.61 (m, 1H(*H2*), 1.47 (s, 2H(NH_2)), 1.25 (dd, J = 6.1, 3.4 Hz, 6H (*H7&H8*)), 0.95 (t, J = 7.5 Hz, 3H(*H1*). **HRMS** (ESI+): calculated $C_7H_{15}NO_2$ $[M+H]^+$ 146.1181, found $[M+H]^+$ 146.1160

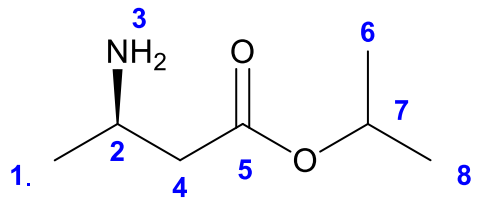

^{1}H NMR (300 MHz, $CDCl_3$) δ= 5.03 (h, *J* = 6.3 Hz, 1H (*H7*)), 4.07– 4.03 (m, 1H(*H2*)), 2.46 – 2.21 (m, 2H (*H4*)), 1.54 (s, 2H(NH_2)), 1.24 (d, *J* = 6.3 Hz, 6H (*H6&H8*)), 1.12 (d, *J* = 6.4 Hz, 3H(*H1*)). **HRMS** (ESI+): calculated $C_7H_{15}NO_2$ $[M+H]^+$ 146.1164, found $[M+H]^+$ 146.1177

Method for % e.e determination.

$$\% \text{ e.e} = \frac{peak\ area\ \ of\ a\ major\ enantiomer - peak\ area\ of\ a\ minor\ enatiomer}{eak\ area\ \ of\ a\ major\ enantiomer + peak\ area\ of\ a\ minor\ enatiomer} \times 100$$

5.4 X-Ray diffraction crystal structure method.

Single crystals of $C_{14}H_{18}N_2O_5$ were grown by slow evaporation of ethyl acetate-hexane**.** A suitable crystal was selected and subjected on a Bruker APEX-II CCD diffractometer. The crystal was kept at 173.00 K during data collection. Using Olex2, the structure was solved with the SHELXT structure solution program using Intrinsic Phasing and refined with the SHELXL refinement package using least squares minimization.

Table 6 Crystal data and structure refinement for 23mb_DeanB3_JM101_Cu_0f.

Identification code	23mb_DeanB3_JM101_Cu_0f
Empirical formula	$C_{14}H_{18}N_2O_5$
Formula weight	294.30
Temperature/K	123.00
Crystal system	orthorhombic
Space group	$P2_12_12_1$
a/Å	5.0930(4)
b/Å	8.7950(6)
c/Å	32.437(2)
α/°	90
β/°	90
γ/°	90
Volume/Å^3	1452.93(18)
Z	4
ρ_{calc}g/cm^3	1.345
μ/mm^{-1}	0.863
F(000)	624.0
Crystal size/mm^3	0.25 × 0.04 × 0.029

Radiation	CuKα (λ = 1.54178)
2Θ range for data collection/°	10.422 to 136.936
Index ranges	-6 ≤ h ≤ 5, -10 ≤ k ≤ 10, -34 ≤ l ≤ 38
Reflections collected	19496
Independent reflections	2621 [R_{int} = 0.0928, R_{sigma} = 0.0620]
Data/restraints/parameters	2621/0/197
Goodness-of-fit on F^2	1.055
Final R indexes [I>=2σ (I)]	R_1 = 0.0603, wR_2 = 0.1253
Final R indexes [all data]	R_1 = 0.0869, wR_2 = 0.1367
Largest diff. peak/hole / e $Å^{-3}$	0.24/-0.27
Flack parameter	0.1(2)

5.5 LCMS data: Ethambutol

5.5.1 Quantitative analysis calculations

Example of calculations carried out to determine the quantity of the product when working in a 1ml -scale reaction

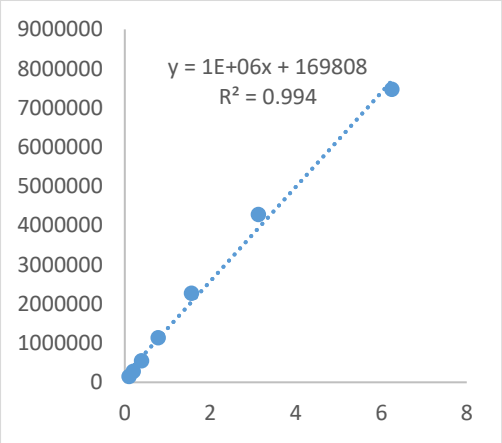

Theoretical yield

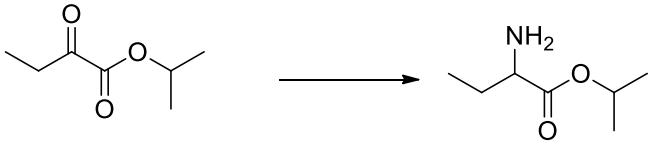

- $c = \frac{n}{v}$, $n = cv$

C (substrate in 1000μL) = 20Mm

- n = (0.02 M) (0.001 L) =2×10^{-5}mol

$n(substate) = n(product) =$ 2×10^{-5}mol

During extraction, 0nly 120 μL of original reaction mixture was extracted, so the maximum number of moles that can be obtained theoretically will be $(2 \times 10^{-5} mol) \times \frac{120}{1000}$= $2.4 \times 10^{-6}\ mol$

Theoretical mass of the product = $2.4 \times 10^{-6}\ mol \times \left(\frac{145.1995 g}{mol}\right) = 0.3484\ mg$

189 –enzyme quantitative

Original area of 189-enzyme = 42168180

Area after 20X dilution = 5793937

Equation of the standard curve straight line graph y=1000000x +169808

From the equation we can estimate the concentration of the product extracted in 500 μL Acetonitrile.

$$y = 1000000x + 169808$$

$$5793937 - 169808 = 1000000\text{x}$$

$$x = 5.6241\ ppm$$

$$= 5.6241\,\frac{mg}{L} \times (dilution\ factor\ 20)$$

$$=112.48\ \text{mg/l}$$

Conversion of ppm into mg

Assumption: 100% extraction of the product into 500 μL ACN (organic layer)

$$112.48\,\frac{mg}{L} \times (0.0005\ L)$$

$$= 0.056241\ mg$$

Theoretical mass = $0.3484\ mg$

% yield = $\frac{0.0562}{0.3484} = 16.139\%$

T*able 7: Quantitative analysis of amino ester **14** in Figure 15.*

Enzyme catalogue number	Mol/mol % yield
ATA-194	22.05
ATA-254	18.39
ATA-81	17.19
ATA-252	19.93
ATA-192	22.07
ATA-187	21.73
ATA-195	22.83
ATA-93	0
ATA-207	21.31
ATA-262	23.42
ATA-31	20.52
ATA-174	15.82
ATA-168	3.04
ATA-170	0
ATA-47	3.95
ATA-26	0
ATA-89	21.13
ATA-188	13.58
ATA-206	6.02
ATA-230	20.70
ATA-190	2.63
ATA-191	14.71

ATA-173	2.38
ATA-169	19.42
ATA-248	0.25
ATA-231	24.58
ATA-251	0.24
ATA-247	0.85
ATA-243	19.27
ATA-250	0.17
ATA-255	18.38
ATA-246	0.23
ATA-232	8.15
ATA-235	0.28
ATA-237	0.24
ATA-240	1.03
ATA-234	6.81

5.5.2 Achiral: HPLC analysis

5.5.2.1 (*S*)-amino ester **11** standard

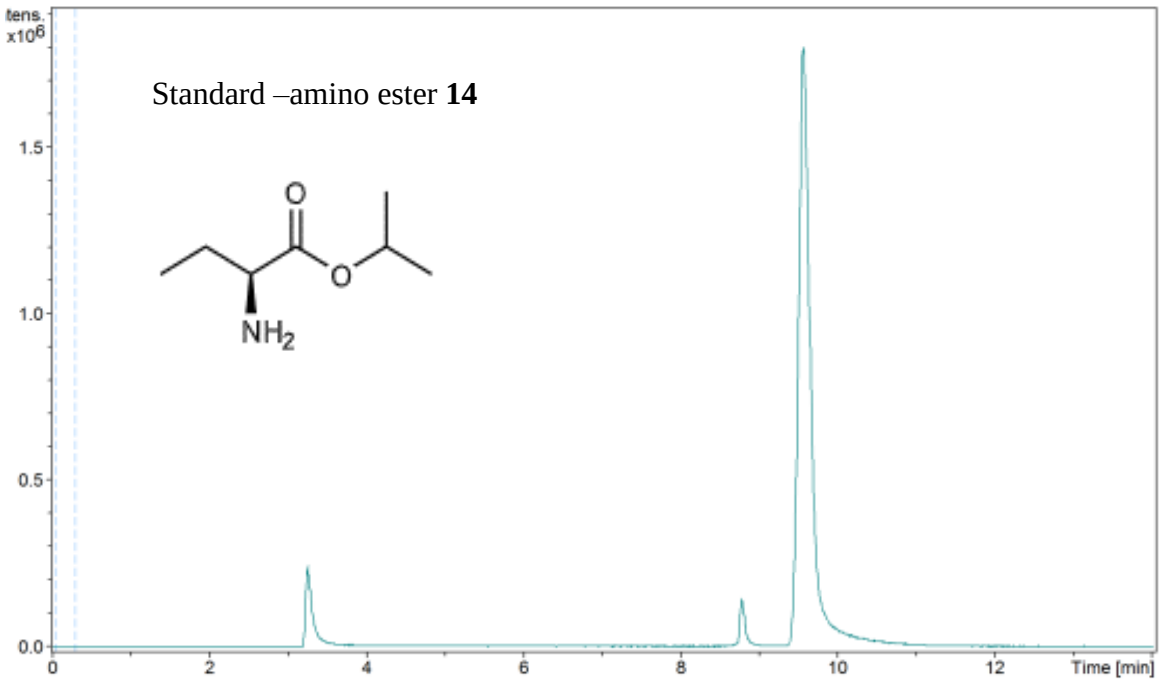

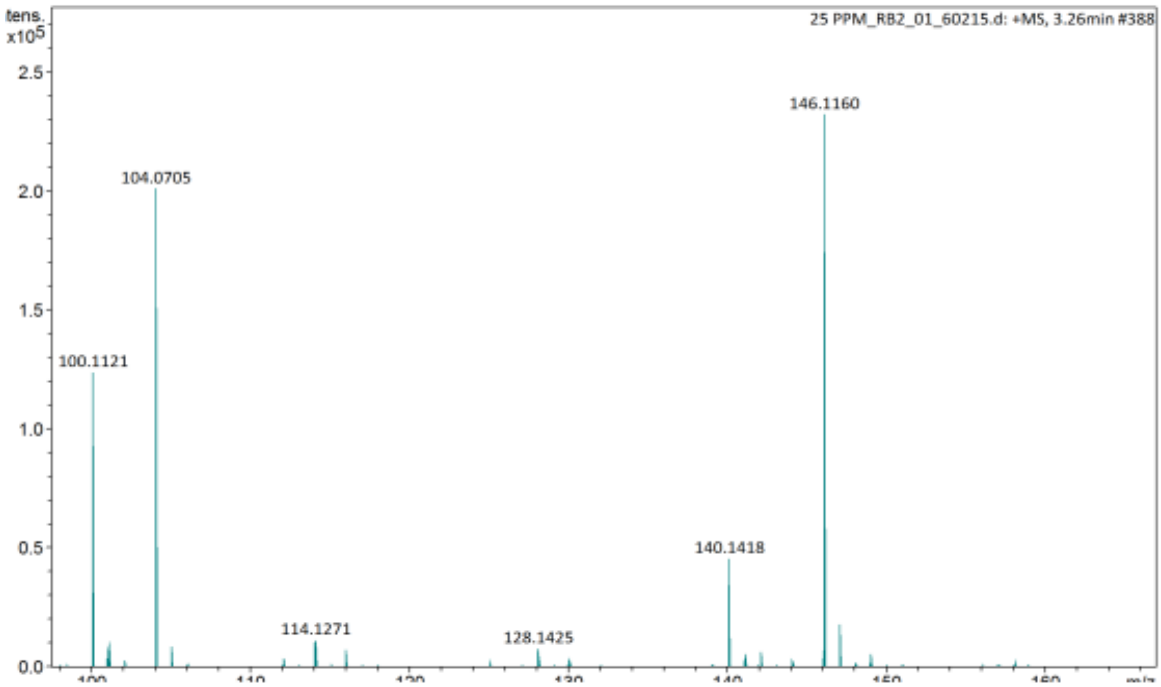

5.5.2.3 (*S*)-amino ester **14** enzyme product

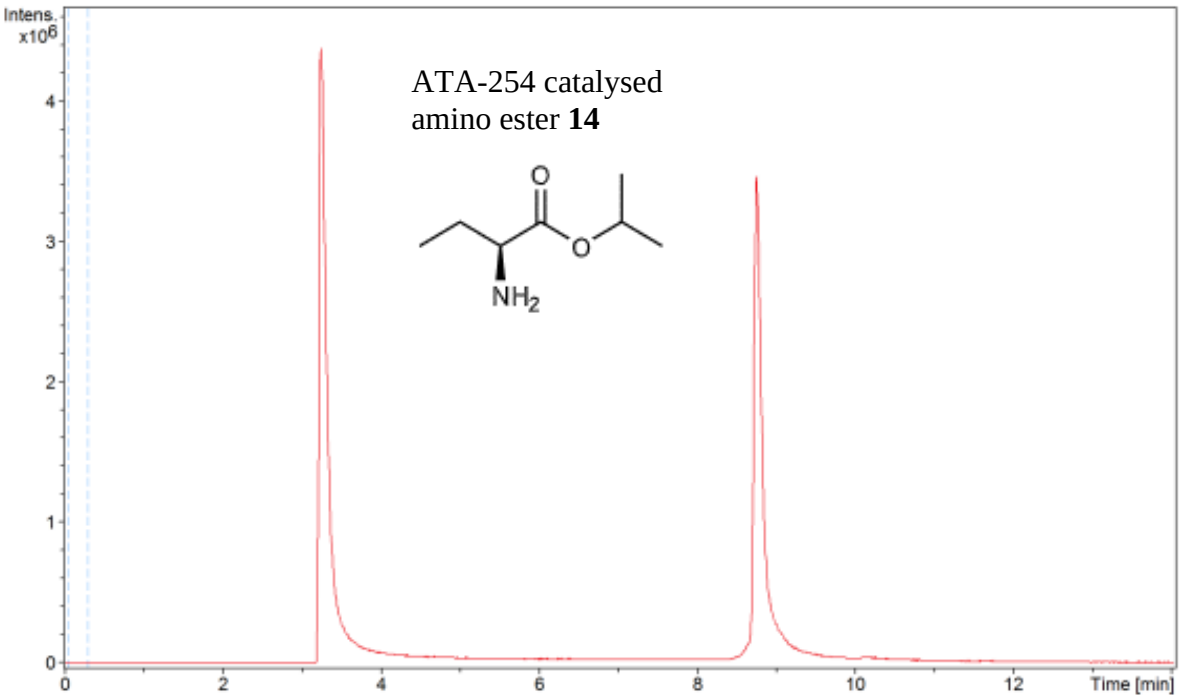
Intens.
x10^6
4
3
2
1
0
0
2
4
6
8
10
12
Time [min]
ATA-254 catalysed
amino ester **14**
O
O
NH2

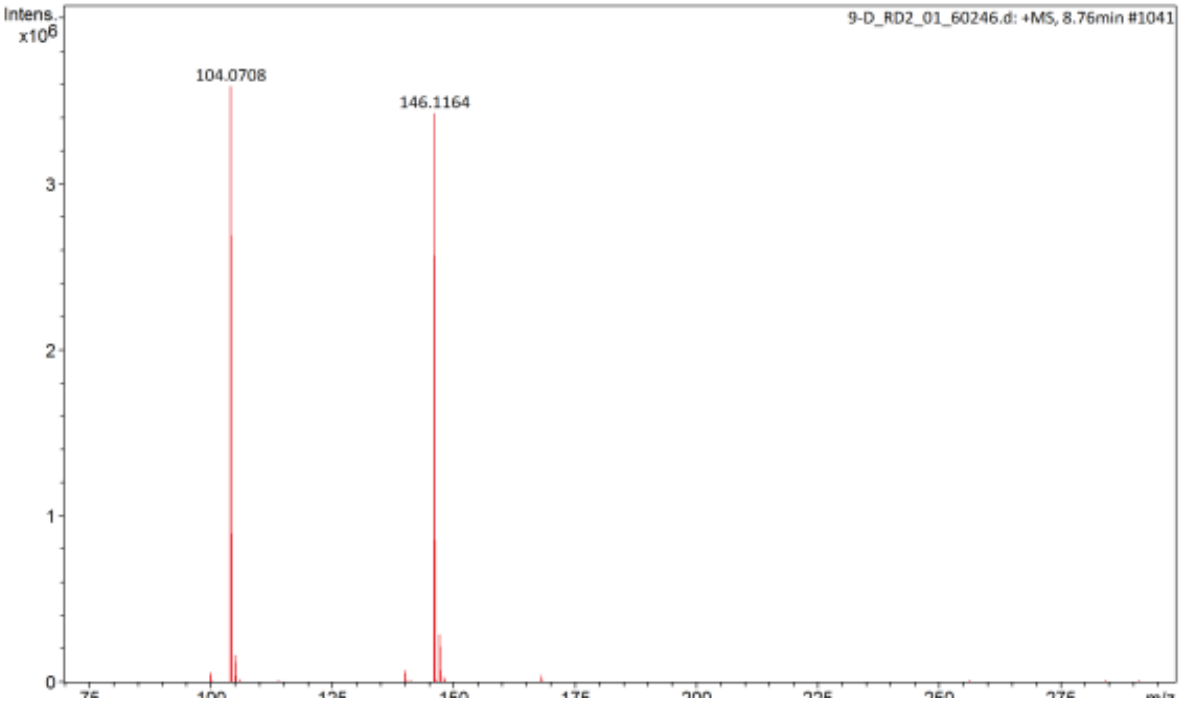
Intens.
x10^6
9-D_RD2_01_60246.d: +MS, 8.76min #1041
104.0708
146.1164
3
2
1
0

5.5.2.4 Chiral: HPLC analysis

(*S*)-Selective enzymes

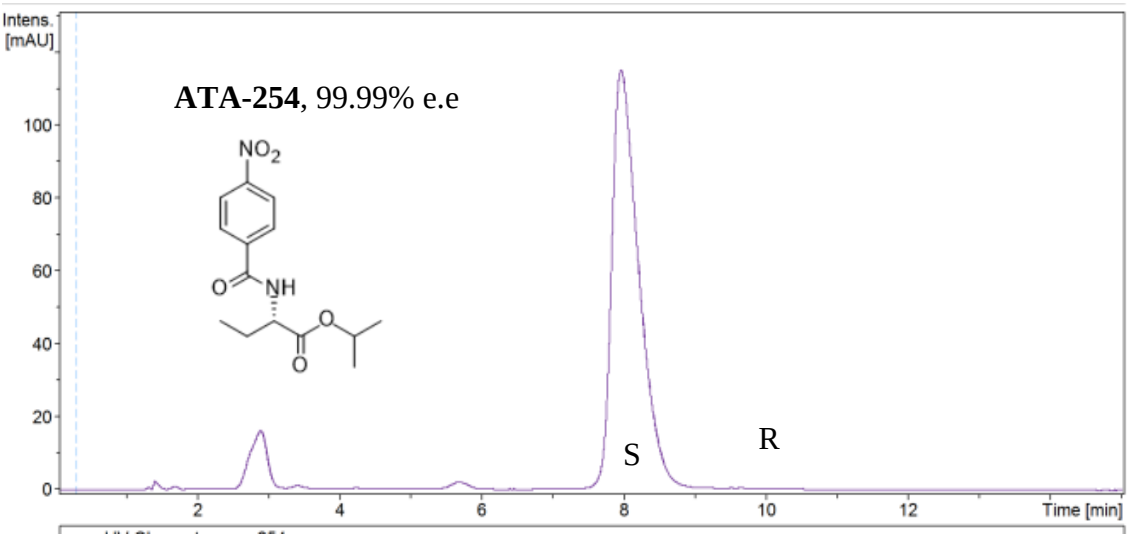

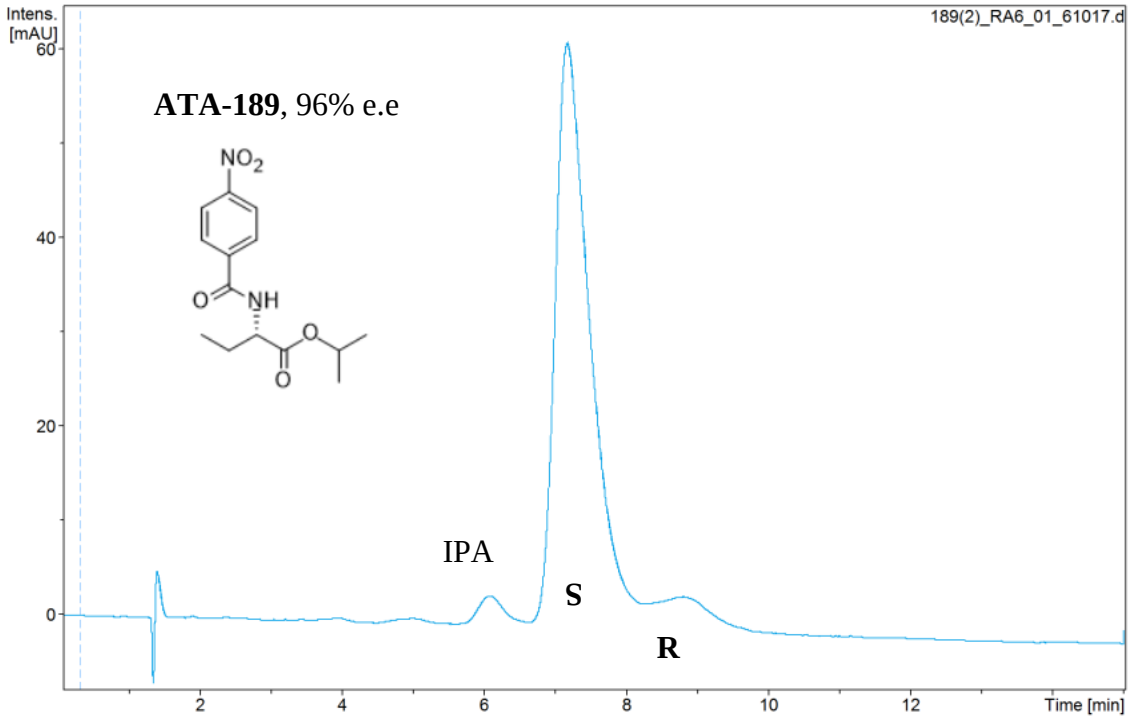

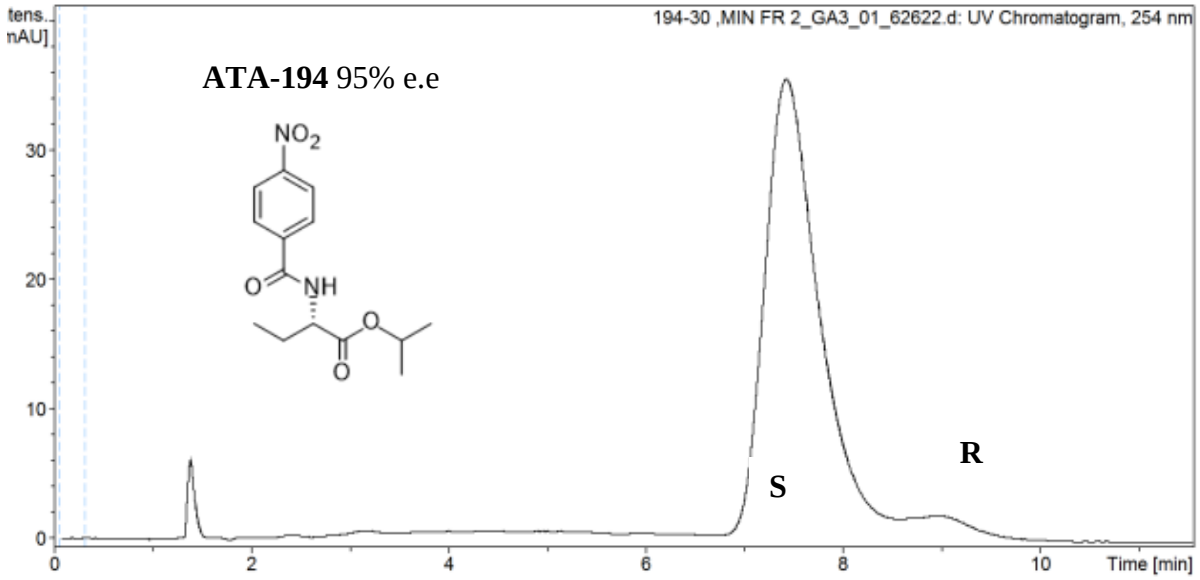

(*R*)-Selective enzymes

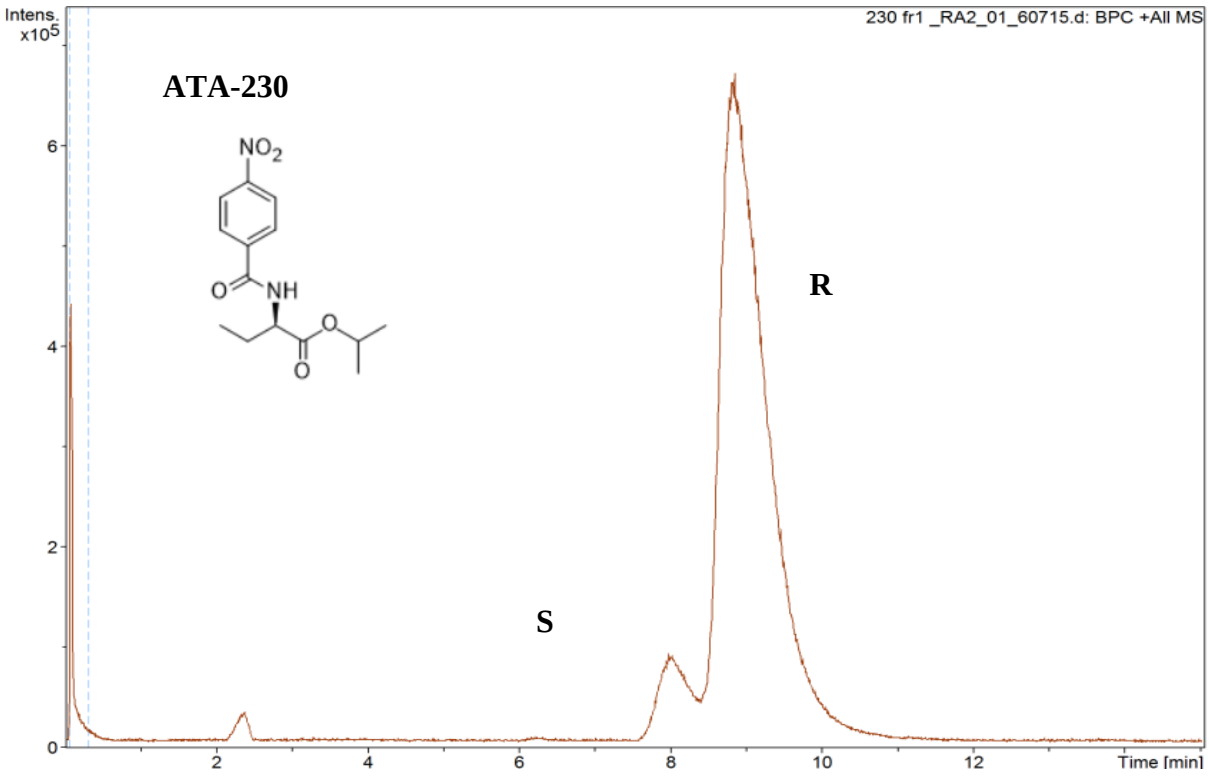

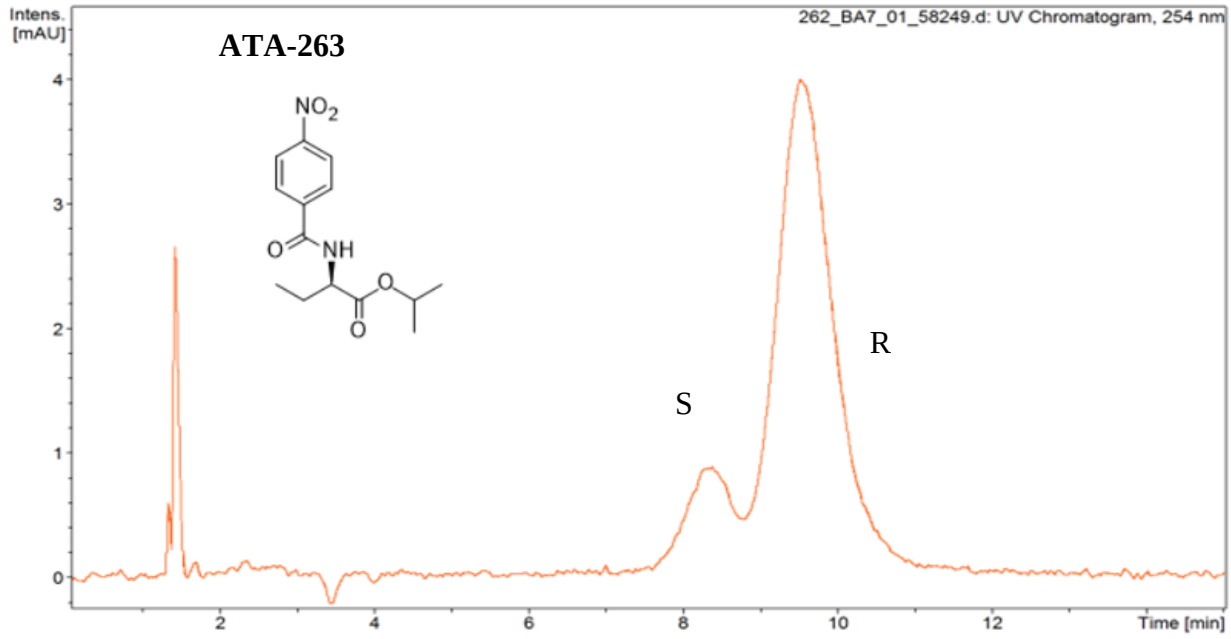

a) MASS SPEC DATA**:** 2-AMINO BUTANOL STANDARD

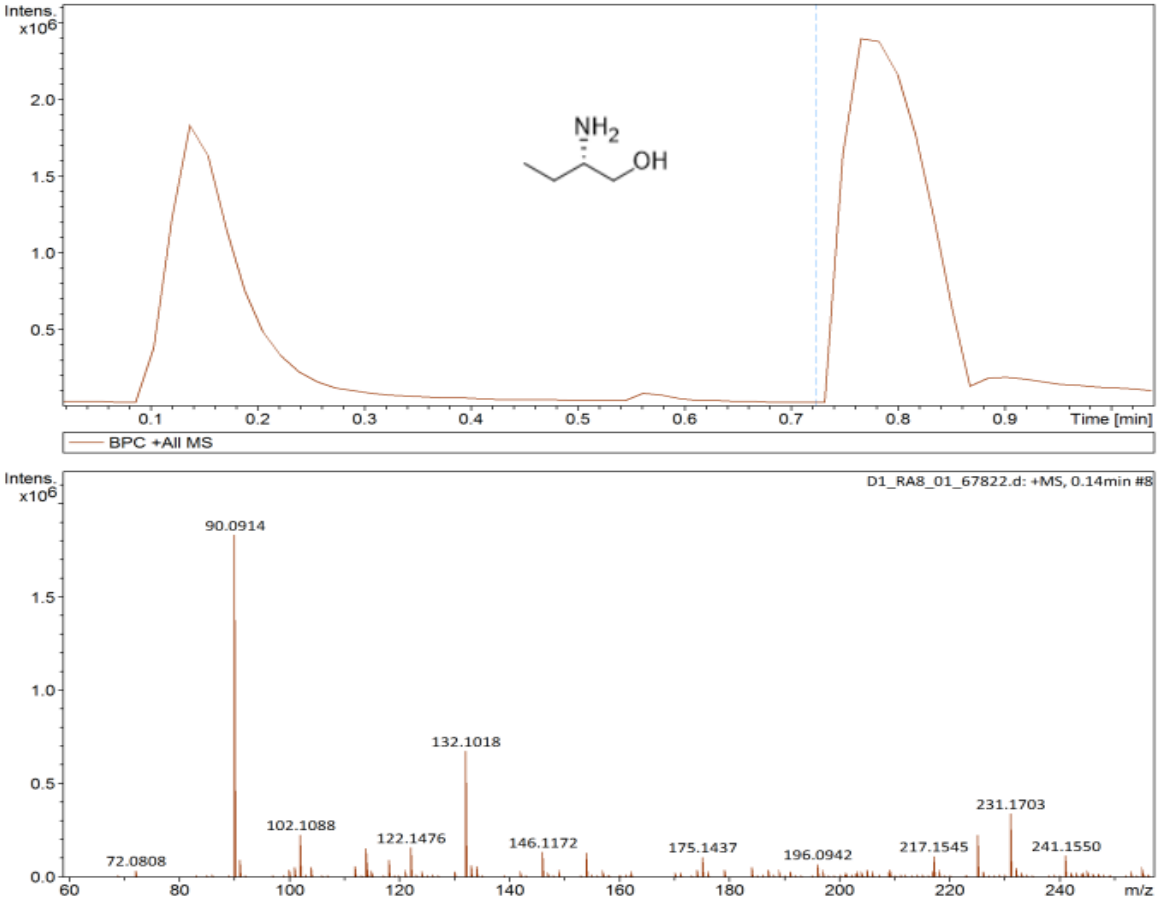

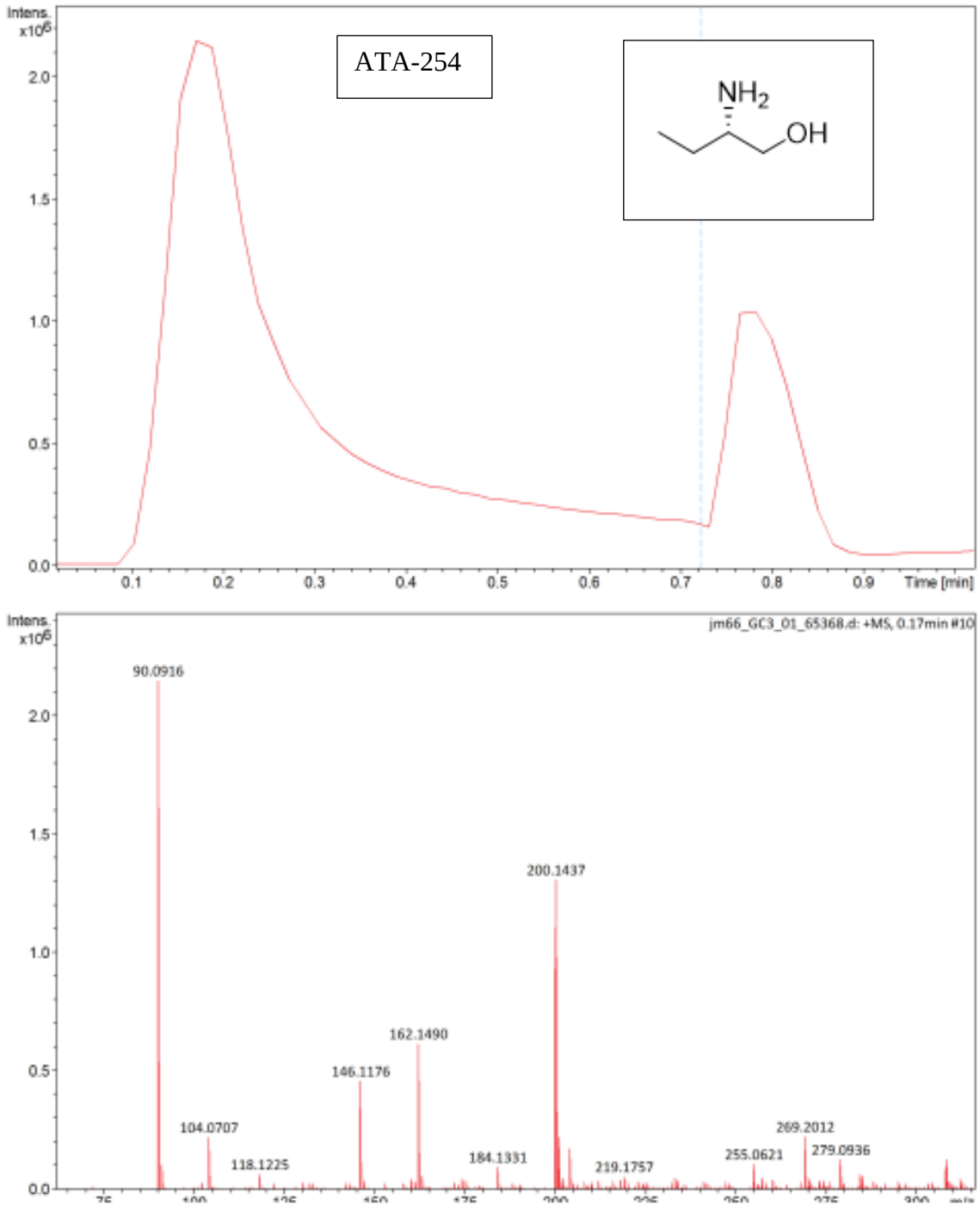
ATA-254
NH2
OH
Intens.
x10^6
2.0
1.5
1.0
0.5
0.0
0.1
0.2
0.3
0.4
0.5
0.6
0.7
0.8
0.9
Time [min]
jm66_GC3_01_65368.d: +MS, 0.17min #10
90.0916
200.1437
162.1490
146.1176
104.0707
118.1225
184.1331
219.1757
255.0621
269.2012
279.0936

5.6 LCMS Data: Dolutegravir intermediate

5.6.1 Achiral: HPLC analysis

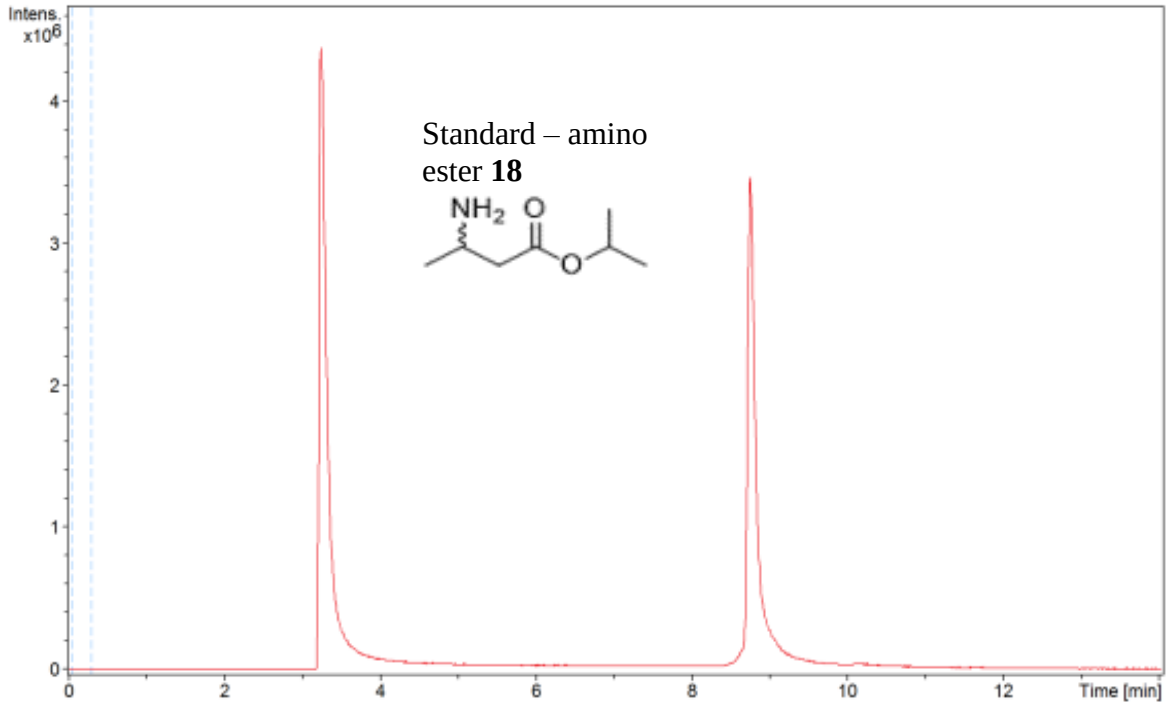

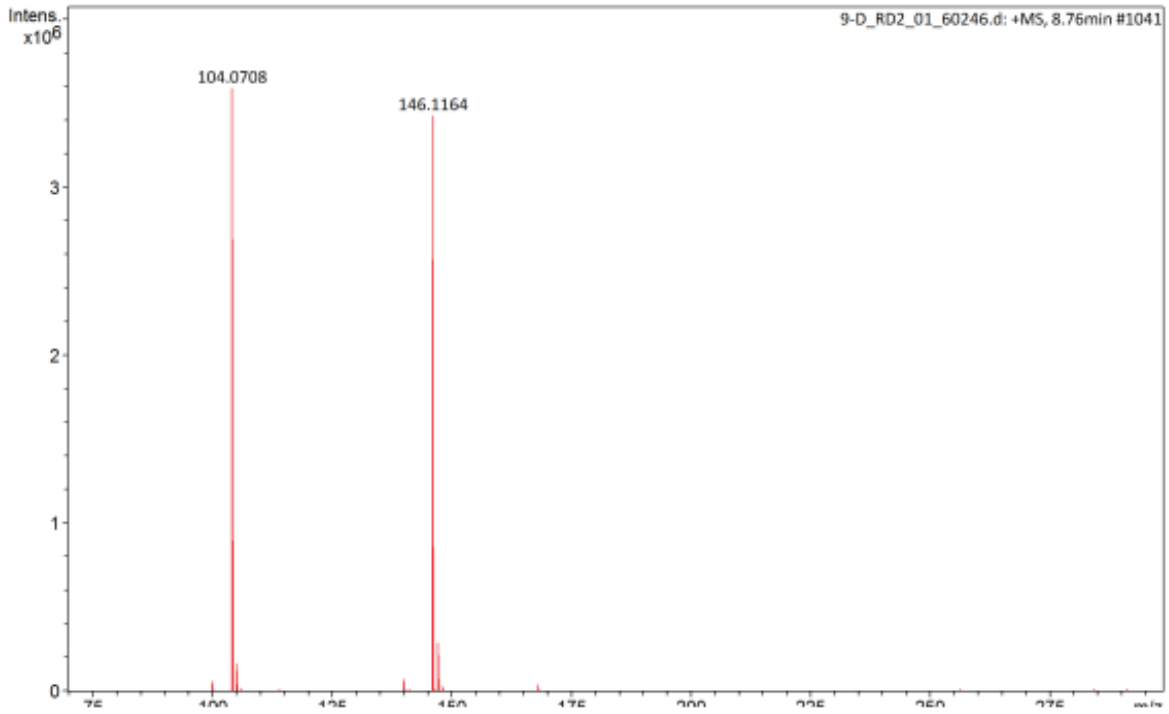

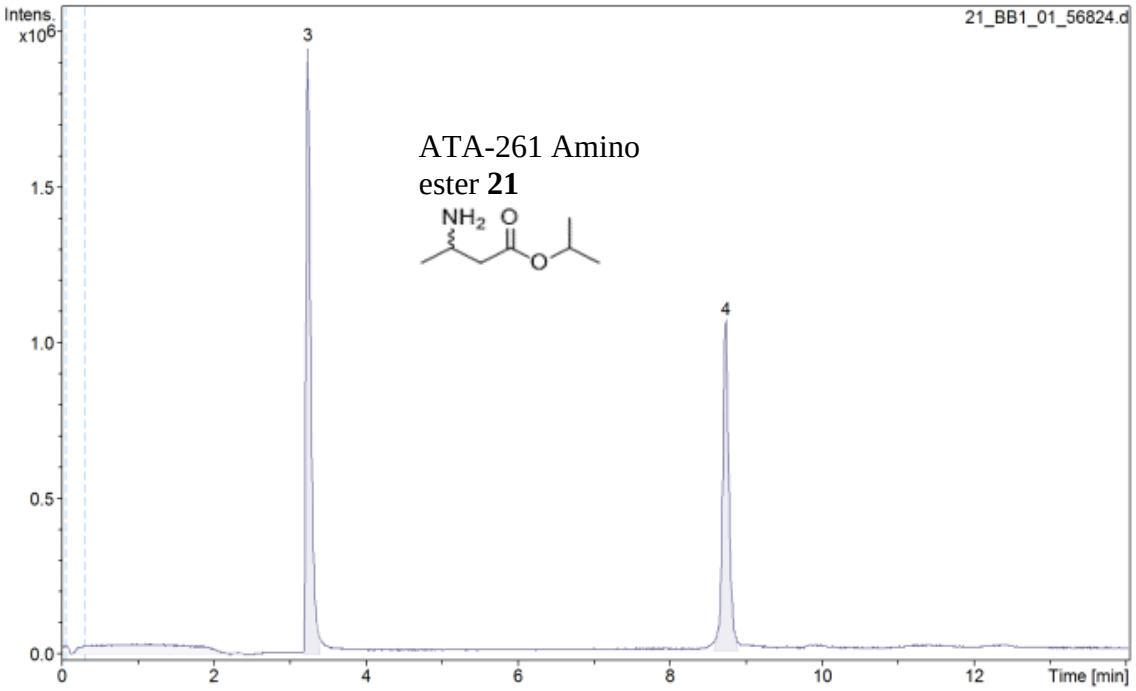

ATA-261 Amino ester **21**

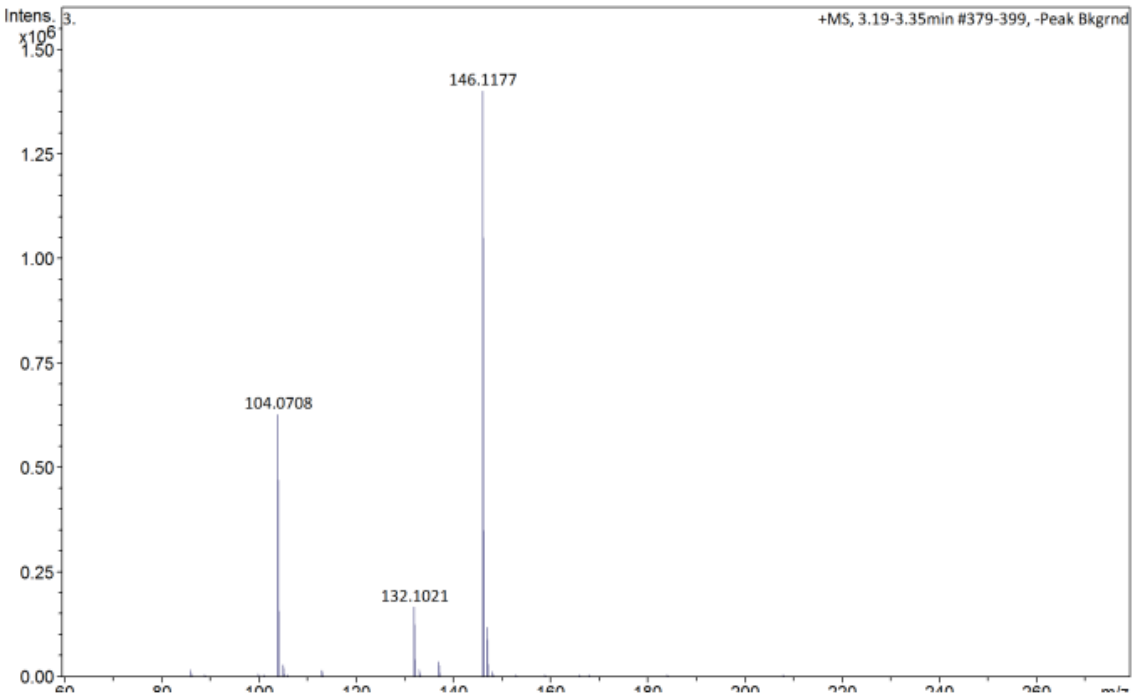

5.6.2 Chiral: HPLC analysis

(R)-selective enzymes

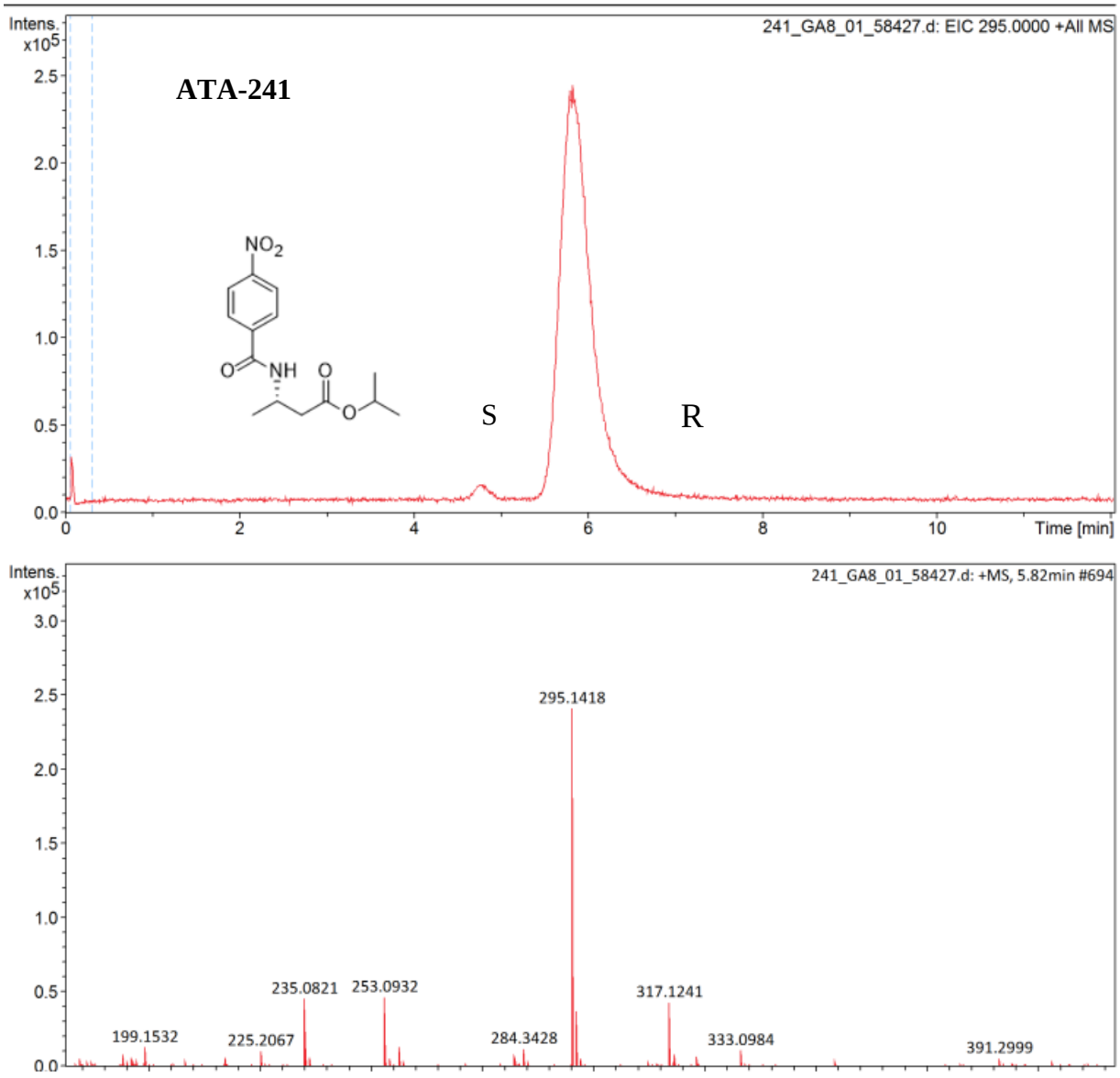

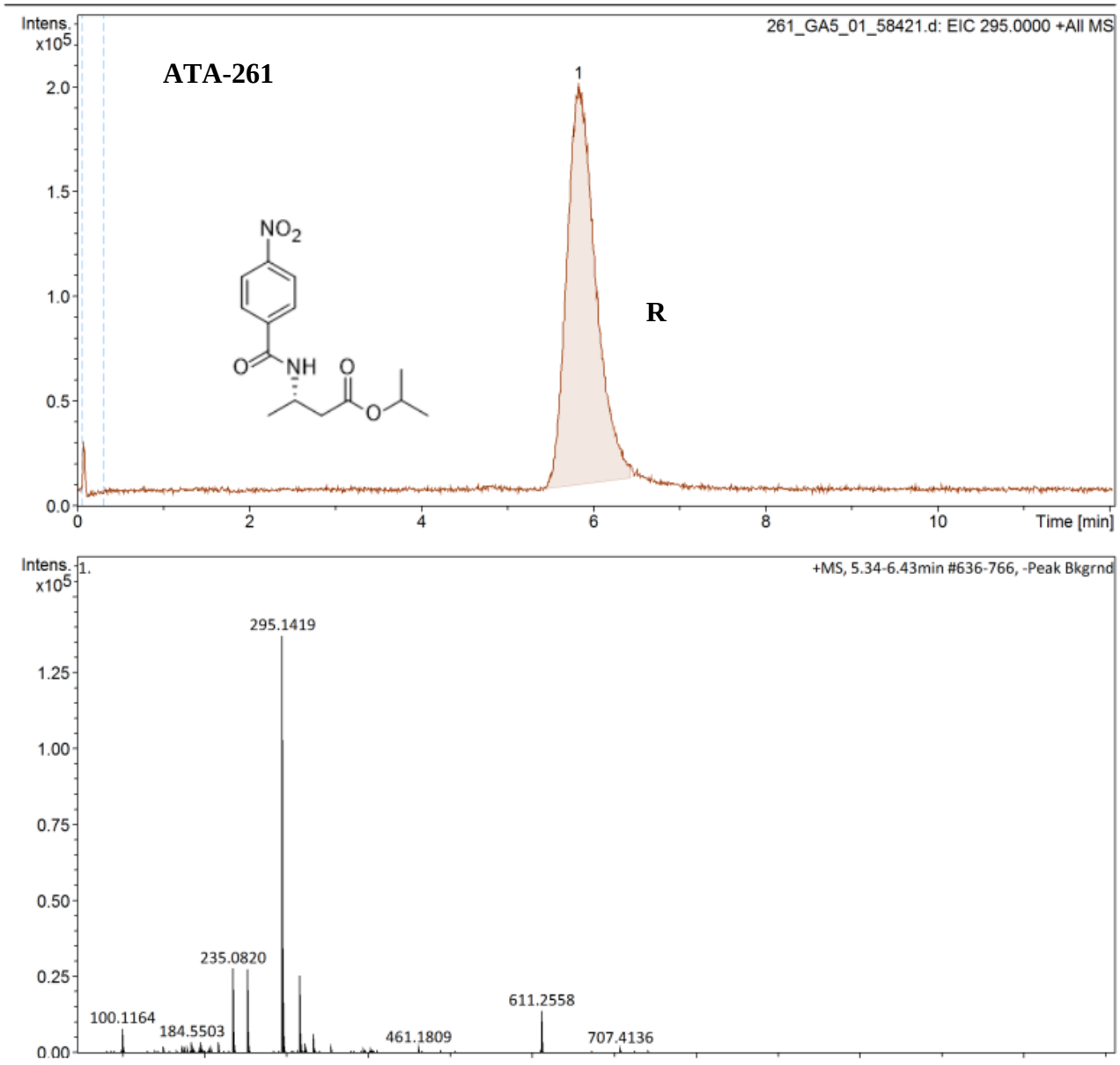
Intens.
x10^5
261_GA5_01_58421.d: EIC 295.0000 +All MS
ATA-261
1
R
NO2
NH
O
O
O
2.0
1.5
1.0
0.5
0.0
0
2
4
6
8
10
Time [min]
Intens.
x10^5
1.
+MS, 5.34-6.43min #636-766, -Peak Bkgrnd
295.1419
235.0820
100.1164
184.5503
461.1809
611.2558
707.4136
1.25
1.00
0.75
0.50
0.25
0.00

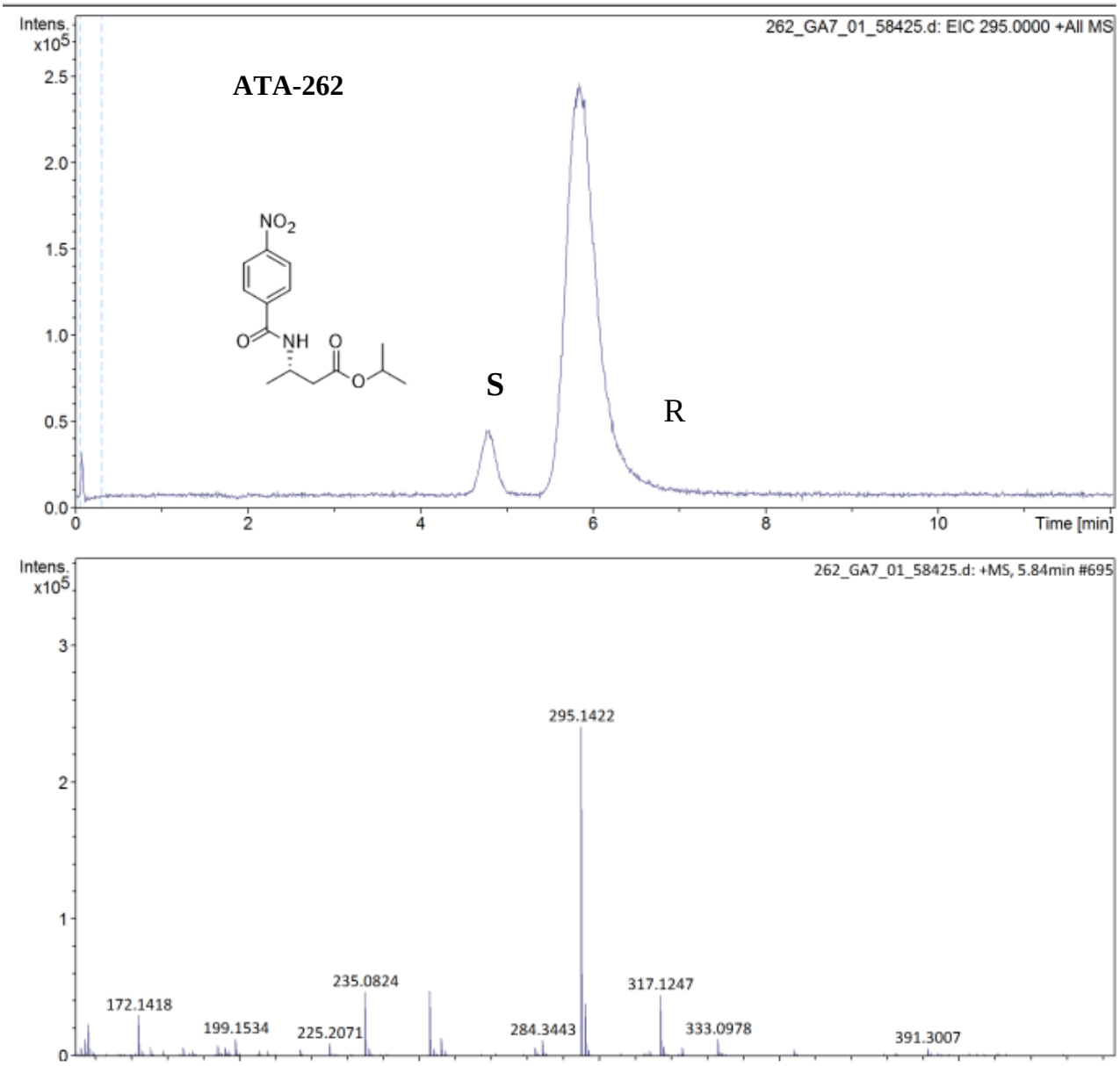
262_GA7_01_58425.d: EIC 295.0000 +All MS
Intens.
x10^5
ATA-262
NO2
NH
O
S
R
Time [min]
262_GA7_01_58425.d: +MS, 5.84min #695
295.1422
235.0824
317.1247
172.1418
199.1534
225.2071
284.3443
333.0978
391.3007

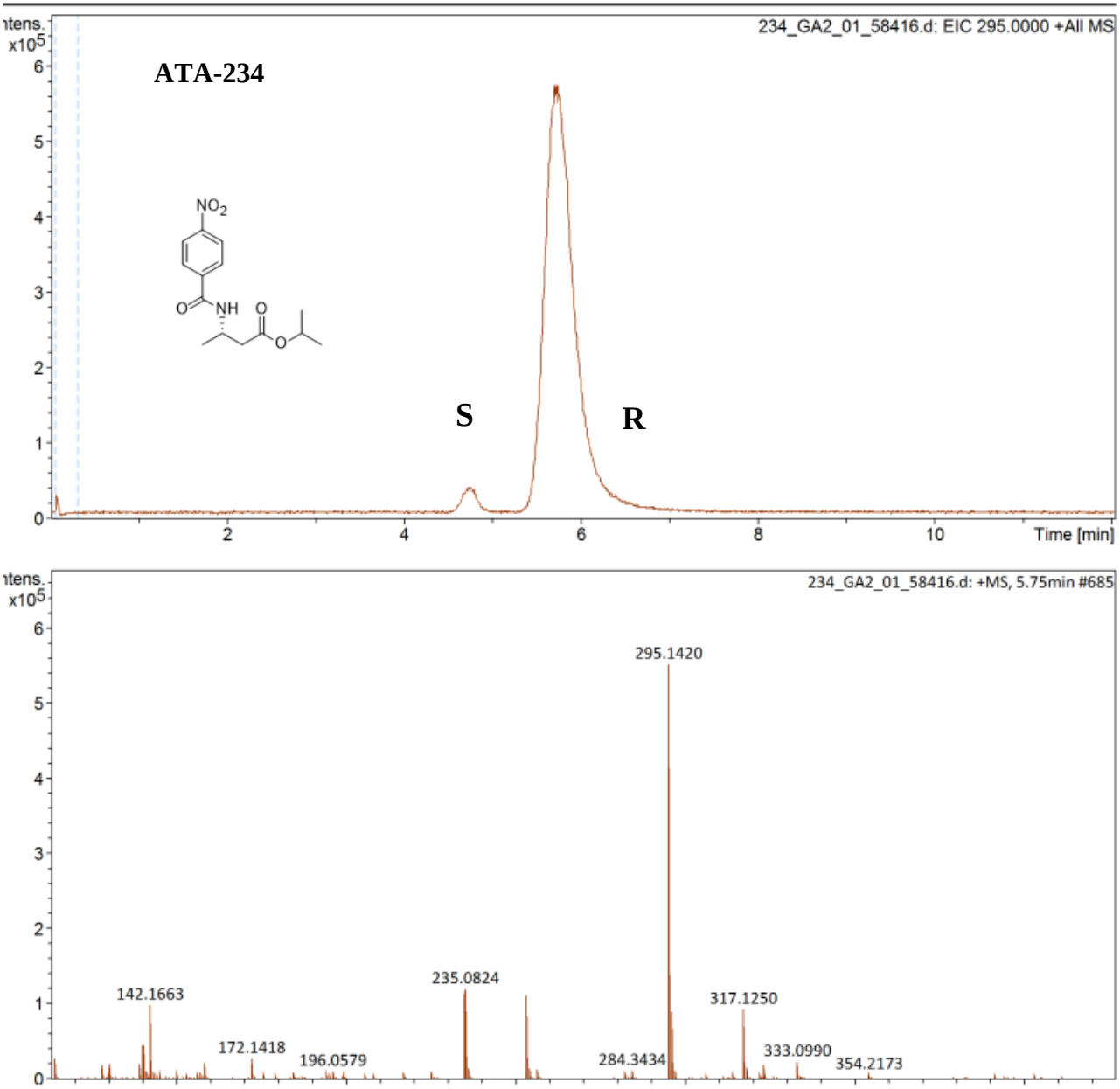

a) MASS SPEC DATA: 3-AMINO BUTANOL STANDARD

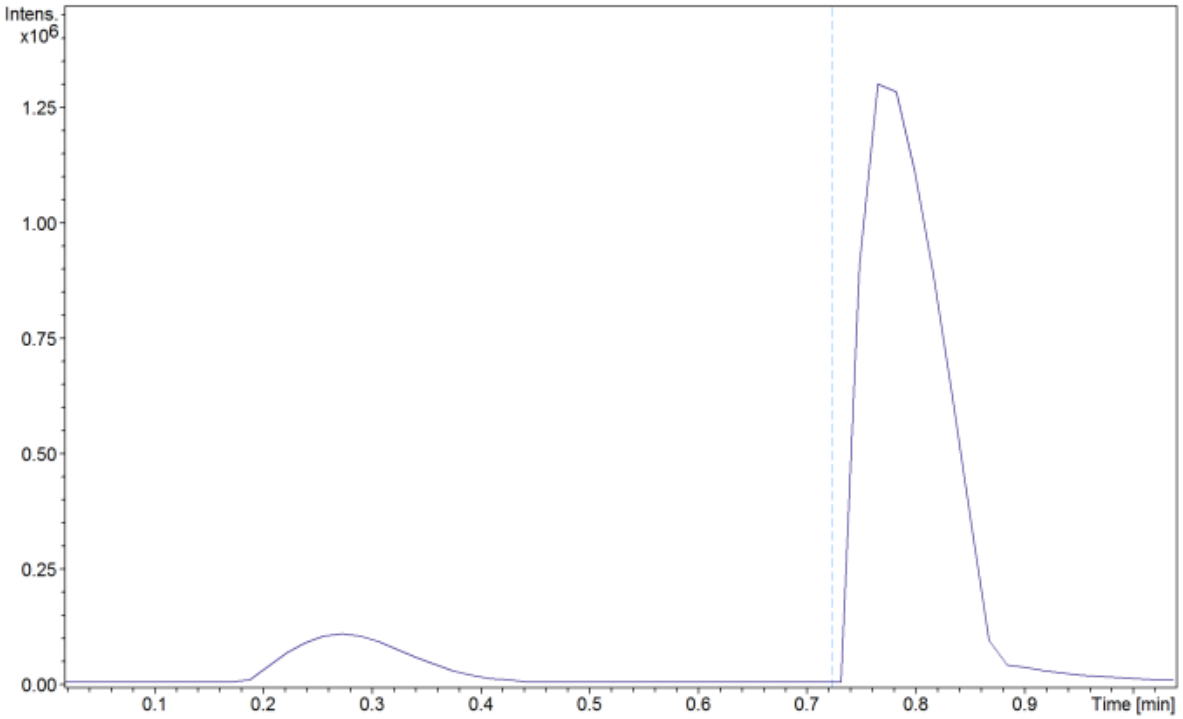
Intens.
x10^6
1.25
1.00
0.75
0.50
0.25
0.00
0.1
0.2
0.3
0.4
0.5
0.6
0.7
0.8
0.9
Time [min]

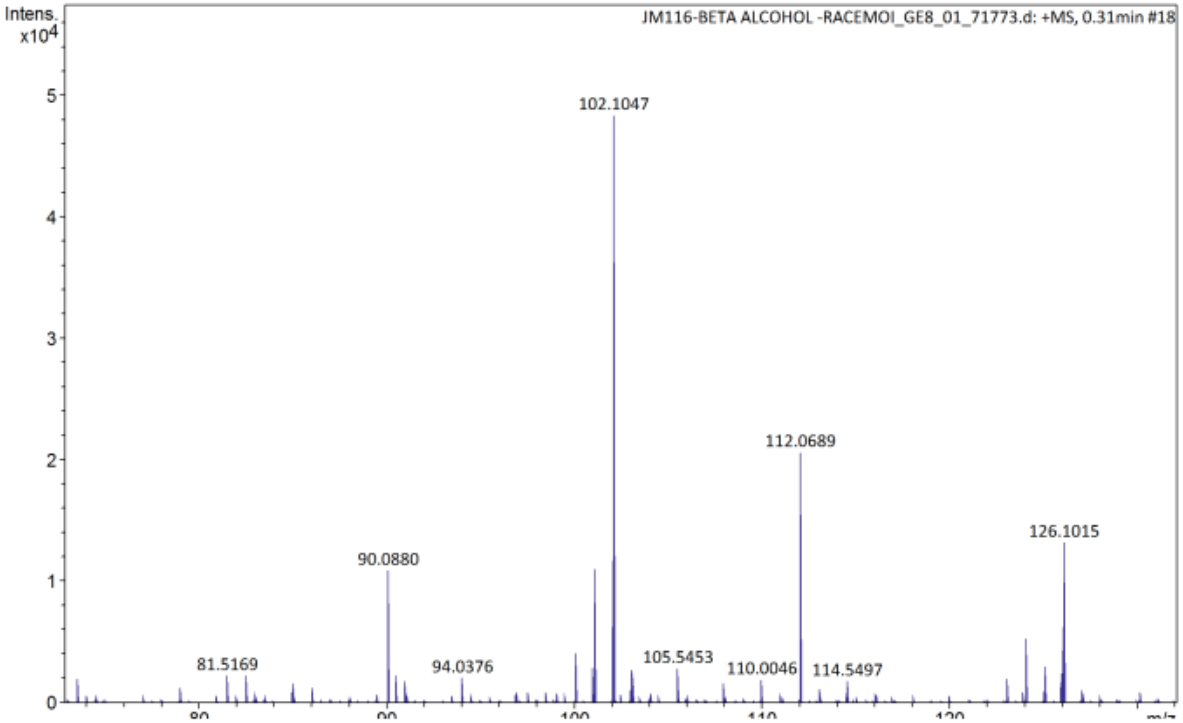
Intens.
x10^4
JM116-BETA ALCOHOL -RACEMOI_GE8_01_71773.d: +MS, 0.31min #18
102.1047
112.0689
126.1015
90.0880
81.5169
94.0376
105.5453
110.0046
114.5497
5
4
3
2
1
0

References

(1) Koper, K.; Han, S. W.; Pastor, D. C.; Yoshikuni, Y.; Maeda, H. A. Evolutionary Origin and Functional Diversification of Aminotransferases. *Journal of Biological Chemistry*. American Society for Biochemistry and Molecular Biology Inc. August 1, 2022. https://doi.org/10.1016/j.jbc.2022.102122.

(2) Rocha, M.; Sodek, L.; Licausi, F.; Hameed, M. W.; Dornelas, M. C.; Van Dongen, J. T. Analysis of Alanine Aminotransferase in Various Organs of Soybean (Glycine Max) and in Dependence of Different Nitrogen Fertilisers during Hypoxic Stress. *Amino Acids* **2010**, *39* (4), 1043–1053. https://doi.org/10.1007/s00726-010-0596-1.

(3) McGill, M. R. The Past and Present of Serum Aminotransferases and the Future of Liver Injury Biomarkers. *EXCLI J* **2016**, *15*, 817–828. https://doi.org/10.17179/excli2016-800.

(4) Miyashita, Y.; Dolferus, R.; Ismond, K. P.; Good, A. G. Alanine Aminotransferase Catalyses the Breakdown of Alanine after Hypoxia in Arabidopsis Thaliana. *Plant Journal* **2007**, *49* (6), 1108–1121. https://doi.org/10.1111/j.1365-313X.2006.03023.x.

(5) Cooper ~, A. J. L.; Meister~, A. *An Appreciation of Professor Alexander E. Braunstein. The Discovery and Scope of Enzymatic Transamination*; 1989; Vol. 71.

(6) Guo, F.; Berglund, P. Transaminase Biocatalysis: Optimization and Application. *Green Chemistry*. Royal Society of Chemistry 2017, pp 333–360. https://doi.org/10.1039/c6gc02328b.

(7) Fuchs, M.; Farnberger, J. E.; Kroutil, W. The Industrial Age of Biocatalytic Transamination. *European Journal of Organic Chemistry*. Wiley-VCH Verlag November 1, 2015, pp 6965–6982. https://doi.org/10.1002/ejoc.201500852.

(8) Patil, M. D.; Grogan, G.; Bommarius, A.; Yun, H. Recent Advances in ω-Transaminase-Mediated Biocatalysis for the Enantioselective Synthesis of Chiral Amines. *Catalysts*. MDPI July 1, 2018. https://doi.org/10.3390/catal8070254.

(9) Iwasaki, A.; Yamada, Y.; Kizaki, N.; Ikenaka, Y.; Hasegawa, J. Microbial Synthesis of Chiral Amines by (R)-Specific Transamination with Arthrobacter Sp. KNK168. *Appl Microbiol Biotechnol* **2006**, *69* (5), 499–505. https://doi.org/10.1007/s00253-005-0002-1.

(10) Liang, J.; Han, Q.; Tan, Y.; Ding, H.; Li, J. Current Advances on Structure-Function Relationships of Pyridoxal 5'-Phosphate-Dependent Enzymes. *Frontiers in Molecular Biosciences*. Frontiers Media S.A. 2019. https://doi.org/10.3389/fmolb.2019.00004.

(11) Rocha, J. F.; Pina, A. F.; Sousa, S. F.; Cerqueira, N. M. F. S. A. PLP-Dependent Enzymes as Important Biocatalysts for the Pharmaceutical, Chemical and Food Industries: A Structural and Mechanistic Perspective. *Catalysis Science and Technology*. Royal Society of Chemistry 2019, pp 4864–4876. https://doi.org/10.1039/c9cy01210a.

(12) Ayad Dawood. Application of Amine Transaminases in the Chemoenzymatic Synthesis of Chiral Amines Using Isopropylamine as Amine Donor, Universität Greifswald, Greifswald, 2018.

(13) Novick, S. J.; Dellas, N.; Garcia, R.; Ching, C.; Bautista, A.; Homan, D.; Alvizo, O.; Entwistle, D.; Kleinbeck, F.; Schlama, T.; Ruch, T. Engineering an Amine Transaminase for the Efficient Production of a Chiral Sacubitril Precursor. *ACS Catal* **2021**, *11* (6), 3762–3770. https://doi.org/10.1021/acscatal.0c05450.

(14) Mathew, S.; Yun, H. ω-Transaminases for the Production of Optically Pure Amines and Unnatural Amino Acids. *ACS Catalysis*. June 1, 2012, pp 993–1001. https://doi.org/10.1021/cs300116n.

(15) Gao, S.; Su, Y.; Zhao, L.; Li, G.; Zheng, G. Characterization of a (R)-Selective Amine Transaminase from Fusarium Oxysporum. *Process Biochemistry* **2017**, *63*, 130–136. https://doi.org/10.1016/j.procbio.2017.08.012.

(16) Patil, M. D.; Grogan, G.; Bommarius, A.; Yun, H. Oxidoreductase-Catalyzed Synthesis of Chiral Amines. *ACS Catalysis*. American Chemical Society December 7, 2018, pp 10985–11015. https://doi.org/10.1021/acscatal.8b02924.

(17) Kim, J. H.; Scialli, A. R. Thalidomide: The Tragedy of Birth Defects and the Effective Treatment of Disease. *Toxicological Sciences* **2011**, *122* (1), 1–6. https://doi.org/10.1093/toxsci/kfr088.

(18) Ghislieri, D.; Turner, N. J. Biocatalytic Approaches to the Synthesis of Enantiomerically Pure Chiral Amines. *Top Catal* **2014**, *57* (5), 284–300. https://doi.org/10.1007/s11244-013-0184-1.

(19) Breuer, M.; Ditrich, K.; Habicher, T.; Hauer, B.; Keßeler, M.; Stürmer, R.; Zelinski, T. Industrial Methods for the Production of Optically Active Intermediates. *Angewandte*

Chemie - International Edition. February 6, 2004, pp 788–824. https://doi.org/10.1002/anie.200300599.

(20) Höhne, M.; Bornscheuer, U. T. Biocatalytic Routes to Optically Active Amines. *ChemCatChem* **2009**, *1* (1), 42–51. https://doi.org/10.1002/cctc.200900110.

(21) Nugent, T. C.; El-Shazly, M. Chiral Amine Synthesis - Recent Developments and Trends for Enamide Reduction, Reductive Amination, and Imine Reduction. *Advanced Synthesis and Catalysis*. Wiley-VCH Verlag March 22, 2010, pp 753–819. https://doi.org/10.1002/adsc.200900719.

(22) Nugent, T. C.; Marinova, S. M. Step-Efficient Access to Chiral Primary Amines. *Synthesis (Germany)* **2013**, *45* (2), 153–166. https://doi.org/10.1055/s-0032-1317589.

(23) France, S. P.; Lewis, R. D.; Martinez, C. A. The Evolving Nature of Biocatalysis in Pharmaceutical Research and Development. *JACS Au*. American Chemical Society March 27, 2022. https://doi.org/10.1021/jacsau.2c00712.

(24) Thalén, L. K.; Zhao, D.; Sortais, J. B.; Paetzold, J.; Hoben, C.; Bäckvall, J. E. A Chemoenzymatic Approach to Enantiomerically Pure Amines Using Dynamic Kinetic Resolution: Application to the Synthesis of Norsertraline. *Chemistry - A European Journal* **2009**, *15* (14), 3403–3410. https://doi.org/10.1002/chem.200802303.

(25) Mitsukura, K.; Suzuki, M.; Tada, K.; Yoshida, T.; Nagasawa, T. Asymmetric Synthesis of Chiral Cyclic Amine from Cyclic Imine by Bacterial Whole-Cell Catalyst of Enantioselective Imine Reductase. *Org Biomol Chem* **2010**, *8* (20), 4533–4535. https://doi.org/10.1039/c0ob00353k.

(26) Zawodny, W.; Montgomery, S. L. Evolving New Chemistry: Biocatalysis for the Synthesis of Amine-Containing Pharmaceuticals. *Catalysts*. MDPI June 1, 2022. https://doi.org/10.3390/catal12060595.

(27) Tseliou, V.; Knaus, T.; Masman, M. F.; Corrado, M. L.; Mutti, F. G. Generation of Amine Dehydrogenases with Increased Catalytic Performance and Substrate Scope from ε-Deaminating L-Lysine Dehydrogenase. *Nat Commun* **2019**, *10* (1). https://doi.org/10.1038/s41467-019-11509-x.

(28) Mayol, O.; David, S.; Darii, E.; Debard, A.; Mariage, A.; Pellouin, V.; Petit, J. L.; Salanoubat, M.; De Berardinis, V.; Zaparucha, A.; Vergne-Vaxelaire, C. Asymmetric Reductive Amination by a Wild-Type Amine Dehydrogenase from the Thermophilic Bacteria: Petrotoga Mobilis. *Catal Sci Technol* **2016**, *6* (20), 7421–7428. https://doi.org/10.1039/c6cy01625a.

(29) Wu, S.; Snajdrova, R.; Moore, J. C.; Baldenius, K.; Bornscheuer, U. T. Biocatalysis: Enzymatic Synthesis for Industrial Applications. *Angewandte Chemie - International Edition*. Wiley-VCH Verlag January 4, 2021, pp 88–119. https://doi.org/10.1002/anie.202006648.

(30) Kelly, S. A.; Mix, S.; Moody, T. S.; Gilmore, B. F. Transaminases for Industrial Biocatalysis: Novel Enzyme Discovery. *Applied Microbiology and Biotechnology*. Springer June 1, 2020, pp 4781–4794. https://doi.org/10.1007/s00253-020-10585-0.

(31) Kelly, S. A.; Pohle, S.; Wharry, S.; Mix, S.; Allen, C. C. R.; Moody, T. S.; Gilmore, B. F. Application of ω-Transaminases in the Pharmaceutical Industry. *Chemical Reviews*. American Chemical Society January 10, 2018, pp 349–367. https://doi.org/10.1021/acs.chemrev.7b00437.

(32) Truppo, M. D.; Turner, N. J.; Rozzell, J. D. Efficient Kinetic Resolution of Racemic Amines Using a Transaminase in Combination with an Amino Acid Oxidase. *Chemical Communications* **2009**, No. 16, 2127–2129. https://doi.org/10.1039/b902995h.

(33) Koszelewski, D.; Pressnitz, D.; Clay, D.; Kroutil, W. Deracemization of Mexiletine Biocatalyzed by ω-Transaminases. *Org Lett* **2009**, *11* (21), 4810–4812. https://doi.org/10.1021/ol901834x.

(34) Tufvesson, P.; Lima-Ramos, J.; Jensen, J. S.; Al-Haque, N.; Neto, W.; Woodley, J. M. Process Considerations for the Asymmetric Synthesis of Chiral Amines Using Transaminases. *Biotechnology and Bioengineering*. July 2011, pp 1479–1493. https://doi.org/10.1002/bit.23154.

(35) Shin, J. S.; Kim, B. G. Asymmetric Synthesis of Chiral Amines with ω-Transaminase. *Biotechnol Bioeng* **1999**, *65* (2), 206–211. https://doi.org/10.1002/(SICI)1097-0290(19991020)65:2<206::AID-BIT11>3.0.CO;2-9.

(36) Dunbabin, A.; Subrizi, F.; Ward, J. M.; Sheppard, T. D.; Hailes, H. C. Furfurylamines from Biomass: Transaminase Catalysed Upgrading of Furfurals. *Green Chemistry* **2017**, *19* (2), 397–404. https://doi.org/10.1039/c6gc02241c.

(37) Kroutil, W.; Fischereder, E. M.; Fuchs, C. S.; Lechner, H.; Mutti, F. G.; Pressnitz, D.; Rajagopalan, A.; Sattler, J. H.; Simon, R. C.; Siirola, E. Asymmetric Preparation of Prim -, Sec -, and Tert-Amines Employing Selected Biocatalysts. *Organic Process Research and Development*. May 17, 2013, pp 751–759. https://doi.org/10.1021/op4000237.

(38) Meng, Q.; Ramírez-Palacios, C.; Wijma, H. J.; Janssen, D. B. Protein Engineering of Amine Transaminases. *Frontiers in Catalysis* **2022**, pp 01-11 https://doi.org/10.3389/fctls.2022.1049179.

(39) Böhmer, W.; Volkov, A.; Engelmark Cassimjee, K.; Mutti, F. G. Continuous Flow Bioamination of Ketones in Organic Solvents at Controlled Water Activity Using Immobilized ω-Transaminases. *Adv Synth Catal* **2020**,362,1858-1867 https://doi.org/10.1002/adsc.201901274.

(40) Andrade, L. H.; Kroutil, W.; Jamison, T. F. Continuous Flow Synthesis of Chiral Amines in Organic Solvents: Immobilization of E. Coli Cells Containing Both ω-Transaminase and PLP. *Org Lett* **2014**, *16* (23), 6092–6095. https://doi.org/10.1021/ol502712v.

(41) Sappino, C.; Mari, A.; Mantineo, A.; Moliterno, M.; Palagri, M.; Tatangelo, C.; Suber, L.; Bovicelli, P.; Ricelli, A.; Righi, G. New Chiral Amino Alcohol Ligands for Catalytic Enantioselective Addition of Diethylzincs to Aldehydes. *Org Biomol Chem* **2018**, *16* (11), 1860–1870. https://doi.org/10.1039/c8ob00165k.

(42) Corrado, M. L.; Knaus, T.; Schwaneberg, U.; Mutti, F. G. High-Yield Synthesis of Enantiopure 1,2-Amino Alcohols from l -Phenylalanine via Linear and Divergent Enzymatic Cascades. *Organic Process Research and Development*. American Chemical Society July 15, 2022, pp 2085–2095. https://doi.org/10.1021/acs.oprd.1c00490.

(43) *Global Tuberculosis ReporT 2022*; 2022. http://apps.who.int/bookorders.

(44) Parai, M. K.; Panda, G.; Chaturvedi, V.; Manju, Y. K.; Sinha, S. Thiophene Containing Triarylmethanes as Antitubercular Agents. *Bioorg Med Chem Lett* **2008**, *18* (1), 289–292. https://doi.org/10.1016/j.bmcl.2007.10.083.

(45) Ma, Z.; Ginsberg, A. M.; Spigelman, M. *7.24 Antimycobacterium Agents*.

(46) Ma, Z.; Lynch, A. S. Development of a Dual-Acting Antibacterial Agent (TNP-2092) for the Treatment of Persistent Bacterial Infections. *J Med Chem* **2016**, *59* (14), 6645–6657. https://doi.org/10.1021/acs.jmedchem.6b00485.

(47) Dobrikov, G. M.; Valcheva, V.; Stoilova-Disheva, M.; Momekov, G.; Tzvetkova, P.; Chimov, A.; Dimitrov, V. Synthesis and in Vitro Antimycobacterial Activity of Compounds Derived from (R)- and (S)-2-Amino-1-Butanol - The Crucial Role of the Configuration. *Eur J Med Chem* **2012**, *48*, 45–56. https://doi.org/10.1016/j.ejmech.2011.11.035.

(48) Weber, N.; Hatsch, A.; Labagnere, L.; Heider, H. Production of (S)-2-Aminobutyric Acid and (S)-2-Aminobutanol in Saccharomyces Cerevisiae. *Microb Cell Fact* **2017**, *16* (1), 51. https://doi.org/10.1186/s12934-017-0667-z.

(49) Kumar, P.; Upadhyay, S. K.; Singh, R. A Study on Recent Trends in Therapy of Air Borne Communicable Disease Caused by Mycobacterium Tuberculosis: The Tuberculosis. *Bulletin of Pure & Applied Sciences- Zoology* **2018**, *37a* (2), 65. https://doi.org/10.5958/2320-3188.2018.00009.8.

(50) Leone, A.; Cerase, A.; Costantini, A. Musculoskeletal Tuberculosis. *Radiologist*. September 2000, pp 227–237. https://doi.org/10.1128/microbiolspec.tnmi7-0046-2017.

(51) Migliori, G. B.; Loddenkemper, R.; Blasi, F.; Raviglione, M. C. 125 Years after Robert Koch's Discovery of the Tubercle Bacillus: The New XDR-TB Threat. Is "Science" Enough to Tackle the Epidemic? *European Respiratory Journal*. March 2007, pp 423–427. https://doi.org/10.1183/09031936.00001307.

(52) *Global Tuberculosis ReporT 2022*; 2022. http://apps.who.int/bookorders.

(53) SANAC National Strategic Plan for HIV, TB and STIs, 2023-2028, https://sanac.org.za/national-strategic-plan-2023-2028

(54) Li, W.; Koay, A.; Kose-Otieno, J.; Rakhmanina, N. HIV Drug Resistance in Children and Adolescents: Always a Challenge? https://doi.org/10.1007/s40471-021-00268-3/Published.

(55) Aoyama, Y.; Hakogi, T.; Fukui, Y.; Yamada, D.; Ooyama, T.; Nishino, Y.; Shinomoto, S.; Nagai, M.; Miyake, N.; Taoda, Y.; Yoshida, H.; Yasukata, T. Practical and Scalable Synthetic Method for Preparation of Dolutegravir Sodium: Improvement of a Synthetic Route for Large-Scale Synthesis. Organic Process Research & Development 2019, 23 (4), 558–564. https://doi.org/10.1021/acs.oprd.8b00409.

(56) Ou, C.-Y.; Takebe, Y.; Luo, C.-C.; Kalish, M.; Auwanit, W.; Bandea.' Nick De La Torre, C.; Moore, J. L.; Schochetman, G.; Yamazaki, S.; Gayle, H. D.; Young,', N. L.; Weniger1', B. G. *Wide Distribution of Two Subtypes of HIV-1 in Thailand*; Mary Ann Liebert, Inc., Publishers 'National Institute of Health, 1992; Vol. 8. www.liebertpub.com.

(57) Lu, D.-Y.; Wu, H.-Y.; Yarla, N. S.; Xu, B.; Ding, J.; Lu, T.-R. HAART in HIV/AIDS Treatments: Future Trends. *Infect Disord Drug Targets* **2017**, *18* (1), 15–22. https://doi.org/10.2174/1871526517666170505122800.

(58) Günthard, H. F.; Saag, M. S.; Benson, C. A.; Del Rio, C.; Eron, J. J.; Gallant, J. E.; Hoy, J. F.; Mugavero, M. J.; Sax, P. E.; Thompson, M. A.; Gandhi, R. T.; Landovitz, R. J.; Smith, D. M.; Jacobsen, D. M.; Volberding, P. A. Antiretroviral Drugs for Treatment and Prevention of HIV Infection in Adults: 2016 Recommendations of the International Antiviral Society-USA Panel. *JAMA - Journal of the American Medical Association* **2016**, *316* (2), 191–210. https://doi.org/10.1001/jama.2016.8900.

(59) Zhao, A. V.; Crutchley, R. D.; Guduru, R. C.; Ton, K.; Lam, T.; Min, A. C. A Clinical Review of HIV Integrase Strand Transfer Inhibitors (INSTIs) for the Prevention and Treatment of HIV-1 Infection. *Retrovirology*. BioMed Central Ltd December 1, 2022. https://doi.org/10.1186/s12977-022-00608-1.

(60) Kandel, C. E.; Walmsley, S. L. Dolutegravir – A Review of the Pharmacology, Efficacy, and Safety in the Treatment of HIV. *Drug Design, Development and Therapy*. Dove Medical Press Ltd. July 7, 2015, pp 3547–3555. https://doi.org/10.2147/DDDT.S84850.

(61) Gonçalves, R. S. B.; Da Silva, E. T.; Vinícius, M.; De Souza,. An Environmentally Friendly, Scalable and Highly Efficient Synthesis of (S,S)-Ethambutol, a First Line Drug against Tuberculosis, *Letters in organic chemistry* ; 2015; Vol. 12.

(62) Vardanyan, R. S.; Hruby, V. J. Antimycobacterial Drugs In Synthesis of Essential Drugs; *Elsevie*r, 2006; pp 525–534. https://doi.org/10.1016/B978-044452166-8/50034-0.

(63) Kwon, S.; Park, H. H. Structural Consideration of the Working Mechanism of Fold Type I Transaminases From Eubacteria: Overt and Covert Movement. *Computational and Structural Biotechnology Journal*. Elsevier B.V. January 1, 2019, pp 1031–1039. https://doi.org/10.1016/j.csbj.2019.07.007.

(64) Zhang, Z.; Liu, Y.; Zhao, J.; Li, W.; Hu, R.; Li, X.; Li, A.; Wang, Y.; Ma, L. Active-Site Engineering of ω-Transaminase from Ochrobactrum Anthropi for Preparation of L-2-Aminobutyric Acid. *BMC Biotechnol* **2021**, *21* (1). https://doi.org/10.1186/s12896-021-00713-7.

(65) Green, A. P.; Turner, N. J.; O'Reilly, E. Chiral Amine Synthesis Using ω-Transaminases: An Amine Donor That Displaces Equilibria and Enables High-Throughput Screening. *Angewandte Chemie - International Edition* **2014**, *53* (40), 10714–10717. https://doi.org/10.1002/anie.201406571.

(66) Teixeira, I. S.; Farias, A. B.; Horta, B. A. C.; Milagre, H. M. S.; de Souza, R. O. M. A.; Bornscheuer, U. T.; Milagre, C. D. F. Computer Modeling Explains the Structural

Reasons for the Difference in Reactivity of Amine Transaminases Regarding Prochiral Methylketones. *Int J Mol Sci* **2022**, *23* (2). https://doi.org/10.3390/ijms23020777.

(67) Cerioli, L.; Planchestainer, M.; Cassidy, J.; Tessaro, D.; Paradisi, F. Characterization of a Novel Amine Transaminase from Halomonas Elongata. *J Mol Catal B Enzym* **2015**, *120*, 141–150. https://doi.org/10.1016/j.molcatb.2015.07.009.

(68) Truppo, M. D.; Rozzell, J. D.; Moore, J. C.; Turner, N. J. Rapid Screening and Scale-up of Transaminase Catalysed Reactions. *Org Biomol Chem* **2009**, *7* (2), 395–398. https://doi.org/10.1039/b817730a.

(69) Cho, Byung Tae. "Recent Development and Improvement for Boron Hydride-Based Catalytic Asymmetric Reduction of Unsymmetrical Ketones." Chem. Soc. Rev. 38, no. 2 (2009): 443–52. https://doi.org/10.1039/b811341f.

(70) Tan, X.; Gao, S.; Zeng, W.; Xin, S.; Yin, Q.; Zhang, X. Asymmetric Synthesis of Chiral Primary Amines by Ruthenium-Catalyzed Direct Reductive Amination of Alkyl Aryl Ketones with Ammonium Salts and Molecular H2. *J Am Chem Soc* **2018**, *140* (6), 2024–2027. https://doi.org/10.1021/jacs.7b12898.

(71) Xianheng Wang, S. C. H. C. Y. H. & C. Z. Three-step synthetic procedure to prepare dolutegravir, cabotegravir, and bictegravir . *Received 11 Jan 2022, Accepted 18 Mar 2022, Published online: 31 Mar 2022* https://doi.org/10.1080/17518253.2022.2057200

(72) Yang, J.; Ji, C.; Zhao, Y.; Li, Y.; Jiang, S.; Zhang, Z.; Ji, Y.; Liu, W. BF3OEt2: An Efficient Catalyst for Transesterification of β-Ketoesters. *Synth Commun* **2010**, *40* (7), 957–963. https://doi.org/10.1080/00397910903029842.

APPENDIX

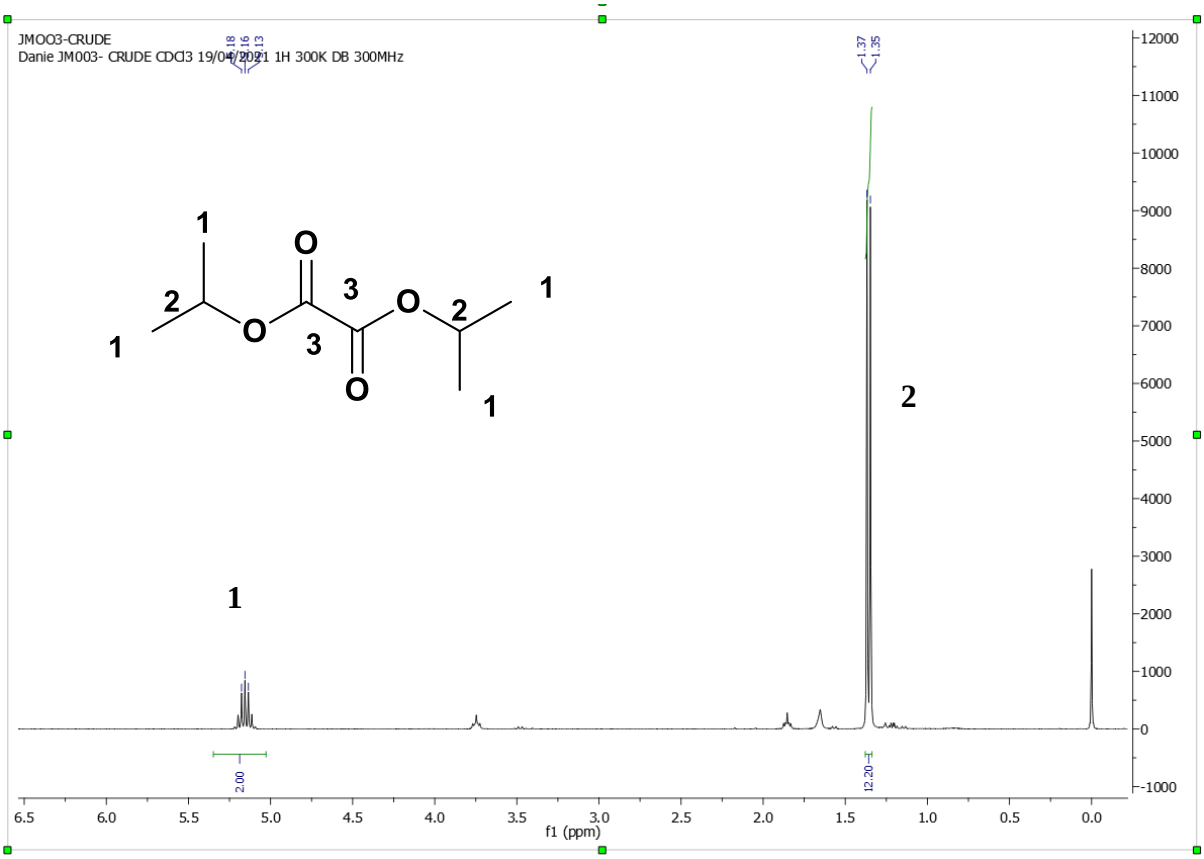
JMOO3-CRUDE
Danie JM003- CRUDE CDCl3 19/04/2021 1H 300K DB 300MHz
1.37
1.35
2.00
12.20
f1 (ppm)

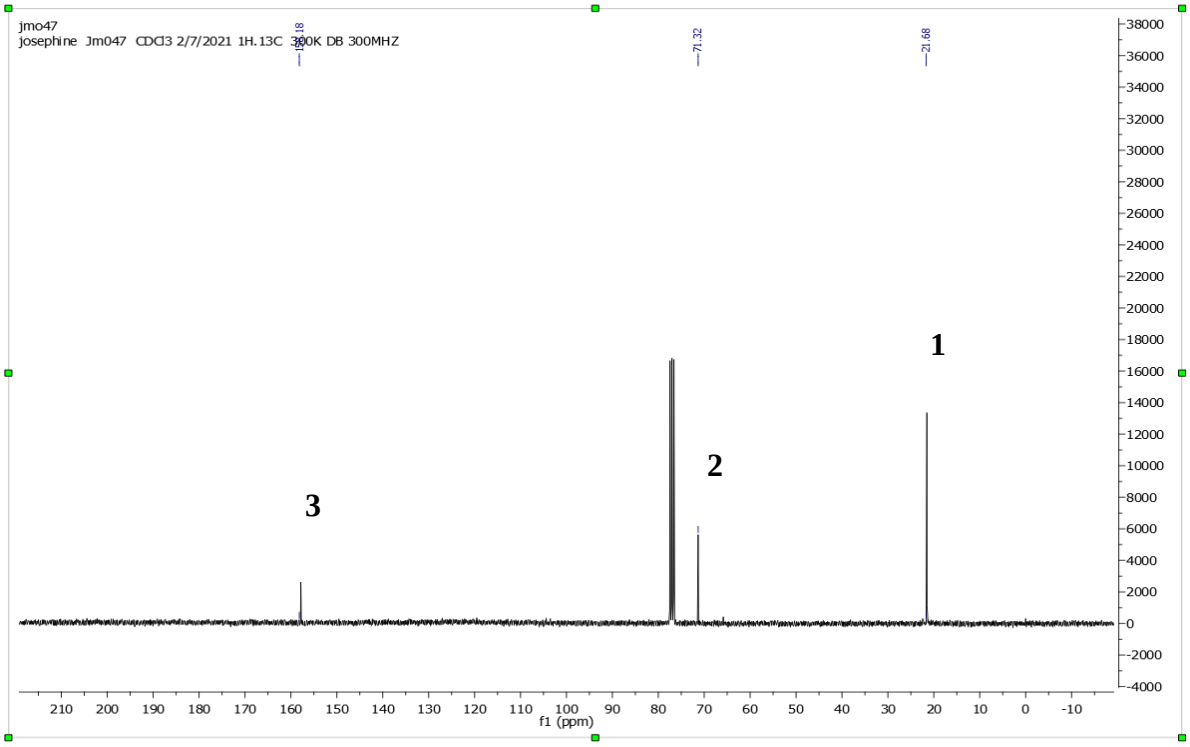
jmo47
josephine Jm047 CDCl3 2/7/2021 1H.13C 300K DB 300MHZ
71.32
21.68
f1 (ppm)

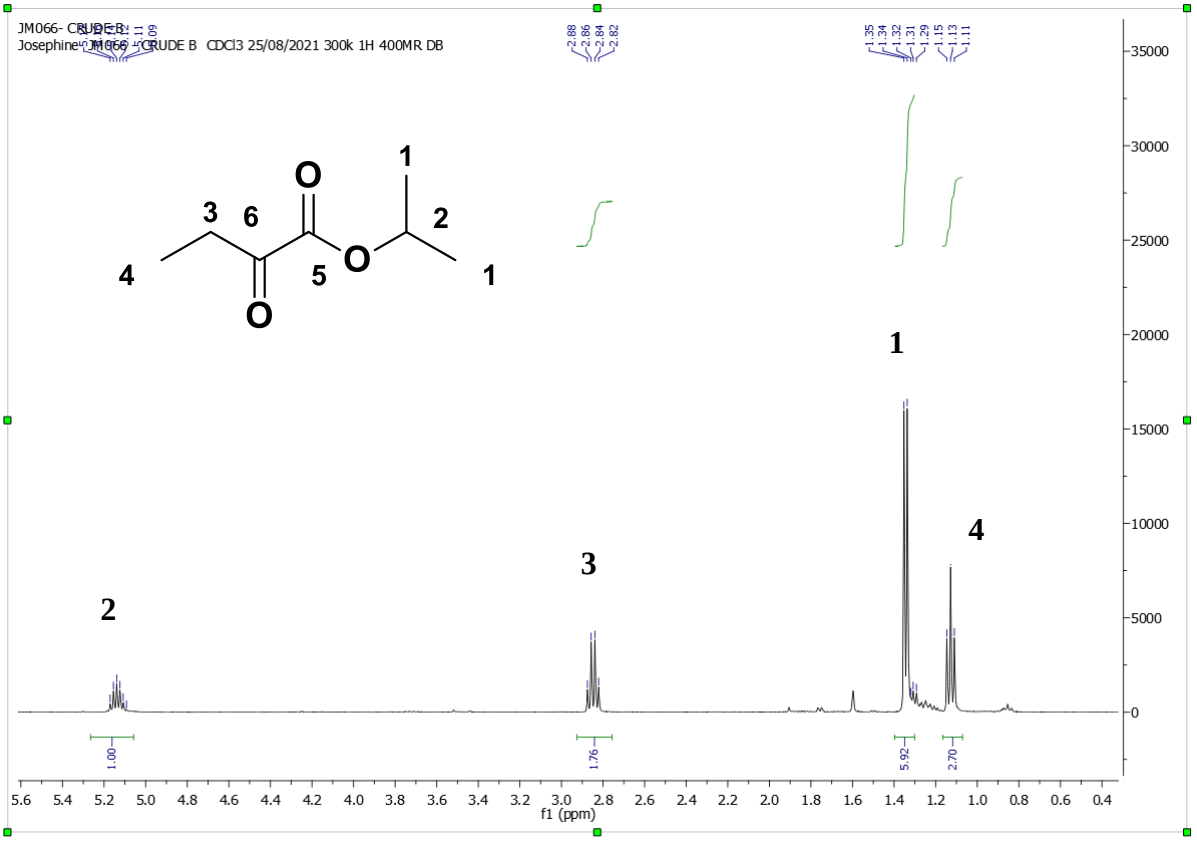
JM066- CRUDE B
Josephine JM066 - CRUDE B CDCl3 25/08/2021 300k 1H 400MR DB
O
O
O
1
2
3
4
5
6
1
2
3
4
f1 (ppm)

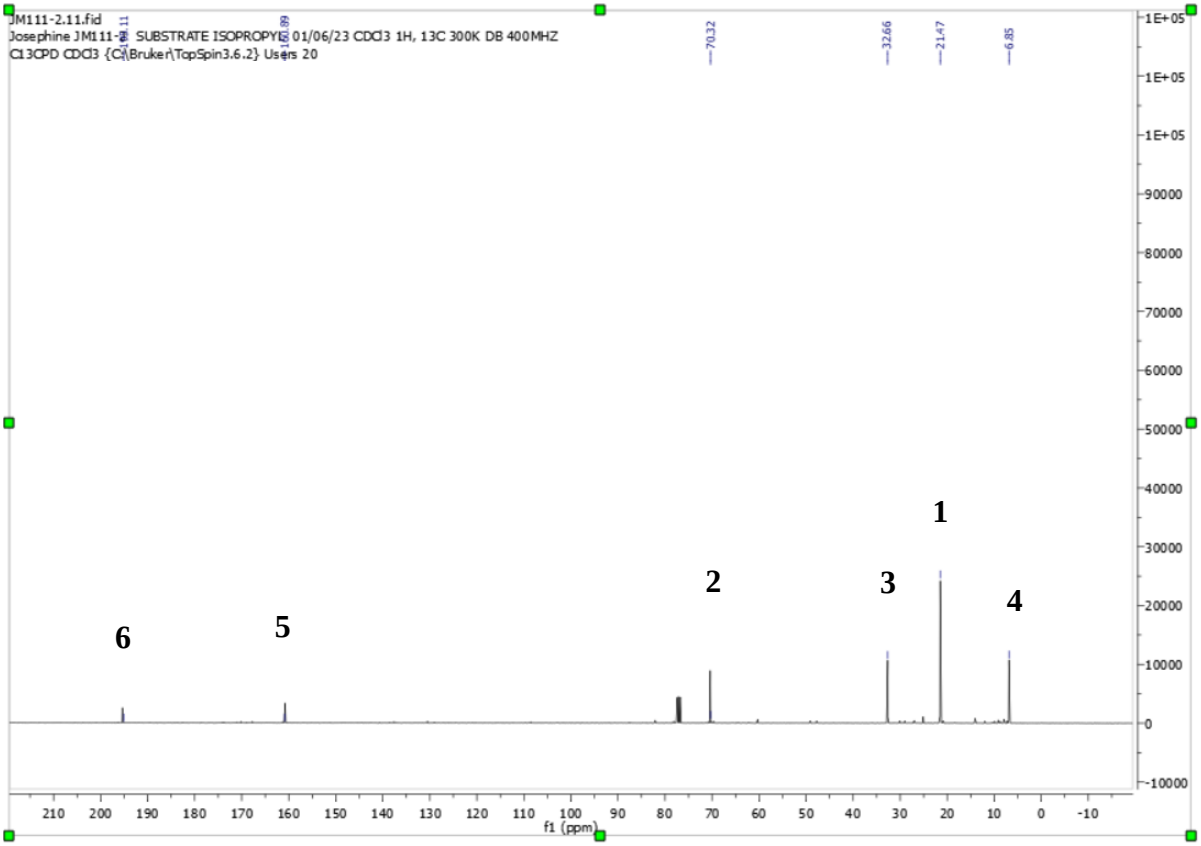
JM111-2.11.fid
Josephine JM111-2 SUBSTRATE ISOPROPYL 01/06/23 CDCl3 1H, 13C 300K DB 400MHZ
C13CPD CDCl3 {C:\Bruker\TopSpin3.6.2} Users 20
70.32
32.66
21.47
6.85
6
5
2
3
1
4
f1 (ppm)

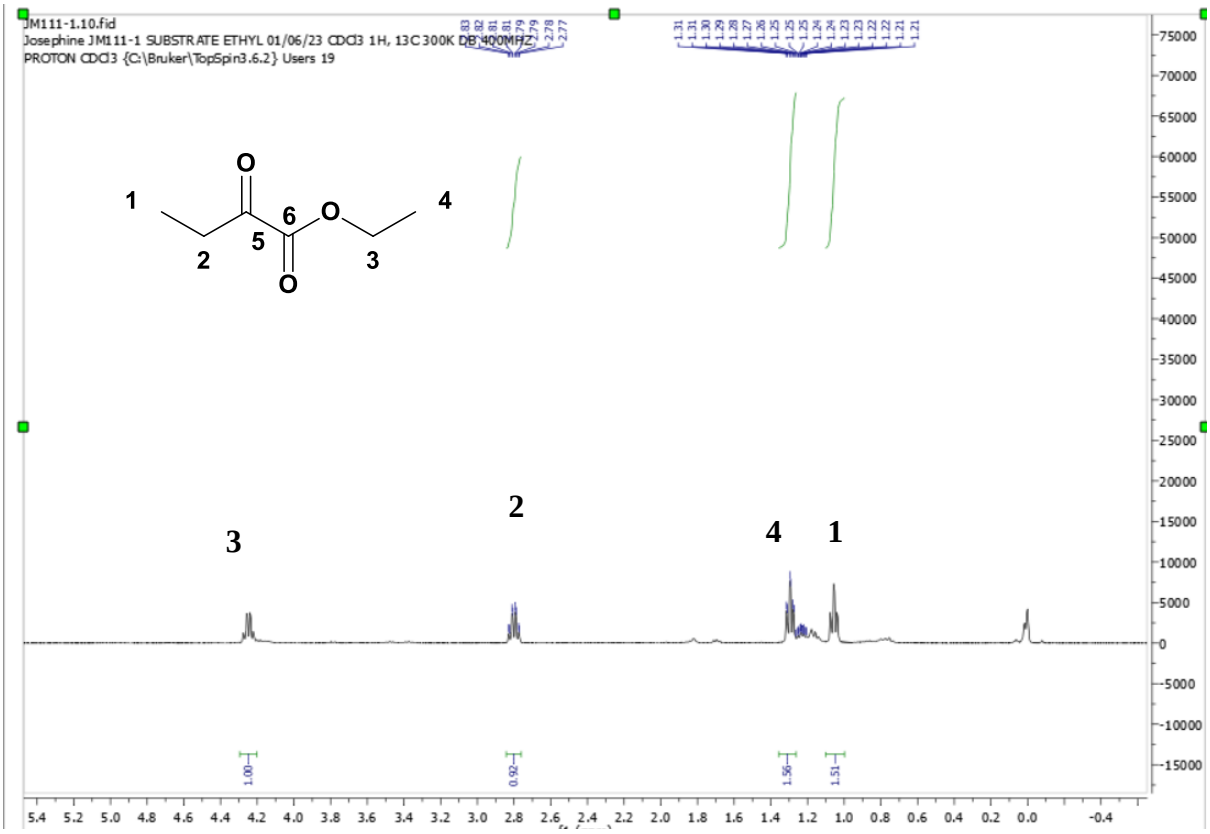
JM111-1.10.fid
Josephine JM111-1 SUBSTRATE ETHYL 01/06/23 CDCl3 1H, 13C 300K DB 400MHZ
PROTON CDCl3 {C:\Bruker\TopSpin3.6.2} Users 19
O
O
O
1
2
3
4
5
6
1
2
3
4
1.00
0.92
1.56
1.51

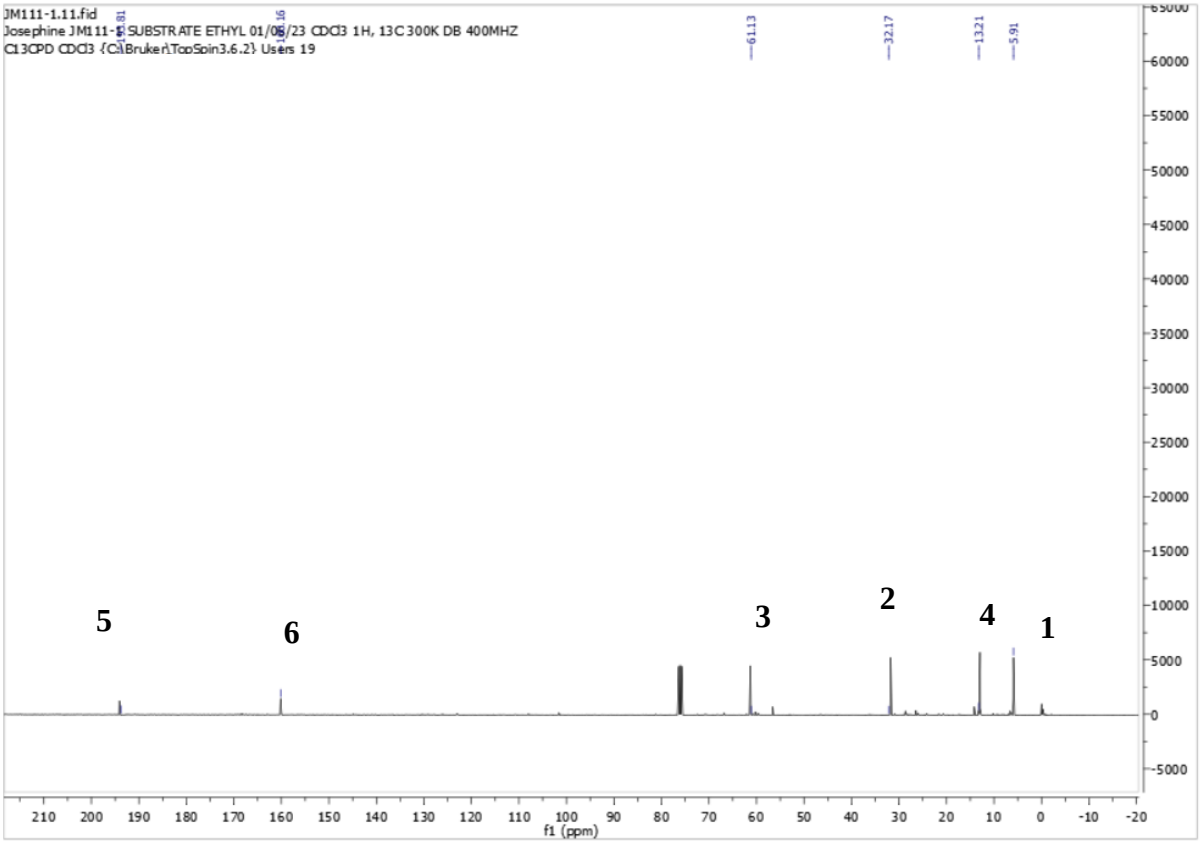
JM111-1.11.fid
Josephine JM111-1 SUBSTRATE ETHYL 01/06/23 CDCl3 1H, 13C 300K DB 400MHZ
C13CPD CDCl3 {C:\Bruker\TopSpin3.6.2} Users 19
61.13
32.17
13.21
5.91
5
6
3
2
4
1
f1 (ppm)

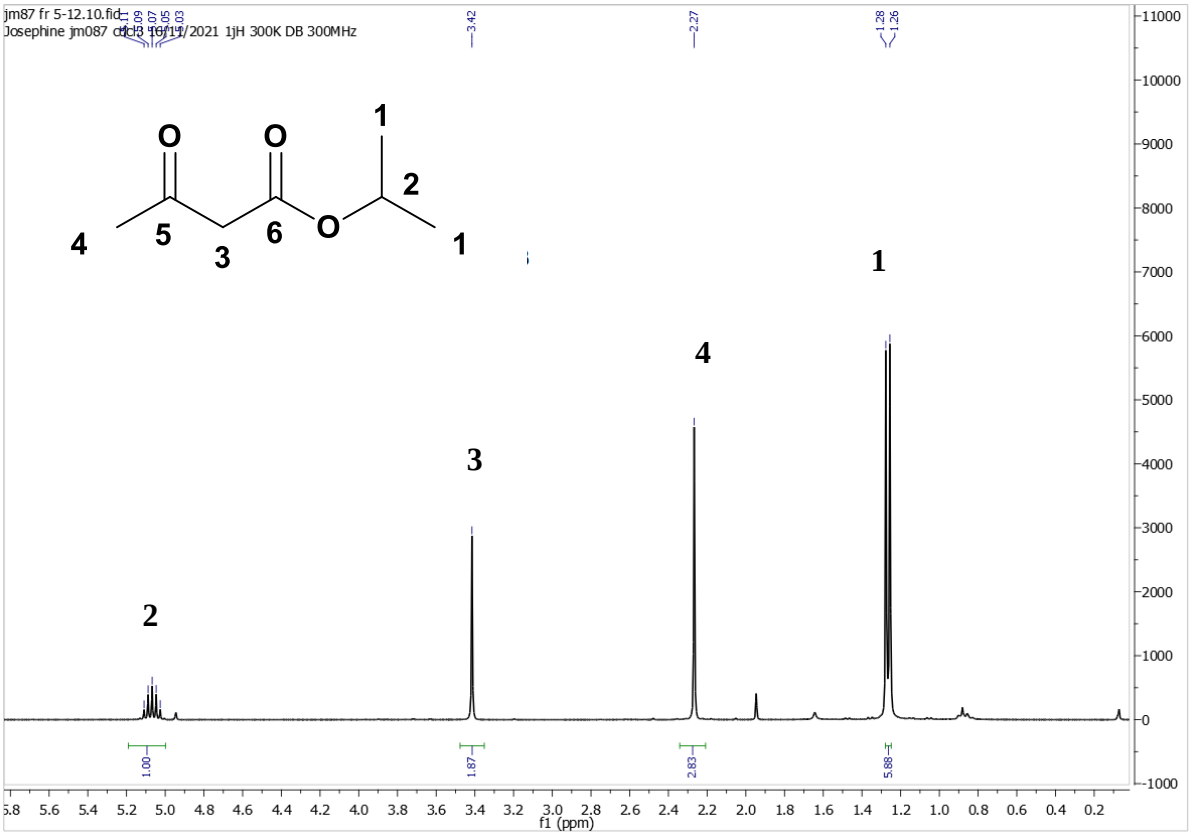
jm87 fr 5-12.10.fid
Josephine jm087 cdcl3 16/11/2021 1jH 300K DB 300MHz
3.42
2.27
1.28
1.26
O
O
O
1
2
4
5
3
6
1
1
4
3
2
1.00
1.87
2.83
5.88
f1 (ppm)

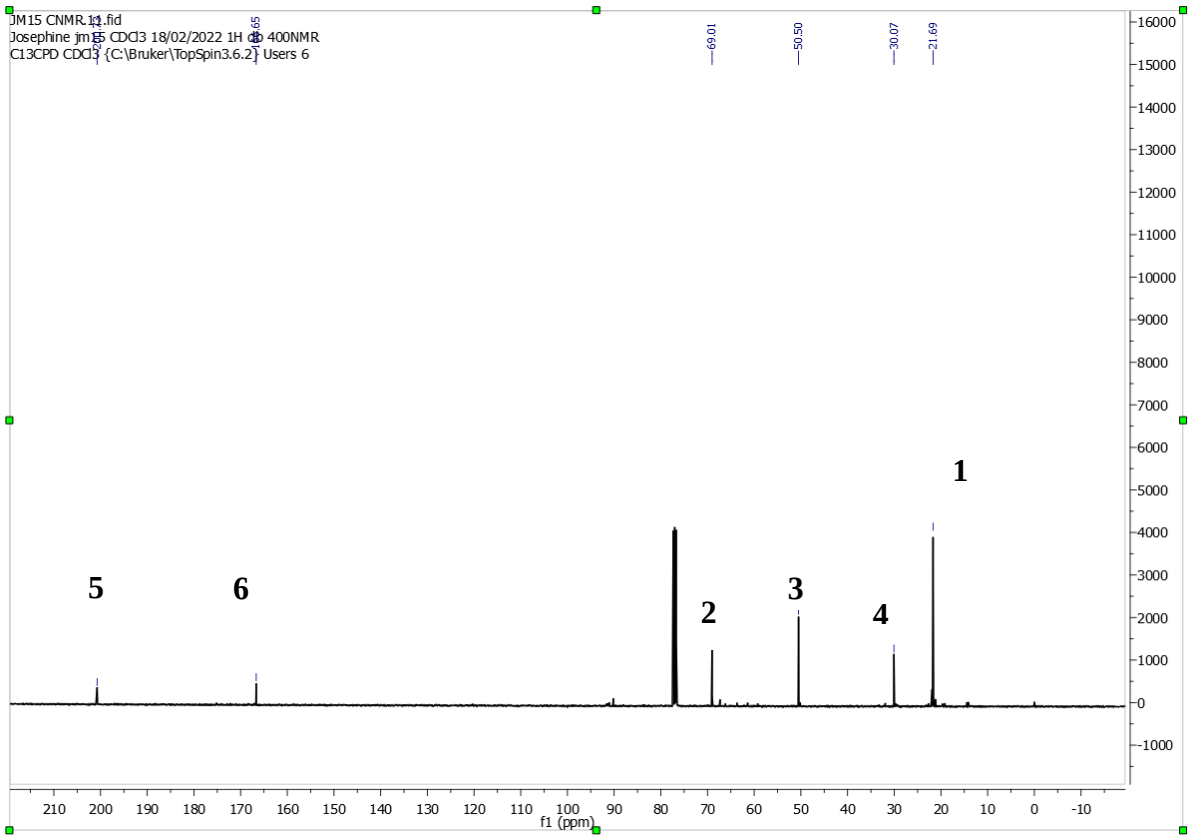
JM15 CNMR.11.fid
Josephine jm15 CDCl3 18/02/2022 1H dh 400NMR
C13CPD CDCl3 {C:\Bruker\TopSpin3.6.2} Users 6
69.01
50.50
30.07
21.69
1
5
6
2
3
4
f1 (ppm)

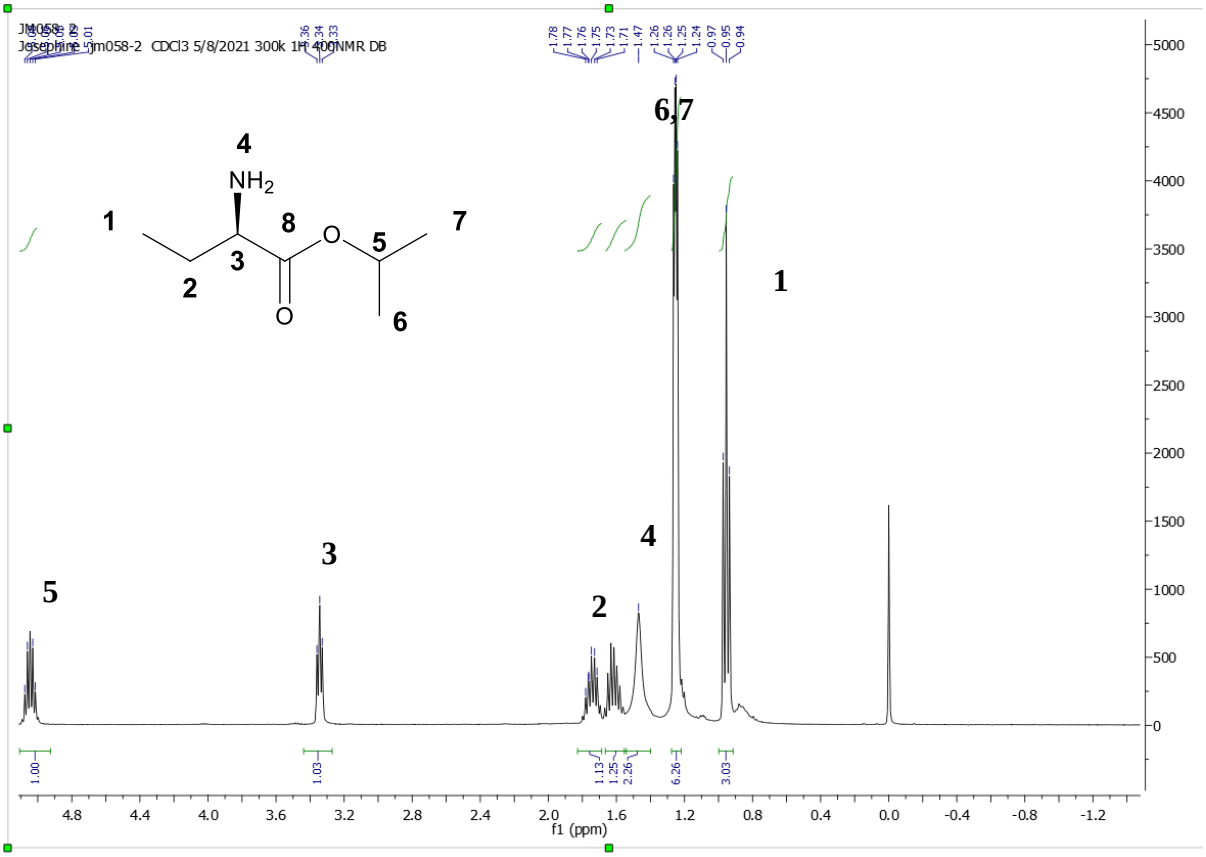
Josephine jm058-2 CDCl3 5/8/2021 300k 1H 400MHz DB
NH2
O
O
1
2
3
4
5
6
7
8
6,7
1
4
3
5
2
f1 (ppm)

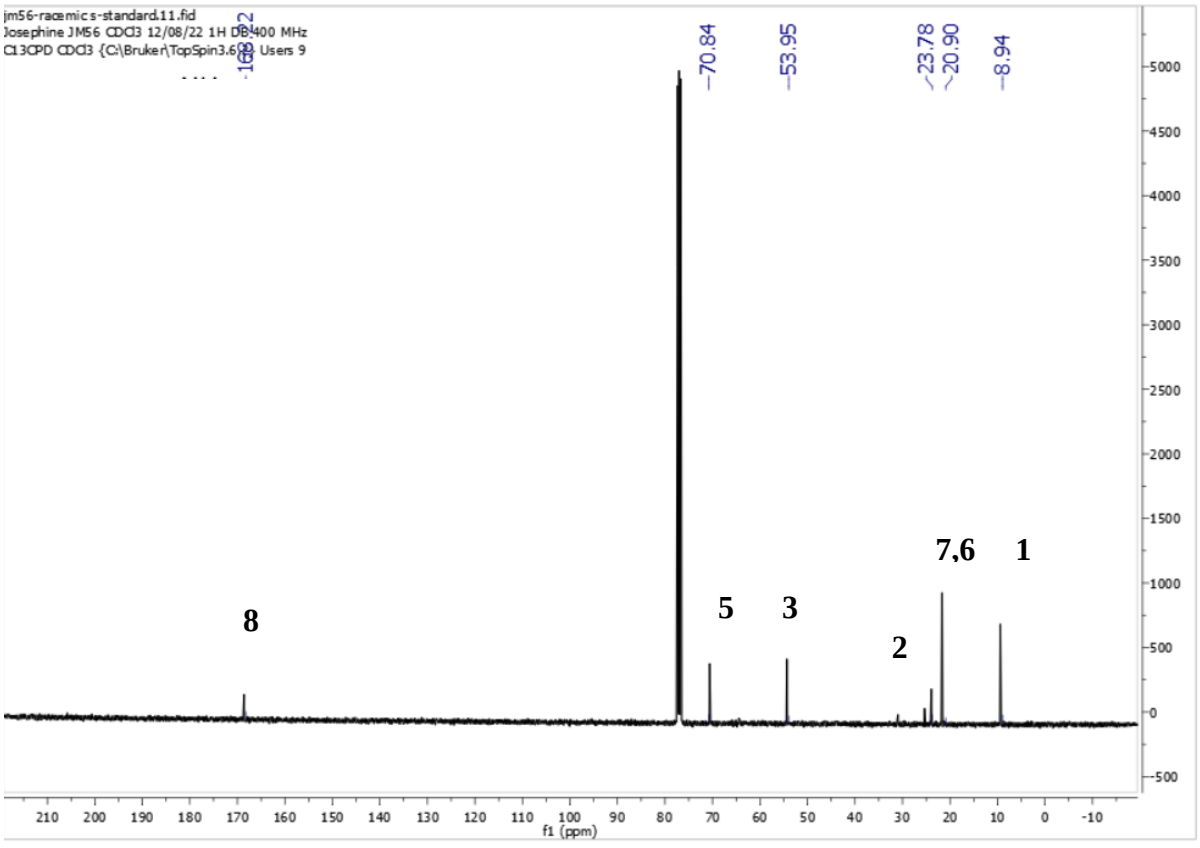
jm56-racemic s-standard.11.fid
Josephine JM56 CDCl3 12/08/22 1H DB 400 MHz
70.84
53.95
23.78
20.90
8.94
8
5
3
2
7,6
1
f1 (ppm)

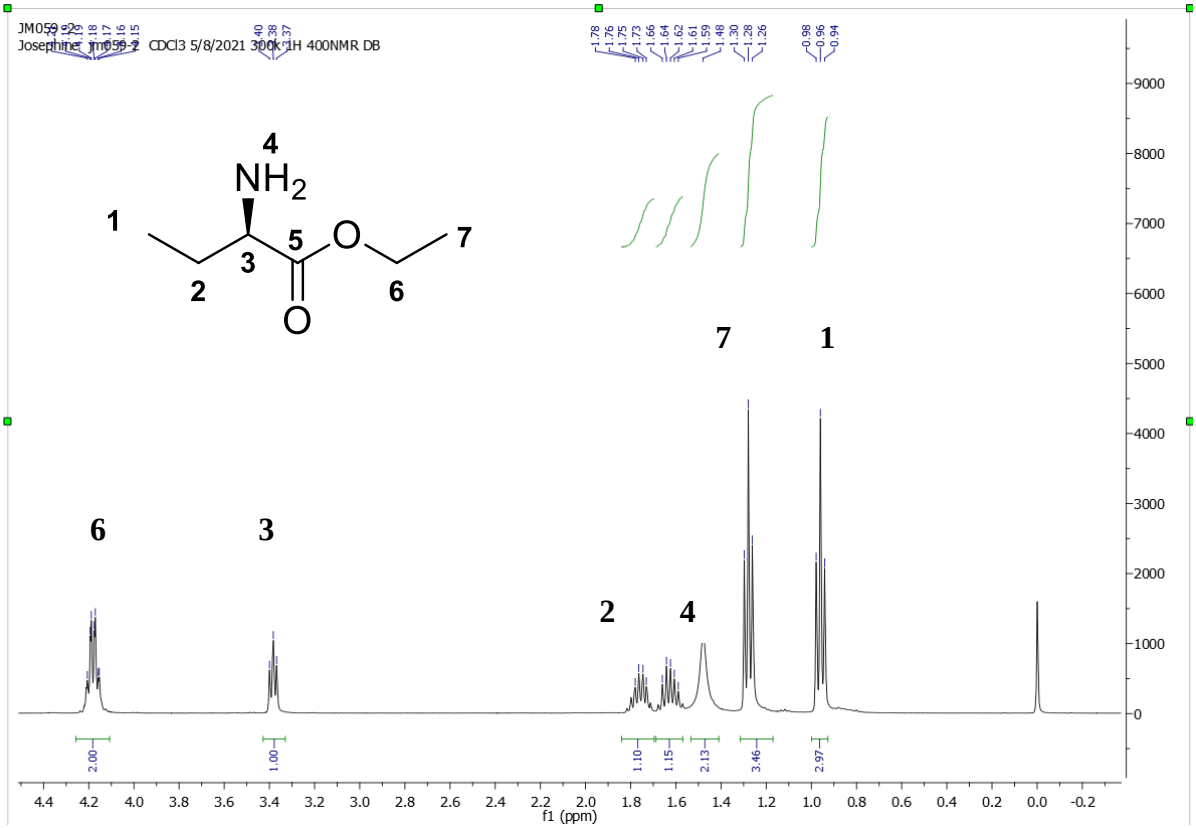
JM059-2
Josephine jm059-2 CDCl3 5/8/2021 300K 1H 400NMR DB
4
NH2
1
3
5
O
7
2
6
O
7
1
6
3
2
4
2.00
1.00
1.10
1.15
2.13
3.46
2.97
f1 (ppm)

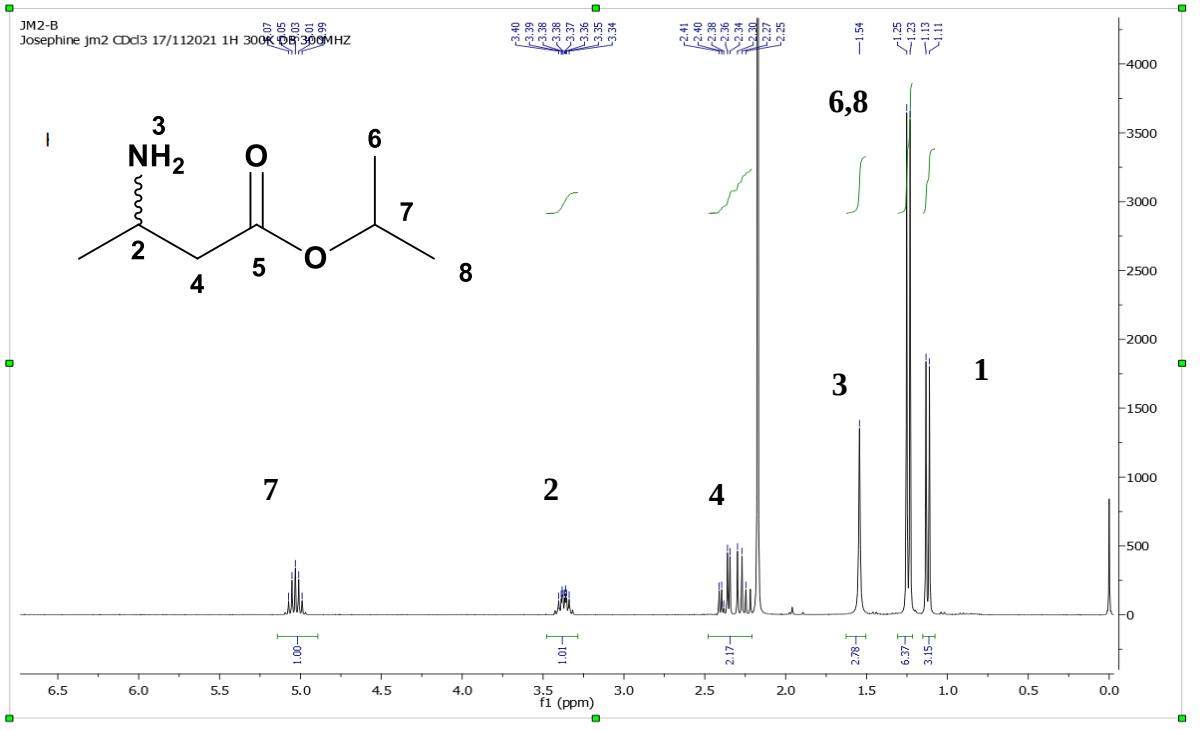
JM2-B
Josephine jm2 CDCl3 17/112021 1H 300K DB 300MHZ
3
NH2
O
6
7
2
5
O
8
4
6,8
3
1
7
2
4
1.00
1.01
2.17
2.78
6.37
3.15
f1 (ppm)

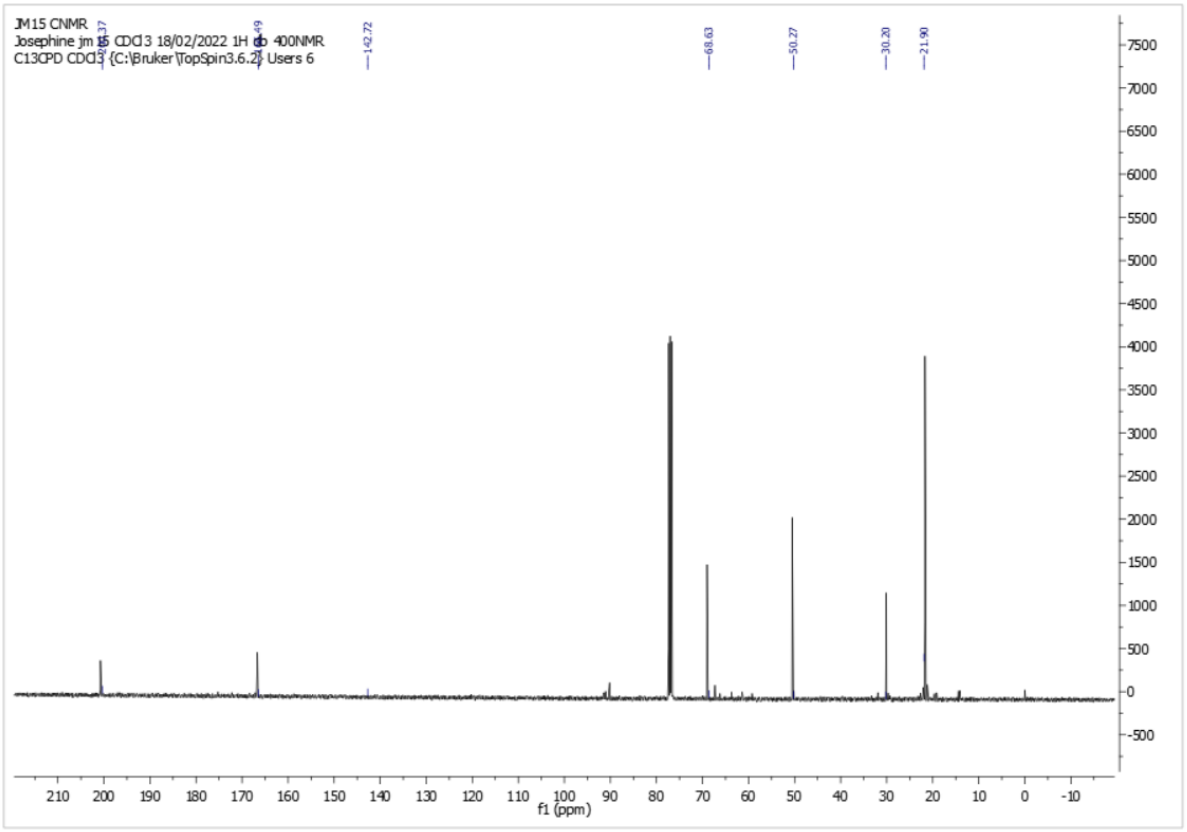
JM15 CNMR
Josephine jm15 CDCl3 18/02/2022 1H 400NMR
C13CPD CDCl3 {C:\Bruker\TopSpin3.6.2} Users 6
142.72
68.63
50.27
30.20
21.90
f1 (ppm)

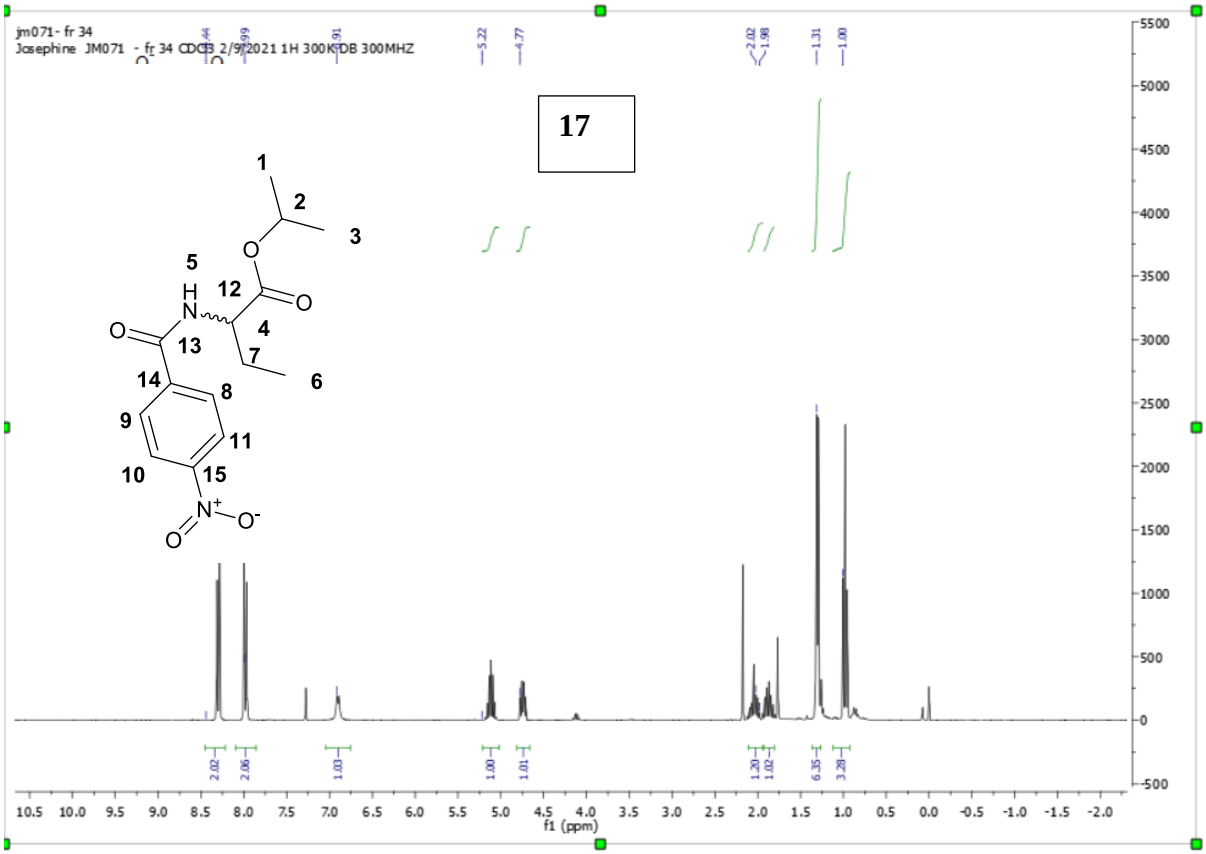
jm071- fr 34
Josephine JM071 - fr 34 CDCl3 2/9/2021 1H 300K/DB 300MHZ
5.22
4.77
2.02
1.98
1.31
1.00
17
1
2
3
5
H
N
12
O
O
13
4
7
6
14
8
9
11
10
15
N+
O-
O
2.02
2.06
1.03
1.00
1.01
1.20
1.02
6.35
3.29
f1 (ppm)

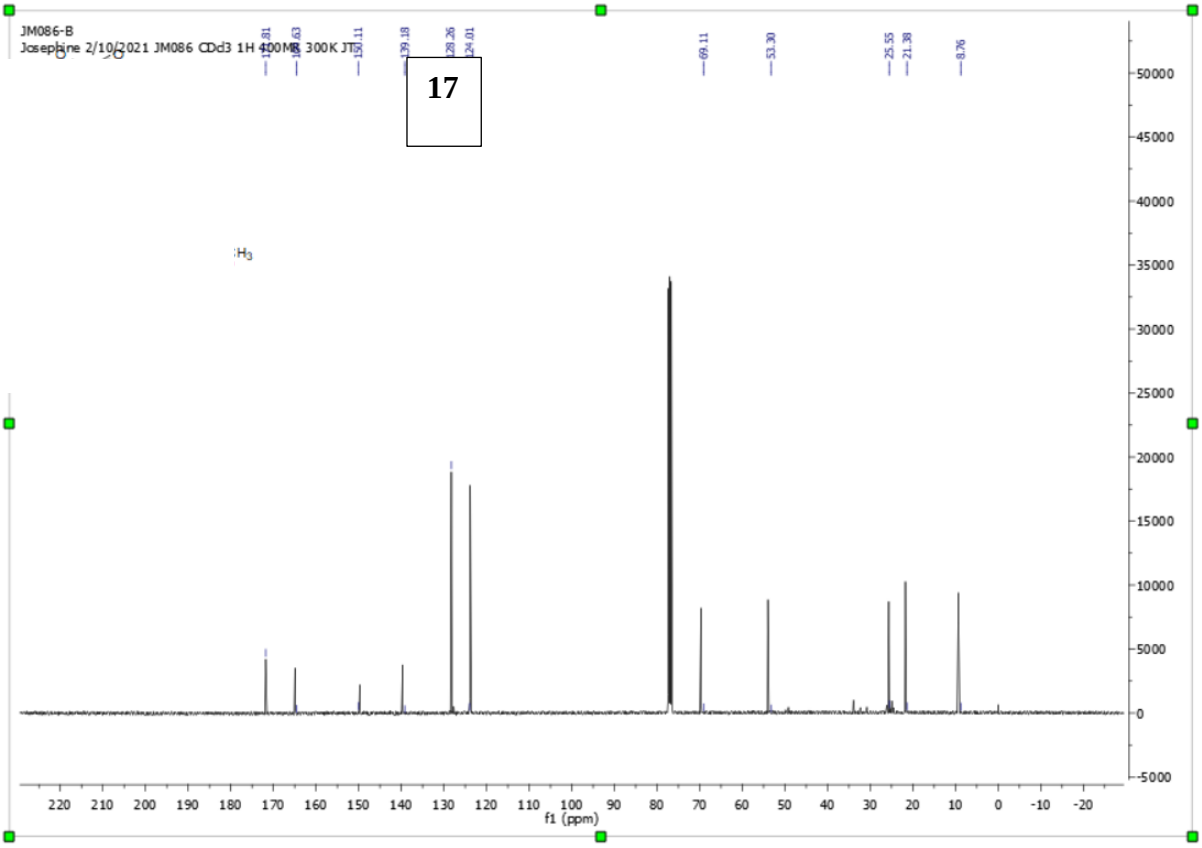
JM086-B
Josephine 2/10/2021 JM086 CDcl3 1H 400MHz 300K JTL
17
69.11
53.30
25.55
21.38
8.76
f1 (ppm)

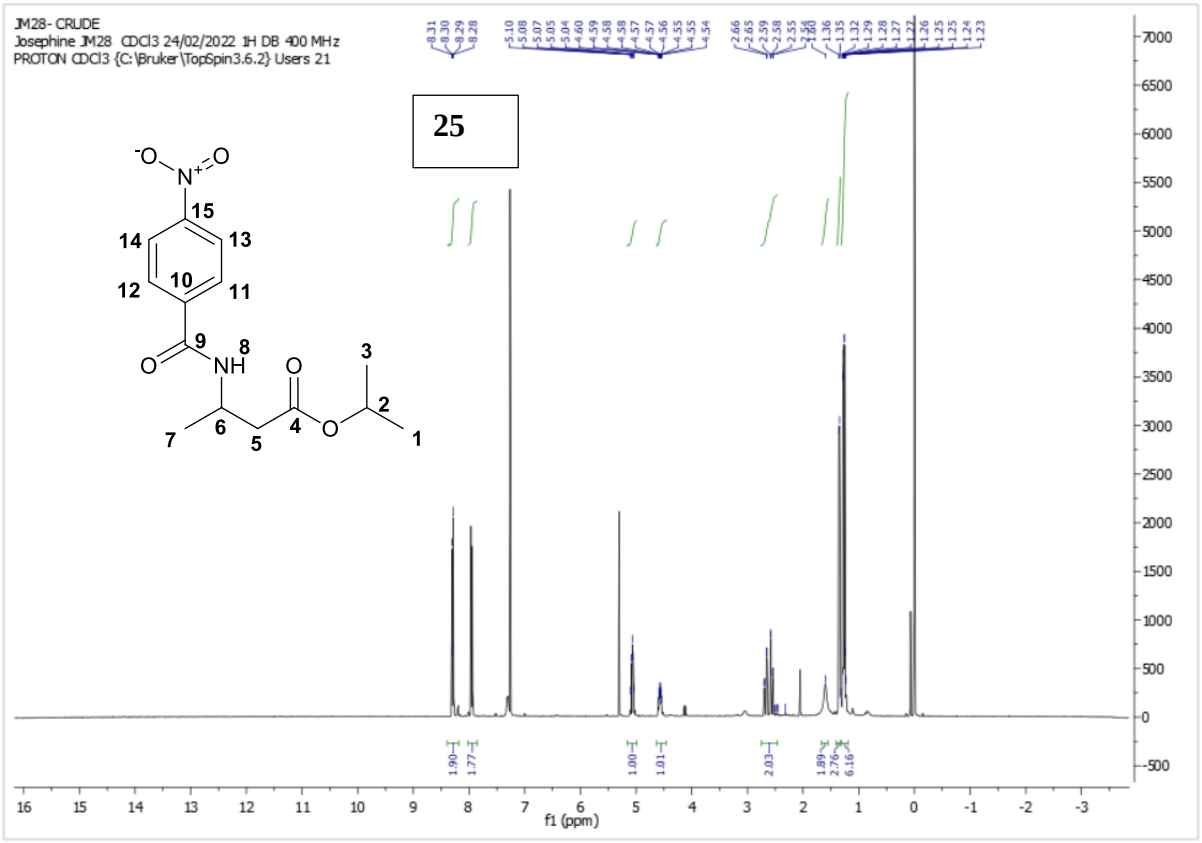
JM28- CRUDE
Josephine JM28 CDCl3 24/02/2022 1H DB 400 MHz
PROTON CDCl3 {C:\Bruker\TopSpin3.6.2} Users 21
25
f1 (ppm)

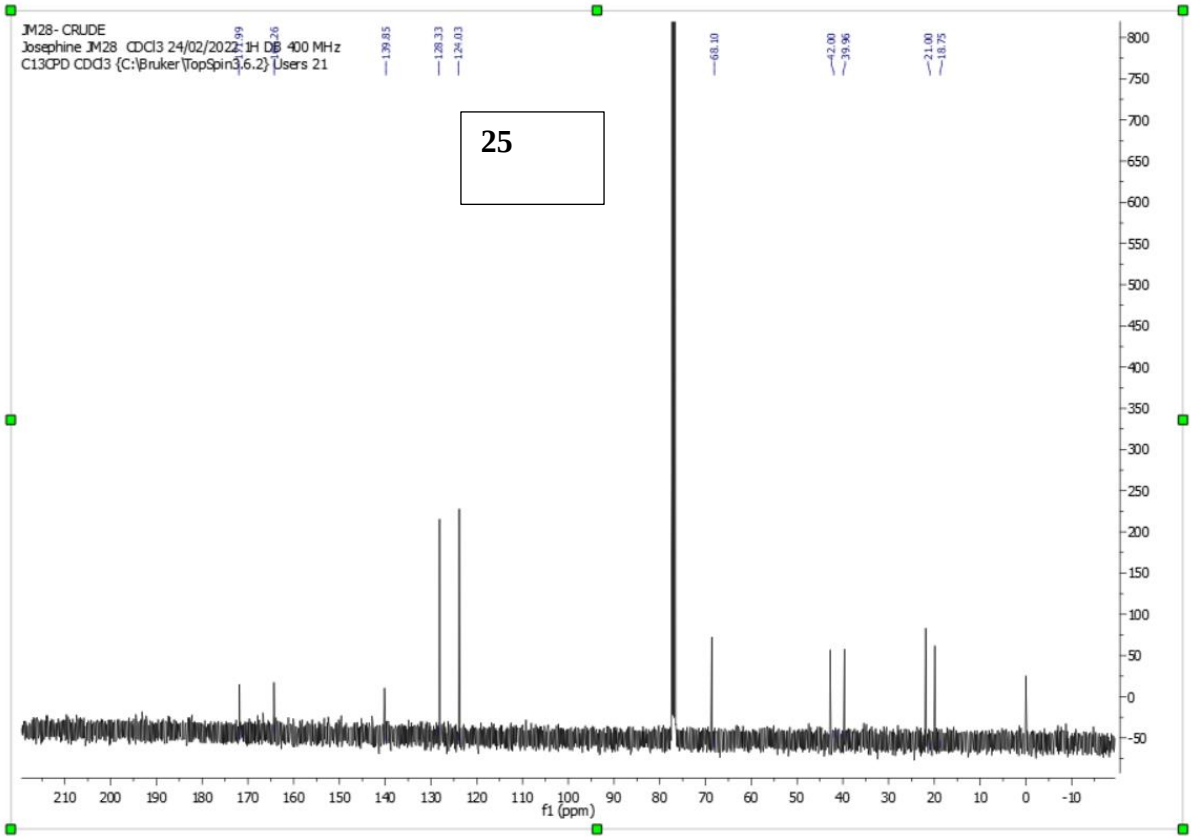
JM28- CRUDE
Josephine JM28 CDCl3 24/02/2022 1H DB 400 MHz
C13CPD CDCl3 {C:\Bruker\TopSpin3.6.2} Users 21
25
f1 (ppm)

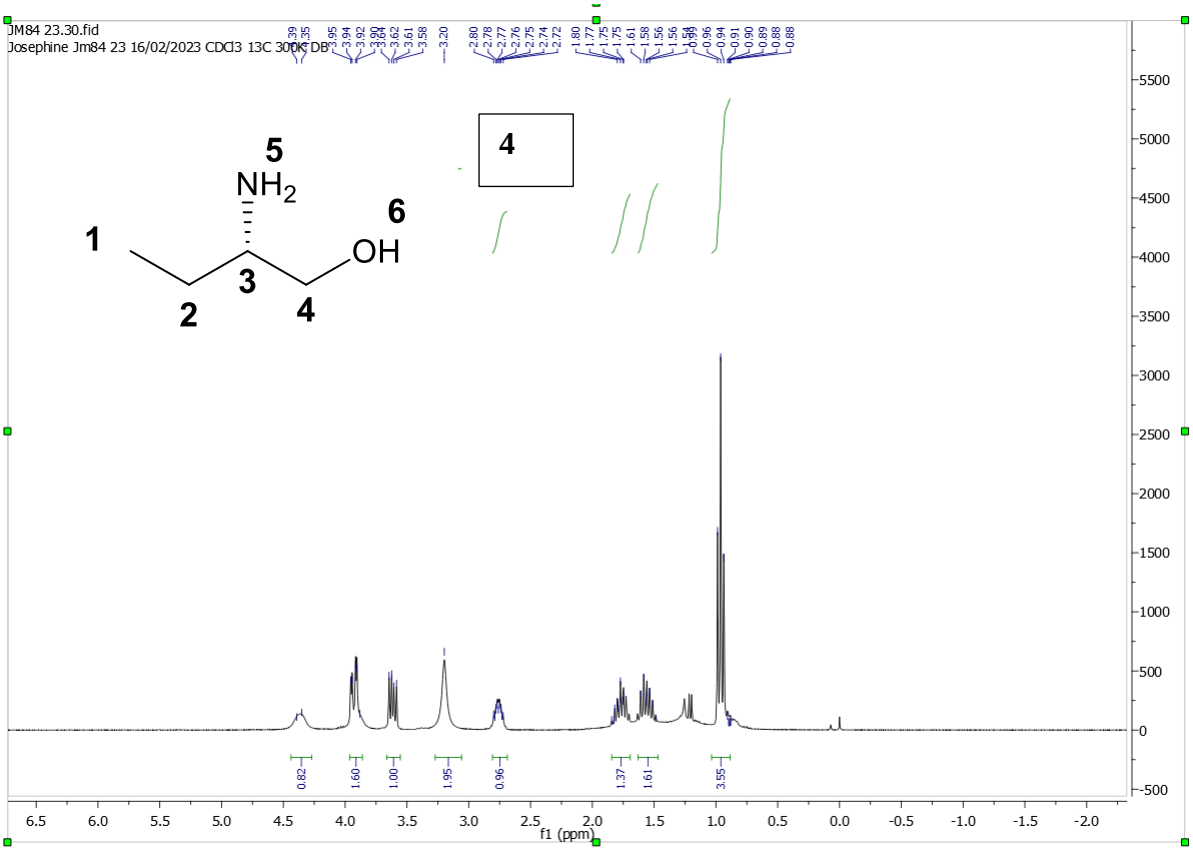
JM84 23.30.fid
Josephine Jm84 23 16/02/2023 CDCl3 13C 300K DB
4
5
NH2
6
1
OH
3
2
4
f1 (ppm)

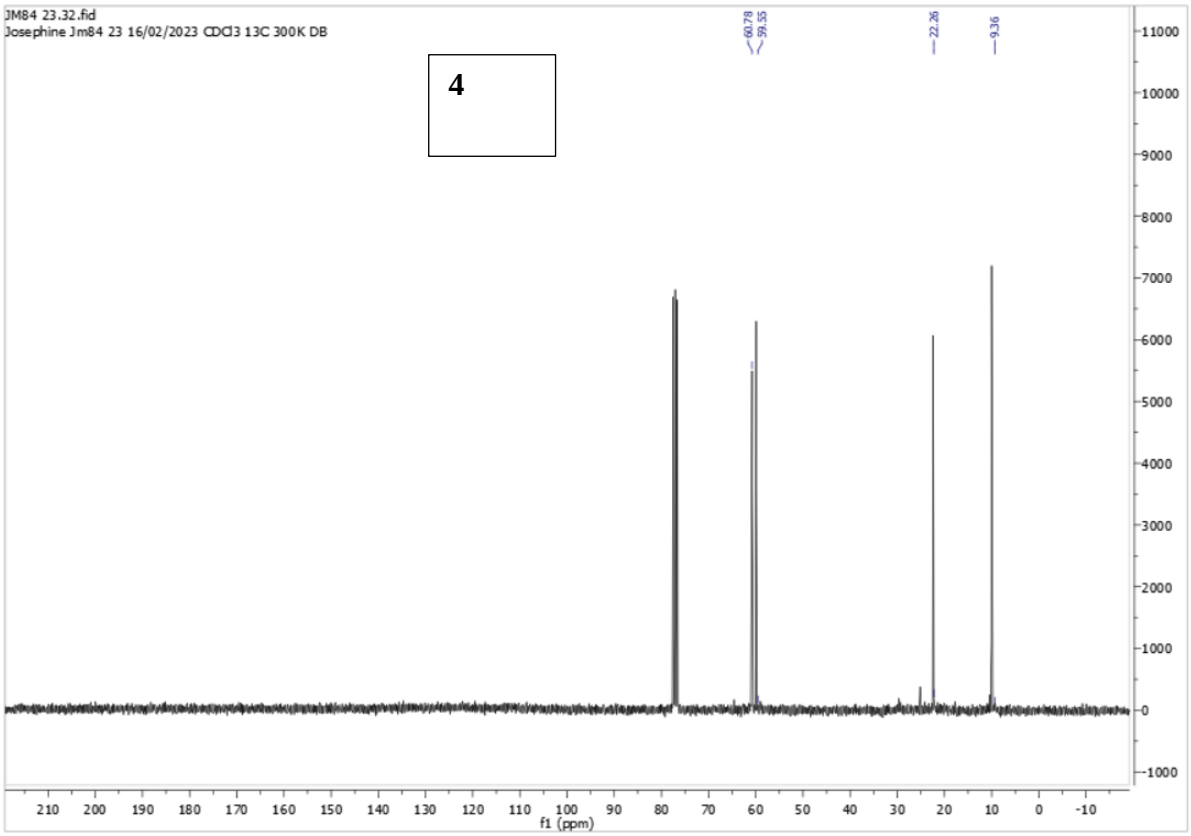
JM84 23.32.fid
Josephine Jm84 23 16/02/2023 CDCl3 13C 300K DB
4
60.78
59.55
22.26
9.36
f1 (ppm)

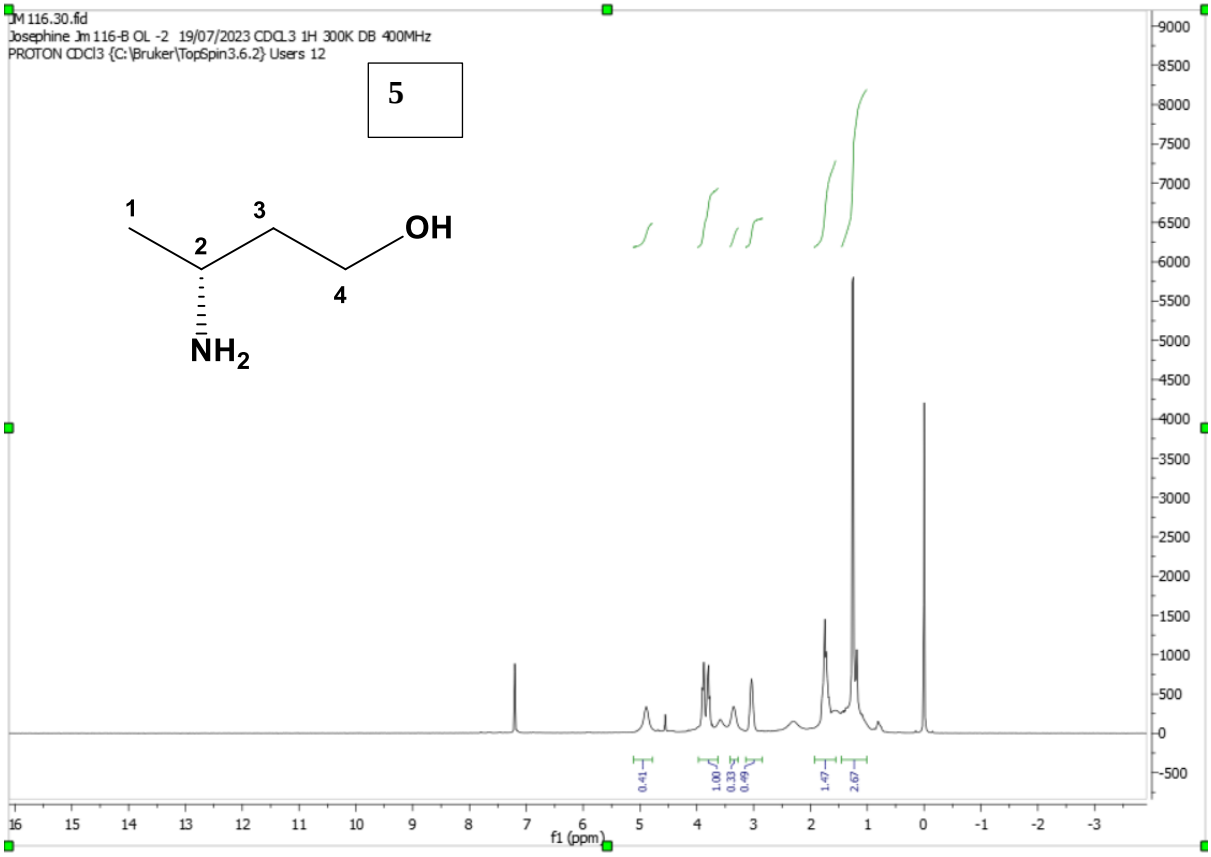
JM 116.30.fid
Josephine Jm 116-B OL -2 19/07/2023 CDCL3 1H 300K DB 400MHz
PROTON CDCl3 {C:\Bruker\TopSpin3.6.2} Users 12
5
1
2
3
4
OH
NH2
0.41
1.00
0.33
0.49
1.47
2.67
f1 (ppm)

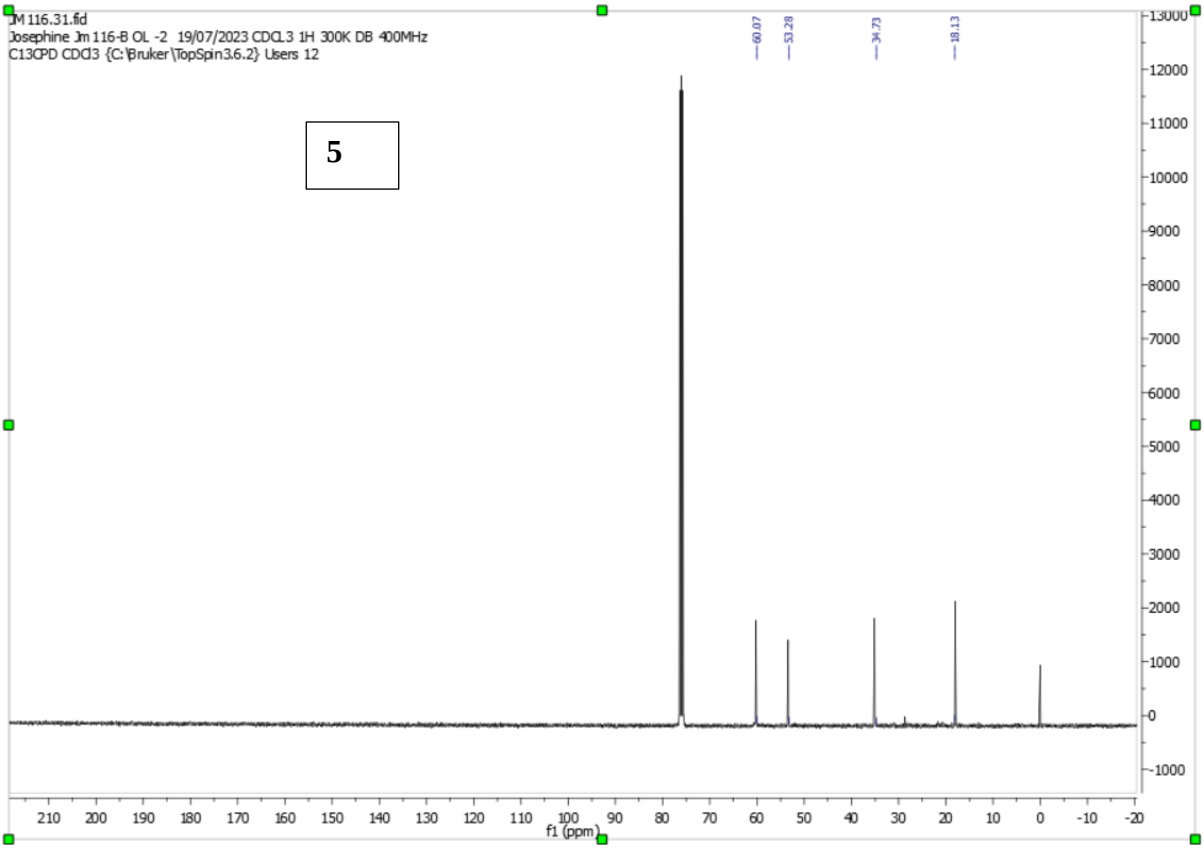
JM 116.31.fid
Josephine Jm 116-B OL -2 19/07/2023 CDCL3 1H 300K DB 400MHz
C13CPD CDCl3 {C:\Bruker\TopSpin3.6.2} Users 12
5
60.07
53.28
34.73
18.13
f1 (ppm)

DEPT NMR of standard **14**

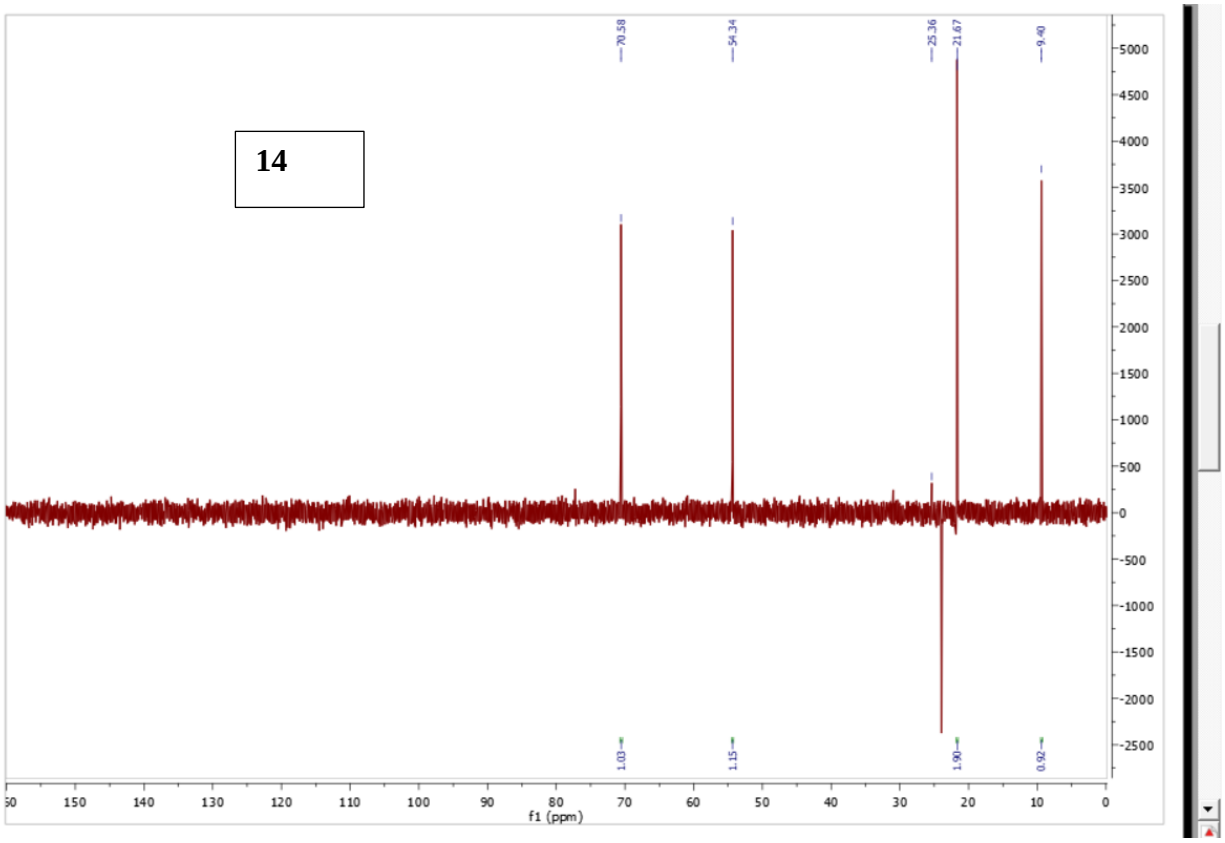

DEPT NMR of enzyme catalysed **14.**

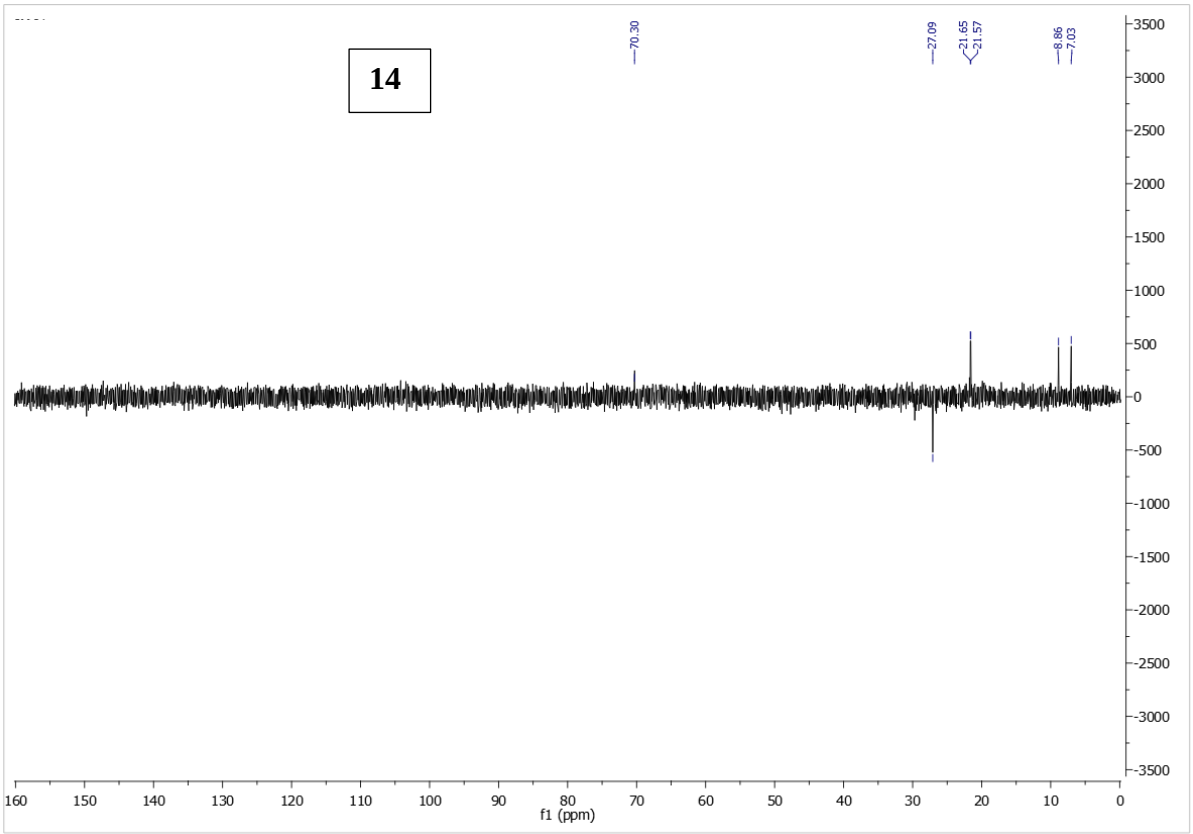

Cost estimation tables

Table8: Cost –estimation of the commercial synthesis of Ethambutol drug .

When (*S*)-2-amino-1-butanol and ethanol are recycled in step 4, according to CN 103772214B, including current costs (in bulk) of the main chemicals :

	Reagent	Mol Weight g/mol	eq wrt step's product moles	mol	mass(g)	Mass(kg)	Cost ($/kg)	Cost ($)
Step 1	1-nitropropane	89.09	1.730	64.24	5723	5.72	10.00	57.23
	paraformaldehyde	30.03	2.247	83.42	2505	2.51	6.00	15.03
	KOH	56.11	0.017	0.64	36	0.04	0.85	0.03
	methanol for rx solution	32.04	0.797	29.60	948	0.95	0.22	0.21
	Raney Nickel				418	0.42	10.00	4.18
	hydrogen gas	2.016	5.190	192.71	388	0.39	6.00	2.33
	methanol for hydrogenation	32.04	17.733	658.39	21095	21.09	0.22	4.64
	***dl*-2-amino-1-butanol**	89.14	1.000	37.13	**3310**	**3.31**		
Step 2	*dl*-2-amino-1-butanol	89.14	2.451	37.13	3310	3.31		
	l-(+)-tartaric acid	150.09	2.491	37.73	5662	5.66	2.50	14.16
	methanol	32.04	49.593	751.24	24070	24.07	0.22	5.30
	methanol for washing							
	crystals	32.04	5.579	84.51	2708	2.71	0.22	0.60
	(S)-2-amino-1-butanol							
	***l*-(+)-tartrate complex**	239.22	1.000	15.15	**3624**	**3.62**		
Step 3	(*S*)-2-amino-1-butanol							
	l-(+)-tartrate complex	239.22	1.316	15.15	3624	3.62		
	KOH	56.11	2.829	32.57	1827	1.83	0.85	1.55
	H2O	18.02	13.329	153.45	2765	2.77		
	(*S*)-2-amino-1-butanol	89.14	1.000	11.51	**1026**	**1.03**		
Step 4	ethylene dichloride	98.96	1.038	5.08	503	0.50	6.00	3.02
	(*S*)-2-amino-1-butanol	89.14	2.352	11.51	1026	1.03		
	ethanol	46.07	0.136	0.67	31	0.03	2.00	0.06
	ethanol for NH4Cl prec.	46.07	0.421	2.06	95	0.09	2.00	0.19

	ammonia	17.03	2.596	12.71	216	0.22	8.00	1.73
	Ethambutol	**204.31**	**1.000**	**4.89**	**1000**	**1.00**		**110.25**

Table 9: Cost –estimation of our proposed synthesis of Ethambutol drug .

								No recycling	>90% THF and EtOH recycled
	Reagent (compound numbers in brackets)	Mol Weight g/mol	eq wrt step's product moles	mol	mass(g)	Mass(kg)	Cost ($/kg)	Cost ($)	Cost ($)
Step 1	diethyl oxalate	89.09	1.250	23.44	2088	2.09	4.00	8.35	8.35
	ethyl bromide	30.03	1.288	24.14	725	0.73	2.80	2.03	2.03
	magnesium	56.11	1.288	24.14	1355	1.35	3.30	4.47	4.47
	tetrahydrofuran	72.11	17.092	320.52	23113	23.11	1.65	38.14	3.81
	ethyl 2-oxobutanoate[1] (8)	130.14	1.000	18.75	**2441**	**2.44**			
Step 2	ethyl 2-oxobutanoate	130.14	1.111	18.75	2441	2.44			
	S-selective transaminase enzyme[2]	50800	0.003	0.05	2441	2.44	3.70	9.03	9.03
	Isopropylamine[3]	59.11	1.111	18.75	1108	1.11	2.00	2.22	2.22
	2 mM PLP in 1 M phosphate buffer[4]								
	ethyl (*S*)-2-aminobutyrate[5] (3)	131.17	1.000	16.88	**2214**	**2.21**			
Step 3	ethyl (*S*)-2-aminobutyrate	131.17	1.379	16.88	2214	2.21			
	Raney Nickel				1107	1.11	10.00	11.07	11.07
	hydrogen gas	2.016	2.759	33.76	553	0.55	6.00	3.32	3.32
	ethanol	46.07	41.314	505.53	23290	23.29	2.00	46.58	4.66
	(*S*)-2-amino-1-butanol[6] (4)	89.14	1.000	12.24	**1091**	**1.09**			
Step 4	ethylene dichloride	98.96	1.250	6.12	605	0.61	6.00	3.63	3.63
	(*S*)-2-amino-1-butanol	89.14	2.500	12.24	1091	1.09			

	ammonia	17.03	3.125	15.30	260	0.26	8.00	2.08	2.08
	Ethambutol[7,8] (1)	**204.31**	**1.000**	**4.89**	**1000**	**1.00**		130.92	**54.68**

Table 10: Cost –estimation of the commercial synthesis of (*R*)-3-amino-1-butanol dolutegravir intermediate (industrial Method A)

	Reagent	Mol Weight g/mol	eq wrt step's product moles	mol	mass(g)	Mass(kg)	Cost ($/kg)	Cost ($)
Step 1	methyl acetoacetate[1]	116.12	1.080	15.73	1827	1.83	18.00	32.89
	ammonium acetate	77.08	1.080	15.73	1213	1.21	1.00	1.21
	acetic acid	60.05	1.296	18.88	1134	1.13	4.00	4.54
	Ru(OAc)2[(*R*)-dm-segphos]	941.94	0.001	0.0157	15	0.015	13.03	0.19
	methanol	32.04	10.940	159.39	14470	14.47	0.22	3.18
	7M NH3 in MeOH	17.03	0.531	17.31	295	0.29	8.00	2.36
	methyl (*R*)-3-aminobutyrate	117.15	1.299	14.57	1707	1.71		
Step 2	methyl (*R*)-3-aminobutyrate	117.15	1.299	14.57	1707	1.71		
	ethanol	46.07	21.751	244.01	11241	11.24	2.00	22.48
	potassium borohydride	49.91	2.908	32.62	1628	1.63	20.00	32.56
	HCl	36.46	1.429	16.03	584	0.58	2.30	1.34
	dichloromethane	17.03	3.247	36.42	620	0.62	2.00	1.24
	Na2CO3	105.99	1.429	16.03	1707	1.71	0.22	0.38
	(R)-3-amino-1-butanol (ee = 92.9%)[2]	**89.14**	**1.000**	**11.22**	**1000**	**1.00**		102.37

Table 11: Cost estimatiom of Current industry chemoenzymatic synthesis of (R)-3-amino-1-butanol dolutegraviv intermediate (industrial METHOD B)

	Reagent	Mol Weight g/mol	eq wrt step's product moles	mol	mass (g)	Mass(kg)	Cost ($/kg)	Cost ($)
Step 2	4-hydroxybutan-2-one[1]	88.11	1.349	15.13	1333	1.33	**70.00**	93.34
	transaminase enzyme[2]	50800	0.004	0.04	2000	2.00	3.70	7.40
	sec-butylamine[3]	73.14	1.349	15.13	1107	1.11	1.00	1.11
	1 mM PLP in phosphate buffer							0.00
	(R)-3-amino-1-butanol (ee = 100%)	**89.14**	**1.000**	**11.22**	**1000**	**1.00**		239.74

Table 12 : cost-estimation of ourproposed chemoenzymatic synthesis of (R)-3-amino-1-butanol

	Reagent	Mol Weight g/mol	eq wrt step's product moles	mol	mass(g)	Mass(kg)	Cost ($/kg)	Cost ($)
Step 1	ethyl acetoacetate[1]	116.12	1.111	16.19	1880	1.88	**31.50**	59.22
	R-selective transaminase enzyme[2]	50800	0.003	0.04	1880	1.88	3.70	6.96
	Isopropylamine[3]	59.11	1.111	16.19	957	0.96	2.00	1.91
	2 mM PLP in 1 M phosphate buffer[4]							
	methyl (*R*)-3-aminobutyrate (ee > 99%)[5]	117.15	1.299	14.57	1707	1.71		
Step 2	methyl (*R*)-3-aminobutyrate	117.15	1.299	14.57	1707	1.71		
	ethanol	46.07	21.751	244.01	11241	11.24	2.00	22.48
	potassium borohydride	49.91	2.908	32.62	1628	1.63	20.00	32.56
	HCl	36.46	1.429	16.03	584	0.58	2.30	1.34
	dichloromethane	17.03	3.247	36.42	620	0.62	2.00	1.24
	Na2CO3	105.99	1.429	16.03	1707	1.71	0.22	0.38
	(R)-3-amino-1-butanol[6,7,8]	**89.14**	**1.000**	**11.22**	**1000**	**1.00**		126.09